UNCLASSIFIED

AD NUMBER

AD815681

LIMITATION CHANGES

TO:

Approved for public release; distribution is unlimited. Document partially illegible.

FROM:

Distribution authorized to U.S. Gov't. agencies and their contractors; Critical Technology; DEC 1966. Other requests shall be referred to Air Force Technical Application Center, Washington, DC. Document partially illegible. This document contains export-controlled technical data.

AUTHORITY

usaf ltr, 25 jan 1972

THIS PAGE IS UNCLASSIFIED

TR 67-13

AD815681

TECHNICAL REPORT NO. 67-13

FINAL REPORT OF THE OPERATION OF THE TONTO FOREST SEISMOLOGICAL OBSERVATORY, PROJECT VT/5055

1 May 1965 Through 31 December 1966

DDC
RECEIVED
JUN 23 1967
A

ORIGINAL CONTAINS COLOR PLATES: ALL DDC REPRODUCTIONS WILL BE IN BLACK AND WHITE. ORIGINAL MAY BE SEEN IN DDC HEADQUARTERS.

STATEMENT #2 UNCLASSIFIED

This document is subject to special export controls and each transmittal to foreign governments or foreign nationals may be made only with prior approval of Chief AFTAC, Wash. D.C.

GEOTECH
A TELEDYNE COMPANY

BEST
AVAILABLE COPY

TECHNICAL REPORT NO. 67-13

FINAL REPORT OF THE OPERATION OF THE TONTO FOREST SEISMOLOGICAL OBSERVATORY, PROJECT VT/5055

1 May 1965 through 31 December 1966

Sponsored by

Advanced Research Projects Agency
Nuclear Test Detection Office
ARPA Order No. 624

GEOTECH
A TELEDYNE COMPANY
3401 Shiloh Road
Garland, Texas

3 April 1967

IDENTIFICATION

AFTAC Project No:	VELA T/5055
Project Title:	Operation of TFSO
ARPA Order No:	624
ARPA Program Code No:	5810
Name of Contractor:	Teledyne Industries Geotech Division Garland, Texas
Date of Contract:	12 April 1965
Amount of Contract:	$758,784.00
Contract Number:	AF 33(657)-14444
Contract Expiration Date:	31 December 1966
Program Manager:	B. B. Leichliter, BR1-2561

ABSTRACT

This is a report of the work accomplished on Project VT/5055 from 1 May 1965 through 31 December 1966. Project VT/5055 includes the operation, evaluation, and improvement of the Tonto Forest Seismological Observatory (TFSO) located near Payson, Arizona. It also includes special research and test functions carried out at TFSO. Research and development tasks performed by the Garland, Texas, staff using TFSO data are included.

CONTENTS

		Page
ABSTRACT		
1.	INTRODUCTION	1
1.1	Authority	1
1.2	History	1
1.3	Work of Project VT/5055	1
2.	OPERATION OF TFSO	3
2.1	General	3
2.1.1	Transfer of management	3
2.1.2	Inventory of equipment and real property	3
2.1.3	Security inspection	4
2.1.4	Vandalism	4
2.2	Seismograph arrays operated during Project VT/5055	4
2.2.1	Thirty-one element short-period array	4
2.2.2	Crossed-linear array	4
2.2.3	Extended array	6
2.2.4	Nineteen-element array	6
2.2.5	Revised numbering system for array seismometers	6
2.3	Standard seismograph operating parameters	6
2.4	Data channel assignment control	13
2.5	Transmission of data from remote sites	13
2.5.1	Application for radio licenses	13
2.5.2	Myrtle Point generator problem	13
2.5.3	LRSM generator problems	15
2.5.4	Telephone transmissions	15
2.5.5	VHF telemetry	15
2.5.6	Control of telemetry data input levels	15
2.5.7	Site clean-up	16
2.6	Astrodata digital data acquisition system	17
2.6.1	Operational problems	17
2.6.2	Special operational procedures	18
2.6.3	Modification of ASDAS	18
2.7	Equipment malfunctions	18
2.8	Calibration of test equipment	20
2.9	Shipment of data to SDL	20
2.10	Safety	22
3.	CHANGES AND ADDITIONS TO THE TFSO INSTRUMENTATION	22
3.1	Short-period vault retrofit	22
3.2	Installation of AEI lightning protection system	26
3.3	Develocorder modifications	27
3.4	Earth powered system	27

CONTENTS, Continued

		Page
3.5	Installation of an improved microbarograph	27
3.6	Modification of intermediate-band and broad-band seismographs	27
3.7	Improved crystal oscillator for Hyperion timing system	32
3.8	Addition of a 1000 watt power amplifier	32
3.9	Additional meteorological instrumentation	32
3.9.1	Recording thermometer	32
3.9.2	Anemometer	34
3.10	Long-period seismograph improvement	34
3.10.1	General system modification	34
3.10.2	Improved operating environment	39
3.11	Installation of new 35-millimeter film recorder	42
3.12	Magnetic-tape recorder heads	42
3.13	Low-gain, short-period seismograph	42
4.	EVALUATION OF STANDARD INSTRUMENTATION	43
4.1	Stability of frequency response	43
4.1.1	General	43
4.1.2	Short-period frequency responses at TFSO	43
4.1.2.1	Average monthly percentage change in the normalized response	43
4.1.3	Long-period frequency responses stability	45
4.1.3.1	Average monthly percentage change in the normalized long-period response	45
4.2	Calibrator motor constants	45
4.2.1	General	45
4.2.2	Routine determination of motor constants	47
4.2.3	Stability of seismograph motor constants	47
4.3	Lightning protection	50
4.3.1	Summary of electrical storms and instrument damage at TFSO	50
4.3.2	Tests of a prototype improved lightning protection system	52
4.4	Operational stability of seismograph magnification at TFSO	52
4.4.1	Stability of isolation amplifier	52
4.4.2	Stability of short-period seismograph	55
4.4.2.1	Average daily percentage magnification change of the primary system	55
4.5	Seismograph reliability	56
4.6	Timing systems	56
4.6.1	Primary timing	56
4.6.2	Secondary timing	57

CONTENTS, Continued

			Page
4.7	Power		57
	4.7.1	Commercial power	57
	4.7.2	Secondary power	57
5.	MAINTENANCE OF TFSO FACILITIES		57
5.1	Engineering laboratory		57
5.2	Air chiller unit		58
	5.2.1	Scale accumulation	58
	5.2.2	Miscellaneous malfunction	58
5.3	Furnace		
5.4	Condensation under the roof of the CRB		59
5.5	Interior of the CRB		60
6.	Routine analysis		60
6.1	Introduction		60
6.2	Analysis procedures		61
	6.2.1	Preliminary analysis	61
	6.2.2	Checking and finalization of preliminary analysis	61
	6.2.3	Daily reporting to the ESSA-G&GS	61
6.3	Publication of the VELA-Uniform earthquake bulletin		62
	6.3.1	Transmittal of raw data to SDL	62
	6.3.2	Final bulletin preparation	62
6.4	Routine analysis of noise data		62
7.	INSTRUMENT TESTS AND EVALUATION		64
7.1	Improvised high-frequency seismograph systems		64
	7.1.1	General	64
	7.1.2	Design and operation	64
	7.1.3	Distortion threshold	78
	7.1.4	Evaluation	84
	7.1.5	Recommendation for optimum system	85
7.2	Long-period system tests		85
	7.2.1	Tests of standard seismograph systems	85
	7.2.2	Tests of experimental seismograph	86
		7.2.2.1 Stability of natural period	86
		7.2.2.2 Response of the modified seismometer to vertical forces	86
		7.2.2.3 Determination of open-circuit damping of the modified seismometer	86
	7.2.3	Operational tests	96
		7.2.3.1 Heat cycling	96
		7.2.3.2 Conclusions	96

CONTENTS, Continued

		Page
7.3	Evaluation of the French seismograph system	101
7.4	Shallow hole tests	109
7.4.1	General	109
7.4.2	Description of test installation	110
7.4.3	Initial installation and operation	110
7.4.4	Parameter stability	112
7.4.5	Seismometer removal and reinstallation	112
7.4.6	Lightning damage	114
7.4.7	Cable leakage	117
7.4.8	General performance	117
7.4.9	Noise characteristics	117
7.4.10	Z102 System noise	127
7.4.11	Theoretical consideration of system noise	127
8.	DEVELOPMENTAL FUNCTION	132
8.1	Automatic calibration	132
8.2	Improved high-frequency seismograph system	133
9.	ASSISTANCE PROVIDED TO OTHER GROUPS	135
10.	RESEARCH INVESTIGATIONS	136
10.1	Signal classification study	136
10.2	Short-period array recommendation	137
10.2.1	General	137
10.2.2	Proposed arrays	137
10.2.2.1	Minor array	137
10.2.2.2	Major array	142
10.2.3	Instrumentation	142
10.2.3.1	Minor array	142
10.2.3.2	Major array	142
10.3	Long-period array recommendation	145
10.3.1	General	145
10.3.2	Assumed TFSO long-period noise	149
10.3.3	Observed characteristics of long-period signals at TFSO	154
10.3.4	Characteristics of the recommended array	155
10.3.4.1	Response of the outer ring	155
10.3.4.2	Response of the inner ring	158
10.3.5	Instrumentation and installation	158
10.3.6	Data recording equipment	158
10.4	Array coupling study	158
10.4.1	Introduction	158
10.4.2	Data selection and reduction	160

CONTENTS, Continued

		Page
	10.4.3 Statistical model	160
	10.4.4 Discussion	163
10.5	Signal amplitude study	165
10.6	Wind noise study	178
10.7	Evaluate various summation seismograph	178
10.8	Evaluation of the effectiveness of various bandpass filters	184
	10.8.1 Filtered summations seismographs	184
10.9	Magnitude studies	184
10.10	Long-period noise study	191
11.	REPORTS AND DOCUMENTS PUBLISHED UNDER PROJECT VT/5055	193
12.	REFERENCES	196

ILLUSTRATION

Figure		Page
1	Location of TFSO	2
2	Tonto Forest Seismological Observatory vault locations	5
3	Locations of TFSO and extended array sites	7
4	Normalized response characteristics of standard seismographs at TFSO	11
5	Normalized response characteristics of long-period seismographs at TFSO prior to Mar. 66. a. Response of three-component system May-August 1965 and vertical only August 1965-March 1966. b. Response of horizontals only August 1965-March 1966	12
6	Lister diesel generator after removal from Myrtle Point	14
7	Witte diesel generator and pier at Myrtle Point	14
8	The rebuilt generator building at Myrtle Point	17
9	Astrodata digital recording equipment	19
10	Modified vault cover	23
11	Vault after retrofit	24
12	AEI protectors installed in protector box	25
13	Modified protector box for Z1 showing typical AEI installation	26
14	Short-period seismogram showing usefulness of low-gain, earth-powered seismograph (BFV) for obtaining measurement of an extremely strong event (epicenter NW New Mexico, Δ about 4.0 degrees, azimuth 056 degrees)	28
15	Frequency response for the BFV (Earth-Powered Seismograph System) at TFSO	29
16	Frequency responses of the high-frequency and low-frequency microbarograph system	30
17	Block diagram of dual-output microbarograph system	31
18	Timing differences between the output of the Hyperion system and the WWV signal for the month of July. The vertical lines indicate the daily range of the time differences	33

ILLUSTRATIONS, Continued

Figure		Page
19	Photographs illustrating the installation of the recording thermometer at TFSO (a). Recording unit installed in the central recording building (b). Sensor mounting shield	35
20	TFSO long-period seismogram showing an anemogram (WI) produced by a 5-mile per hour wind from the east. (X10 enlargement of 16-millimeter film)	36
21	Long-period seismogram recorded at TFSO exhibiting the response of the dual output long-period system to a P wave during a period of normal background activity. (X10 enlargement of 16-millimeter film)	37
22	Frequency responses of the long-period system at TFSO performed in April 1966. The approximate parameters of the system were T_s = 20 sec, λ_s = 0.74, T_g = 110 sec, and λ_g = 0.83	38
23	Marine door installation in the TFSO long-period vault	40
24	Marine door installation in the TFSO long-period vault	41
25	Comparison of number of storm-caused outages at TFSO in 1964 (seismometers protected by fuses and carbon blocks) and 1966 (seismometers protected by AEI lightning protectors)	53
26	Simplified schematic diagram of the modified lightning protection system	54
27	Frequency responses and block diagrams for ZHF1 and ZHF2	65
28	Frequency responses and block diagrams for ZHF3 and ZHF4	67
29	Block diagram and estimated frequency response for the geophone seismograph (ΣGF)	68
30	P arrival from Chase IV as recorded by the standard (Z99) and high-frequency short-period seismographs at TFSO. Note signal partially masked by local blast. (X10 enlargement of 16-millimeter film)	69

ILLUSTRATIONS, Continued

Figure		Page
31	Normal background noise recorded by standard (Z99) and high-frequency short-period seismographs at TFSO. (X10 enlargement of 16-millimeter film)	70
32	Frequency responses for the high-frequency seismographs. (These responses are plotted for constant amplitude input and apply to the film recordings	71
33	Simplified circuit diagram and calculated frequency response for the filter amplifier for the ZHF5 high-frequency seismograph. The maximum gain of this channel is approximately 10 at 6 cps	72
34	Simplified circuit diagram and calculated frequency response for the filter amplifier for the ZHF6 high-frequency seismograph. The maximum gain of this channel is approximately 6 at 6 cps	73
35	Short-period recording exhibiting the response of the shallow-well seismometers, improvised high-frequency seismometers, and JMZ to a teleseismic event. (X10 enlargement of 16-millimeter film)	74
36	Short-period recording exhibiting the response of the shallow-well seismometers, the improvised high-frequency seismometers and JMZ to a teleseismic event from Borneo. Epicentral data: $\Delta = 121.8^{\circ}$, azimuth 297° 42 km, o = 18:05:54.4. (X10 enlargement of 16 millimeter film)	75
37	Short-period recording exhibiting the response of the shallow-well seismometers, the improvised high-frequency seismometer, and JMZ to a local event. (X10 enlargement of 16-millimeter film)	76
38	Distortion threshold curve for the ZHF seismograph at normal gain setting, and the ZHF6 seismograph for frequencies below 2.5 cps. This curve indicates the maximum input that the seismograph can amplify without distortion	79
39	Block diagram and oscillogram for test of ZHF5 components with a PTA output level of 10 volts p-p	80

ILLUSTRATIONS, Continued

Figure		Page
40	Block diagram and oscillogram for test of ZHF5 components with a PTA output level of 20 volts p-p	81
41	Block diagram and oscillogram for test of ZHF5 components with a PTA output level of 30 volts p-p	82
42	Output waveforms and approximate distortion curve for a short-period PTA	83
43	Typical background as displayed by long-period, broad-band, and intermediate band seismographs at TFSO, near beginning of reporting period. Note magnifications of horizontal components of long-period system. (X10 view of 16-millimeter film)	87
44	Typical background and weak surface waves as displayed by broad-band and long-period seismographs at TFSO at close of reporting period. (X10 view of 16-millimeter film)	88
45	Long-period experimental seismogram comparing Z57LP and Z54LP (housed in a surface tank vault) to Z51LP and Z44LP (located in a large walk-in concrete vault) during period of pressure change. WI register at about 10 mph. (X10 view of 16-millimeter film)	89
46	Long-period experimental recording comparing Z57LP and Z54LP (notched) (housed in a surface tank vault) to Z51LP and Z44LP (located in a large walk-in concrete vault) during period of little pressure change. (X10 view of 16-millimeter film)	90
47	Suspension system of the Geotech Model 8700C seismometer equipped with cross-ribbon flexures	91
48	Suspension system of the Geotech Model 8700C long-period horizontal seismometer equipped with a wire hinge system. Dashed lines indicate the lines that contain the wire flexures. Dotted lines indicate actual location of flexures	92
49	Mass position versus natural period for the Geotech Model 8700C seismometer equipped with wire flexures	93

ILLUSTRATIONS, Continued

Figure		Page
50	Typical natural period versus mass-position curve of the Geotech Model 8700C seismometer	94
51	Long-period seismogram recorded at TFSO showing spikes on N54LPX. Note absence of spikes on control instruments N46LP and E45LP. Signal at 01:21, from unknown epicenter, is comparable on all instruments. (Direct print from Helicorder record)	97
52	Long-period seismogram illustrating the similarity of the data recorded by the control seismographs (E45LP, N46LP, E52 LP, and N53LP) and the experimental seismographs (N57LPX and N54LPX). (X10 enlargement of 16-millimeter (film)	98
53	Seismogram illustrating close correlation of data produced by the Geotech Model 8700C seismometer (control seismometer No. 1) and the Geotech Model 8700C seismometer equipped with wire flextures (modified seismometer)	99
54	Seismogram illustrating differences in the character of the data produced by the control seismometers (E45LP, N46LP, E52LP and N53LP) and the modified seismometers (N57LPX and N54LPX) during period when convection currents were present in the vault. (X10 enlargement of 16-millimeter film)	100
55	Seismograms of a quarry blast from San Manuel Magma at a distance of 1.5 degrees recorded by the French seismograph and by standard seismographs at TFSO. The time bases of these seismograms are approximately equal. The lower seismogram is an X6 enlargement of 16-millimeter film	102
56	Seismogram of a teleseismic event from southern Peru recorded by the French seismograph and by standard seismographs at TFSO. The time bases of these seismograms are approximately equal. The lower seismogram is an X6 enlargement of 16-millimeter film. Epicentral data o = 13:53:57.1, $\Delta \cong 63.9^{o}$, h ≅ 62 km, azimuth = ≅ 136^{o}, magnitude 45	103

ILLUSTRATIONS, Continued

Figure		Page
57	Seismograms of a near regional event (epicenter unknown) recorded by the French seismograph and by standard seismographs at TFSO. The time bases of these seismograms are approximately equal. The lower seismogram is an X6 enlargement of 16-millimeter film	104
58	TFSO short-period seismogram showing a P arrival from eastern Arizona, $\Delta \simeq 1.0$ degrees. (X10 enlargement of 16-millimeter film)	105
59	TFSO short-period seismogram showing a P arrival from southern California, $\Delta \simeq 5.8$ degrees. (X10 enlargement of 16-millimeter film)	106
60	TFSO short-period seismogram showing a P arrival from the Leeward Islands, $\Delta \simeq 47.6$ degrees, azimuth = 98°, h = 89 km, o = 08:00:00.7, m$\simeq$ 5.4 (C&GS) (X10 enlargement of 16-millimeter film)	107
61	Frequency responses of the Z74, ZFX, ZHF5, and ZHF6 seismographs operated at TFSO	108
62	General configuration of test seismograph systems	111
63	Spread in magnification during test period 20171/23168-A (Z102SG)	115
64	Spread in magnification during test period HS-10-1/ARPA/RA-5 (Z103SH)	116
65	Short-period recording exhibiting the response of the shallow-well seismometers and JMZ to a local event. (X10 enlargement of 16-millimeter film)	118
66	Short-period recording exhibiting response of shallow-well seismometers and the JMZ to a near-regional event from northwest New Mexico $\Delta \cong 4.0$, azimuth $\cong 56°$. (X10 enlargement of 16-millimeter film)	119
67	Spectral relations of low level seismic background and system noise Z100 - CH 67 JM/4300 PTA	120
68	Spectral relations of low level seismic background and system noise Z103SH - CH 69 HS-10-1/ARPA/RA-5	121

ILLUSTRATIONS, Continued

Figure		Page
69	Noise pulses (arrows) on Z102SG during interval of low seismic background (magnification approximately 10,000K at 1 cps) (Analog conversion of digital-tape seismogram)	123
70	Spectral relations of low level seismic background and system noise - PTA at 12 dB, TFO Z74 - (Astrodata CH 19) JM/4300 PTA TFO, 8 Dec 66	124
71	Spectrum of seismic background during interval of low activity Z102 - (CH 74, File 1) JM/25220 TFO, 8 Dec 66	125
72	Spectral relations of low level seismic background and system noise - PTA at 0 dB, TFO Z74 - (Astrodata CH 19) JM/4300 PTA TFO, 8 Dec 66	126
73	Spectrum of seismic background during interval of low activity Z102 - (CH 74, File 2) JM/25220 TFO, 8 Dec 66	128
74	Z74 time series used for computing noise spectrum of system with dummy source (PTA at 12 dB, magnification = 32,000K at 1 cps) (analog conversion of digital-tape seismogram)	129
75	Z102 (JM/25220) time series of system noise with dummy source (magnification = 32,000K at 1 cps)(analog conversion of digital-tape seismogram)	130
76	Comparison of representative TFSO seismic background level with minimum thermal noise levels of the HS-10-1/ARPA and 20171-A seismographs (with noiseless amplifiers)	131
77	Block diagram of existing calibration equipment and the basic components of the automatic calibration system planned for TFSO	134
78	Proposed 19-element array at TFSO	138
79	k Plane response for equally weighted 19 seismometer hexagonal array with seismometer spacing d (from TI-1961)	139

ILLUSTRATIONS, Continued

Figure		Page
80	Comparison of the principle lobes of the present 31-element array and the proposed minor array	140
81	Comparison of S/N improvement for the summed output of the present 31-element array and the beam-steered output of the proposed 37-element array	141
82	Proposed 37-element array at TFSO	143
83	k Plane response for equally weighted 37 seismometer hexagonal array with seismometer spacing of 5 km (from TI-1961)	144
84	Composite $\vec{k}$ response for 30 beams of 37-element array	146
85	Composite $\vec{k}$ response for 30 beams of 37-element array	147
86	Composite $\vec{k}$ response for 30 beams of 37-element array	148
87	Power density spectra of long-period noise sample 3 for vertical, radial, and transverse components (1 cps bandwidth) of TFSO and extended array seismographs (from TI 1966a)	150
88	Relative power density spectral estimate of long-period noise for TFSO vertical component (not corrected for seismograph response)	151
89	Relative power density spectral estimate of long-period noise for TFSO vertical component (not corrected for seismograph response)	152
90	Relative power density spectral estimate of long-period noise for TFSO vertical component (not corrected for seismograph response)	153
91	Recommended configuration of TFSO long-period array	156
92	$\vec{k}$-space response for equally weighted seven-element hexagonal array with seismometer spacing of 23.3 kilometers (outer ring plus center element of recommended array) showing predominant microseismic noise wave-number bands	157

ILLUSTRATIONS, Continued

Figure		Page
93	$\vec{k}$-space response for equally weighted seven-element hexagonal array with seismometer spacing of 10.8 kilometers (inner ring plus center element of recommended array) showing predominant microseismic noise wave-number bands	159
94	Epicentral regions considered, as a function of distance and azimuth from TFSO	161
95	Estimates of seismometer effect ($\hat{\beta}_j$)	166
96	Estimates of region-seismometer interaction effect for Region 1 ($\hat{\gamma}_{1j}$)	167
97	Estimates of region-seismometer interaction effect for Region 2($\hat{\gamma}_{2j}$)	168
98	Estimates of region-seismometer interaction effect for Region 3 ($\hat{\gamma}_{3j}$)	169
99	Estimates of region-seismometer interaction effect for Region 4 ($\hat{\gamma}_{4j}$)	170
100	Estimates of region-seismometer interaction effect for Region 5 ($\hat{\gamma}_{5j}$)	171
101	Estimates of region-seismometer interaction effect for Region 6 ($\hat{\gamma}_{6j}$)	172
102	Estimates of region-seismometer interaction effect for Region 7 ($\hat{\gamma}_{7j}$)	173
103	Estimates of region-seismometer interaction effect for Region 8 ($\hat{\gamma}_{8j}$)	174
104	Estimates of region-seismometer interaction effect for Region 9 ($\hat{\gamma}_{9j}$)	175
105	Estimates of region-seismometer interaction effect for Region 10 ($\hat{\gamma}_{10j}$)	176
106	Tonto Forest Seismological Observatory vault locations	177

Figure		Page
107	Response of four quietest and four noisiest short-period vertical seismographs selected from 19 seismographs of the 31 element array	179
108	Short-period recording exhibiting response of experimental summation and ΣT to wind noise during wind with velocities of 25 mph.(X10 enlargement of 16 millimeter film)	180
109	Short-period experimental recording exhibiting response of experimental summations and ΣT to microseisms during interval when background level is unusually low. (X10 enlargement of 16 millimeter film)	182
110	Short-period experimental recording exhibiting response of experimental summations and ΣT to microseism during period of typical background level. (Note: Teleseismic signal from Solomon Islands Δ = 96.8°, azimuth = 267°, h = 68 km, o = 18:39:47.2, m = 5.4) (X10 enlargement of 16-millimeter film)	183
111	Frequency response of filtered summation systems TFSO	185
112	Short-period experimental seismogram exhibiting response of ΣTF and ΣTFK to a low-level teleseismic signal from the Aleutian Islands with period of 0.8 sec. Filter settings are:	186
		High cutoff / Low cutoff
	ΣTF	1.755 cps 12 dB/oct / 0.7 cps 24 dB/oct
	ΣTFK	3.0 cps 24 dB/oct / 0.8 cps 24 dB/oct
	Hypocentral data: Δ = 56.1°, azimuth = 315°, h = 33 km o = 02:39:50.0, m = 3.9 (X10 enlargement of 16 millimeter film	
113	Short-period experimental recording exhibiting response of ΣTF and ΣTFK to a low-level teleseismic event from unknown epicenter having period of 0.6 sec at the following filter settings:	187
		High cutoff / Low cutoff
	ΣTF	1.755 cps 12 dB/oct / 0.7 cps 24 dB/oct
	ΣTFK	3.0 cps 24 dB/oct / 0.8 cps 24 dB/oct
	(X10 enlargement of 16 millimeter film)	

ILLUSTRATIONS, Continued

Figure		Page
114	Short-period experimental seismogram exhibiting response of ΣTF and ΣTFK to a low-level teleseismic event having a period of 0.9 sec. Filter settings are: ΣTF: High cutoff 1.755 cps 12 dB/oct; Low cutoff 0.7 cps 24 dB/oct ΣTFK: High cutoff 3.0 cps 24 dB/oct; Low cutoff 0.8 cps 24 dB/oct Epicenter unknown. (X10 view of 16-millimeter film)	188
115	Short-period experimental recording showing the response of ΣTF and ΣTFK to a teleseismic signal having a period of 1.1 sec. Filter settings are: ΣTF: High cutoff 1.755 cps 12 dB/oct; Low cutoff 0.7 cps 24 dB/oct ΣTFK: High cutoff 3.0 cps 24 dB/oct; Low cutoff 1.0 cps 24 dB/oct Epicenter unknown. (X10 enlargement of 16-millimeter film)	189
116	Short-period recording of primary data exhibiting the effectiveness of an experimental summation (ΣTFK) in detecting low-level signal having a period of 0.8 sec. Filter settings are: ΣTF: High cutoff 1.755 cps 12 dB/oct; Low cutoff 0.7 cps 24 dB/oct ΣTFK: High cutoff 3.0 cps 24 dB/oct; Low cutoff 1.0 cps 24 dB/oct Epicenter unknown. (X10 enlargement of 16-millimeter film)	190
117	Estimated error ($\hat{\alpha}$) in Q_p (Δ, h) for those values of epicentral distance and hypocentral depth for which there were at least 10 observations	192
118	Long-period test array configuration	194

TABLES

Table		Page
1	Element number designators used at TFSO before and after 9 December 1966	8
2	Operating parameters and tolerances of standard seismographs at TFSO	10
3	Sample output of COMPFAIL	21
4	Average monthly percentage change from 1 July through 8 December 1966 in the normalized response of a representative group of short-period seismographs	44
5	Average monthly percentage change from 1 June through 31 December 1966 in the normalized response of the TFSO long-period system	46
6	TFSO 1966 annual motor constant check	48
7	Equipment at TFSO damaged on 10 July 1965	51
8	Average daily percentage change in the magnification of a selected group of short-period seismographs at TFSO	55
9	Earthquake data reported to the C&GS	6
10	High-frequency seismograph recording intervals	77
11	Response of Geotech Model 8700C seismometer (equipped with wire flexures) to the removal of test weights from the inertial mass	95
12	Nominal parameter values of test seismometer/amplifier combinations	113
13	Estimates of seismometer effect ($\hat{\beta}_j$) and region-seismometer interaction effect ($\hat{\gamma}_{ij}$)	164
14	Analysis of variance	165
15	Station magnitude corrections (S) for BMSO, CPSO, TFSO, UBSO, and WMSO	191

OPERATION OF THE TONTO FOREST SEISMOLOGICAL OBSERVATORY

1. INTRODUCTION

1.1 AUTHORITY

The research described in this report was supported by the Advanced Research Projects Agency, Nuclear Test Detection Office, and was monitored by the Air Force Technical Applications Center (AFTAC) under Contract AF 33(657)-14444, dated 12 April 1965.

1.2 HISTORY

The Tonto Forest Seismological Observatory (TFSO), located near Payson, Arizona, was originally constructed by the United States Corps of Engineers in 1963. TFSO was designed to record seismic events and to be used as a laboratory for testing, comparing, and evaluating advanced seismograph equipment and seismometric recording techniques. The instrumentation was assembled, installed, and operated until 30 April 1965 by United Electrodynamics (UED) (now Earth Sciences A Teledyne Company under Contract AF 33(657)-7747. In March 1964, the Long-Range Seismic Measurements (LRSM) Program provided eight mobile seismic recording vans to extend the existing instrument arrays at TFSO. On 1 May 1965, Geotech assumed the responsibility for operating TFSO. The LRSM mobile vans were phased out of the TFSO operation on 3 October 1965.

The location of TFSO is shown in figure 1.

1.3 WORK OF PROJECT VT/5055

During the 20-month period from 1 May 1965 through 31 December 1966, the work of Project VT/5055 was similar to the work performed at the Blue Mountains, Uinta Basin, and Wichita Mountains Seismological Observatories under Projects VT/1124, VT/4054, and VT/5054. When reasonable, operating procedural changes, observatory instrumentation improvements, and special research investigations were accomplished simultaneously at all observatories for greater operational efficiency. In other instances, improvements, modifications, and/or procedures that had been developed and proven at another observatory were incorporated into the TFSO configuration to improve the effectiveness of the observatory.

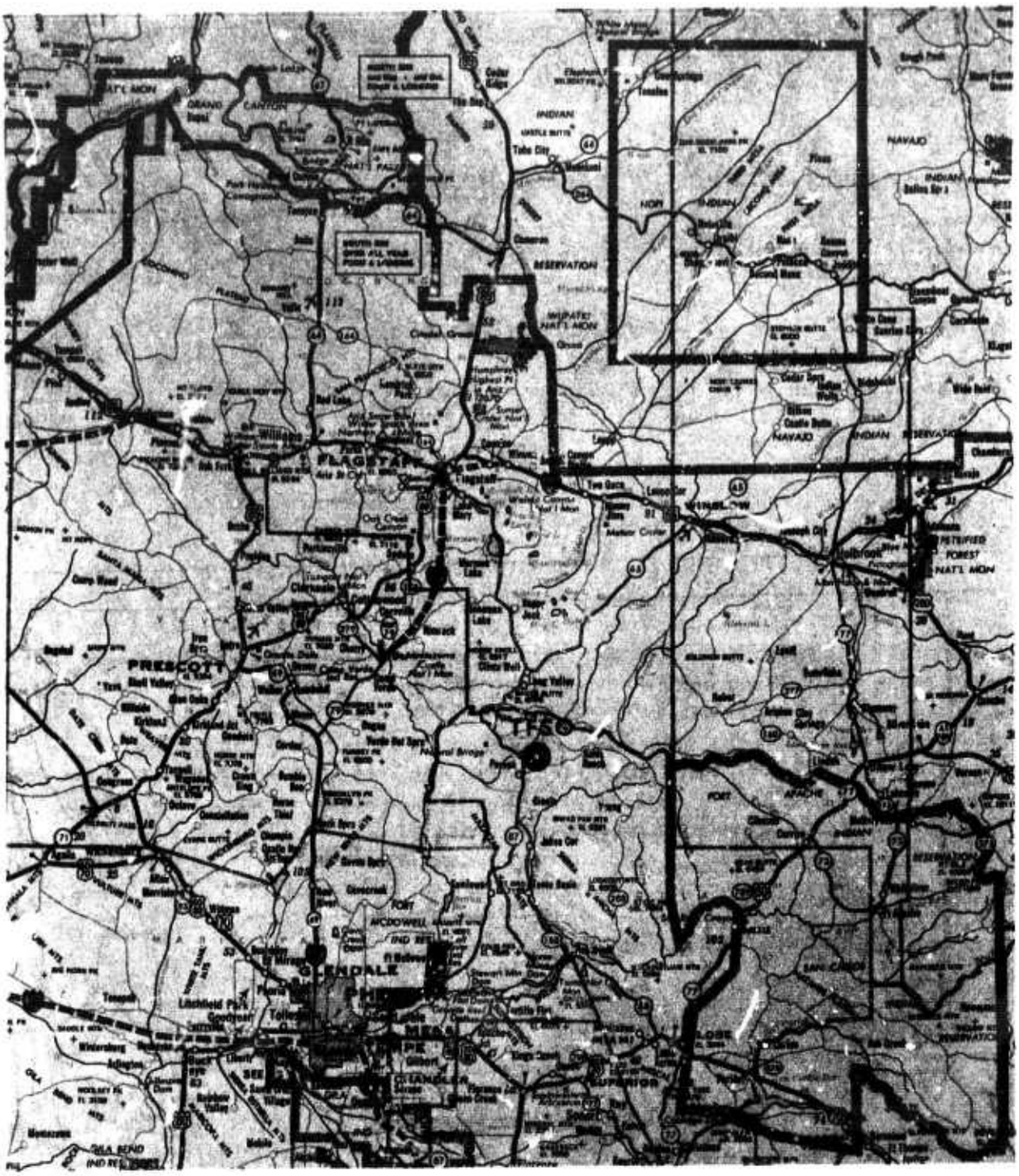

Figure 1. Location of TFSO

G 650

The work of the past 20 months can be subdivided into four categories:

a. Continued operation of TFSO;

b. Evaluation of standard and experimental detection equipment to provide a more effective observatory;

c. Design and/or development of new and improved instrumentation;

d. Routine and special analysis of resulting seismometric data.

The detailed work statement for Contract 14444 is included in this report as an appendix.

2. OPERATION OF TFSO

2.1 GENERAL

2.1.1 Transfer of Management

Four Geotech employees went to TFSO on 19 April 1965 to work with the UED personnel for the purpose of familiarizing themselves with the instrumentation and routine operating procedures in preparation for the transfer of the responsibility for operating the observatory. The UED personnel were quite helpful during the orientation period. A smooth transition of routine operations and change of personnel was completed by 1 May 1965. The AFTAC/VSC Project Officer visited TFSO in late April 1965 and reviewed the status of the TFSO operations with both UED and Geotech representatives. He also discussed the TFSO procedures and special studies that were underway or planned, with the Geotech personnel.

2.1.2 Inventory of Equipment and Real Property

Mr. W. O. Grimpe, Headquarters, Aeronautical Systems Division, Wright-Patterson Air Force Base, visited TFSO on 27 April 1965 to inspect facilities. The facilities inventory was checked on 28 April and the contract equipment inventory was signed on 30 April.

Mr. Thomas Muir, Real Property Clerk from Williams Air Force Base, was at TFSO on 22 July 1965 to make a real property inventory. All of the original TFSO real property inventory records were changed to show

subsequent improvements. While Mr. Muir was at TFSO, he also updated the original building drawings to show the modifications and additions that had been made to the facilities.

2.1.3 Security Inspection

Mr. D. P. Posage, Security Inspector from the Western Contract Management Region, San Diego Office, visited to inspect the facilities before issuing a SECRET facility clearance for TFSO. All was in order, including the standard practice procedures observed at the observatory,

Subsequently, routine security inspections of the observatory were made in April and August of 1966. During each of these visits, all items relating to station security were found to be in proper order.

2.1.4 Vandalism

Vandals shot into and damaged two sections of spiral-four cable on 21 August 1966. At this time, two junction boxes were shot and a cable road crossing sign was destroyed. This damage occurred at points in the array closest to a small area that was being developed for summer homes. This type of vandalism has been rare.

2.2 SEISMOGRAPH ARRAYS OPERATED DURING PROJECT VT/5055

2.2.1 Thirty-One Element Short-Period Array

The basic short-period seismograph system in use at TFSO during this reporting period was an array of 31 vertical Johnson-Matheson (JM) seismometers. The elements of this array are uniformly distributed at intervals of approximately 2000 feet, within an area of about 6 square miles.

The configuration of this array is shown in figure 2; the seismometer locations are designated in black as vaults 1 through 31.

2.2.2 Crossed-Linear Array

A crossed-linear array consisting of 21 short-period vertical elements and 24 short-period horizontal elements was operated until 9 December 1966, at which time the operation of all crossed-linear array elements except those consisting of three-component systems and the element common to both legs was discontinued. This array utilized selected elements of the 31-element array plus sites 60 through 74 as shown in figure 2. The approximate seismometer spacing of the vertical elements of the crossed-linear array was 1 kilometer. The twelve three-component sets were spaced at intervals of about 2 kilometers.

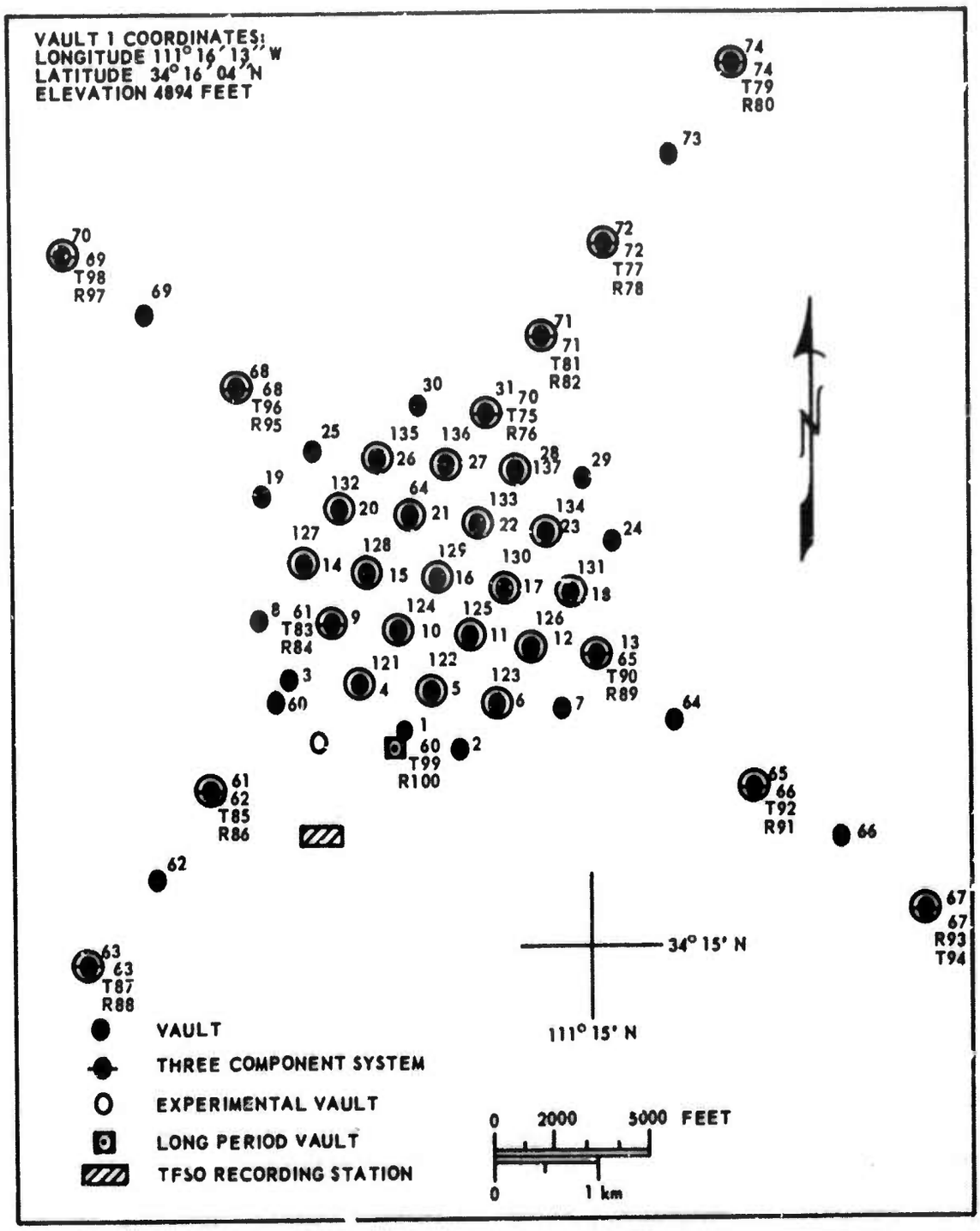

Figure 2. Tonto Forest Seismological Observatory vault locations

2.2.3 Extended Array

Eight mobile seismic recording vans provided extensions to the legs of the crossed-linear array between the beginning of Project VT/5055 and 3 October 1965. The locations of these sites are shown in figure 3. Data from the extended array were transmitted to the TFSO central recording building (CRB) via a telephone and VHF telemetry system.

2.2.4 Nineteen-Element Array

A temporary 19-element short-period array was formed from the original 31-element array on 9 December 1966, and the remaining seismographs from the 31-element array were deactivated. The designators of the elements of the 19-element array and the element locations are shown in red in figure 2.

2.2.5 Revised Numbering System for Array Seismometers

In anticipation of the expansion of the short-period array, new seismometer location number-designators were assigned on 9 December to all active and planned elements. A cross index of element number designators before and after this date is given in table 1.

2.3 STANDARD SEISMOGRAPH OPERATING PARAMETERS

The operating parameters and tolerances for the TFSO standard seismographs are shown in table 2. Frequency response calibrations are made routinely, and parameters are checked and reset to maintain the specified tolerances. Normalized response characteristics of all TFSO standard seismographs, as they were being operated at the close of the contract, are shown in figure 4. Responses of the long-period seismographs as operated earlier in the contract period are shown in figure 5.

In addition, two band-pass filtered summation seismographs are operated at the observatory. The filtered-summation seismograms are used as "flag" seismograms during the routine on-line analysis of data. One of the filtered seismographs (ΣTF) employs a UED filter with a pass band from 0.7 cps to 1.75 cps with slopes of 24 dB per octave.

The other filtered seismograph (ΣTFK) employs a Krohn-Hite filter operated with a pass band of 1.0 cps to 3.0 cps with skirt slopes of 24 dB per octave. The second of the filtered seismographs was activated on 15 February 1966 when it was added to Develocorder Data Trunk 1.

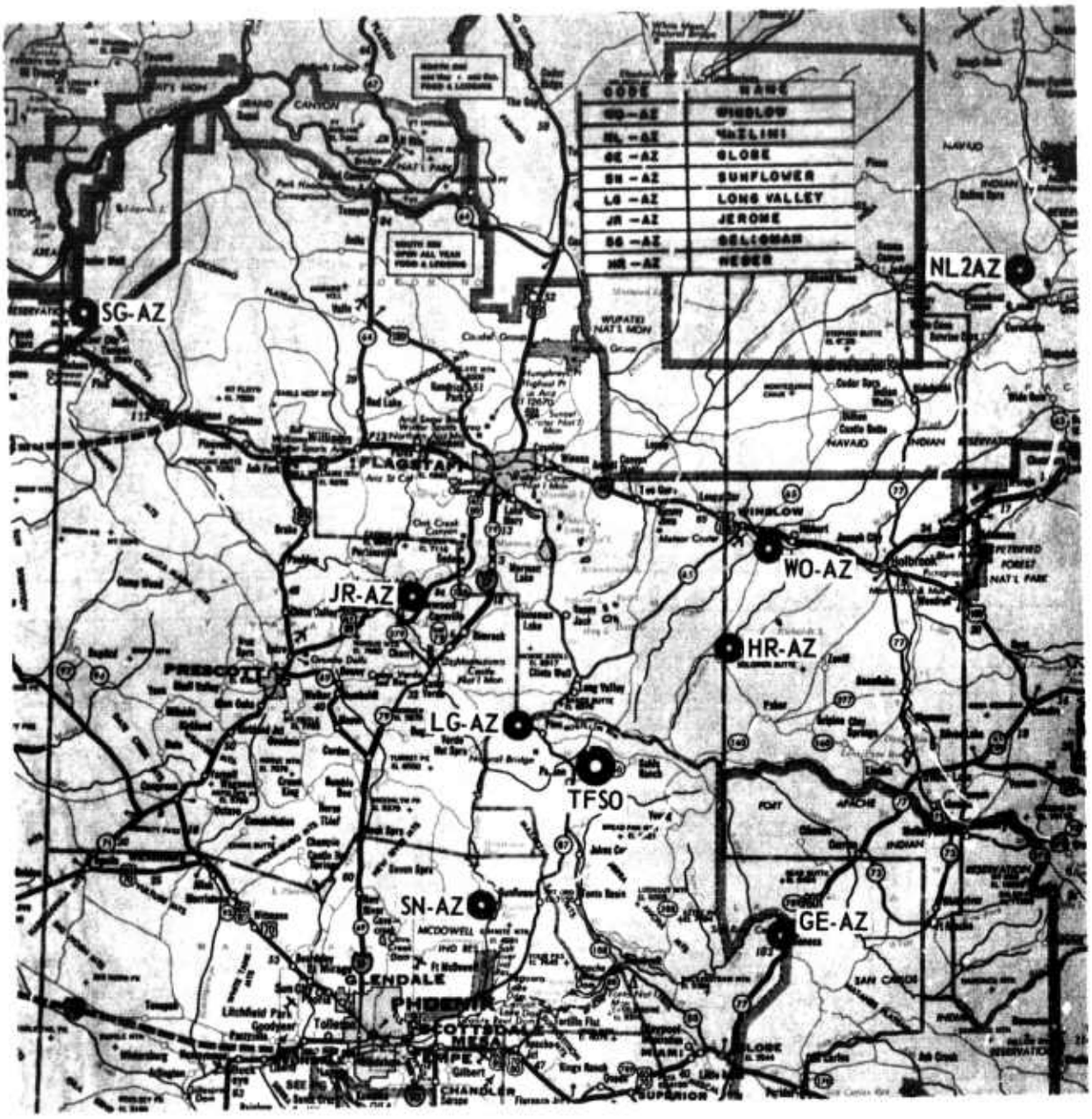

Figure 3. Locations of TFSO and extended array sites

G 2581

Table 1. Element number designators used at TFSO before and after 9 December 1966

New system	Old system	New system	Old system
Z 1	-	Z 74	Z 99
Z 2	-	T 75	T 75
	-	R 76	R 76
thru	-	T 77	T 77
	-	R 78	R 78
Z 37	-	T 79	T 79
Z 38 BB	Z 38 BB	R 80	R 80
E 39 BB	E 39 BB	T 81	T 81
N 40 BB	N 40 BB	R 82	R 82
Z 41 IB	Z 41 IB	T 83	T 83
E 42 IB	E 42 IB	R 84	R 84
N 43 IB	N 43 IB	T 85	T 85
Z 44 LP	Z 44 LP	R 86	R 86
E 45 LP	E 45 LP	T 87	T 87
N 46 LP	N 46 LP	R 88	R 88
Z 47 BF	Z 47 BF	R 89	R 89
E 48 BF	E 48 BF	T 90	T 90
N 49 BF	N 49 BF	R 91	R 91
Z 51 LP	Z 51 LP	T 92	T 92
E 52 LP	E 52 LP	R 93	R 93
N 53 LP	N 53 LP	T 94	T 94
Z 54 LPX	N 54 LPX	R 95	R 95
Z 57 LPX	N 57 LPX	T 96	T 96
Z 60	Z 1	R 97	R 97
Z 61	Z 9	T 98	T 98
Z 62	Z 61	E 99 SP	E 36 SP
Z 63	Z 63	N 100 SP	N 37 SP
Z 64	Z 21	1 A	1 A
Z 65	Z 13	1 B	1 B
Z 66	Z 65	1 C	1 C
Z 67	Z 67	1 D	1 D
Z 68	Z 68	1 E	1 E
Z 69	Z 70		
Z 70	Z 31		
Z 71	Z 71		
Z 72	Z 72		
Z 73	Z 74		

Table 1. (Continued)

New system	Old system
Z 121	Z 4
Z 122	Z 5
Z 123	Z 6
Z 124	Z 10
Z 125	Z 11
Z 126	Z 12
Z 127	Z 14
Z 128	Z 15
Z 129	Z 16
Z 130	Z 17
Z 131	Z 18
Z 132	Z 20
Z 133	Z 22
Z 134	Z 23
Z 135	Z 26
Z 136	Z 27
Z 137	Z 28
Σ B	Σ B
Σ C	Σ C
Σ T	Σ T
Σ TF	Σ TF
Σ TFK	Σ TFK

Σ B - Sum of R 76, R 84, R 89, R 95
Σ C - Sum of T 75, T 83, T 90, T 96
Σ T, Σ TF, Σ TFK - Sums of Z 121, 122, 123, 61, 124, 125, Z 126, 127, 128, 129, 130, 131, 132, 64, Z 133, 134, 135, 136, 137

Table 2. Operating parameters and tolerances of standard seismographs at TFSO

Seismograph				Operating parameters and tolerances				Filter settings		
System	Comp	Type	Model	Ts	λs	Tg	λg	δ^2	Bandpass at 3 dB cutoff (sec)	Cutoff rate at SP side (dB/oct)
SP	Z	Johnson-Mathesor	6480	1.25 ±2%	0.54 ±5%	0.33 ±5%	0.65 ±5%	0.0117	0.1 - 100	12
SP	H	Johnson-Mathes.n	7515	1.25 ±2%	0.54 ±5%	0.33 ±5%	(.65 ±5%	0.0117	0.1 - 100	12
SP	Z	Benioff	1051	1.0 ±2%	1.0 ±5%	0.2 ±5%	1.0 ±5%	0.0104	0.1 - 100	12
SP	H	Benioff	1101	1.0 ±2%	1.0 ±5%	0.2 ±5%	1.0 ±5%	0.0104	0.1 - 100	12
SP	Z	UA Benioff	1051	1.0 ±2%	1.0 ±5%	0.75	1.0 ±5%	0.0245		
SP	H	UA Benioff	1101	1.0 ±2%	1.0 ±5%	0.75	1.0 ±5%	0.0245		
SP	H	Wood-Anderson	TS 220	0.8	0.78					
IB	Z	Melton	10012	2.25 ±5%	0.65 ±5%	0.64 ±5%	1.2 ±5%	0.0006	0.05 - 100	18
IB	H	Lehner-Griffith	SH-216	2.25 ±5%	0.65 ±5%	0.64 ±5%	1.2 ±5%	0.0004	0.05 - 100	18
BB	Z	Press-Ewing	SV-232	12.0 ±5%	0.425 ±10%	0.64 ±5%	9.0 ±10%	0.00027	0.05 - 100	18
BB	H	Press-Ewing	SH-242	12.0 ±5%	0.425 ±10%	0.64 ±5%	9.0 ±10%	0.00027	0.05 - 100	18
LP[a]	Z	Geotech	7505A	20.0 ±5%	0.74 ±10%	110.0 ±10%	0.83 ±10%	0.66	25 - 1000	12
									20 - 200[c]	12
LP[a]	H	Geotech	8700C	20.0 ±5%	0.74 ±10%	110.0 ±10%	0.83 ±10%	0.66	25 - 1000	12
									20 - 200[c]	12
LP[b]	Z	Geotech	7505A	20.0 ±5%	0.74 ±10%	110.0 ±10%	0.83 ±10%	-	25 - 1000	12
LP[b]	H	Geotech	8700C	20.0 ±5%	0.620 ±10%	30.0 ±10%	0.591 ±10%	-	25 - 1000	12
									20 - 1000[c]	12

KEY

SP Short period
IB Intermediate band
BB Broad band
LP Long period
UA Unamplified (i.e., earth powered)

Ts Seismometer free period (sec)
Tg Galvanometer free period (sec)
λs Seismometer damping constant
λg Galvanometer damping constant
δ^2 Coupling coefficient

[a] Since March 1966
[b] Prior to March 1966
[c] With a 6-second notch filter

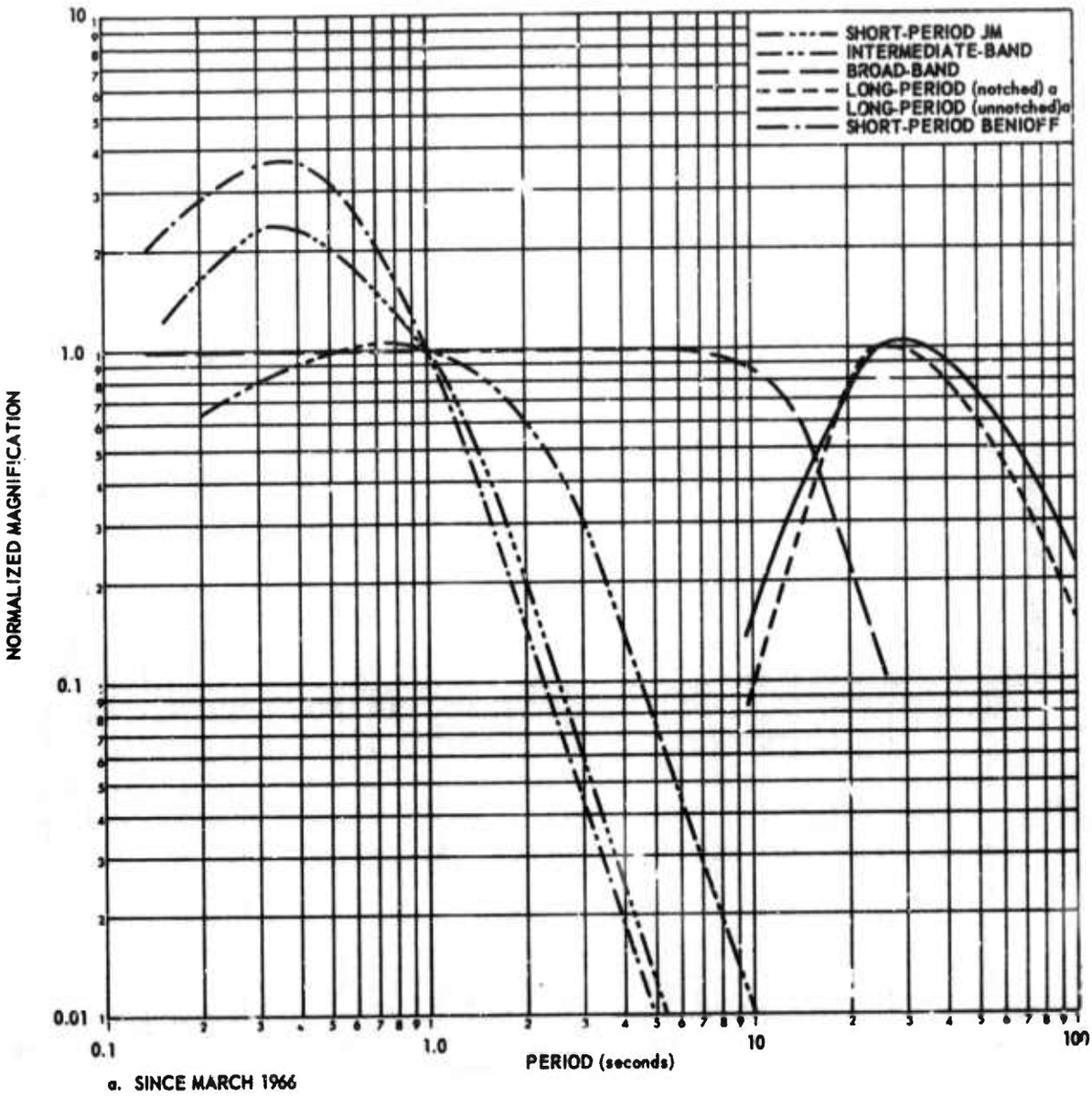

Figure 4. Normalized response characteristics of standard seismographs at TFSO G 1418

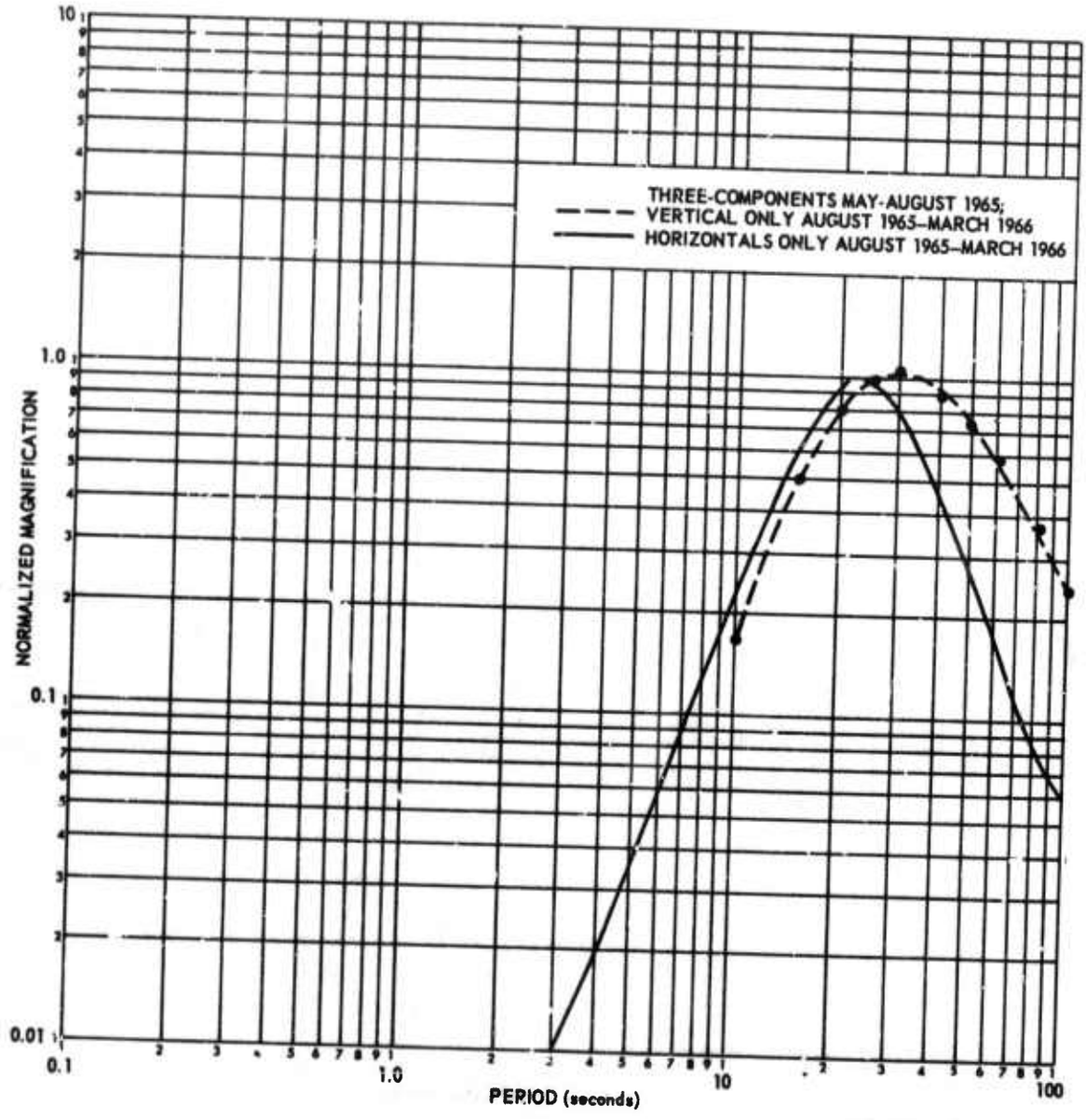

Figure 5. Normalized response characteristics of long-period seismographs at TFSO prior to March 1966

G 2582

2.4 DATA CHANNEL ASSIGNMENT CONTROL

Each data format recorded at TFSO was assigned a data group number. When the data assigned to a channel of any format was changed, a new data group number was assigned to the format. Data format change notices with the new channel assignments and data group numbers were submitted to the Project Officer and to frequent users of TFSO data when formats were changed.

2.5 TRANSMISSION OF DATA FROM REMOTE SITES

2.5.1 Application for Radio Licenses

Radio licenses required for transmittal of data from the sites of the LRSM extended array to the CRB were obtained by 1 May 1965. The close liaison maintained with the Federal Communications personnel by the Project Officer was most helpful in obtaining the licenses on schedule.

Telegraphic approval of our application for citizens band license was received on 22 June 1965 from the Federal Communications Commission.

We were authorized to operate a five-station citizens band radio network until 22 September on a temporary permit. On 28 June, a permanent license for this network was received; the call sign is KMV 4469.

2.5.2 Myrtle Point Generator Problem

The operation of the Lister generator (figure 6) which supplied power for the Myrtle Point relay station had not given satisfactory service prior to 1 May 1965. Because of malfunctions of the generator, UED had experienced frequent and prolonged outages. Servicing of the generator at Myrtle Point was frequently delayed because the area was generally inaccessible during the winter months. On 6 May 1965, during routine refueling of the generator, the generator was shut down, and preventative maintenance was performed. On 8 May, data transmission was lost because a power cable broke at the generator due to vibration. A new cable with standard conductors was installed the same day, and the data transmission was restored. The generator was operated continuously until 9 June 1965 when it again failed, apparently because of an oil leak. The engine consumed the 20-gallon oil reserve in a 3-week period and the bearings overheated, causing a rod to break. A 5 kW gasoline-powered generator was rented and placed in temporary service on 11 June.

A new 9 kW Witte diesel generator was ordered from Socorro, New Mexico, and installed on a concrete pier on 16 June (see figure 7). This new generator was operated throughout the term of the extended array program without trouble.

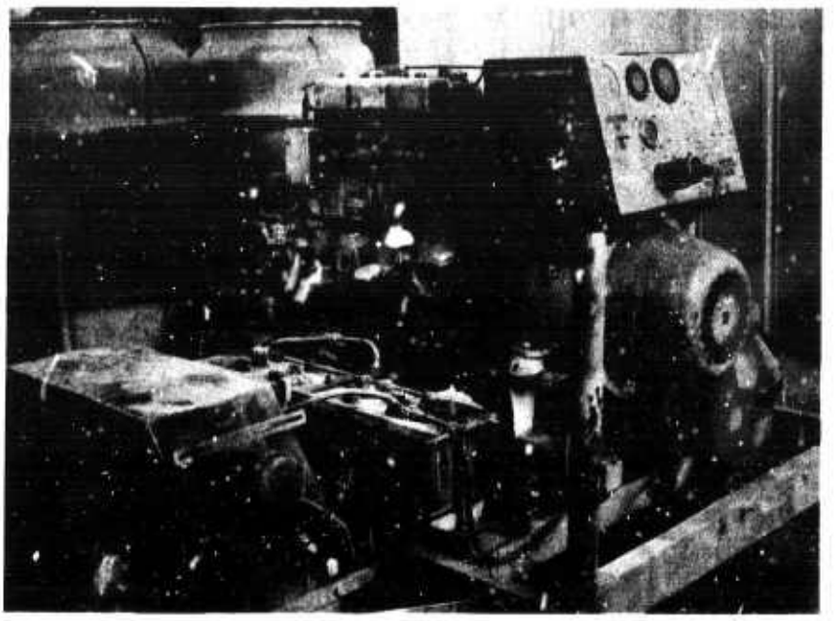

Figure 6. Lister diesel generator after removal from Myrtle Point

G 2582

Figure 7. Witte diesel generator and pier at Myrtle Point

G 2583

2.5.3 LRSM Generator Problems

The 1.5 kW generators used at the Globe and Heber, Arizona, extended array sites, to supply power for the two VHF links, developed problems during July 1965. Heat build-up in the generator buildings apparently activated the overheating cutoff switches. The problem was remedied by providing better ventilation for the generator housing buildings.

2.5.4 Telephone Transmissions

The LRSM van sites of the extended array, located at Long Valley, Arizona, (LG-AZ); Nazlini, Arizona, (NL2AZ); Seligman, Arizona, (SG-AZ); Jerome, Arizona (JR-AZ); Winslow, Arizona, (WO-AZ); and Sunflower, Arizona, (SN-AZ) employed four-wire telephone service for transmitting data to TFSO after mid-July 1965. Four-wire service was not available at the beginning of the extended array program; however, the quality of the transmitted data and the reliability of the original telephone data transmission system was so poor that Mountain States Telephone Company installed the necessary equipment for four-wire transmission beginning in early July 1965. The four-wire system resulted in an immediate improvement in signal-to-noise ratio.

On 4 October 1965, data transmission from the LRSM van sites was suspended, and on 13 December, at the request of the Project Officer, we notified Mountain States Telephone Company that the six telephone circuits would no longer be required.

2.5.5 VHF Telemetry

Data from the extended array sites at Heber, Arizona, and at Globe, Arizona, were transmitted using VHF radio equipment. Each of the sites transmitted their carriers to a repeater station located at Myrtle Point where the signals were retransmitted to TFSO. Transmission from these stations also was discontinued on 4 October 1965.

2.5.6 Control of Telemetry Data Input Levels

The input signal levels from the telemetry systems were too high to be recorded on Develocorder film and no attenuation controls were available in the circuits between the discriminators and the Develocorders. Attenuators were installed in these circuits during June 1965 to facilitate equalization of the discriminator outputs to the normal TFSO Develocorder input levels.

2.5.7 Site Clean-Up

Clean-up and restoration of the LRSM van sites of the extended array was accomplished between February and August 1966 under the supervision of Project VT/5055 personnel. The Winslow and Heber sites, including the microwave installation, were restored during February. The bulk of the restoration was completed during the summer months, however. During June and July, the telemetry equipment at the sites at Sunflower, Long Valley, Globe, and Nazlini was picked up and the sites were restored. Approximately 85 reels of spiral-four cable and the microwave equipment from the Globe station were recovered. Seligman, the last of the sites to be restored, was completed in August; 38 reels of spiral-four cable was recovered from this site. Funds for restoration of the extended array sites were furnished by the LRSM program.

We recommended that the Myrtle Point relay station site be maintained on a standby basis so that it was available for reuse if required in the future. Our recommendation was approved by the Project Officer, and in compliance with suggestions made by the U. S. Forest Service, the following site improvements were made beginning in late July:

a. About 0.2 mile of access road was graded and filled as required, and drainage ditches were constructed at each end;

b. The generator building which had been blown down by high winds was rebuilt and screened in;

c. The electrical wiring in the generator was installed in metal conduit to minimize the fire hazard in the event of a short circuit;

d. The area surrounding the site was cleaned.

Figure 8 shows the rebuilt generator house. The Myrtle Point site was inspected by Forest Service personnel, and the improvements were approved in August.

Figure 8. The rebuilt generator building at Myrtle Point G 1420

2.6 ASTRODATA DIGITAL DATA ACQUISITION SYSTEM

2.6.1 Operational Problems

Some problems were encountered with the discriminators in the Astrodata system in early May 1965. Modification of the discriminators by Astrodata, and air conditioning of the engineering laboratory at TFSO improved the operation of the system.

Digital data were lost from 1400Z on 11 September to 0000Z on 16 September 1965, because of a failure of the Astrodata system. High voltage from the power supply caused several components to fail. A total of 42 transistors and 38 diodes, in addition to capacitors and lamps, were damaged. The power supply was modified to prevent a recurrence of this type of failure in the future. A detailed report of this failure was submitted to the Project Officer.

In May of 1966, a system failure occurred in the Astrodata equipment. The cause of the failure is unknown. Thirty transistors and two diodes were replaced to correct the problem. After this work was completed a special test tape was prepared and sent to Garland for processing. The processed

results indicated that the system was functioning properly. Figure 9 shows the Astrodata digital recording equipment.

2.6.2 Special Operational Procedures

a. Massachusetts Institute of Technology - Between 1 May and 1 July 1965, a UED program of recording digital seismic data from the LRSM extended array and from TFSO for the Massachusetts Institute of Technology (MIT) was completed. This operation was started before 1 May.

b. Texas Instruments - Texas Instruments (TI) required digital data from TFSO for a special research program study. Originally, we planned to begin recording digital data for TI during July, 1965; however, digital recording was delayed while system modifications were completed. Modifications were required in the telemetry system between the LRSM extended array sites and the CRB. Also, modifications were made in the TFSO instrumentation parameters (see also 3.10.1).

Operational amplifiers were installed, the necessary circuit changes were completed, and recording of digital data for TI was started on 16 August 1965. All recordings were made with the low-magnification (normal) short-period recording format until 26 August when "high-magnification" recording of short-period data was started on a 24-hour basis. Two temporary employees were added to the TFSO staff to assist with the 24-hour operation of the equipment at the request of the Project Officer. Twenty-four hour recording of digital data with the Astrodata equipment was continued until 4 October 1965 when the operation of the extended array was terminated.

2.6.3 Modification of ASDAS

After recording of the digital data for MIT was completed in July 1965, the Project Officer requested that we check the feasibility of modifying the Astrodata system to provide a digital packing density on magnetic tape of 556 bpi. Modification of the system to decrease the packing density from the original 800 bpi configuration was required to provide digital data suitable for processing with the CDC 1604 computer at SDL. Modification of the Astrodata system was completed on 11 August; the change in packing density changed the recording time from approximately 96 minutes per reel to approximately 67 minutes per reel.

2.7 EQUIPMENT MALFUNCTIONS

Component failure information received from the observatories is coded in Garland and punched onto standard 80-column IBM cards. The computer program, Program MISERABLE, used to process these data from the other observatories was revised to be compatible with our CDC 3100 computer

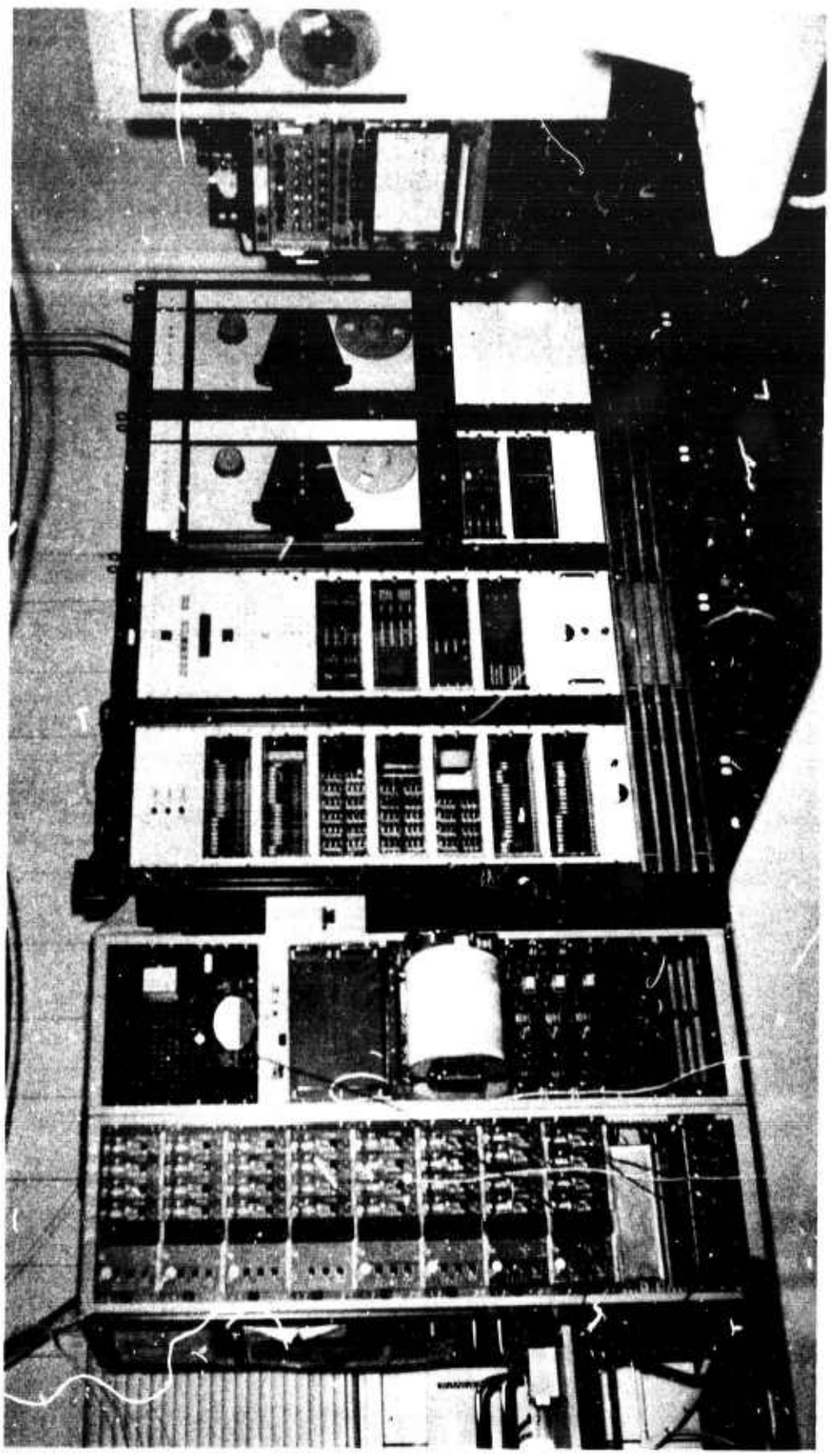

Figure 9. Astrodata digital recording equipment G 110

and was renamed Program COMPFAIL. Presorting of the cards by observatory, general function, and subassembly pertaining to a general function is required before the data can be processed. If, when more data are accumulated, it is necessary, we will write a program for computer sorting so that data stored on magnetic tape can be automatically updated at periodic intervals. The program accommodates up to 10 different types of subassemblies and 25 different components for each subassembly. The output data are similar to those shown in table 3 which gives a summary of the equipment malfunctions experienced at TFSO from 1 August 1965 to 1 January 1967.

The output of COMPFAIL for data from 1 August 1965 to 1 January 1967 shows that various components in 4300 FTA's failed 83 times for a total outage time of 262.1 hours, the highest failure rate in the study; several components failed only once.

2.8 CALIBRATION OF TEST EQUIPMENT

In October 1965, three of the observatory test instruments were sent to Metercraft Inc. of Phoenix, Arizona, for routine calibration. In an effort to establish a more efficient and satisfactory procedure for accomplishing the routine calibration of test equipment, Mr. Dewey Jones of our Quality Assurance Department visited TFSO in April 1966, to assist and train station personnel in the repair and calibration of all test equipment. At this time, a routine calibration schedule was established for the observatory, and the responsibility for routine calibration of test equipment was assigned to the station operations engineer. Routine calibration of test equipment, as specified by the Government, was subsequently accomplished at the observatory.

2.9 SHIPMENT OF DATA TO SDL

The magnetic-tape seismograms are shipped from TFSO each week. Three of the magnetic-tape units are used to record data for the AFTAC/VELA Seismological Center (VSC); these data are sent to our Garland laboratory. The other three units are used to record data for universities; these data are shipped directly to the universities from the observatory. When any or all of the recorders normally assigned to the universities are not required, the observatory notifies VSC and the Project Officer frequently assigns an alternate recording format. The VSC data are shipped routinely to SDL from Garland about 15 days after the end of the month in which they were recorded.

Table 3. Sample output of COMPFAIL

Specific function	Model No.	Sub assembly	Total failures	Repair time	Time inop.	Prevent.	Catas.	Component	No.
TR	(7460)	TSP	45	11.5	33.3	25	20		
								Bearing	10
								Belt	10
								DS102A1	2
								DS102A2	2
								DS102	6
								Roller	5
								CR103	1
								CR102	1
								CR101	1
								L105	1
								R141	1
								CR104	1
								DS101	4
		OSC	20	4.7	10.7	0	20		
								DS1	10
								DS101	2
								Q2	3
								Q1	4
								Q4	1
		DISC	16	7.0	11.5	0	16		
								DS1	3
								Q3	3
								Q2	3
								Q1	2
								Q503	1
								Q504	1
								Q305	1
								Q306	1
								DS	1
		AMP	5	1.5	15.0	0	5		
								V101	2
								V103	2
								V102	1
		PS	47	14.7	40.3	22	25		
								V2	1
								F101	2
								Q11	1
								Q9	1
								Q7	1
								F103	1
								Q17	1

Sixteen-millimeter film seismograms from 10 Develocorders are routinely shipped to data users about 45 days after the end of the month in which they were recorded. Original operation and calibration logs for the 16-millimeter film and magnetic tape seismograms accompany the shipment; copies of the logs are retained at TFSO as back-up. Thermofax copies of selected data are routinely sent to our Garland support group, and copies are sent to other interested parties as requested and/or approved by the Project Officer.

Routine shipments of 16-millimeter film seismograms recorded through October 1966 and shipment of magnetic-tape seismograms recorded through 30 November 1966 were made to SDL before the end of the reporting period.

2.10 SAFETY

To assure maximum cognizance of routine safety procedures and available safety aids, TFSO personnel are assigned responsibility, on a rotational basis, for the monitoring and administration of routine safety procedures established for the observatory. It is the duty of the responsible person to check and brief other observatory personnel regarding the availability and location of safety aids (for example, first-aid and snake-bite kits, the 24 observatory fire extinguishers, and 2 outside fire hydrants and hoses), discuss the importance of safety procedures, and to publish a safety memorandum each month.

3. CHANGES AND ADDITIONS TO THE TFSO INSTRUMENTATION

3.1 SHORT-PERIOD VAULT RETROFIT

In May 1965, we found several features of the short-period seismometer operating environments to be unsatisfactory for optimum seismograph operation. Following is a summary of the major faults found:

a. The vault lids were made of a circular piece of 6.4-millimeter steel which was anchored to the vault by only four anchor bolts. These lids did not adequately seal the vaults against water and wind.

b. A soft putty-like gasket material which was water absorbent was used to seal the vaults; this did not provide an adequate "permanent seal."

c. The cable inlet-tee threads were not sealed, and the sealant with which the cable inlet was filled was water absorbent.

d. About 25 percent of the short-period vaults had water standing in them; the depth of the water ranged from 1/2 to 19 inches.

A program of retrofitting the short-period vaults and checking the seismometers was started in June and completed by 20 July 1965. The major items of the retrofit were:

a. The vault lids were notched to accommodate eight additional anchor bolts, and reinforcing strips were welded to the lids (see figure 10).

b. Eight additional anchor bolts were welded to the outside of each vault.

c. The cable inlet-tee was replaced and sealed, and the cable inlet was sealed with Chico A5 cement.

d. A permanent type gasket was installed between the lid and the tank.

e. In all instances in which the level of the water had been above the seismometer case seal, the seismometer was replaced, and the seismometer removed from the vault was thoroughly cleaned and checked to assure that it was operating properly before it was installed in another vault.

Figure 10. Modified vault cover

G 2585

Two of the short-period horizontal vaults were reopened about 3 weeks after the vault retrofit program had been completed. The "high-water mark" in the pits surrounding the vaults was above the vault lids. The removal of the lids showed that the insides of the vaults were dry and no evidence of water leakage was present. Figure 11 shows a typical interior and exterior of a retrofitted vault.

After completion of the retrofit program, the vaults housing the short-period horizontal instruments were reopened so that final weight-lifts and motor-constant (G) checks could be made. All calibrator motor constants were standardized to a value with ±2 percent of 0.296 newton per ampere to facilitate calibration of all short-period seismographs with a constant value of calibration current. While the vaults were open, the horizontal seismometers oriented southeast-northwest were reoriented 180 degrees because these seismometers had been originally installed in an unconventional manner. As originally installed, weight lifts and dc pulses produced seismograph outputs of polarity opposite to that conventionally produced. Consequently, interpretation of seismograph polarities from weight lift data was confusing. All short-period horizontal seismometer orientations were checked and set to 127.5 degrees and 217.5 degrees, where necessary. Effective 1 October 1965, the designators for the horizontal seismographs of the linear array were changed from "SE" to "R" (radial) and from "NE" to "T" (transverse). No seismograph number designations were changed at this time. Motor constant calibrations and seismometer orientation checks of the horizontal instruments were completed on 8 October 1965.

Figure 11. Vault after retrofit G 2586

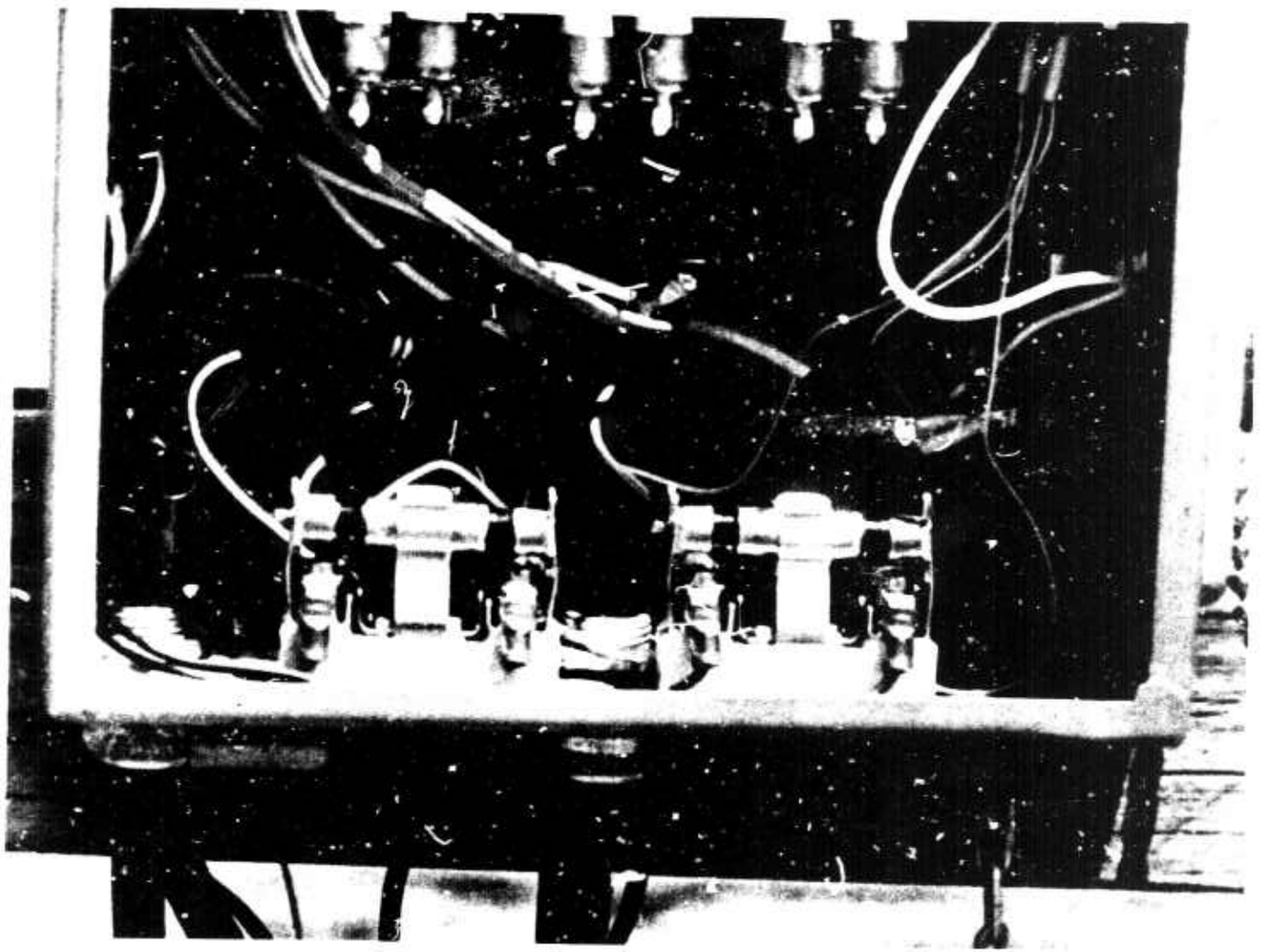

Figure 12. AEI protectors installed in protector box

G 2587

3.2 INSTAI LATION OF AEI LIGHTNING PROTECTION SYSTEM

After reviewing the lightning protection system at TFSO, and based on the performance of the gas-triode protection system successfully tested at the Wichita Mountains Seismological Observatory, we recommended that the TFSO lightning protection system be updated. Our recommendation was approved by the Project Officer, and the carbon blocks of the existing system were replaced with Associated Electronics Industries, Limited (AEI), Type 16A lightning protectors (figure 12). The AEI protectors are gas-filled triode protectors widely used in the protection of telephone and power circuits in Great Britain.

Modification of the lightning protection portions of the data circuits, calibration circuits, and field telephone circuits was completed by November 1965. Figure 13 shows a typical installation of the AEI protectors.

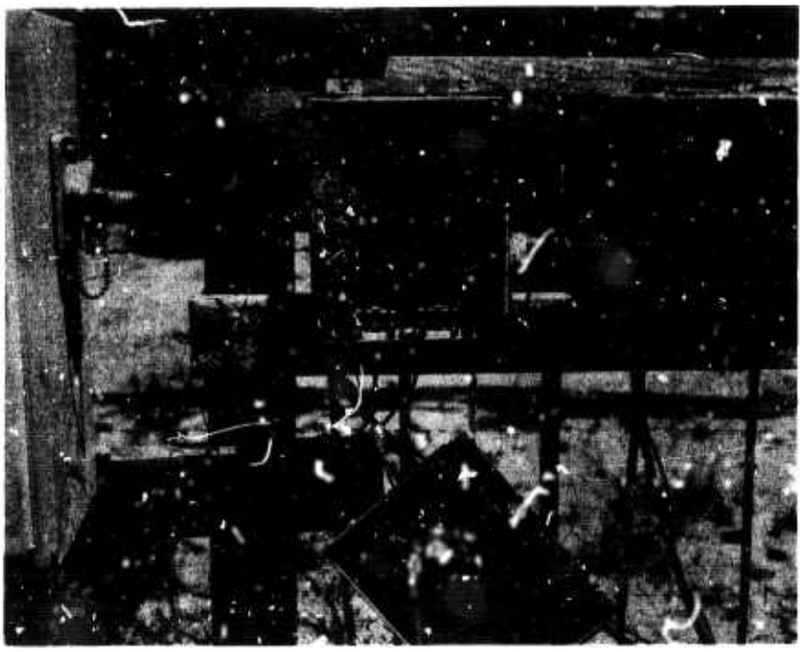

Figure 13 Modified protector box for Z1 showing typical AEI installation G 2588

3.3 DEVELOCORDER MODIFICATIONS

Peristaltic pumps were installed in the nine "on-line" Develoccrders by the end of August 1965. These pumps are, in general, more reliable than the reciprocating pumps used previously and provide better processing quality because an even rate of chemical flow is maintained to the processor.

Model 16041 processing kits which utilize fixed fluid applicators alsc were installed in the Develocorders. In addition to improving film quality by essentially eliminating the occurrence of film scratching, the time and effort required for cleaning and maintenance of the processing units was reduced.

3.4 EARTH POWERED SYSTEM

A low-gain (4.5K at 1.0 cps), short-period, vertical seismogram was added to Develocorder Data Group 7177. This seismogram has been of aid in the analysis of signal arrivals from large events. Figure 14 shows a signal arrival from a large event. Figure 15 shows the response and block diagram of this seismograph system.

3.5 INSTALLATION OF AN IMPROVED MICROBAROGRAPH

The Naval Electronics Laboratories (NEL) T-21-B Microbarograph was replaced by a dual-output infrasonic microbarograph system, the design of which is based on the system developed by the National Bureau of Standards. This new microbarograph has greater temperature stability than the NEL microbarograph and is identical to the microbarograph operated at the other observatories. Frequency response curves for the long- and short-period outputs of the new system are shown in figure 16. Figure 17 is a block diagram of the system.

3.6 MODIFICATION OF INTERMEDIATE-BAND AND BROAD-BAND SEISMOGRAPHS

During the early months of Project VT/5055, the stability of the intermediate-band and broad-band seismographs was poor. During March 1966, the Model 5240 phototube amplifiers (PTA's) with Lehner-Griffith Model GS-250 galvanometers used in these systems were replaced by Model 4300 PTA's with Model 4100-112 galvanometers. This change resulted in a significant improvement in the frequency response and magnification stability of these systems.

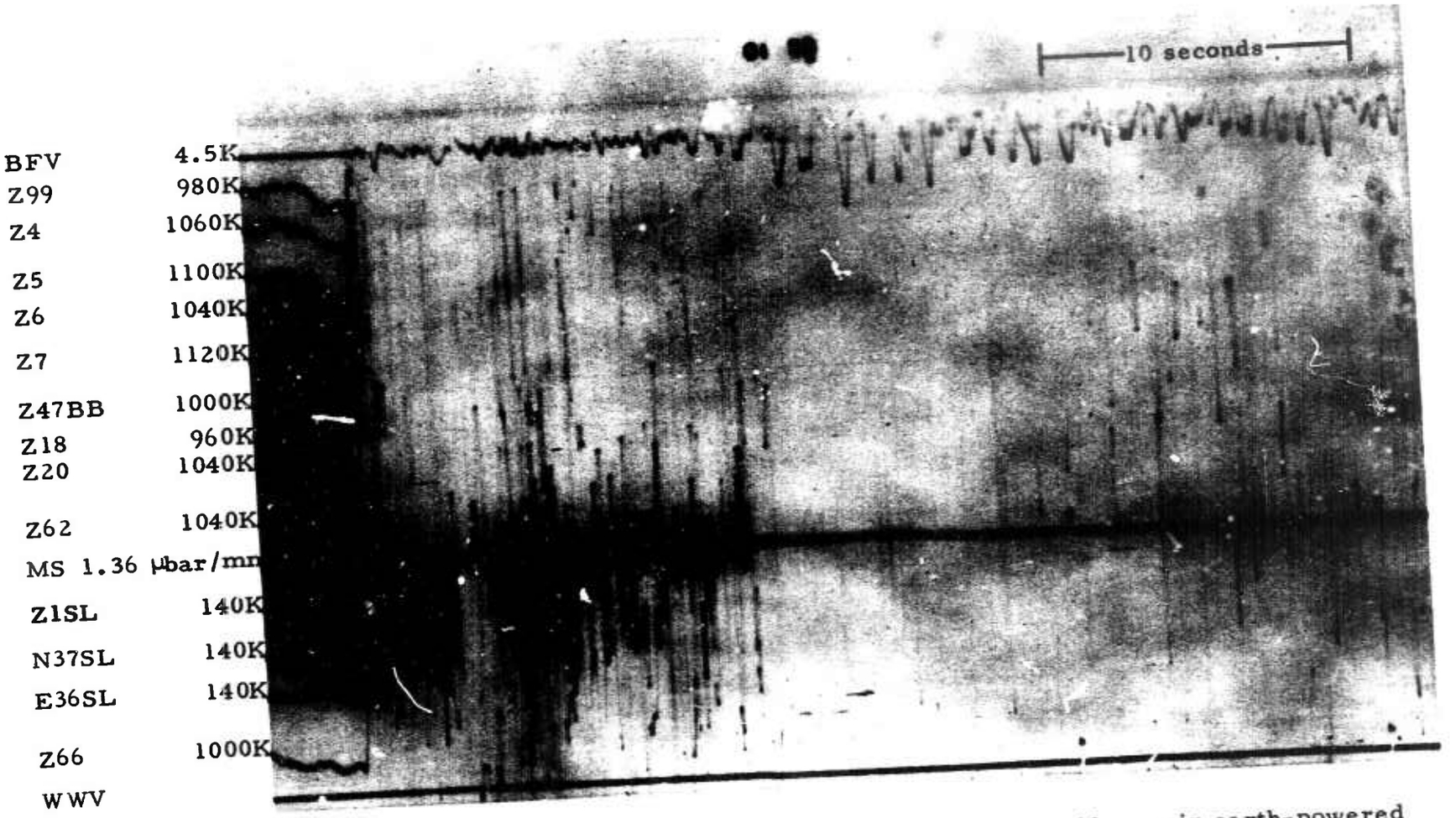

Figure 14. Short-period seismogram showing usefulness of low-gain earth-powered seismograph (BFV) for obtaining measurement of an extremely strong event (Epicenter NW New Mexico, Δ about 4.0 degrees, azimuth 056 degrees).

TFSO
Run 023
23 Jan 1966
Data Group 7177

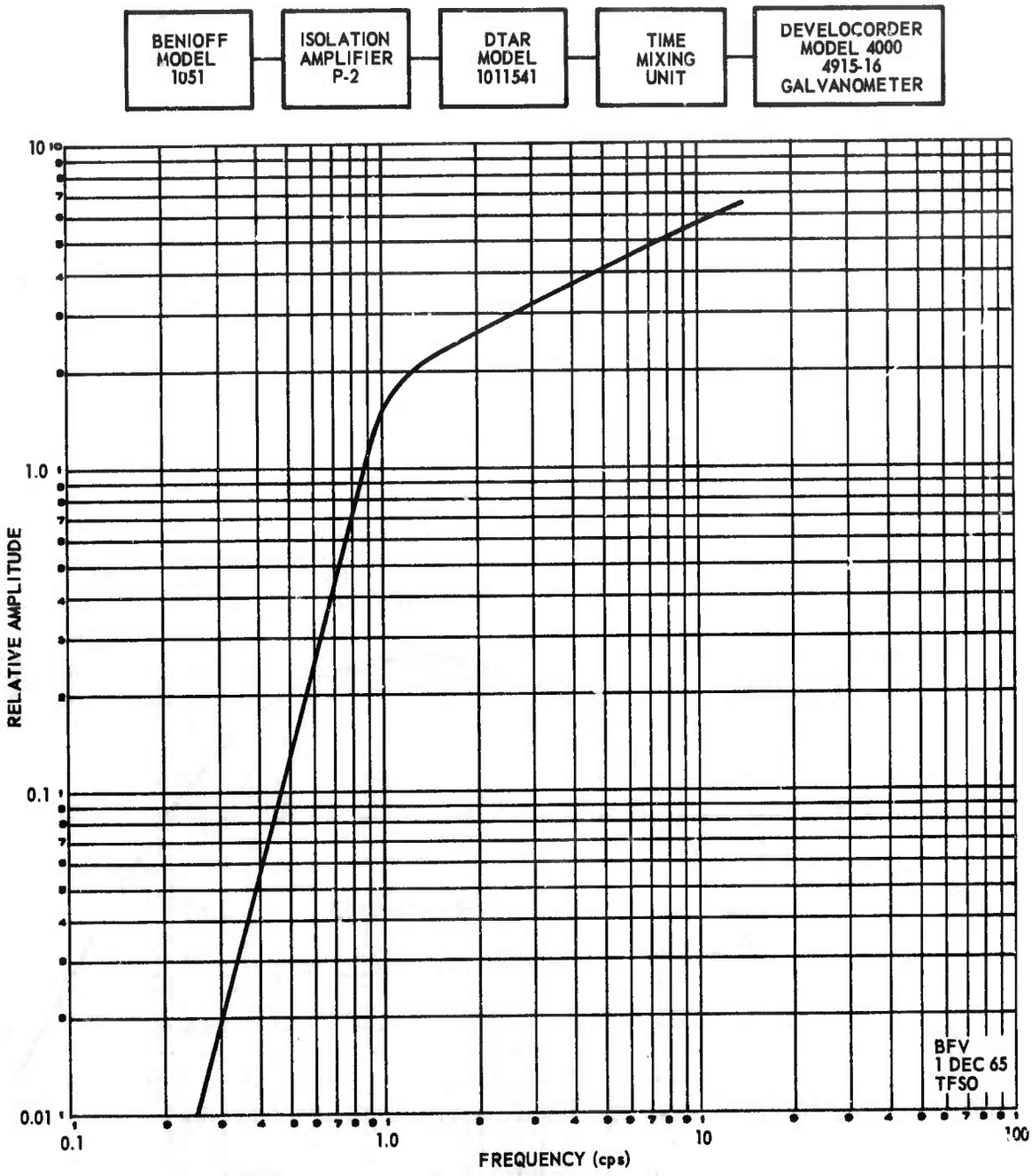

Figure 15. Frequency response for the BFV (Earth-Powered Seismograph System) at TFSO

G 651

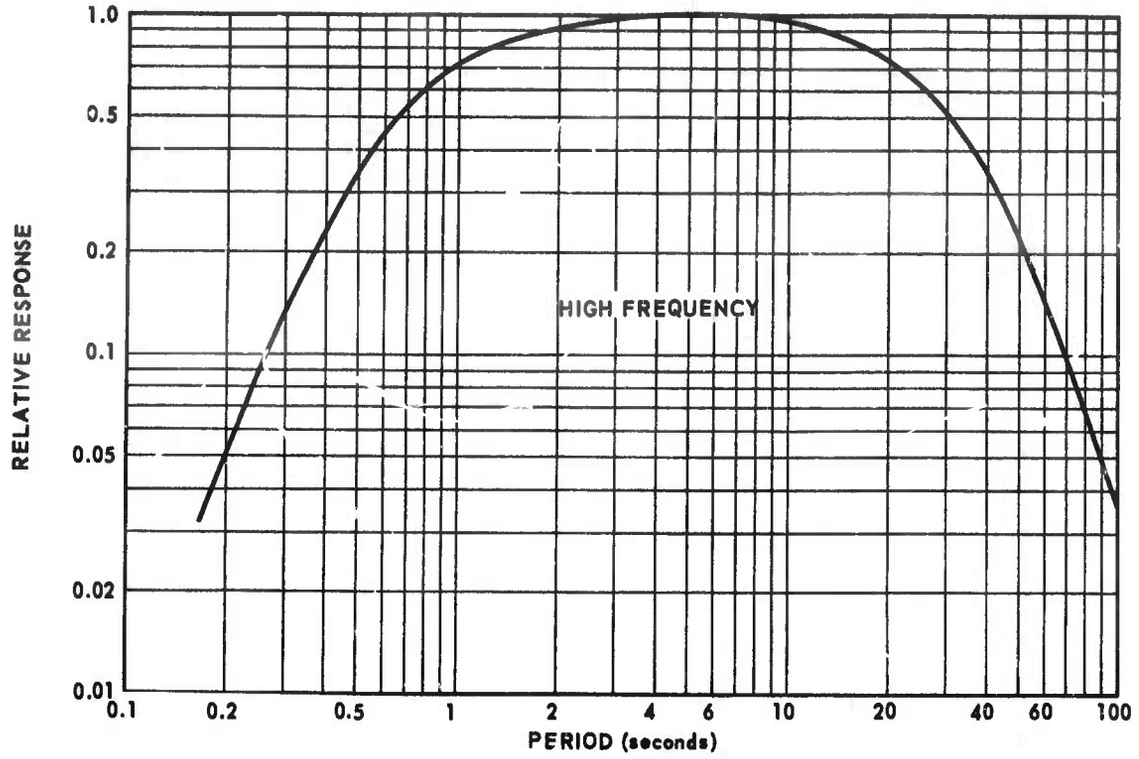

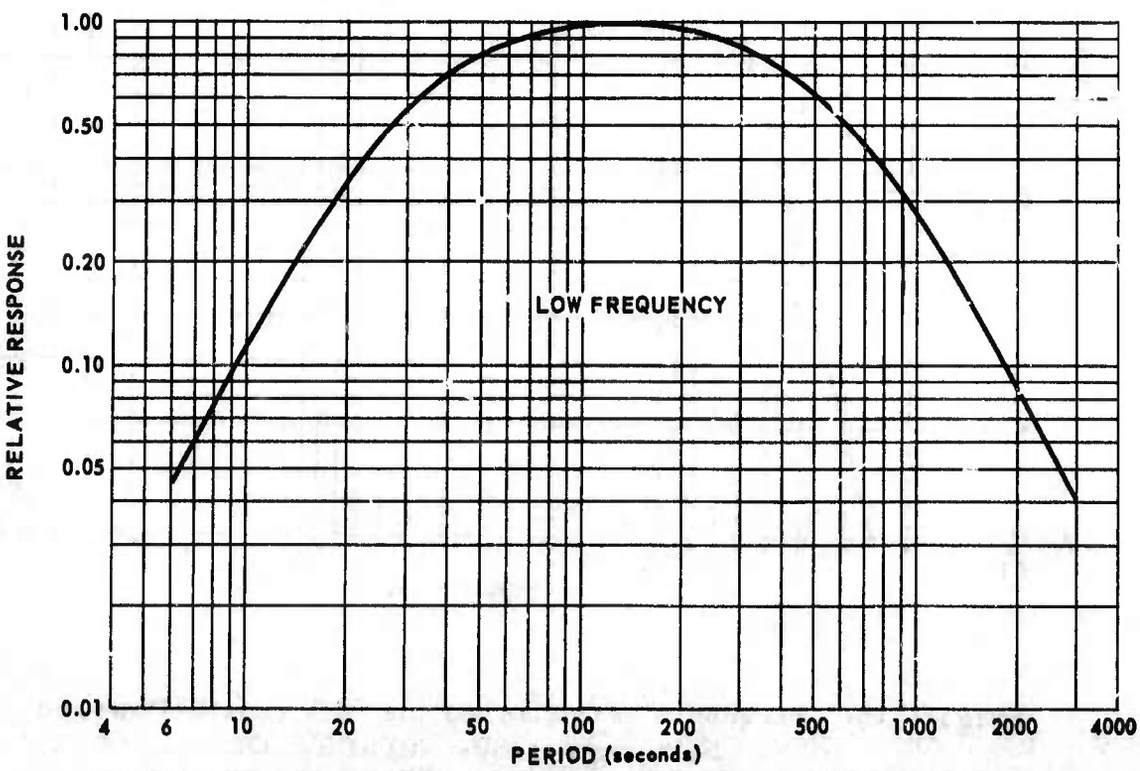

Figure 16. Frequency responses of the high-frequency and low-frequency microbarograph system G 675

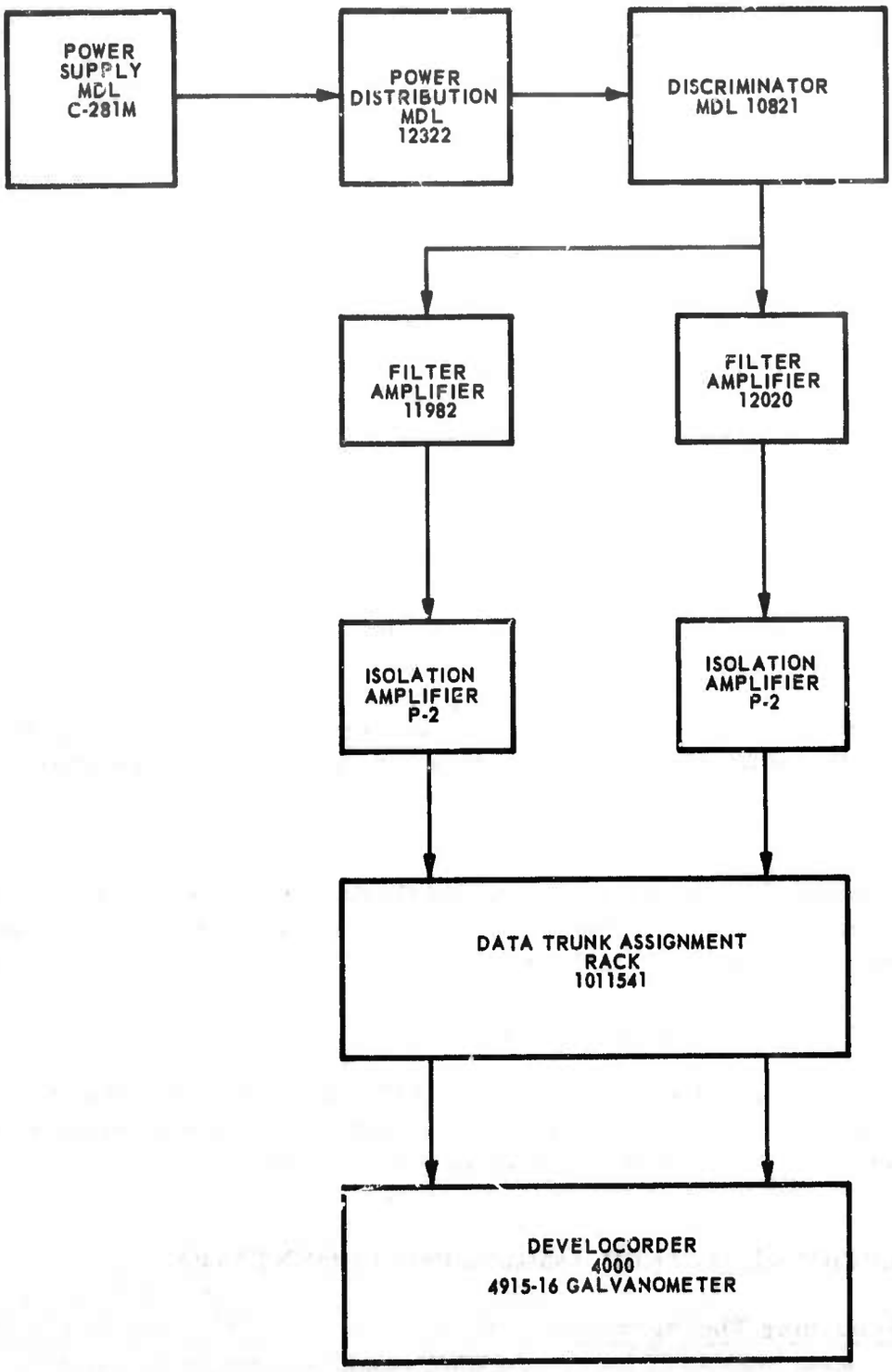

Figure 17. Block diagram of dual-output microbarograph system

G 652

3.7 IMPROVED CRYSTAL OSCILLATOR FOR HYPERION TIMING SYSTEM

In November 1965, a study was initiated to determine a suitable replacement for the crystal oscillator in the Hyperion timing system. We learned that a direct replacement for this oscillator which had five times the frequency stability of the existing unit was available. An improved crystal oscillator was ordered from Hyperion Industries.

The new crystal oscillator for the Hyperion timing system was received and installed during June 1966. During the first three weeks of operation with the improved oscillator, the time error did not exceed 12 milliseconds, and no adjustments were made. Several adjustments were made during the latter part of July 1966; however, these adjustments were required because of work on the power and timing circuits, not because of oscillator drift. Daily drift variations of the timing system during July 1966 are shown in figure 18.

3.8 ADDITION OF A 1000 WATT POWER AMPLIFIER

A Model 22183 power amplifier with a power capability of 1000 watts and a Model 26212 power control unit were received at TFSO in July 1966. Initially, problems were encountered because of asymmetry of the waveform of the precision 60 cps signal furnished to the power amplifier from the Model 5400A timing system, and because of noise spikes on the signal from the Hyperion timing system. These problems were overcome by modification of the circuits in the power control unit. However, we found that the overload circuits were causing the power amplifier to shut down when certain of the loads were switched.

The power amplifier was returned to the Garland laboratory for tests and modification in November 1966. Current plans call for the installation of a self-contained oscillator which can be synchronized from either the primary or secondary timing system and replacement of any malfunctioning components in the overload circuits.

The power amplifier will be returned to TFSO to replace ten 100-watt Bogan amplifiers presently supplying frequency regulated power for the observatory instrumentation when these modifications are complete.

3.9 ADDITIONAL METEROLOGICAL INSTRUMENTATION

3.9.1 Recording Thermometer

A recording thermometer with a remote sensor was installed on 10 June 1966. The sensor was installed outside of the CRB on a special mounting which was

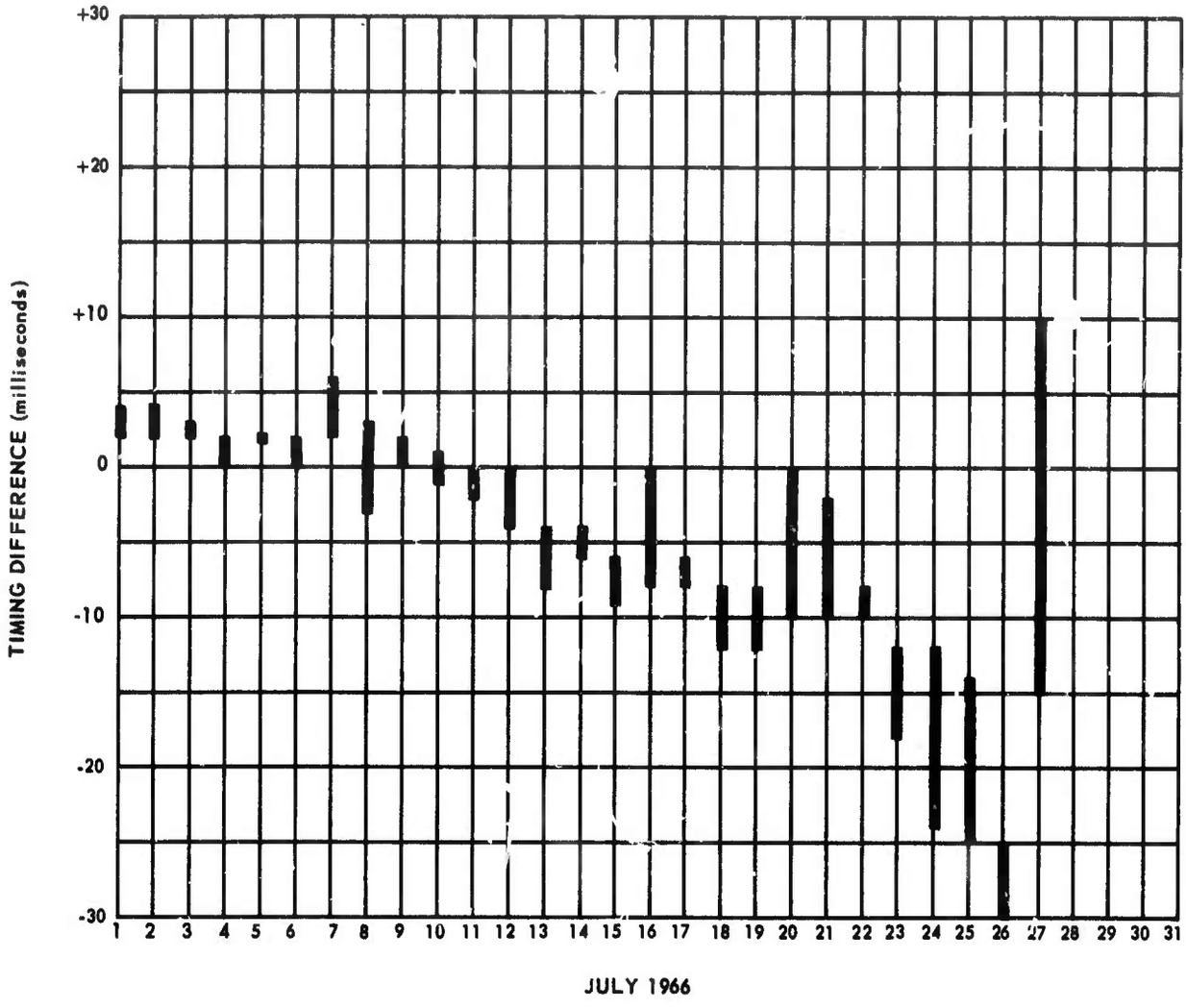

Figure 18. Timing differences between the output of the Hyperion system and the WWV signal for the month of July. The vertical lines indicate the daily range of the time differences.

G 1415

made to shield it from radiated building heat. (Pictures of the thermometer and sensor mounting are shown in figure 19.)

3.9.2 Anemometer

An anemometer was received and installed during May 1966. Data from this system are recorded on several Develocorder formats. The system is calibrated so that at X10 view, a downward shift from the base line shows direction (0 and 8 millimeters = S, 2 millimeters = W, 4 millimeters = N, and 6 millimeters = E), and an upward deflection from the base line shows speed (1 millimeter = 3 mph). This instrument was installed near the long-period vault. Figure 20 includes a typical anemogram (WI).

3.10 LONG-PERIOD SEISMOGRAPH IMPROVEMENT

3.10.1 General System Modification

Initial tests and adjustments of the long-period seismograph system after May 1965 failed to produce the desired frequency responses for the long-period seismographs. A thorough examination of the circuitry of the system showed the following undesirable features:

a. Eighty-ohm attenuator circuits for control of system magnification were mounted on the PTA's. With this circuitry, the correct galvanometer damping could not be obtained.

b. A line-equalization and free-period module was built into the line in order to adjust the seismometer damping, but the correct damping was not obtainable.

Three of the major modifications of the system were (a) replacement of the UED type G51 galvanometers in the horizontal seismographs with Model 8530-1 Harris long-period galvanometers to standardize the seismographs with those at the other observatories; (b) installation of Model 14415 junction assemblies in the three-component long-period seismograph systems; and (c) installation of dual-output PTA's in the seismograph system. A Model 6824-2 filter (unnotched) was installed in one output channel of each PTA, and a Model 6824-15 filter (notched) was installed in the other output channel.

Line-noise tests indicated no deleterious effects from line noise when the long-period PTA's were operated in the PTA room of the CRB rather than in the vault with the seismometers. All three PTA's were moved and are presently being operated in the CRB. Figure 21 shows the dual-output long-period seismograms as they were being recorded during April 1966. Figure 22 shows system frequency responses.

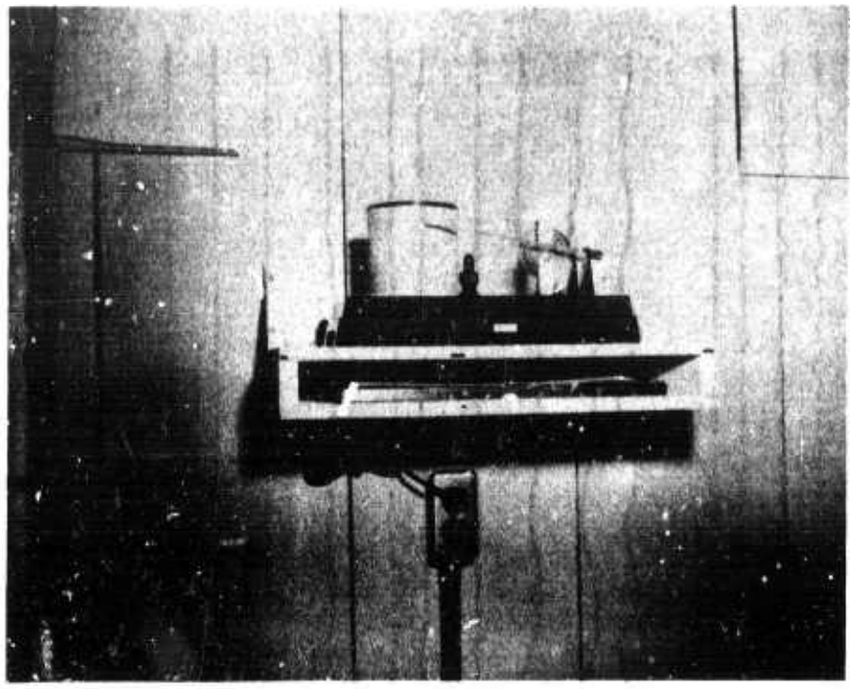

(a)

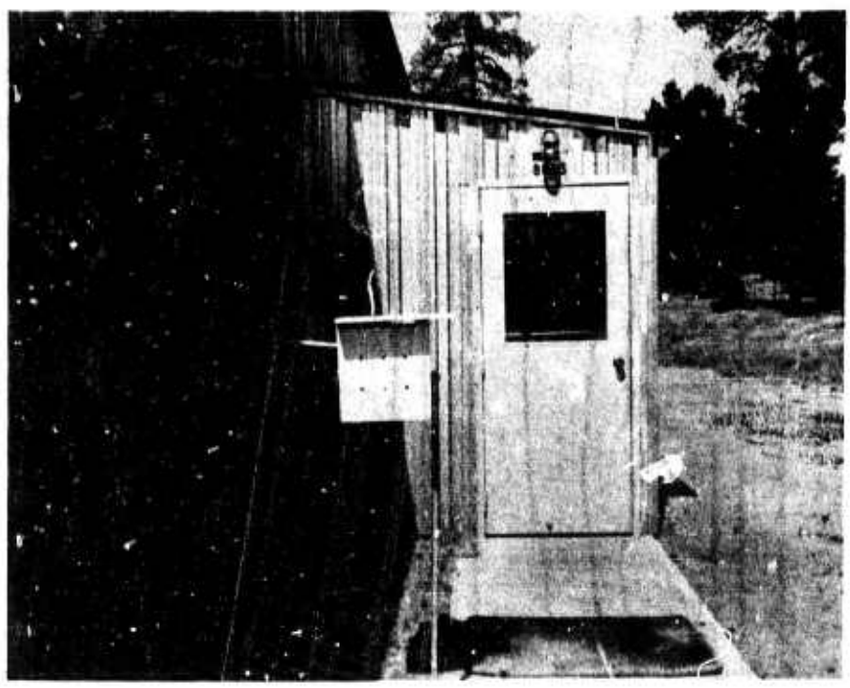

(b)

Figure 19. Photographs illustrating the installation of the recording thermometer at TFSO (a). Recording unit installed in the central recording building (b). Sensor mounting shield

G 1416

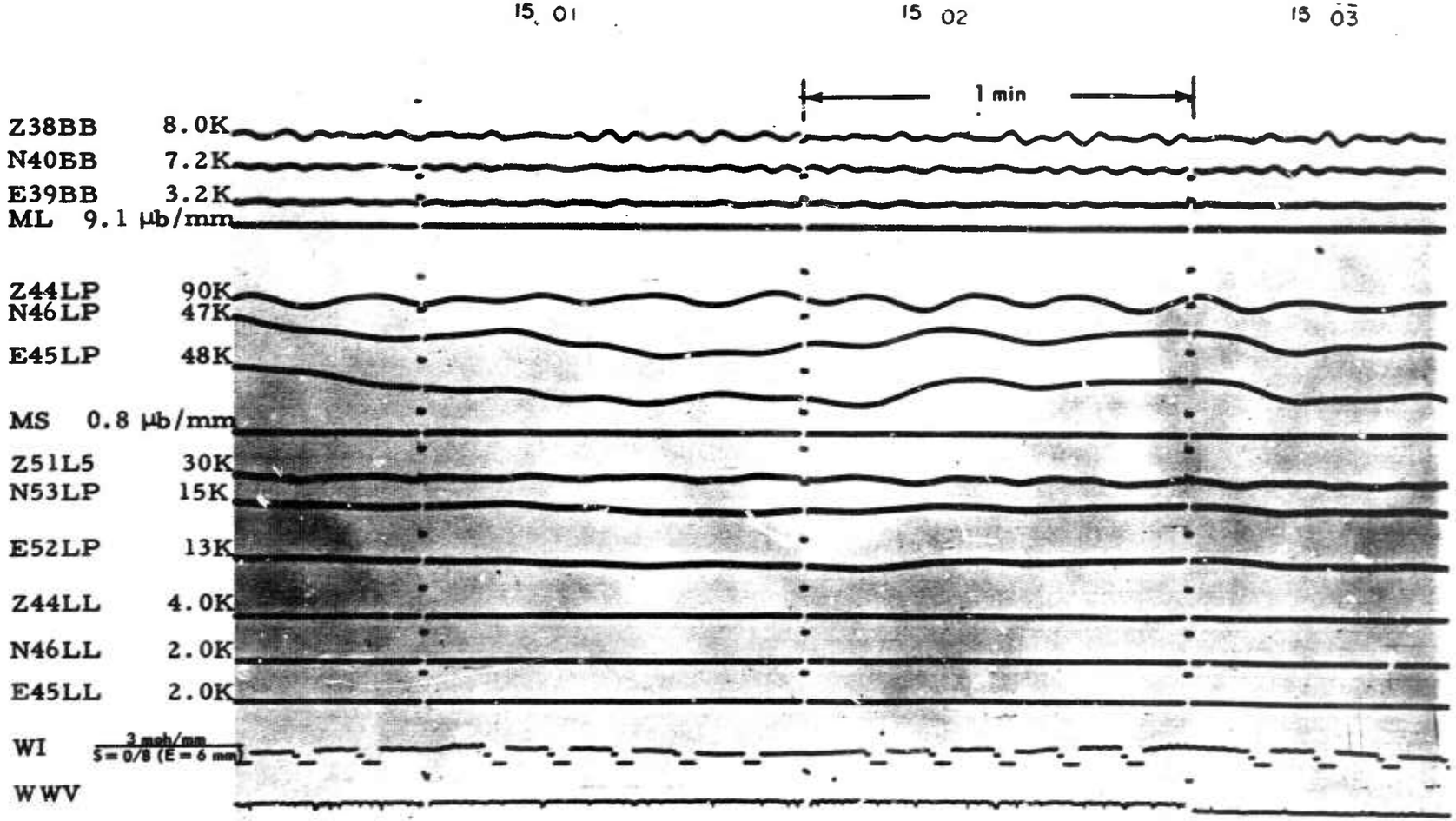

TFSO
Run 208
27 July 1966
Data Group 7184

Figure 20. TFSO long-period seismogram showing an anemogram (WI) produced by a 5-mile per hour wind from the east. (X10 enlargement of 16-millimeter film).

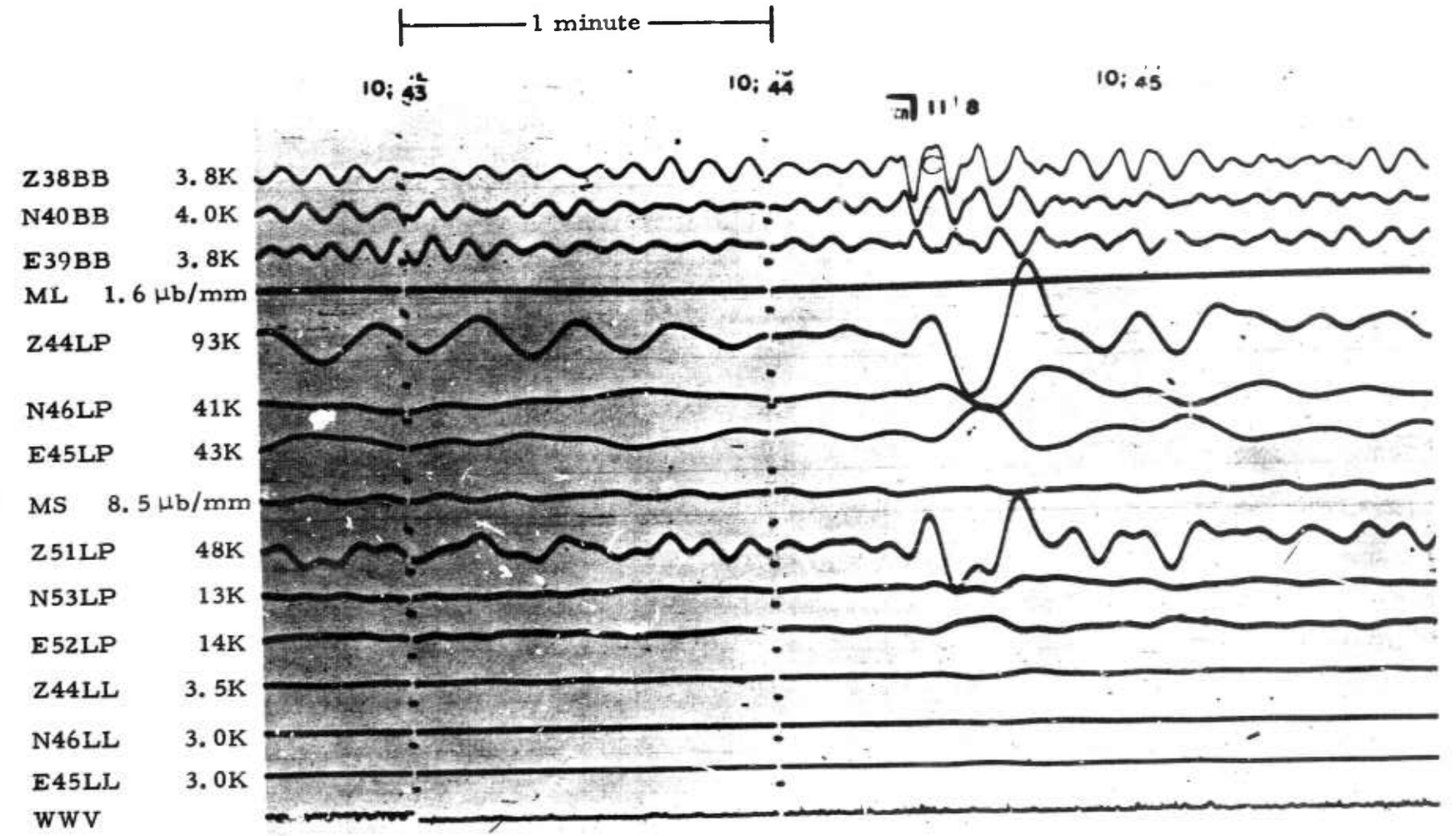

TFSO
Run 118
28 April 1966
Data Group 7181

Figure 21. Long-period seismogram recorded at TFSO exhibiting the response of the dual output long-period system to a P wave during a period of normal background activity. (X10 enlargement of 16-millimeter film)

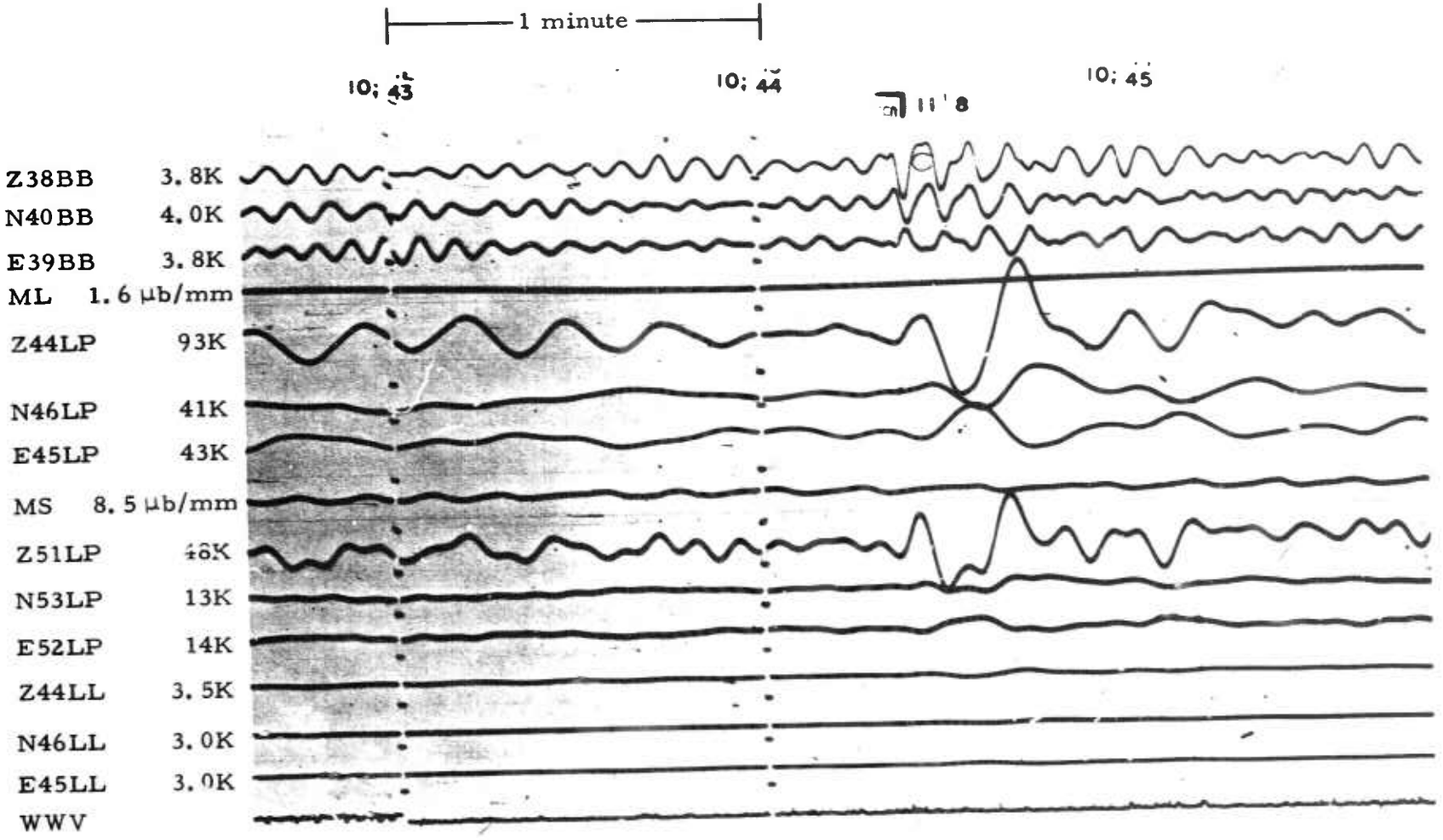

TFSO
Run 118
28 April 1966
Data Group 7181

Figure 21. Long-period seismogram recorded at TFSO exhibiting the response of the dual output long-period system to a P wave during a period of normal background activity. (X10 enlargement of 16-millimeter film)

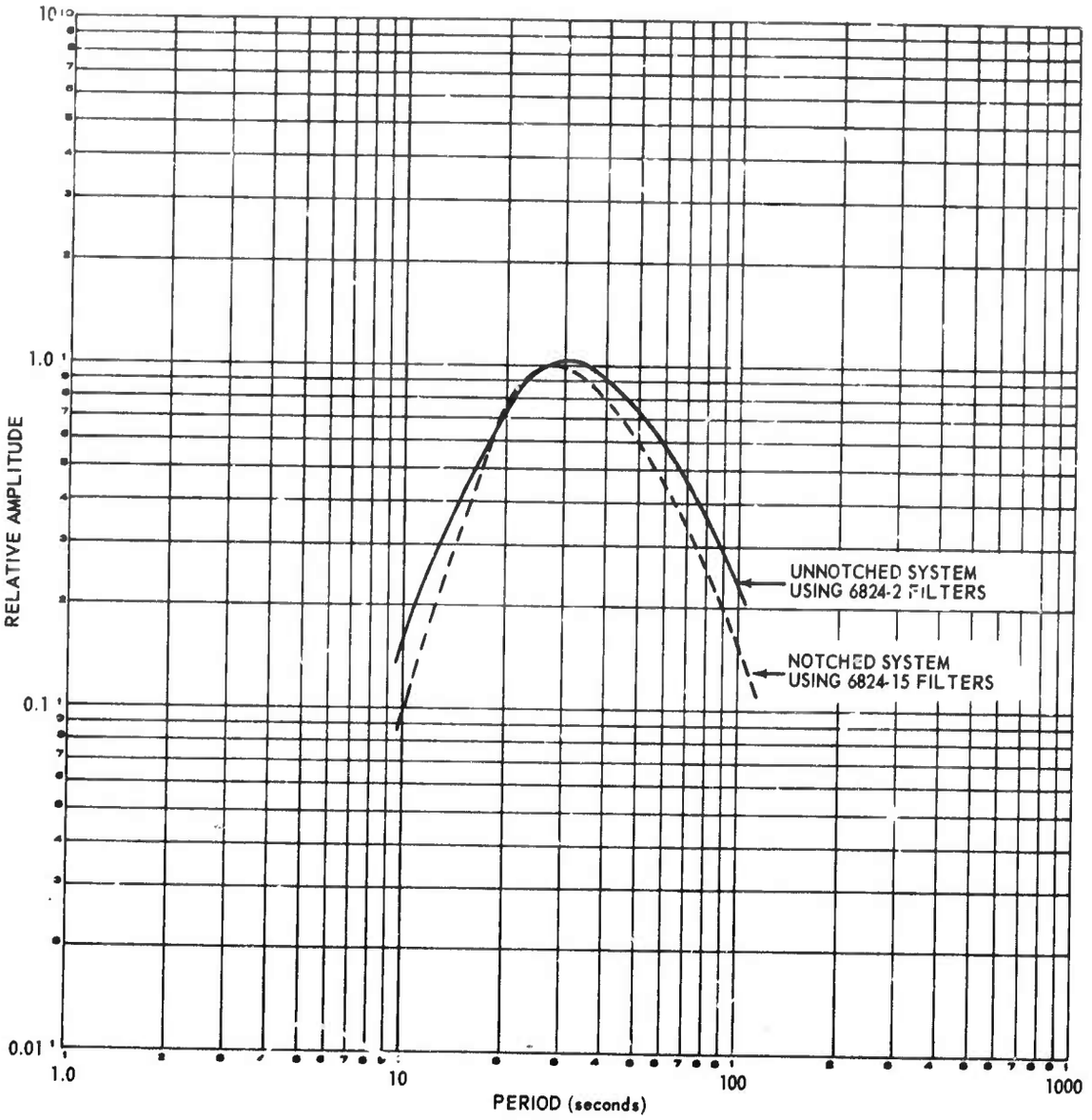

Figure 22. Frequency responses of the long-period system at TFSO performed in April 1966. The approximate parameters of the system were T_s = 20 sec, λ_s = 0.74, T_g = 110 sec, and λ_g = 0.83

G 994

3.10.2 Improved Operating Environment

The installation of a pressure-tight door for one of the pier rooms in the long-period vault at TFSO was approved by the Project Officer. A suitable marine door and frame were ordered and installed (see figures 23 and 24).

The first pressure test of the room indicated a time constant of 25 minutes. Checks proved that the ceiling and walls were leaking. Two coats of filler block sealer (Glidden Y1952) was applied to the walls and ceiling. The next pressure test indicated a 45-minute time constant. Tests were made by producing a partial vacuum in the pressure room and covering the walls with a film of soapy water. Small bubbles appeared in the film on the walls, indicating that these surfaces were still leaking. An epoxy base paint was applied to all interior surfaces in the long-period vault, and RTV-30 silicon rubber compound was applied around the base of the pier on which the long-period seismometers are located. A check made after this work indicated a pier-room pressure time constant of 1 hour and 40 minutes.

After the seismometers for the vertical and the north-south components were moved to the pier in the pressure room, and the seismometer for the east-west component was reoriented, the pressure room was sealed.

We were then able to operate the seismograph at the magnifications listed in the following table:

Seismometer	PTA filter	Operating magnification
Z44 LP	6824-15	100K
Z44 LP	6824-2	50K
N45 LP	6824-15	40K
N46 LP	6824-2	20K
E45 LP	6824-15	40K
E45 LP	6824-2	20K

A considerable improvement in the quality of the data produced by the long-period system is believed to have been obtained by operating the long-period seismometers in the sealed vault; however, the exact degree of improvement cannot be determined because the response of the system was changed at the time the seismometers were placed in the sealed vault, and also because Model 23471 convection shields were installed on the seismometers when the seismometers were placed in the sealed vault.

All vegetation in the area surrounding the long-period vault was removed early in August 1966, and the ground was sprayed with whitewash to provide a reflecting surface. This was done to determine whether the effects of

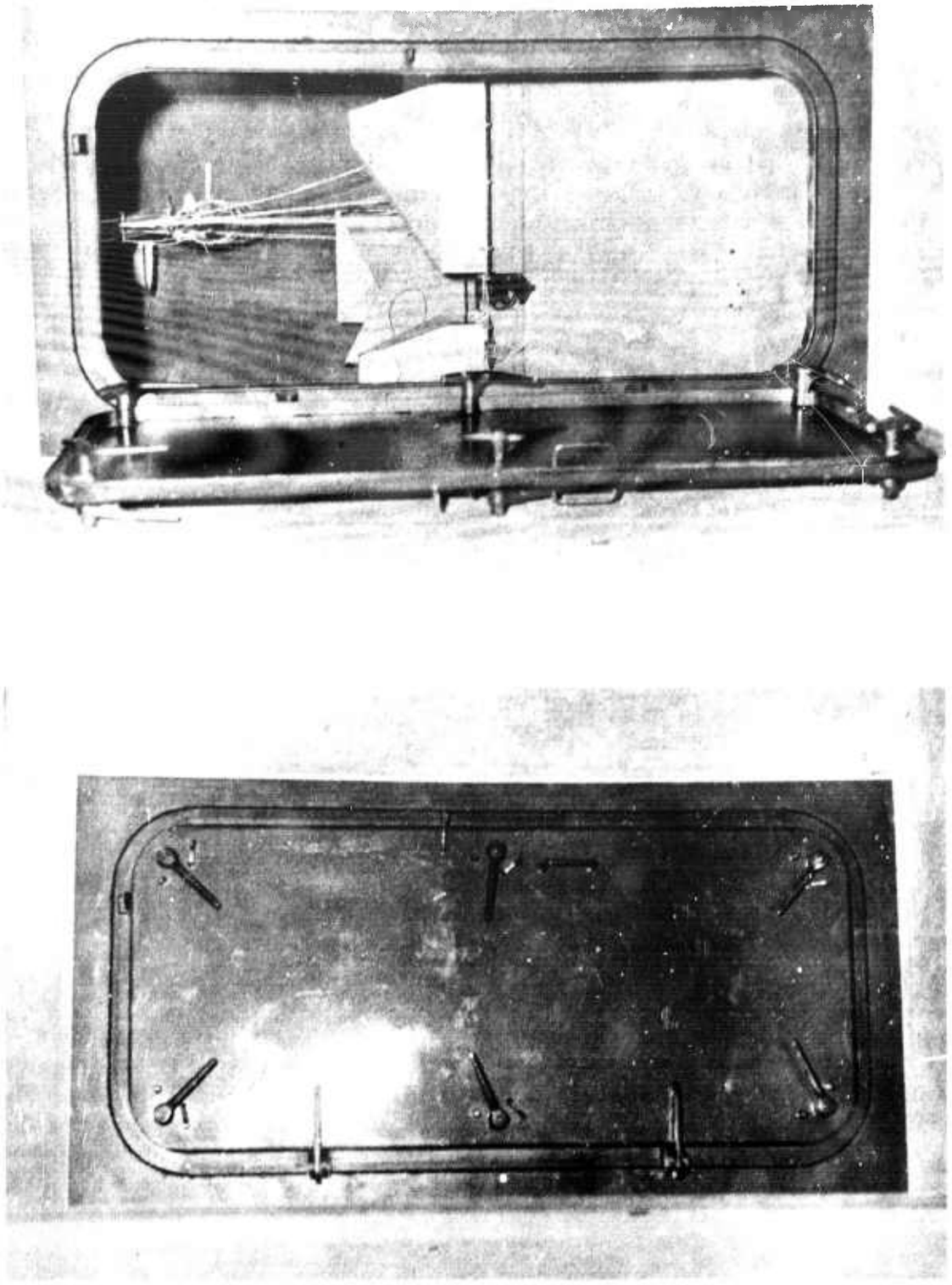

Figure 23. Marine door installation in the TFSO long-period vault G 108

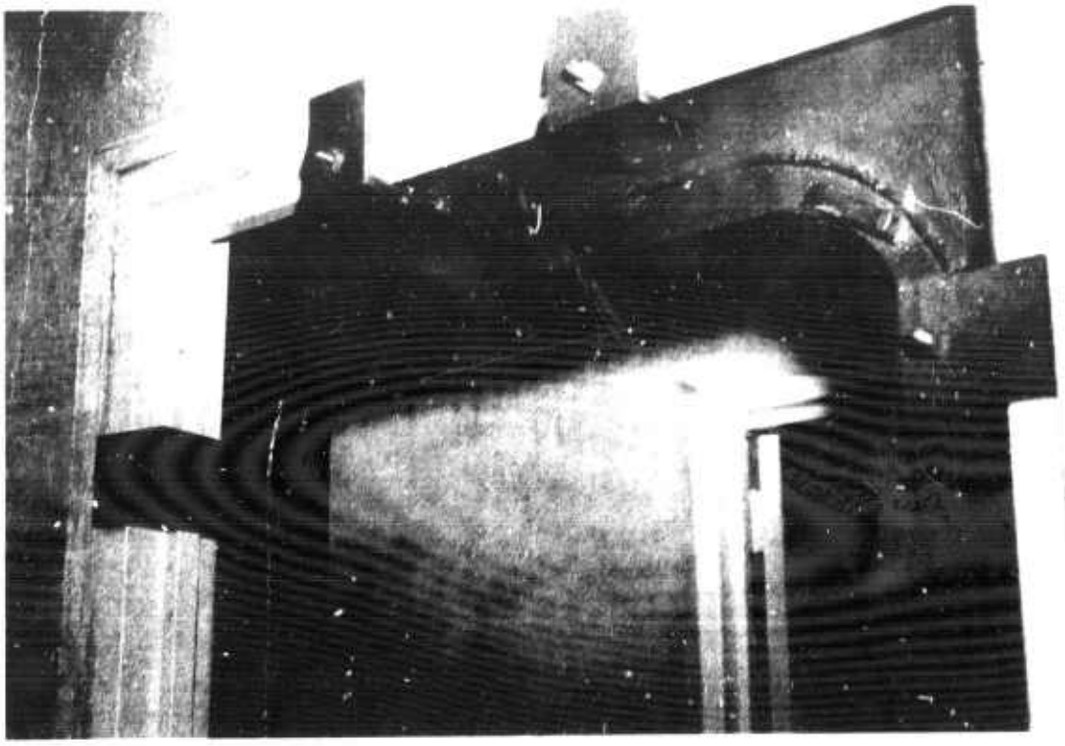

a. Inside top

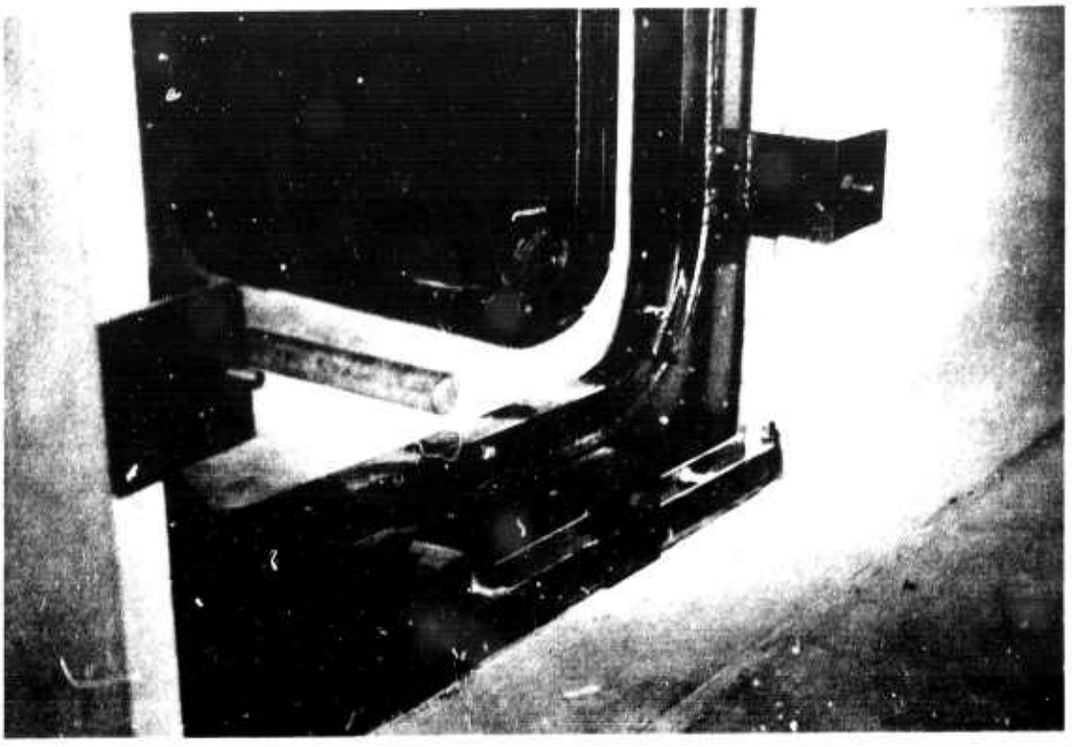

b. Inside bottom

Figure 24. Marine door installation in the TFSO long-period vault

G 109

diurnal temperature variations on the seismometers could be significantly reduced, thereby affording improved long-period seismograms. Initial results appeared encouraging; however, rain washed away 50 percent of the solution within a week. The spraying operation was repeated. Seismograms recorded before the rain again washed away a major part of the solution indicated that no significant improvement of the long-period environment was achieved.

3.11 INSTALLATION OF NEW 35-MILLIMETER FILM RECORDER

In June 1965, the Project Officer approved our recommendation to replace the two Wood-Anderson seismographs recorded on the five-channel, 35-millimeter film recorder with earth-powered vertical Benioff seismographs. The recorder, however, could not be readily modified to accommodate earth-powered data; therefore, a Geotech Mark II 35-millimeter film recorder was installed. The data recorded on this recorder and the approximate seismograph magnifications at 1 cps follow:

Short-period earth-powered vertical	- 10K
Short-period earth-powered vertical	- 1K
Short-period earth-powered north	- 10K
Short-period earth-powered east	- 10K

3.12 MAGNETIC-TAPE RECORDER HEADS

The recording heads of the Minneapolis-Honeywell magnetic-tape recorders were closely checked. Indications are that the heads of three of the recorders will require replacement within the next few months. The heads of the remaining recorders appear to be in satisfactory condition.

3.13 LOW-GAIN, SHORT-PERIOD SEISMOGRAPH

A three-component, low-gain, short-period system is currently recorded on Tape Data Trunk 2 and Develocorder Date Trunk 10 at a magnification of 5K (designated Z60LL, N100LL, and E99LL). This system became operational on 24 November.

4. EVALUATION OF STANDARD INSTRUMENTATION

4.1 STABILITY OF FREQUENCY RESPONSE

4.1.1 General

Soon after Geotech assumed responsibility for the operation of TFSO, frequency responses were performed on all of the seismographs. Eight of the frequency responses were found to be out of tolerance. Five of these were short-period seismograph responses, one was an intermediate-band seismograph response, and two were broad-band seismograph responses. The systems that were out of tolerance were adjusted. The parameters and instrument frequency responses of all systems were within operating tolerances by 31 July 1965.

Monthly measurement of the frequency response of each seismograph was continued throughout the reporting period. Adjustments were made whenever the response deviated beyond the specified tolerances.

The norms and allowable tolerances for each seismograph system are given in table 2. The standard frequency response of each system is presented in figure 4. To study the frequency-response stability of a representative group of short-period seismographs and the long-period seismographs at TFSO, the average monthly percentage change of the normalized response at two frequencies was computed. Examination of individual frequency responses indicated that the variations in the relative amplitudes at the selected frequencies were representative of the variations which occurred at the other test frequencies. This conclusion is based on frequency responses measured each month before adjustments were made to the seismographs.

4.1.2 Short-Period Frequency Responses at TFSO

4.1.2.1 Average Monthly Percentage Change in the Normalized Response

The average monthly percentage change in the normalized response at the frequencies of 0.4 and 3.0 cps were selected for evaluation of the stability of the frequency responses of a group of short-period seismographs both because they were representative and because the recorded amplitudes at these frequencies were large enough to minimize the effects of inaccuracies resulting from measurement error. The average monthly percentage change in the normalized response at 0.4 and 3.0 cps for a representative group of short-period seismographs between July and December 1966 is listed in table 4. In addition, the allowable tolerances at these frequencies are given.

Table 4 shows that the short-period seismographs were relatively stable throughout the sampling interval.

Table 4. Average monthly percentage change from 1 July through 8 December 1966 in the normalized response of a representative group of short-period seismographs

Seismograph	Average monthly percentage change at 0.4 cps	Allowable percentage tolerance at 0.4 cps	Average monthly percentage change at 3.0 cps	Allowable percentage tolerance at 3.0 cps
Z31	2.71	±7.5	10.9	±7.5
Z8	3.26	±7.5	2.05	±7.5
Z2	5.41	±7.5	2.26	±7.5
Z13	1.18	±7.5	3.25	±7.5
Z16	1.95	±7.5	2.12	±7.5
Z20	2.71	±7.5	1.23	±7.5
Z4	0.616	±7.5	2.95	±7.5
Z7	2.95	±7.5	5.82	±7.5
Z1	1.8	±7.5	2.38	±7.5
N37	1.7	±7.5	1.63	±7.5
E36	3.21	±7.5	4.83	±7.5

4.1.3 Long-Period Frequency Responses Stability

4.1.3.1 Average Monthly Percentage Change in the Normalized Long-Period Response

The average monthly percentage change for a 7-month interval in the normalized frequency response of the long-period seismographs at TFSO at 0.067 cps (15 seconds) and 0.025 cps (40 seconds) were selected as indicators of the overall stability of the long-period seismograph system. The periods of 15 and 40 seconds were used because the individual frequency responses indicated that the variations in the relative amplitudes at these periods were representative of the relative amplitude variations that occurred at the other periods.

Also, the recorded amplitudes at these frequencies were large enough to minimize the effect of inaccuracies in measurement. The average monthly percentage change in the normalized response at 15 and 40 seconds for the long-period system at TFSO are presented in table 5. In addition, the allowable tolerance at these frequencies are given.

Table 5 shows that on the average, the responses of all but two of the long-period seismographs were within the allowed 10 percent tolerance and that N66 and Z51 exceeded the tolerances by 0.3 and 1.4 percent, respectively.

4.2 CALIBRATOR MOTOR CONSTANTS

4.2.1 General

The motor constants (G)[1] are determined by comparing the seismogram trace deflection produced by manual weight lift and deflections produced by dc current pulses of known value applied through the calibration coil. Weight lifts are made with the smallest practical weight with which a high signal-to-noise ratio can be obtained. The smallest weight used on any of the seismographs is 0.2 gram; however, except for the short-period Johnson-Matheson (JM) seismometers, larger weights are used when necessary because of the level of the background noise.

The 0.2-gram weight was specified for use on short-period JM seismographs because it is the smallest weight that can be lifted manually without introducing significant error and because the dc current required to produce trace deflections equivalent to the deflections produced by larger weight falls within the nonlinear range of the calibration actuator used in the JM seismometers at the observatories.

[1]The motor constant, "G", is defined as the force in newtons exerted on the mass per ampere of current passed through the calibrator coil.

Table 5. Average monthly percentage change from 1 June through 31 December 1966 in the normalized response of the TFSO long-period system

Seismo-graph	Average monthly percentage change at 15 seconds	Allowable tolerance at 15 seconds (percent)	Average monthly percentage change at 40 seconds	Allowable tolerance at 40 seconds (percent)
E52	4.29	±10	4.34	±10
N53	7.36	±10	7.55	±10
Z44	1.43	±10	8.48	±10
E45	5.6	±10	6.56	±10
N66	5.49	±10	10.3	±10
Z51	11.4	±10	8.61	±10

The motor constants of the calibration actuators of all seismographs were set to their specified values prior to 9 October 1965. Since that time, they have been checked on an annual basis and when seismometers were replaced or repaired. The motor constants were adjusted when their measured values deviated by more than 3 percent from the specified values shown in table 6.

A brief description of the method of adjustment of motor constants for each type of seismometer follows:

a. Short-period JM - by adjusting the outer pole piece of the calibration actuator;

b. Three-component long-period, three-component broad-band, and intermediate-band vertical by changing the strength of the magnetic field through shunting;

c. Intermediate-band horizontal - by adjusting a resistive shunt in the line termination module at the CRB.

4.2.2 Routine Determination of Motor Constants

Soon after Geotech began operation of TFSO, a program was initiated to check the motor constants used in the determination of the magnification of each seismograph.

On 17 May 1965, the intermediate-band motor constants were checked, and we found that the magnification factors used to calculate the seismograph magnifications were in error by a factor of about 4.

On 24 May, the motor constants for the intermediate-band system were values of 0.0206, 0.0471, and 0.0472 newtons/ampere for the vertical, north-south, and east-west components, respectively.

By 9 October 1965, the motor constants of all calibrator actuators had been adjusted to the values listed in table 6 as "G after 1965 determination."

4.2.3 Stability of Seismograph Motor Constants

The calibrator motor constants of all JM short-period seismometers (47 verticals and 26 horizontals) were checked by manual weight lifts during the period 1 August to 9 October 1965. The observed value of the motor constant was in each case compared with the value determined during the previous checks which, for most seismometers, occurred prior to 1 May 1965. Average changes of 1.7 percent and 5.5 percent were noted

Table 6. TFSO 1966 annual motor constant check

System	G after 1965 determination (newtons/ampere)	1st check 1966	Adjusted 1966	Currently used for calibration
Z1	0.296	0.2975		0.296
Z2	0.2935	0.310	0.216	0.296
Z3	0.305	0.295		0.296
Z4	0.299	0.295		0.296
Z5	0.3025	0.300		0.296
Z6	0.298	0.300		0.296
Z7	0.297	0.303		0.296
Z8	0.2965	0.301		0.296
Z9	0.298	0.2875		0.296
Z10	0.2945	0.2935		0.296
Z11	0.2975	0.2861	0.296	0.296
Z12	0.3005	0.3041		0.296
Z13	0.2955	0.289		0.296
Z14	0.3075	0.293		0.296
Z15	0.3035	0.3055	0.2925	0.296
Z16	0.302	0.321	0.2915	0.296
Z17	0.303	0.2885		0.296
Z18	0.296	0.296		0.296
Z19	0.297	0.300		0.296
Z20	0.2945	0.3175	0.2955	0.296
Z21	0.295	0.284	0.2955	0.296
Z22	0.297	0.294		0.296
Z23	0.294	0.2915		0.296
Z24	0.295	0.296		0.296
Z25	0.294	0.2995		0.296
Z26	0.299	0.304		0.296
Z27	0.3015	0.302		0.296
Z28	0.2925	0.303		0.296
Z29	0.291	0.2945		0.296
Z30	0.2765	0.2965		0.296
Z31	0.292	0.285	0.2995	0.296
E36	0.2945	0.2995		0.296
N37	0.303	0.3125	0.2965	0.296
Z38BB	0.185	0.186		0.188
E39BB	0.1865	0.186		0.188
N40BB	0.187	0.1725	0.190	0.188
Z41IB	0.02075	0.0212		0.0206
E42IB	0.04675	0.0491	0.0474	0.0474
N43IB	0.0476	0.0482		0.0474
Z44LP	0.03175	0.0303		0.32 [a]
E45LP	0.0311	0.0301		0.32 [a]
N46LP	0.0322	0.0250		0.32 [a]
Z47BF	2.38	2.385		2.43
E48BF	2.28	2.31		2.26
N49BF	2.27	2.305		2.26
1A	2.12	2.10		2.12
1B	2.21	2.20		2.20
1C	2.18	2.085	2.18	2.20

Table 6. (Continued)

System	G after 1965 determination (newtons/ampere)	1st check 1966	Adjusted 1966	Currently used for calibration
Z60	0.300	0.298		0.296
Z61	0.304	0.296		0.296
Z62	0.304	0.290		0.296
Z63	0.302	0.295		0.296
Z64	0.291	0.298		0.296
Z65	0.2975	0.296		0.296
Z66	0.2965	0.2875		0.296
Z67	0.3025	0.3025	0.2965	0.296
Z68	0.297	0.295		0.296
Z69	0.3015	0.304		0.296
Z70	0.295	0.2955		0.296
Z71	0.300	0.300		0.296
Z72	0.296	0.295		0.296
Z73	0.297	0.292		0.296
Z74	0.289	0.296		0.296
T75	0.300	0.275	0.293	0.296
R76	0.2925	0.280	0.2945	0.296
T77	0.3905	0.275	0.293	0.296
R78	0.2945	0.251	0.295	0.296
T79	0.3015	0.284	0.294	0.296
R80	0.2915	0.2825	0.294	0.296
T81	0.2965	0.277	0.298	0.296
R82	0.2955	0.277	0.292	0.296
T83	0.2945	0.272	0.2925	0.296
R84	0.292	0.2705	0.292	0.296
T85	0.2955	0.293		0.296
R86	0.2975	0.290		0.296
T87	0.2945	0.288		0.296
R88	0.2975	0.294		0.296
R89	0.2985	0.281	0.296	0.296
T90	0.299	0.2765	0.296	0.296
R91	0.296	0.308	0.2935	0.296
T92	0.2945	0.288		0.296
R93	0.2945	0.2775	0.293	0.296
T94	0.295	0.296		0.296
R95	0.295	0.2285	0.299	0.296
T96	0.293	0.2725	0.2965	0.296
R97	0.292	0.299		0.296
T98	0.298	0.2755	0.296	0.296
Z99	0.2995	0.2985		0.296
Z100	0.298	0.2965		0.296

[a] 0.0300 used for daily calibrations after 27 October 1966

for the motor constants of the vertical and horizontal instruments, respectively. A change of more than 5 percent was observed on 4 of the vertical seismometers and 15 of the horizontal seismometers. The maximum deviations measured were 6.7 percent for the vertical seismometers and 13 percent for the horizontal seismometers. The larger percentage change in the horizontal seismometers is attributed primarily to the fact that prior to 1 May 1965, an effective weight of 0.5 gram was used instead of the specified 0.2 gram effective weight. Also, motor constant determinations for short-period horizontal seismographs in the field are inherently more susceptible to measurement errors than are motor constant determinations for vertical seismographs because the precision required in installing the weight-lift jig on the seismometer is difficult to obtain repeatedly under field conditions.

The 1966 annual seismometer calibrator motor-constant checks were made between August and October. Table 6 shows the results of these motor constant determinations. The large number of horizontal seismograph calibrators that required adjustment can be attributed at least in part to the difficulties involved in installing the weight-lift jig on these seismometers.

4.3 LIGHTNING PROTECTION

4.3.1 Summary of Electrical Storms and Instrument Damage at TFSO

Several minor electrical storms occurred during June and July 1965; a major storm occurred on 10 July. Most of the damage to the equipment resulting from this storm was confined to those systems that were not yet fully protected by the AEI lightning protection system. Equipment damaged on 10 July is listed in table 7. Of the 25 circuits affected, 17 were calibration circuits that were protected by the AEI system only at the seismometer vault. Of the remaining 8 circuits damaged, 6 were data circuits that were not yet protected by the AEI system, and 2 were fully protected by the AEI protectors.

Analysis of the failure of the two AEI-protected circuits (Z69 and Z18) indicates that neither failure could be attributed to failure of the AEI protection system. The diodes in the power supply of the Z69 data line failed, probably because of a power surge during transfer of the current load from commercial power to the standby generator. The galvanometer-diode protector portion of the lightning protection system failed in the Z18 circuit, but the AEI lightning protector did not.

By November 1965, all data and calibration circuits were protected by AEI protectors. Protection of the TFSO seismographs with the AEI protection system did not eliminate the incidence of lightning-induced damage to the systems; however, the AEI system was much more effective in protecting the TFSO seismographs than was the fuse and carbon-block system previously used.

Table 7. Equipment at TFSO damaged on 10 July 1965

System	Circuit	Fuses	Carbon blocks	Galvo diode protector	
Z2	Calibration	X	X		
Z3	Calibration	X	X		
Z5	Calibration	X	X		
Z7	Calibration	X	X		
Z8	Calibration	X	X		
Z9	Calibration	X	X		
Z13	Calibration	X	X		
Z18	Calibration	X	X		
Z18	Data			X	
Z22	Calibration	X	X		
Z37	Calibration	X	X		
NBB39	Calibration		X		
NBB39	Data		X		
ZIB41	Calibration	X	X		
ZJB41	Data	X	X		
EIB42	Data		X		(flipped galvanometer)
ZLP44	Data		X		
NLP45	Data		X		
Z61	Calibration	X	X		
Z63	Calibration	X	X		
Z65	Calibration	X	X		
Z67	Calibration	X	X		
Z69	Data				(power supply)
Z99	Calibration	X	X		
Z99	Data	X	X		

Figure 25 shows a comparison of outages caused by storms that occurred in 1964 when fuses and carbon blocks were used for lightning protection and those that occurred in 1966 when AEI gas-triode protectors were used.

4.3.2 Tests of a Prototype Improved Lightning Protection System

Two 1-millihenry inductors were installed in the data circuit of Z8 on 21 July 1966. These components were installed between the AEI protector and the galvanometer protection diodes to provide additional protection for the PTA galvanometer. The inductors provide a high impedance to the sharp voltage spikes induced by lightning strikes, limiting the current in the galvanometer coil caused by these spikes; the impedance of the inductors at data frequencies is negligible. Two storms have occurred since this installation with no damage to this circuit; however, until the circuit has been subjected to more lightning storms, no conclusive evaluation of this circuit is possible. Examination of the Z8 seismograph indicates that no noise or pickup has been introduced into the system by this modification. Figure 26 is a simplified schematic of the modified protection system.

4.4 OPERATIONAL STABILITY OF SEISMOGRAPH MAGNIFICATION AT TFSO

The operating magnification of the short-period, intermediate-band, broad-band, and long-period seismographs was determined by calibrating them daily with a single frequency sine-wave. If the deviation of the operating magnification from the standard magnification exceeded the specified operational tolerance for a given seismograph (see TR 64-59), adjustments were made and the seismograph was recalibrated.

4.4.1 Stability of Isolation Amplifier

Operational amplifiers are used in the seismographs at TFSO to isolate the instruments in the system from each other. Early experience with these amplifiers showed that the amplifier gain drifted. Observatory personnel indicated that the problem appeared to be associated with the feedback potentiometers in the amplifiers. Ten of these units were modified by installing dust-sealed feedback potentiometers. There was no case of gain instability associated with these ten circuits after modification. Subsequently, we found that adjustment of the potentiometers served to keep the contact surfaces clean, eliminating the erratic output problems; therefore, no additional amplifiers were modified.

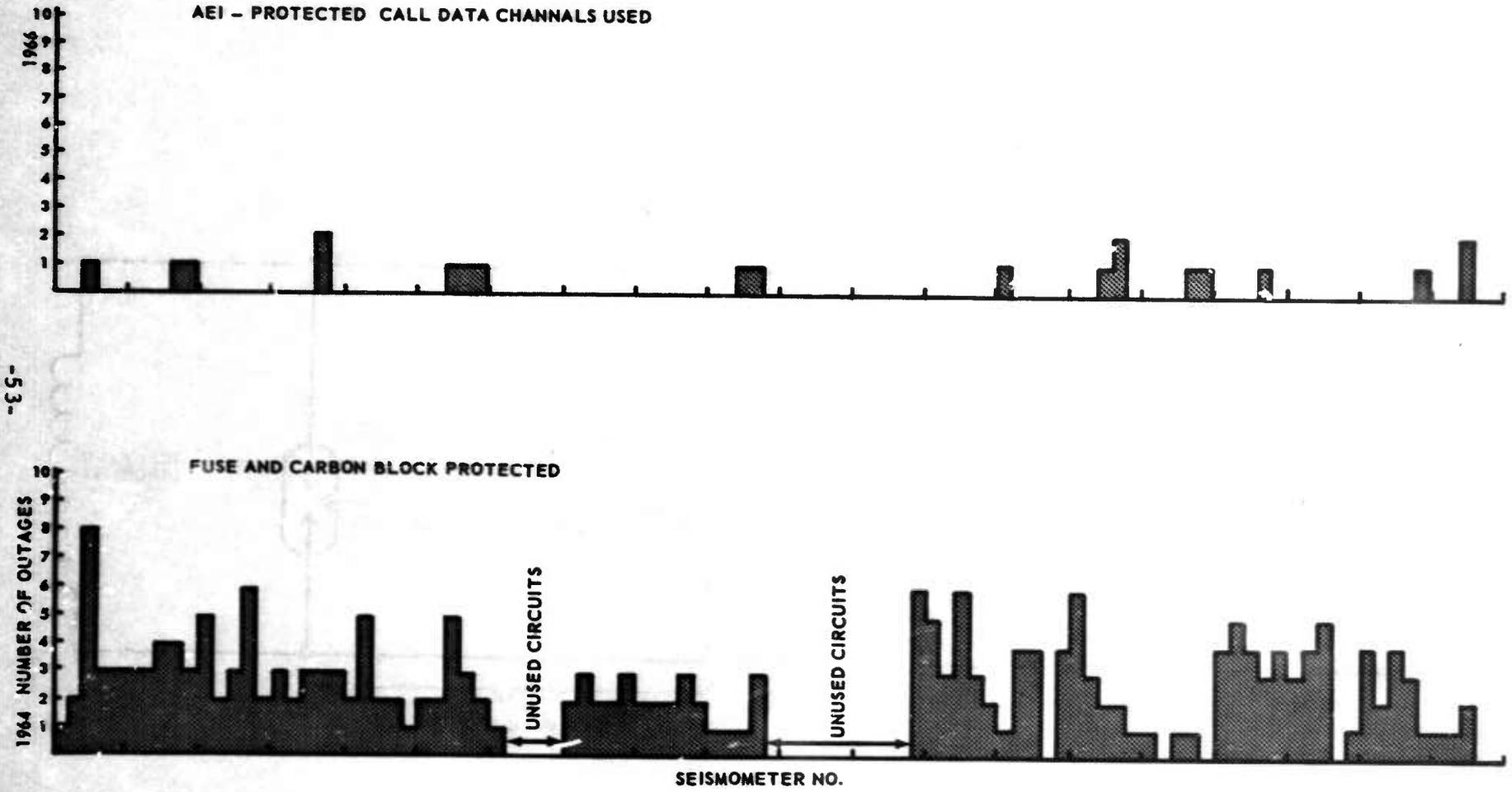

Figure 25. Comparison of number of storm-caused outages at TFSO in 1964 (seismometers protected by fuses and carbon blocks), and 1966 (seismometers protected by AEI lightning protectors

G 1840

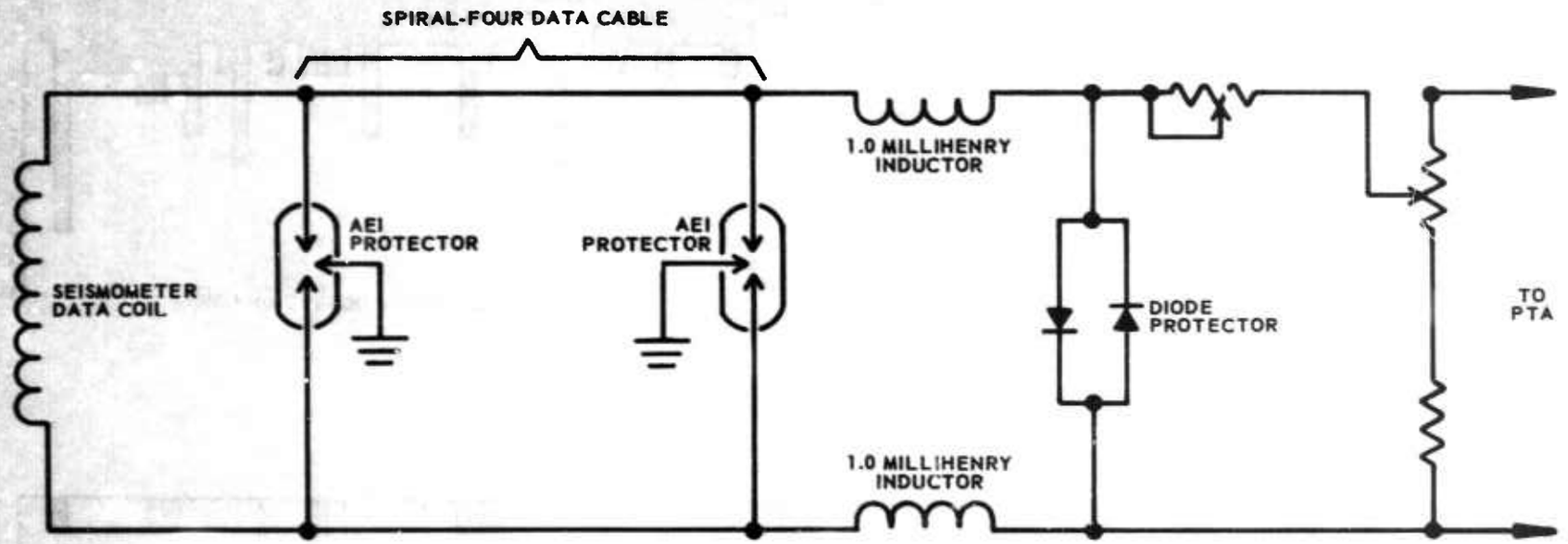

Figure 26. Simplified schematic diagram of the modified lightning protection system

G 1417

4.4.2 Stability of Short-Period Seismograph

4.4.2.1 Average Daily Percentage Magnification Change of the Primary System

The average daily percentage magnification variation was computed for each of several selected short-period seismographs as follows:

$$f = \sum_{n=1}^{n=N} \frac{G_{n+1} - G_n}{G_n (N-1)}$$

f = the average daily percentage magnification variation;

G = the magnification at daily calibration;

N = the total number of days;

n = the nth day.

The average daily percentage magnification change for the primary system is presented in table 8.

Table 8. Average daily percentage change in the magnification of a selected group of short-period seismographs at TFSO

Seismograph	Average daily percentage magnification change
Z31	2.21
Z8	2.07
Z2	3.37
Z13	2.55
Z16	6.11
Z20	4.48
Z4	2.28
Z7	1.64
Z1	2.36
N37	3.11
E36	2.46

4.5 SEISMOGRAPH RELIABILITY

The average outage time for all seismographs was much less than 1 percent, including outages required to perform routine frequency-response checks, motor-constant checks, and polarity tests. As shown in figure 25 the outage time decreased with the fuse-type protectors were replaced with three-electrode, gas-filled protectors.

4.6 TIMING SYSTEMS

4.6.1 Primary Timing

Primary time at TFSO is furnished by a Hyperion Model 1551A combination timing system and programmer. Observatory primary time was normally adjusted twice daily, if necessary, to maintain the time difference between observatory time and the time base, Radio Station WWV, at less than 50 milliseconds. When this time differential exceeded 50 milliseconds, the correction required to realign the observatory time with WWV was entered in the station log.

Excessive drift rates were experienced with the Hyperion timing system. In November 1965, we began a search for a suitable replacement for the crystal oscillator in the Hyperion timing system. We learned that a direct replacement for this oscillator which had five times the frequency stability of the existing unit was available. A crystal oscillator of this type was ordered. The new crystal was received on 24 June 1966 and installed on 28 June. During the first 3 weeks of operation with the new crystal, the time error of the Hyperion system did not exceed 12 milliseconds, and no adjustments were made. Several adjustments were made during the last part of July. These adjustments were not required because of oscillator drift, but because of work performed on power and timing circuits. The Hyperion timing system became temporarily inoperative on 19 August due to the failure of capacitors which were damaged by overheating of the oven. Failure of the thermostat to open the oven circuit resulted in overheating of the oven. The thermostatically controlled heaters were temporarily bypassed, and the timing system was returned to operation.

On 14 September, the Hyperion timer again stopped operating. Adjustments were made to the Schmidt trigger (ST 1-A), and the timer was restarted. No faulty components were found. The thermostat in the oven assembly was replaced at this time. The unit was operating satisfactorily at the end of the reporting period.

4.6.2 Secondary Timing

Secondary time at TFSO is furnished by a Timing System, Geotech Model 11880, and a Programmer, Geotech Model 11395. The secondary time was normally adjusted daily, if necessary, to maintain the time difference between the observatory time and Radio Station WWV at less than 50 milliseconds. No significant problems were encountered with secondary timing systems during this contract period.

4.7 POWER

4.7.1 Commercial Power

Commercial power at TFSO is supplied by Arizona Public Service Company. During this reporting period, all commercial power failures were caused by lightning storms. The commercial power failed twice during the contract period for a total of 9 hours.

4.7.2 Secondary Power

Secondary power at TFSO is supplied by a 100-kilowatt diesel generator. The power output of the generator is sufficient to provide emergency power for the amplifiers, timing systems, and recording equipment. The generator can be started remotely from the CRB. An indicator lamp in the CRB serves to signal the return of commercial power.

The station generator is operated each month for approximately 5 hours to facilitate the performance of routine tests, service, and maintenance. The secondary power system functioned properly during the two commercial power outages.

5. MAINTENANCE OF TFSO FACILITIES

5.1 ENGINEERING LABORATORY

Work on air conditioning of the engineering laboratory to provide cooling adequate for proper operation of the Astrodata system was completed during May 1965. This work, planned and started under the previous contract, included lowering the ceiling, insulating the room, and installing two 5-ton air-conditioning units and the required duct work.

In an effort to reduce the level of environmental noise recorded on the digital magnetic-tape system, the Project Officer requested that the TFSO

engineering laboratory be operated as a "clean" room and that it be used only for equipment and work requiring a controlled environment. The conversion of the engineering laboratory to a clean room was completed in early July 1965. All of the air-conditioning ducts were equipped with air filters, the outside door and windows were locked and sealed, doors into the darkroom and drafting areas were kept closed, smoking was prohibited, and all dust-creating materials were removed. Daily maintenance was performed on the floor, electronic equipment, and work benches to maintain a stable environment for equipment operation.

5.2 AIR CHILLER UNIT

5.2.1 Scale Accumulation

During a visit on 27 April 1965, Mr. W. Grimpe, an engineer from ASD, noted a buildup of scale in the chiller units of the air-conditioning system caused by excessive quantities of minerals in the local water supply. An acid treatment had been used to remove the scale about every 6 months by the previous contractor. Treating was done by a Phoenix firm and was quite expensive. In addition, repeated use of the acid was damaging the chiller units and complete replacement of the chillers, heat exchangers, and so forth, would have been inevitable had these treatments been continued.

At the suggestion of Mr. Grimpe, we arranged for a Phoenix water treatment firm, Sullbrook Water Services, to examine the scale build-up and to recommend a solution to the problem. Based on an analysis of the water, Sullbrock Services recommended a chemical mixture which would eliminate the necessity of periodic cleaning and would inhibit scale accumulation. (Sullbrook Services guaranteed a free acid treatment and scale removal if their product was not successful.) Initially, a 5-month supply of the recommended chemicals and a feeder were purchased. The treatment successfully retarded the accumulation of the scale, and was used routinely throughout the reporting period.

5.2.2 Miscellaneous Malfunction

The two sealed water-chiller units in the TFSO air-conditioning system were operated continuously for 3 years. In the spring of 1966, the oil level in one of the units dropped intermittently, to a very low level. Because no external oil leaks could be found, and because the oil normally returned to its original level after the chiller unit had been shut down, we assumed that the oil was being trapped somewhere within the chiller unit. Continued operation of the unit with the oil at a low level could have resulted in damage to the unit; therefore, a Phoenix air-conditioning firm was contacted to service the unit.

A prechiller unit was found to be operating incorrectly. A set of O-rings and check valves were replaced in the unloader assembly of the unit, and it was returned to satisfactory operating condition.

During late June and early July, both units developed an increase in the discharge head-pressure. The head-pressure often exceeded the preset limit, activating a safety relay which shut the units down. The cooling-water system, which is common to both units, was examined, and the inside of the condenser tubes was found to contain a slimy algae buildup. The water system was subsequently treated with a copper sulfate solution to control the algae. Since this treatment, the head pressure has remained in the safe operating range.

5.3 FURNACE

During Mr. Grimpe's visit, he observed that the boiler was overheating and recommended that it be repaired or replaced. On 21 October a representative of the Plumbing and Heating Division of American Standard visited TFSO and reported that the furnace, an A-5 diesel oil-fired boiler, did not have a completely enclosed heating chamber inside the outer cover. Fire and smoke had been escaping around the inspection plate, especially during initial combustion.

The following remedial action was taken:

a. The inspection plate was clamped in place and putty was forced into the gaps;

b. New insulation was packed into the side of the unit;

c. The jacket was cleaned and painted;

d. The draft controls were carefully adjusted so that most of the draft comes up through the bottom of the unit, and the oriface in the top of the unit was decreased so that the flame is primarily contained in the bottom of the unit.

Subsequently, only minor adjustments to the furnace were required. Moderate soot deposits necessitate cleaning the boiler room quite often; however, this cannot be avoided because of the design of the boiler flue.

5.4 CONDENSATION UNDER THE ROOF OF THE CRB

Mr. Grimpe also reported that in the past, a problem existed in the attic of the CRB where condensation accumulated on the inside of the insulated

metal roof, especially during the winter months. The condensation collected here because the vapor barrier on the warm side of the insulation was inadequate. Mr. Grimpe recommended that attic ventilation be provided to remedy this problem.

During May 1965 the attic was ventilated, and the ceiling in the CRB was insulated. Because the warmer air is contained below the attic, and because of the increased efficiency of the ventilation in the attic, the temperature was expected to remain below the dew-point. TFSO personnel periodically checked for condensation during the winter of 1965-66, and no buildup of moisture was noted.

5.5 INTERIOR OF THE CRB

Repainting of the interior of about 40 percent of the central recording building was accomplished by summer employees on a room-by-room basis during the summer of 1966.

6. ROUTINE ANALYSIS

6.1 INTRODUCTION

Seismometric data were recorded at TFSO continuously throughout this reporting period. The recorded data were routinely analyzed, the analysis checked, and a daily tabulation of arrival times of P phases and selected later phases of earthquake signals were transmitted to the Environmental Science Services Administration's Coast and Geodetic Survey (ESSA-C&GS). Analysis data were finalized at SDL where they were associated, when possible, with known earthquakes using the Automated Bulletin Process (ABP). Automated Bulletin Process association is based on hypocentral information furnished by the (ESSA-C&GS). Using these data, a monthly earthquake bulletin was prepared and published at our Garland laboratory.

Sixteen-millimeter film seismograms and associated preliminary analysis data were routinely selected on a random basis by our Garland laboratory personnel for review by a quality-control analyst. Recorded data were also used to evaluate routine and special seismograph systems operated at TFSO and to obtain data for research studies (see sections 4, 7 and 10).

6.2 ANALYSIS PROCEDURES

6.2.1 Preliminary Analysis

Film seismograms recorded were analyzed during each 24-hour period. Preliminary analysis was conducted on an "on line" basis and the analysis data were recorded on worksheets compatible to both observatory use and direct transcription of data to IBM cards. Data recorded during preliminary analysis consist of:

1. Phase arrival time;
2. Peak amplitude and signal period of each phase arrival;
3. Preliminary phase identification when possible;
4. Classification of events by general type (for example, local, near regional);
5. Estimated station-to-epicenter distance and/or azimuth (when possible);
6. Seismograph system and component.

6.2.2 Checking and Finalization of Preliminary Analysis

The seismograms were reviewed by a second analyst who checked the arrival time, period, and amplitude data recorded on the worksheets, and reviewed portions of the seismogram classified as "possible signal" by the preliminary analyst. Data from the analysis sheets were used for compilation of information for ESSA-C&GS, the monthly earthquake bulletin, and for various statistical analyses.

Before the analysis sheets were sent to our Garland laboratory, events are assigned sequence numbers for ABP control.

6.2.3 Daily Reporting to the ESSA-G&GS

Throughout the reporting period, arrival time, signal period, signal amplitude, and estimates of epicentral locations (when estimates were possible) of events recorded at TFSO were reported daily to the ESSA-C&GS in Washington D.C. Daily messages, sent by TWX, are relayed to Washington, D. C., by the General Services Administration in Phoenix on week days, and are sent directly to Washington, D. C., on weekends and holidays. Data are used by the C&GS in their hypocenter location program. A monthly tabulation of

the number of events of each type reported, the number of hypocenters reported by the C&GS, and the percentage of hypocenters in which TFSO data were used is given in table 9.

Prior to 28 June 1965, the C&GS had requested that both suspected and confirmed pP arrivals be reported in our daily messages. On 28 June, Mr. April of the C&GS requested, through the Project Officer, that we report pP arrivals that were definitely identifiable or in the identity of which we had a high degree of confidence.

6.3 PUBLICATION OF THE VELA-UNIFORM EARTHQUAKE BULLETIN

6.3.1 Transmittal of Raw Data to SDL

Data from TFSO were keypunched into IBM cards directly from the analysis sheets. The cards were checked for proper sequencing, anomalous data values, and incomplete data using a CDC 3100 computer program written under Project VT/1124. Necessary corrections were made, and the data were transcribed onto digital magnetic tape and shipped to SDL for processing by the ABP.

6.3.2 Final Bulletin Preparation

After the raw analysis data were processed by the ABP at SDL, the associated data were returned to our Garland laboratory for final processing. Until January 1966, the data were transcribed onto IBM cards and checked by the Geotech CDC 160A computer; necessary minor corrections were made to the card deck; and offset masters were prepared on an IBM 407 printer. In January, when our CDC 3100 computer became operational, updating of the bulletin data was fully automated. Currently, after the ABP output is checked for anomalous data, the updating program makes the necessary corrections; automatically calculates ground displacement values and magnitudes that may be missing from the APB output; and associates Love and Rayleigh wave arrivals with the proper hypocenters (Love and Rayleigh arrival associations made during the preliminary analysis are accepted by the ABP). Subsequently, a third program controls the preparation of the offset masters by the ABP.

6.4 ROUTINE ANALYSIS OF NOISE DATA

Microseismic noise analysis was routinely accomplished at the observatory. Nine samples of noise in the period range between 0.4 and 1.4 seconds are measured from the film seismogram from each day. The data are processed, and monthly probability of occurrence curves are prepared for both X10

Table 9. Earthquake data reported to the C&GS

May 1965					June 1965					July 1965				
L	N	R	T	Per[a]	L	N	R	T	Per[a]	L	N	R	T	Per[a]
2	71	18	933	71.8	3	128	21	991	76.1	0	185	19	953	79.3
C&GS signals located - 418					C&GS signals located - 469					C&GS signals located - 421				
August 1965					September 1965					October 1965				
L	N	R	T	Per[a]	L	N	R	T	Per[a]	L	N	R	T	Per[a]
9	120	20	1050	71.8	19	156	41	977	78.0	25	132	14	1048	83.7
C&GS signals located - 531					C&GS signals located - 396					C&GS signals located - 399				
November 1965					December 1965					January 1966				
L	N	R	T	Per[a]	L	N	R	T	Per[a]	L	N	R	T	Per[a]
11	99	25	1385	81.6	5	63	21	1165	77.3	8	388	17	1244	85.8
C&GS signals located - 387					C&GS signals located - 375					C&GS signals located - 366				
February 1966					March 1966					April 1966				
L	N	R	T	Per[a]	L	N	R	T	Per[a]	L	N	R	T	Per[a]
12	152	12	1116	76.9	9	119	16	1130	71.8	10	122	19	1135	78.3
C&GS signals located - 360					C&GS signals located - 432					C&GS signals located - 401				
May 1966					June 1966					July 1966				
L	N	R	T	Per[a]	L	N	R	T	Per[a]	L	N	R	T	Per[a]
24	204	52	1089	76.2	13	122	30	1238	73.5	10	126	12	1287	76.9
C&GS signals located - 442					C&GS signals located - 446					C&GS signals located - 363				
August 1966					September 1966					October 1966				
L	N	R	T	Per[a]	L	N	R	T	Per[a]	L	N	R	T	Per[a]
11	179	23	1458	80.1	36	609	35	1243	73.6	10	325	20	1371	74.6
C&GS signals located - 469					C&GS signals located - 419					C&GS signals located - 387				
November 1966					December 1966									
L	N	R	T	Per[a]	L	N	R	T	Per[a]					
9	179	22	1229	79.3	2	140	8	1212	71.3					
C&GS signals located - 365					C&GS signals located - 320									

Key:

L - Local
N - Near regional
R - Regional
T - Teleseism

a - Percentage of those events located by the C&GS that were reported by the observatory, based on C&GS "Earthquake Data Report"

trace amplitude and ground displacement for an individual seismogram, the summation seismogram, and the filtered summation seismogram. These data are routinely sent to the Project Officer.

7. INSTRUMENT TESTS AND EVALUATION

7.1 IMPROVISED HIGH-FREQUENCY SEISMOGRAPH SYSTEMS

7.1.1 General

It has been postulated that the characteristics of the high-frequency components of seismic signals might be a valuable aid in the determination of the nature of seismic source mechanisms. The standard short-period seismographs, which were primarily designed to detect signals in the frequency range from 0.2 to 3.0 cps, furnish very little useful data in the region above 3.0 cps. To provide systems more suitable for recording the high-frequency components of seismic signals, improvised high-frequency seismographs were designed and installed at TFSO at the request of the Project Officer. Examination of the available data indicated that the amplitudes of the earth motion caused by the majority of teleseismic events decreased with increasing frequency, and that they are from 40 to 60 dB less in the frequency range from 4 to 5 cps than in the frequency range center about 1 cps. Consideration of these amplitude ratios indicated that an effective high-frequency seismograph should be capable of being operated at very high magnifications at frequencies above 4.0 cps, and that the magnification should be sufficiently low at 1.0 cps to prevent the large-amplitude, low-frequency components of seismic signals from interfering with the recording of the high-frequency components.

7.1.2 Design and Operation

On 8 September 1965, the Project Officer requested that we install and operate five special high-frequency seismograph systems at TFSO. Four of these systems, ZHF1, ZHF2, ZHF3, and ZHF4, were essentially identical to systems being operated at WMSO.

The design of the ZHF1, ZHF2, ZHF3, and ZHF4 high-frequency seismographs was based on the attainment of the desired system characteristics, but it was limited by the characteristics of the instruments available and by stringent time restrictions.

Krohn-Hite filters were used to shape the responses of ZHF1 and ZHF2 which peak at 6 and 8 cps, respectively. Figure 27 shows the responses and block diagrams of the systems. The response of ZHF3 was similar to that of ZHF1, and the response of ZHF4 was similar to that of SHF2;

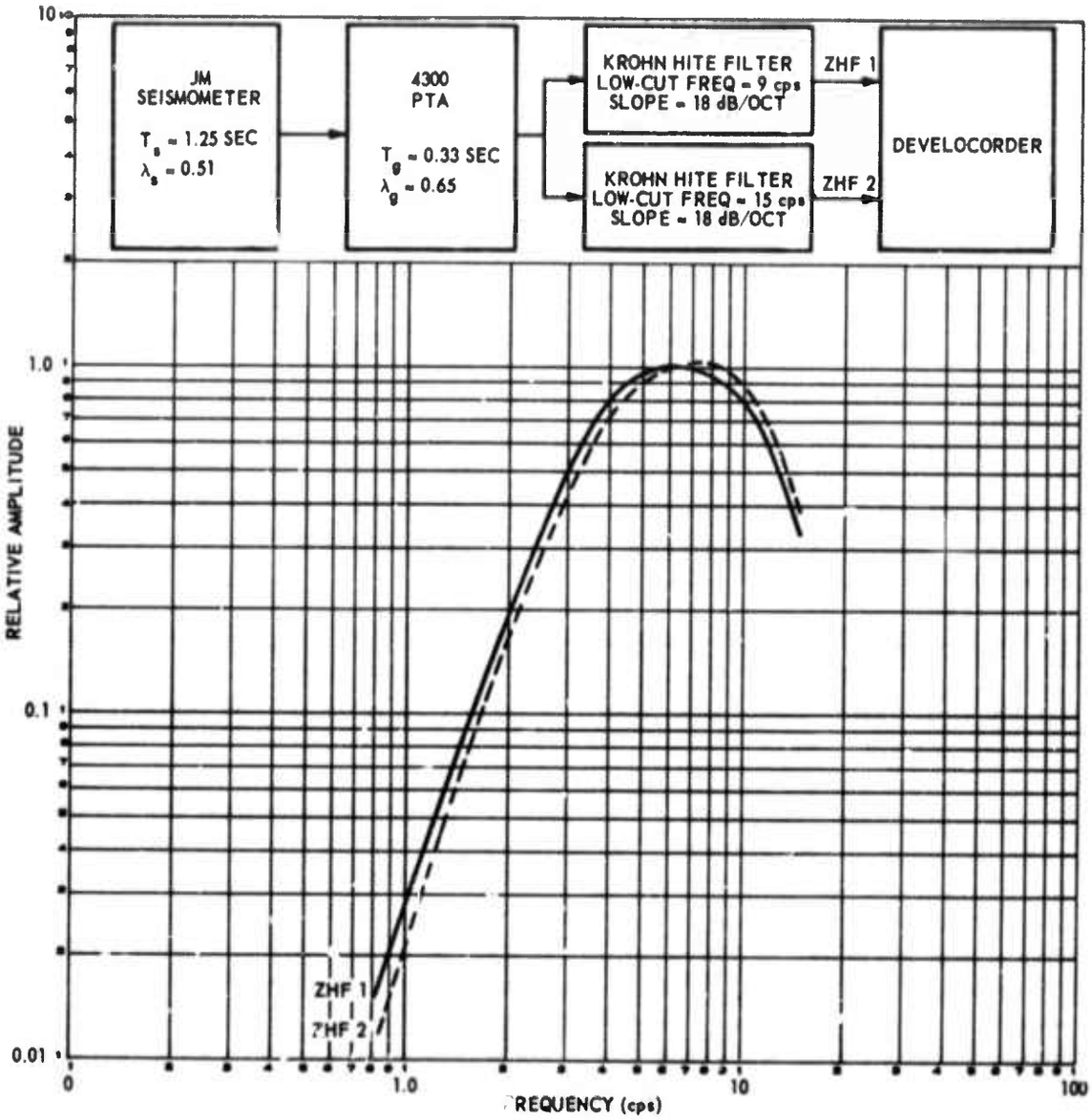

Figure 27. Frequency responses and block diagrams for ZHF1 and ZHF2

G 42

however, shaping of the responses of ZHF3 and ZHF4 was accomplished by modification of the PTA. The PTA modification included replacement of the 3 cps galvanometer with a 5 cps galvanometer, replacement of the Model 6824-1 filter with a Model 6824-7 filter, and the addition of a filter amplifier. These seismographs were operated with magnifications up to 10,000K at 6.0 cps. The frequency responses and block diagrams of these systems are shown in figure 28. Another high-frequency system, ΣGF, was produced by summation of the outputs of 24 Century geophones, Model 12FL, arranged in an 880-foot array. The estimated frequency response of ΣGF is shown in figure 29. These systems were activated between 13 and 16 September, with the exception of ZHF1, which was not activated immediately due to a malfunction in the Krohn-Hite filter. Data from these systems were recorded on both magnetic-tape and 16-millimeter film. Periodic recording of 16-millimeter film seismograms at a rate twice the normal short-period recording speed was accomplished in an effort to better resolve some of the higher-frequency signals recorded.

Figure 30 shows the signal from CHASE IV, partially masked by the signal from a local blast, and figure 31 shows typical microseismic background noise recorded by the high-frequency systems. On 1 October, the Project Officer requested that all high-frequency seismographs be recorded at three levels on both FM and digital magnetic tape. The three levels were adjusted to be 10, 30, and 50 dB below clipping level.

On 20 October, at the request of the Project Officer, recording of the ZHF1, ZHF2, and ZHF4 seismographs was discontinued and two new seismographs, ZHF5 and ZHF6, were activated. Figure 32 shows the frequency responses of these new systems.

In designing the ZHF5 and ZHF6 high-frequency seismographs, a moderate improvement in the signal-to-system noise ratio in the frequency range above 5.0 cps was achieved by using Model 4100-300 PTA galvanometers with natural frequencies of 10 cps directly coupled to the seismometer data coils. Also, the response of the new seismographs to the low-frequency components of seismic signals was reduced by including 2 additional low-cut filter sections in the circuits of the ZHF5 seismographs and 4 additional low-cut filter sections in the circuits of the ZHF6 seismographs. Block diagrams of the filter circuits and their responses are shown in figures 33 and 34.

Figures 35, 36, and 37 show the response of ZHF3, ZHF5, and ZHF6 to two teleseismic and one local event.

The high-frequency systems were recorded during the intervals listed in table 10. Recording of the high-frequency seismographs was discontinued on 7 July at the request of the Project Officer.

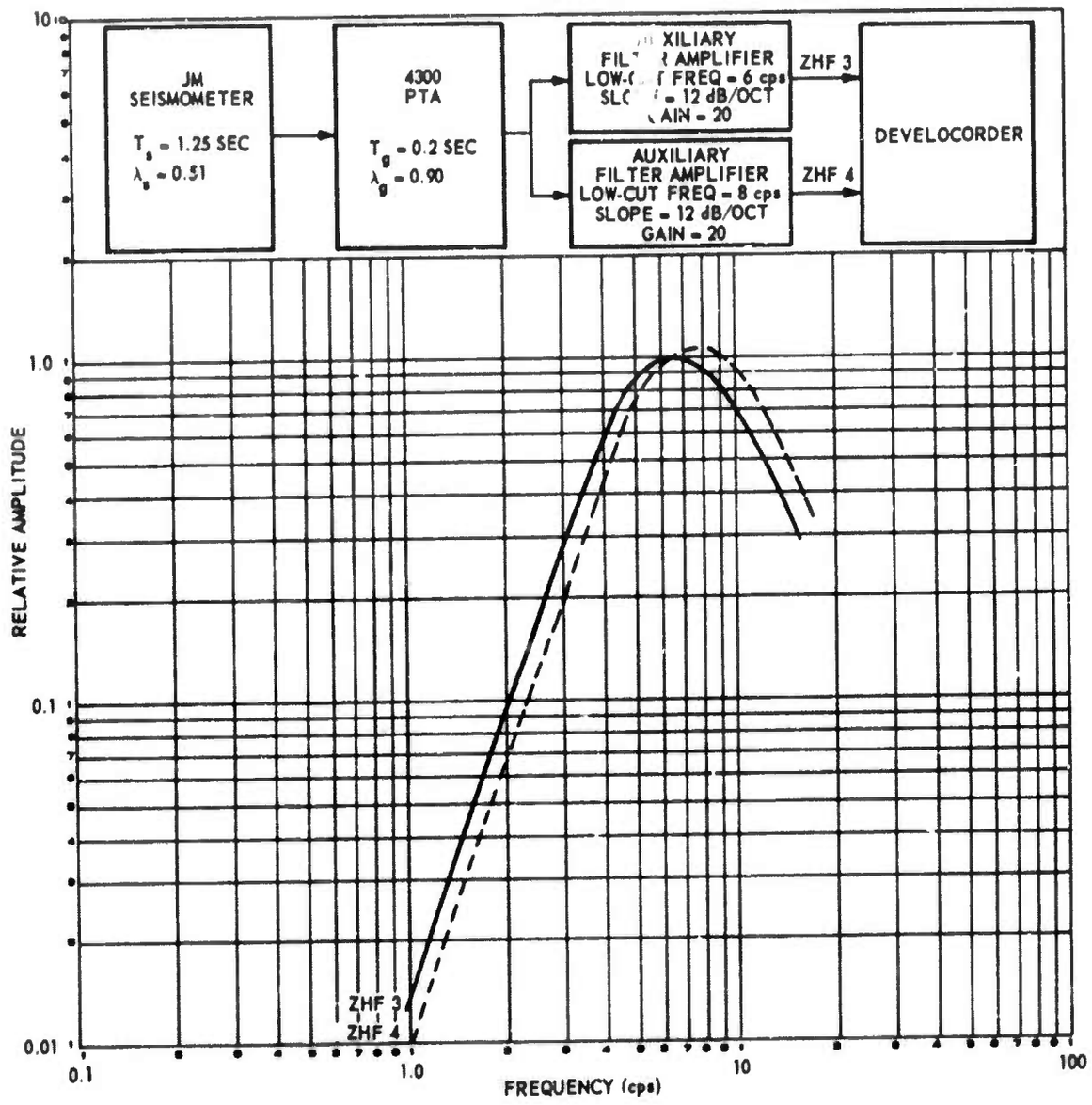

Figure 28. Frequency responses and block diagrams for ZHF3 and ZHF4

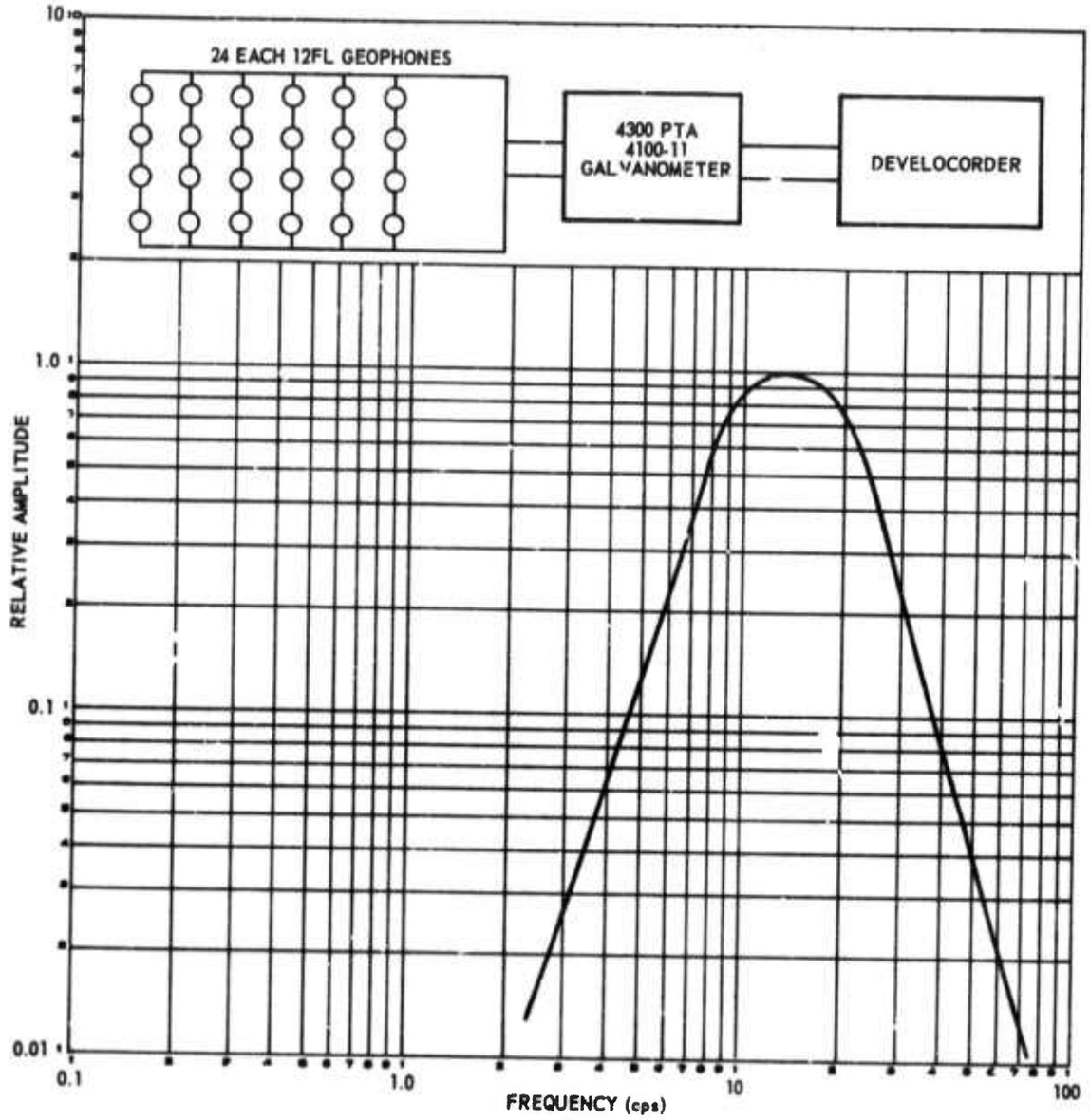

Figure 29. Block diagram and estimated frequency response for the geophone seismograph (ΣGF)

G 44

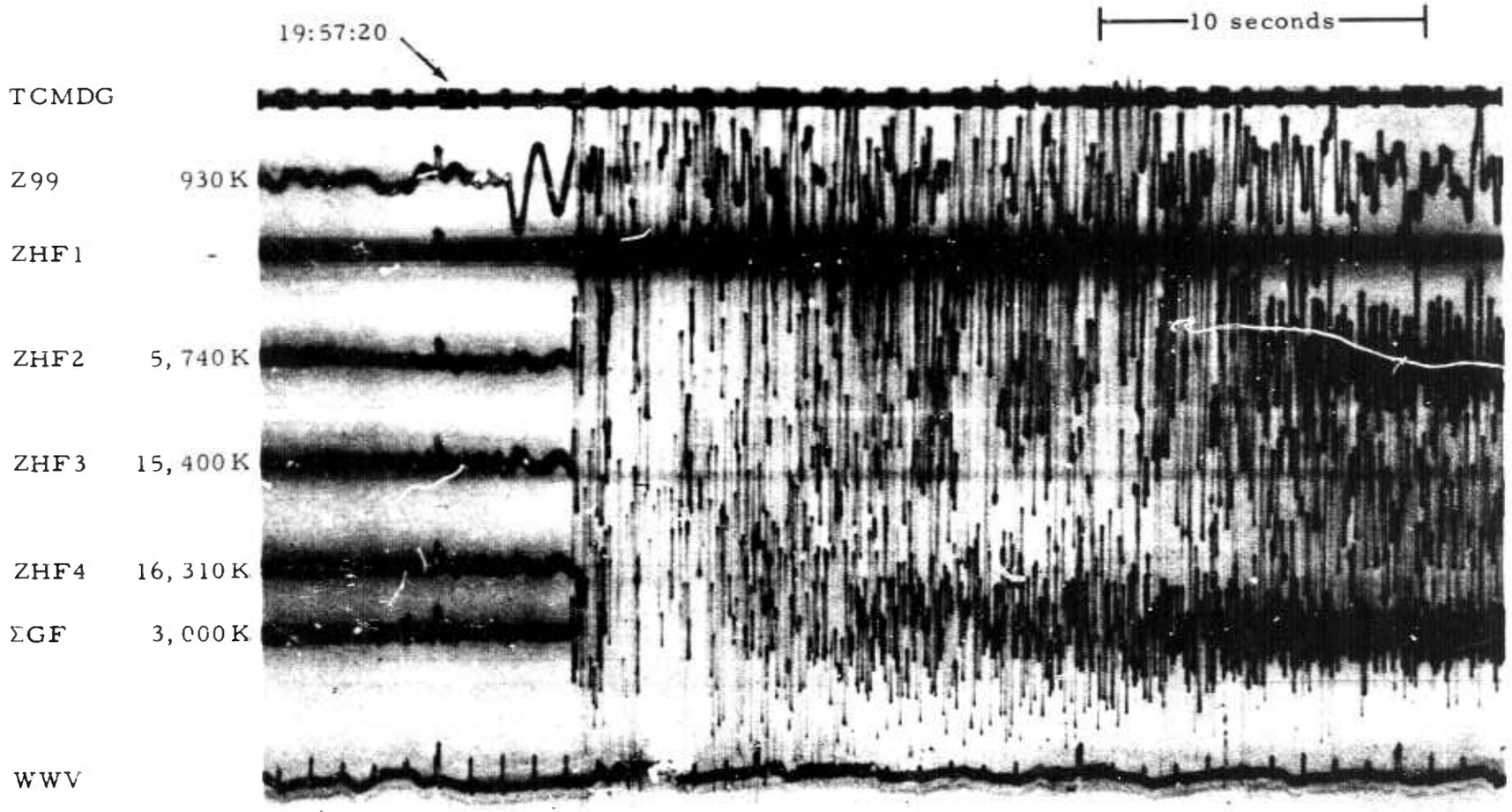

TFSO
16 Sept 65
Run 259
DG 7162
DT 9

Figure 30. P arrival from Chase IV as recorded by the standard (Z99) and high-frequency short-period seismographs at TFSO. Note signal partially masked by local blast. (X10 enlargement of 16-millimeter film)

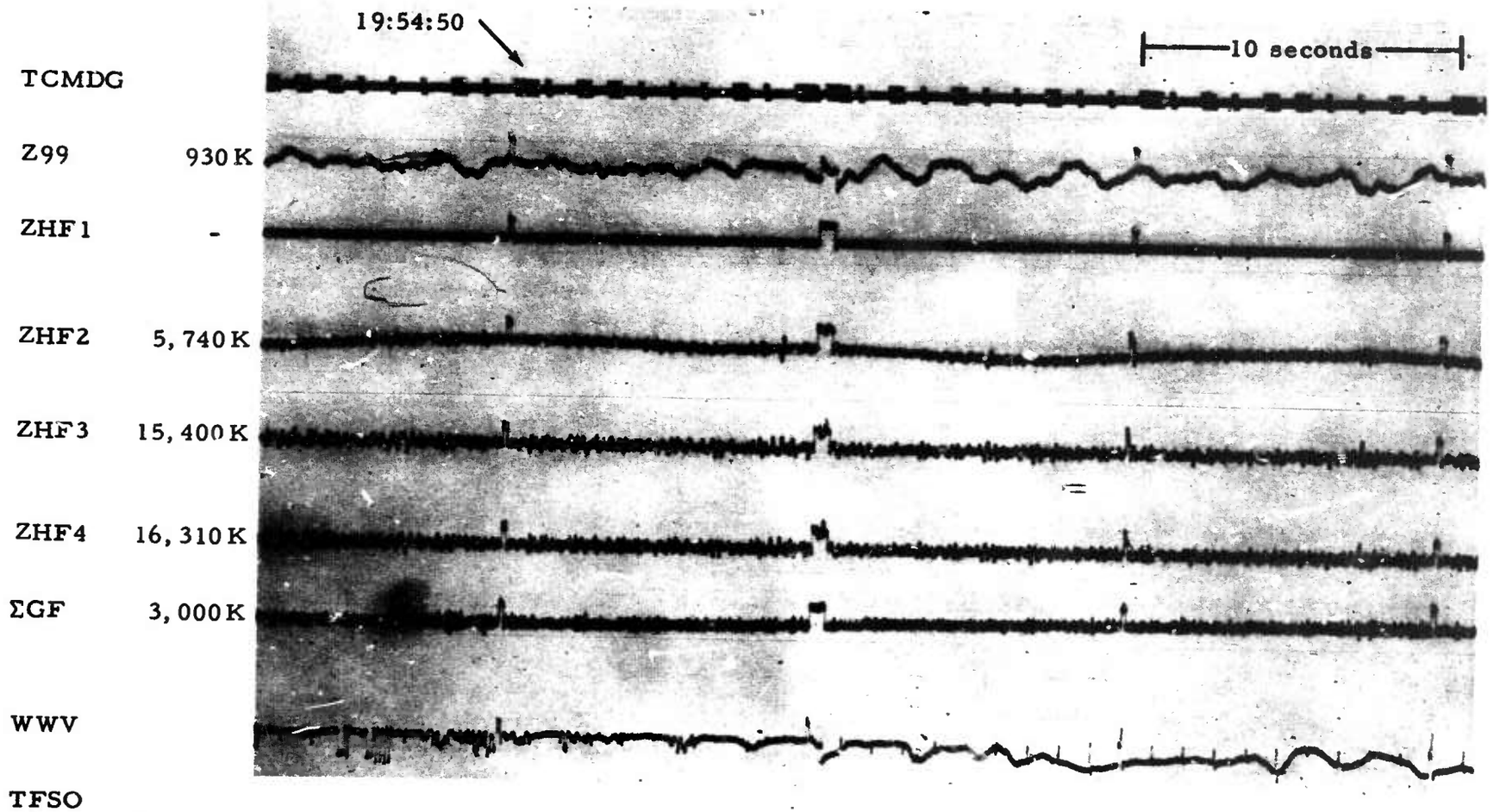

Figure 31. Normal background noise recorded by standard (Z99) and high-frequency short-period seismographs at TFSO. (X10 enlargement of 16-millimeter film)

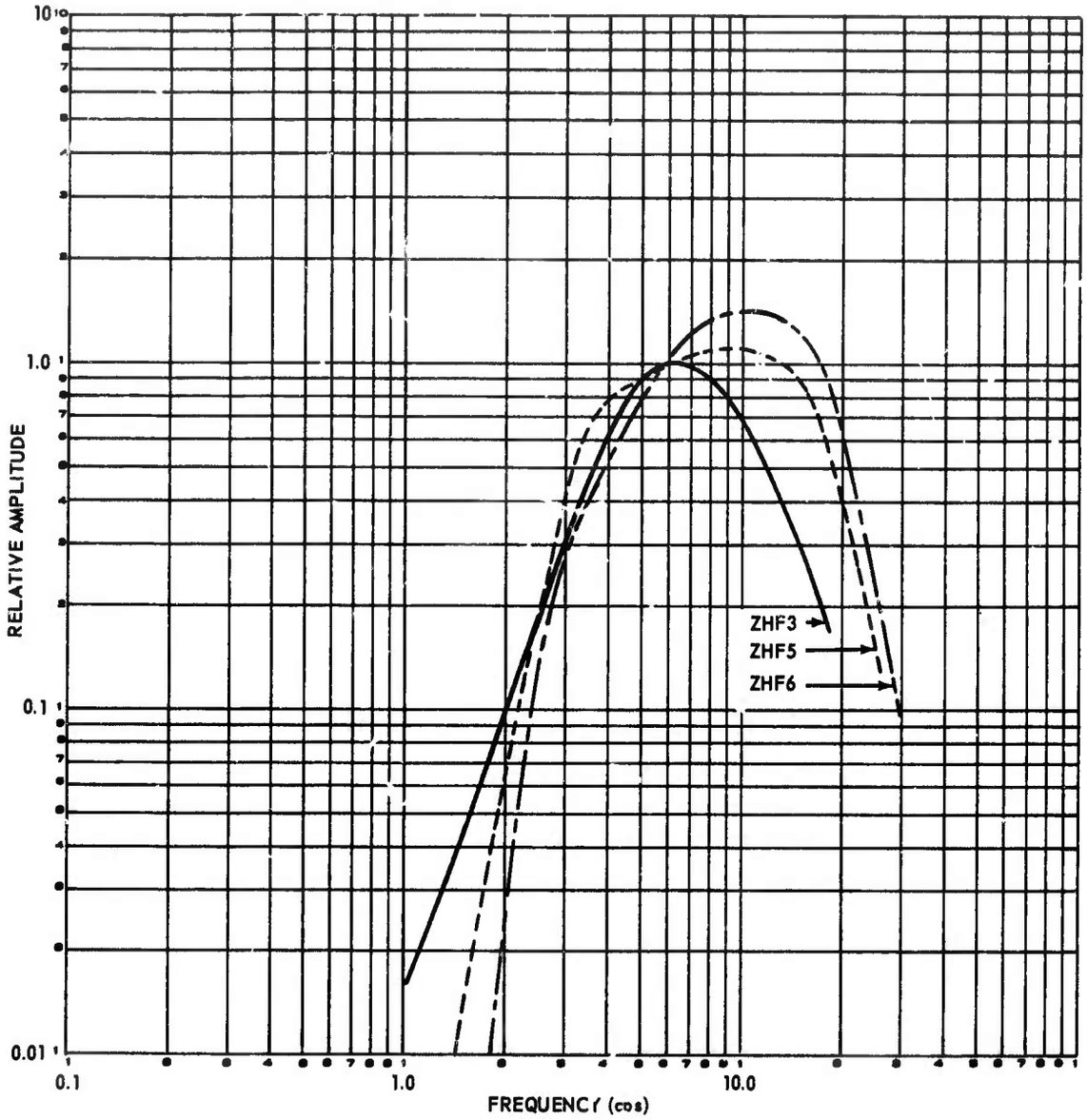

Figure 32. Frequency responses for the high-frequency seismographs. (These responses are plotted for constant amplitude input and apply to the film recordings.

G 45

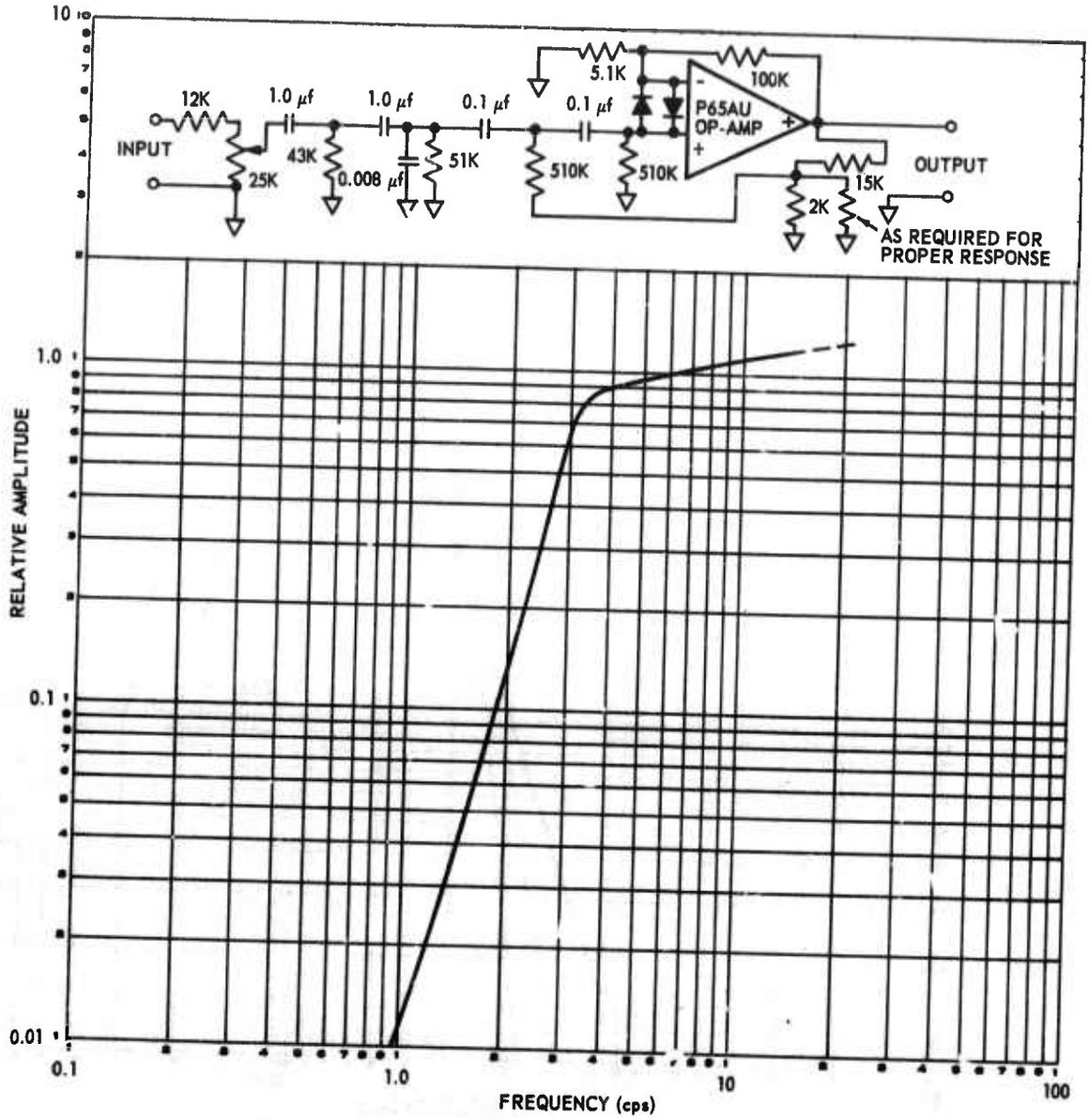

Figure 33. Simplified circuit diagram and calculated frequency response for the filter amplifier for the ZHF5 high-frequency seismograph. The maximum gain of this channel is approximately 10 at 6 cps

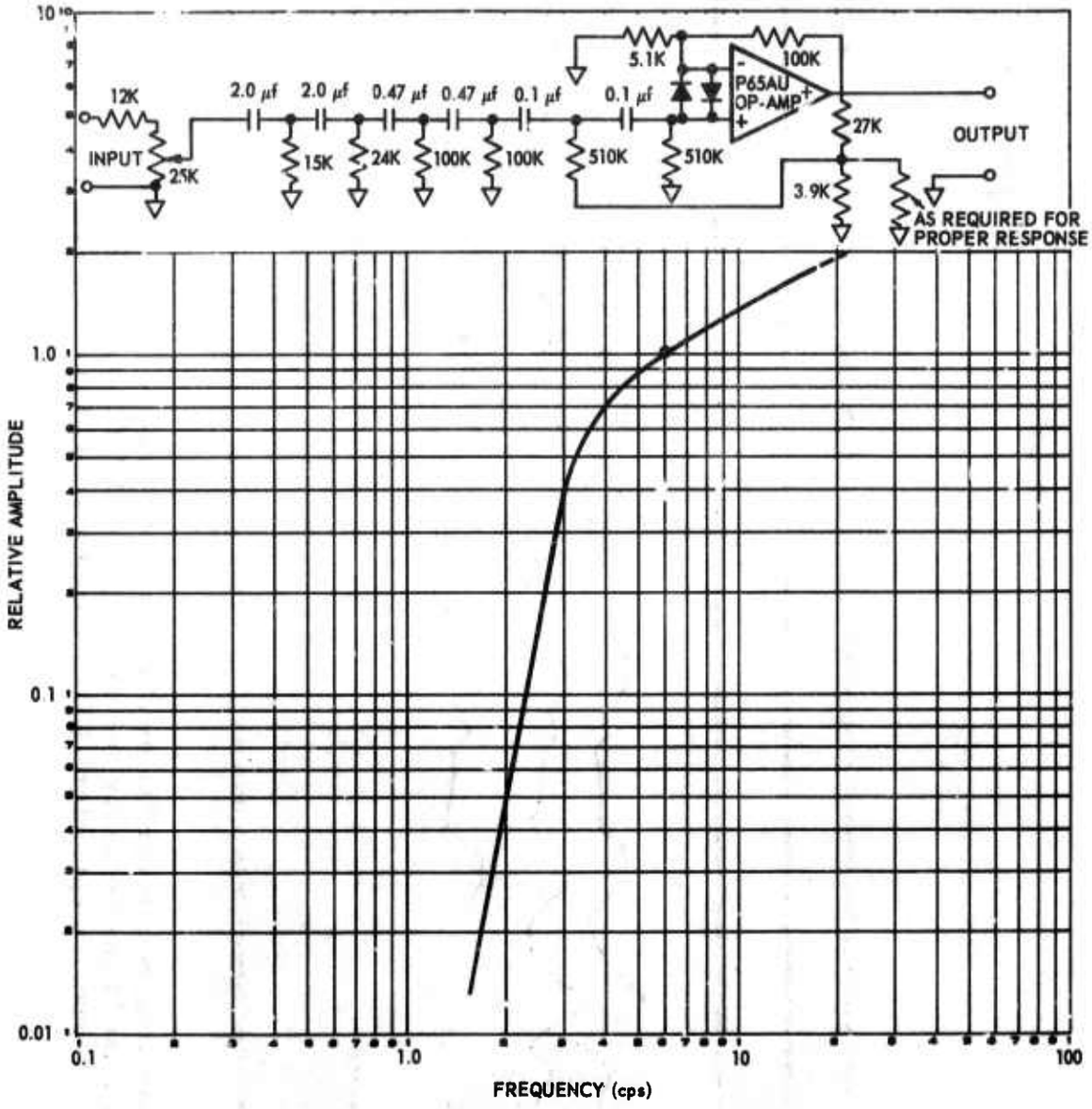

Figure 34. Simplified circuit diagram and calculated frequency response for the filter amplifier for the ZHF6 high-frequency seismograph. The maximum gain of this channel is approximately 6 at 6 cps

G 35

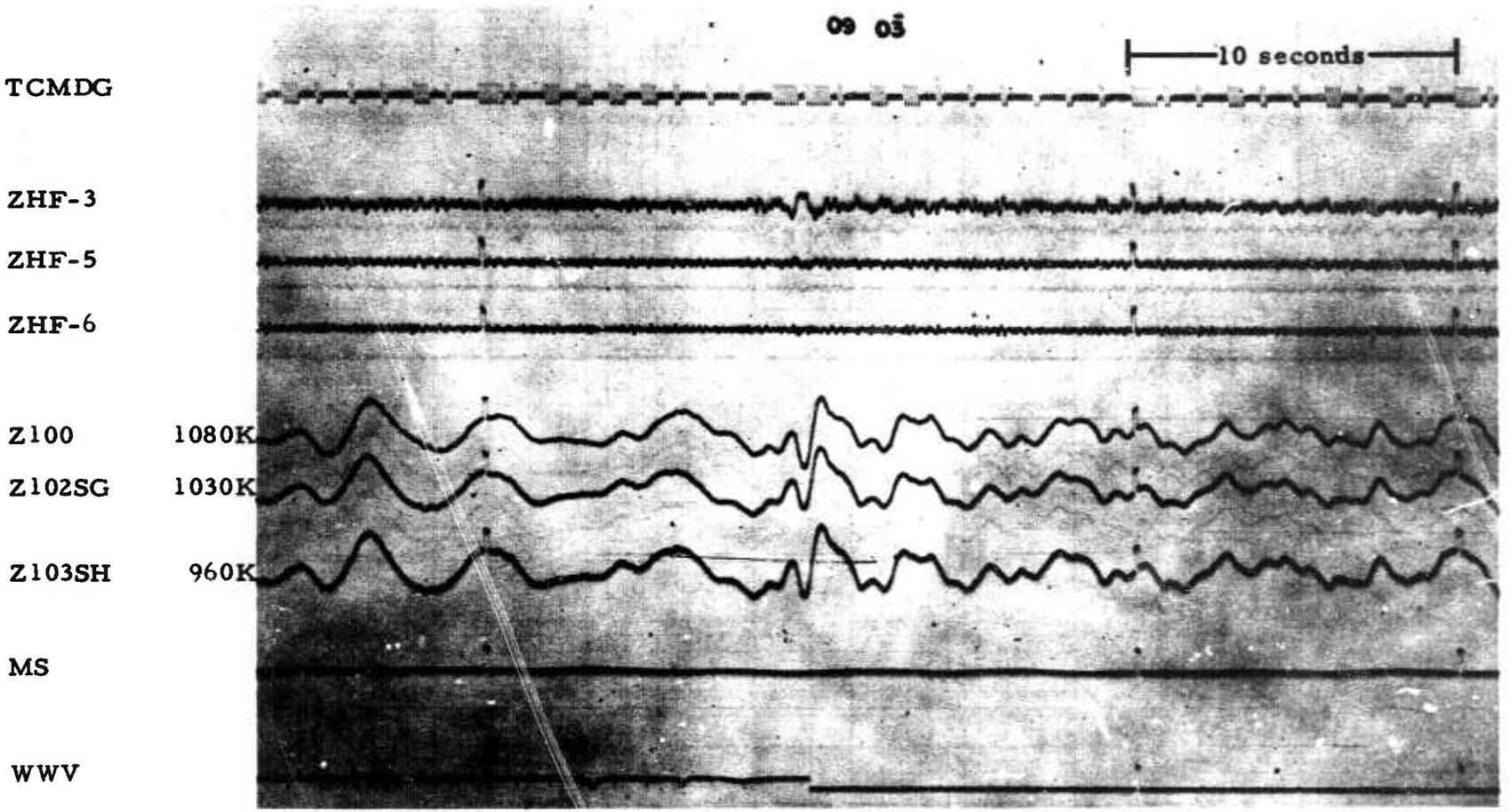

TFSO Figure 35. Short-period recording exhibiting the response of the shallow-well seismometers, improvised high-frequency seismometers, and JMZ to a teleseismic event from unknown epicenter. (X10 enlargement of 16 millimeter film)
Run 025
25 Jan 1966
Data Group 7178

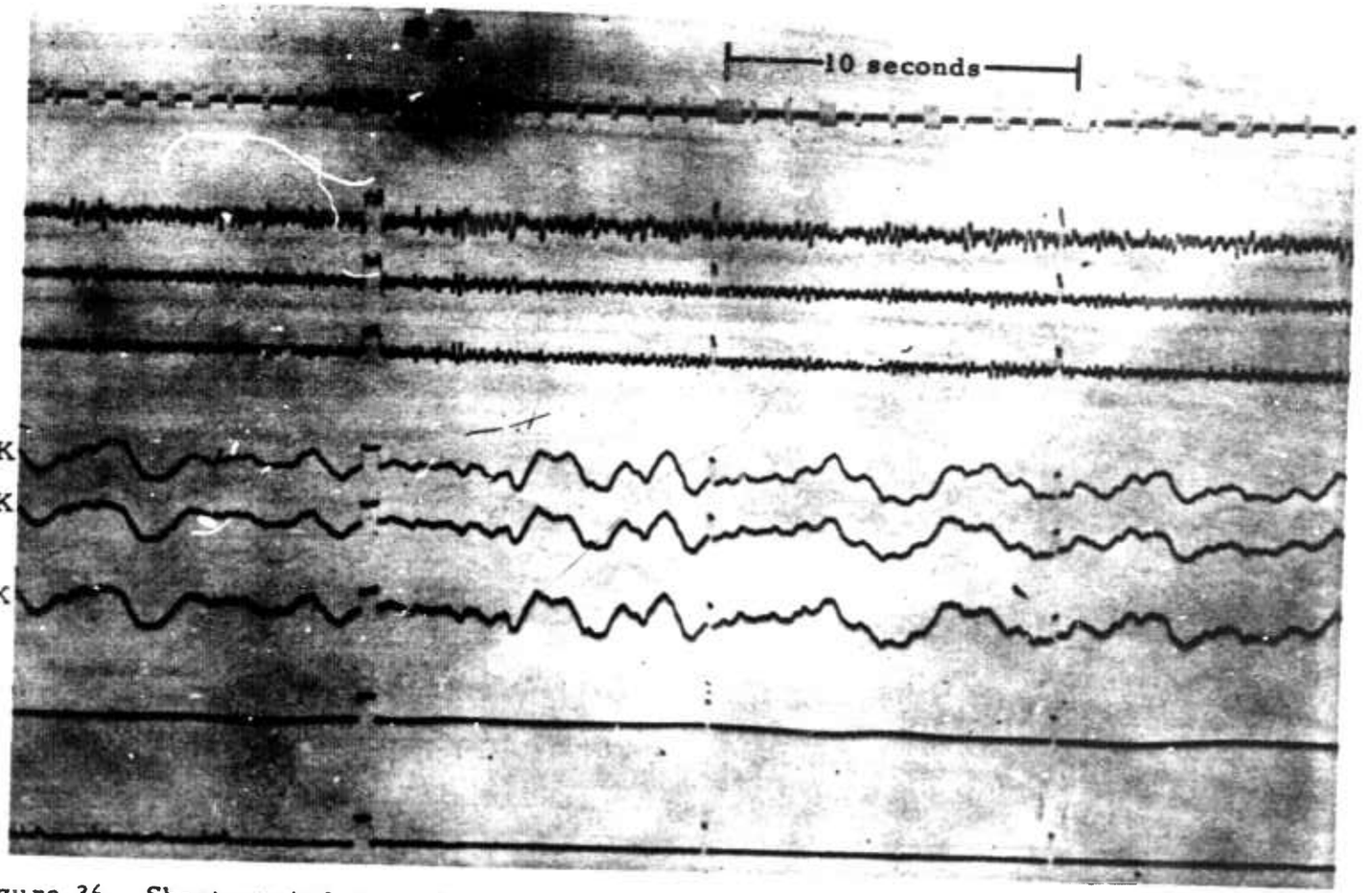

Figure 36. Short-period recording exhibiting the response of the shallow-well seismometer, the improvised high-frequency seismometers and JMZ to a teleseismic event from Borneo. Epicentral data: $\Delta = 121.8^{o}$, Azimuth = 297^{o}, h = 42 km, o = 18:05:54.4 (X10 enlargement of 16-millimeter film)

TFSO
Run 025
25 Jan 1966
Data Group 7178

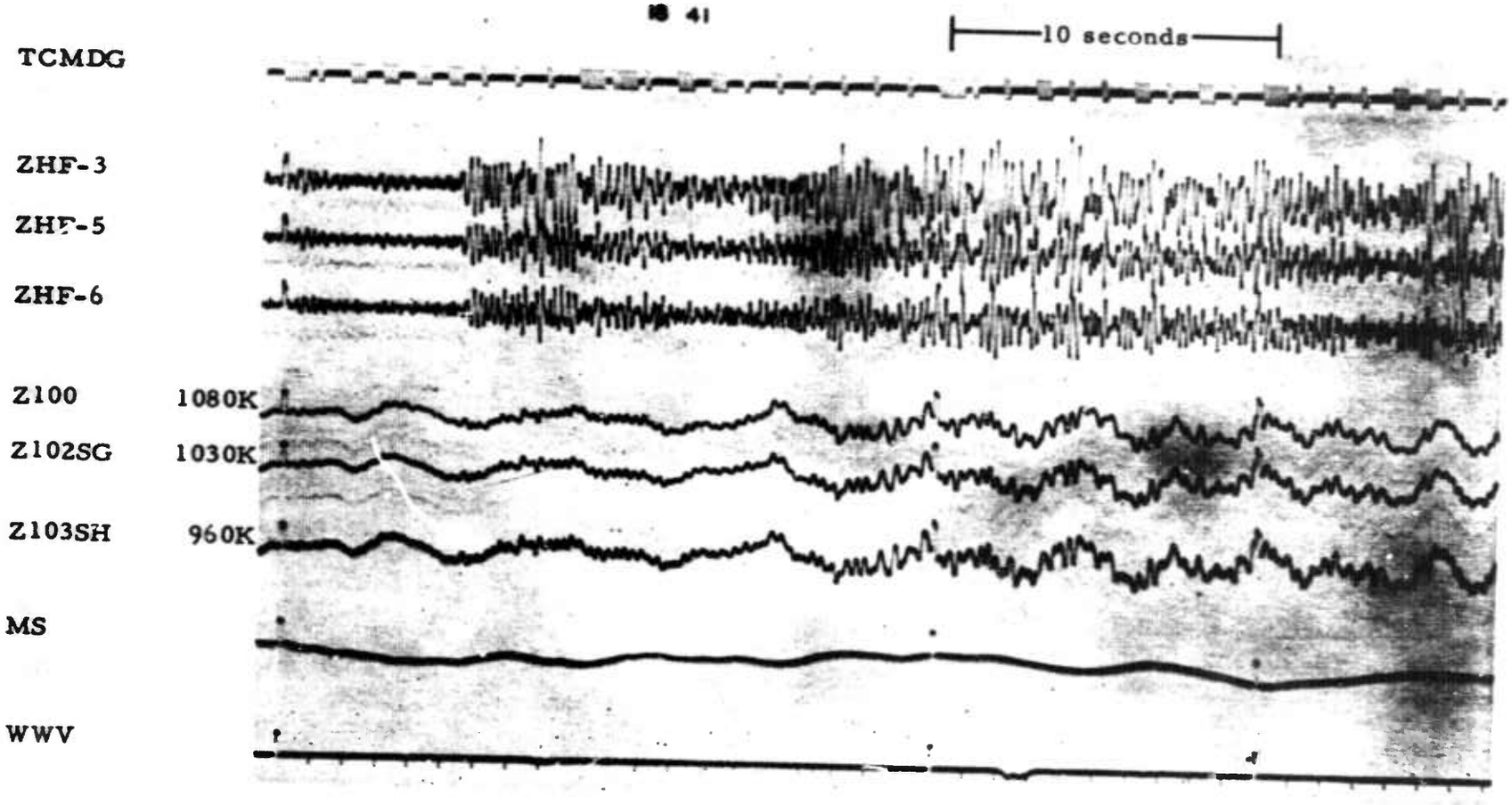

TFSO
Run 025
25 Jan 1966
Data Group 7178

Figure 37. Short-period recording exhibiting the response of the shallow-well seismometer, the improvised high frequency seismometer, and JMZ to a local event. (X10 enlargement of 16-millimeter film)

Table 10. High-frequency seismograph recording intervals

Period of operation	Develocorder	Tape (FM)	Tape (digital)
15 September to 13 October	ZHF 1 ZHF 2 ZHF 3 ZHF 4 ΣGF	ZHF 1 ZHF 2 ZHF 3 ZHF 4 ΣGF	
13 October to 20 October	ZHF 1 ZHF 2 ZHF 3 ZHF 4	ZHF 1 (hi, med, lo) ZHF 2 (hi, med, lo) ZHF 3 (hi, med, lo) ZHF 4 (hi, med, lo)	ZHF 1 (hi, med, lo) ZHF 2 (hi, med, lo) ZHF 3 (hi, med, lo) ZHF 4 (hi, med, lo)
20 October to 7 July 1966	ZHF 3 ZHF 5 ZHF 6 ΣGF	ZHF 3 (hi, med, lo) ZHF 5 (hi, med, lo) ZHF 6 (hi, med, lo) ΣGF (hi, med, lo)	ZHF 3 (hi, med, lo) ZHF 5 (hi, med, lo) ZHF 6 (hi, med, lo) ΣGF (hi, med, lo)

KEY

ZHF 1 Peaked at 6 cps
ZHF 2 Peaked at 8 cps
ZHF 3 Peaked at 6 cps
ZHF 4 Peaked at 8 cps
ZHF 5 Peaked at 10 cps
ZHF 6 Peaked at 10 cps
ΣGF Summation of Century Geophones

7.1.3 Distortion Threshold

A study of the high-frequency 16-millimeter film seismograms, spectrograms, and filtered playbacks produced from the magnetic-tape seismograms indicated that the ratio of the seismic-signal level to system-noise level of the systems was inadequate in the frequency range above 5 cps. In addition, it is probable that because of the low-frequency response characteristics of these high-frequency systems, the high-amplitude, low-frequency components of some strong seismic signals produced high-frequency distortion components that tend to obscure the high-frequency signal components.

The distortion threshold curve, figure 38, which was previously published in TR 65-133 and TR 66-54, applies to the ZHF5 seismographs at all observatories. The solid portion of the curve, which extends across the frequency range from 0.5 to 2.5 cps, indicates the equivalent ground motion that will produce a PTA output of 10 volts peak-to-peak. At this output level, a well adjusted PTA should produce no more than 1 percent total harmonic distortion.

At the request of the Project Officer, subsequent tests were conducted at TFSO to verify the distortion threshold curve and to examine the system distortion when large input signals were applied. Oscillograms made during these tests are presented in figures 39 through 41. The PTA output voltage, which is presented on the lower trace of each oscillogram, was set to 10, 20, and 30 volts peak-to-peak for the three tests and was passed through the isolation amplifier (iso-amp). The upper traces of the oscillograms show the PTA output filtered by the ZHF5 filter amplifier unit. The frequency response shown in fugure 33 indicates that this unit amplifies the second and third harmonic components of a 1 cps signal 10 and 50 times more, respectively, than the fundamental component is amplified. Thus, the percentage distortion on the upper trace should be at least 10 times greater than on the lower trace. In figure 39, there is about 10 percent distortion on the upper trace indicating approximately 1 percent distortion on the lower trace, even though this distortion is not visible. This percentage distortion and output level correspond to the data used to plot the curve in figure 38.

With the function generator set to produce 20 volts at the PTA output, the distortion is clearly visible on the lower trace (figure 40). The corresponding upper trace has been resolved into the fundamental and distortion components in figure 42. Taking into account the frequency response of the filter amplifier, the PTA output signal contains about 7 percent distortion at this output level. Also shown in figure 42 is a curve indicating the approximate percentage distortion for a PTA at various output levels.

We computed that the LONG SHOT event (TFSO peak amplitude 380 millimicrons at 1.25 cps) produced about 27 volts peak-to-peak at the output of the ZHF5 PTA, with approximately 10 percent harmonic distortion (about

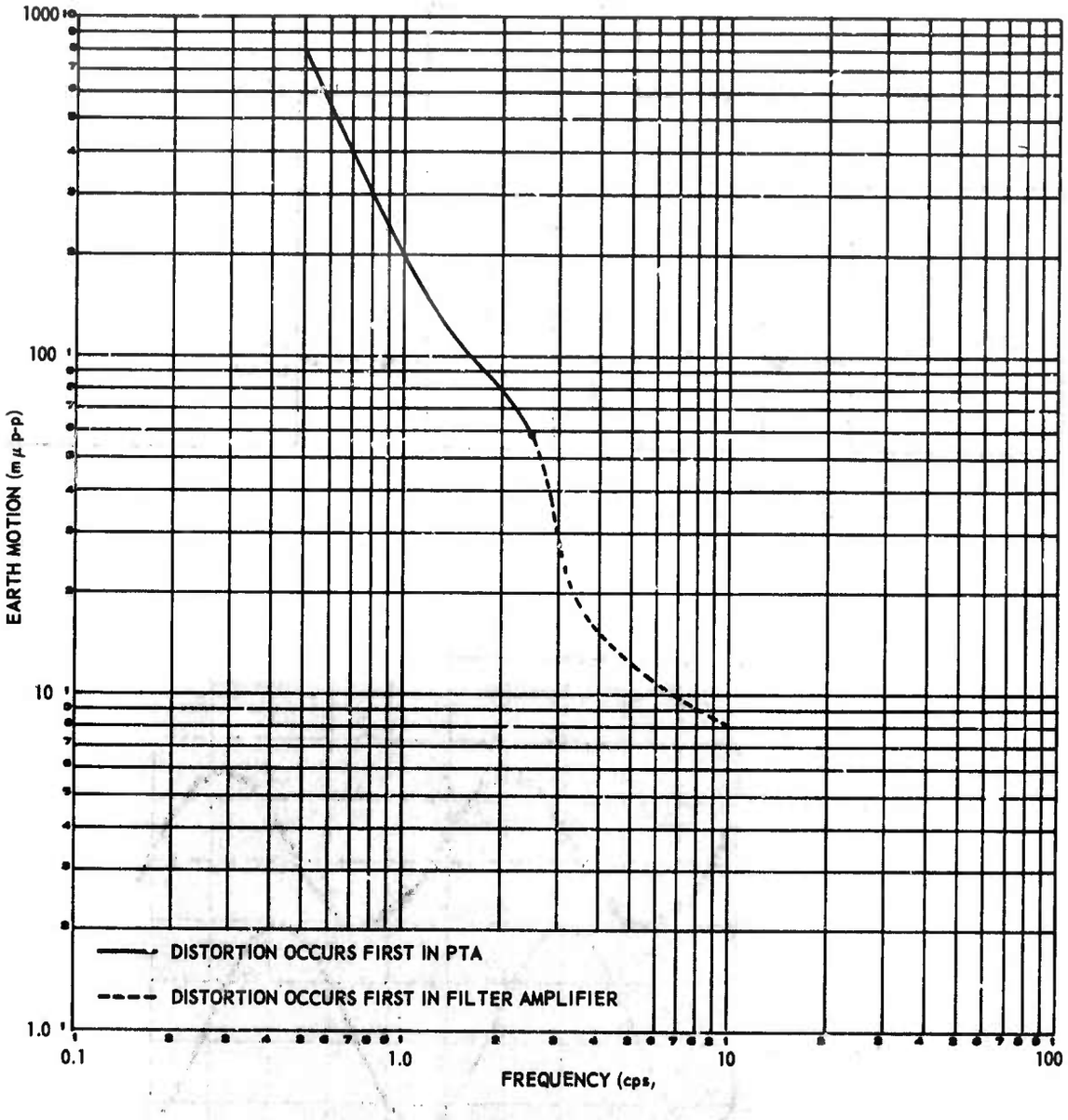

Figure 38. Distortion threshold curve for the ZHF5 seismograph at normal gain setting, and the ZHF6 seismograph for frequencies below 2.5 cps. This curve indicates the maximum input that the seismograph can amplify without distortion

G 433

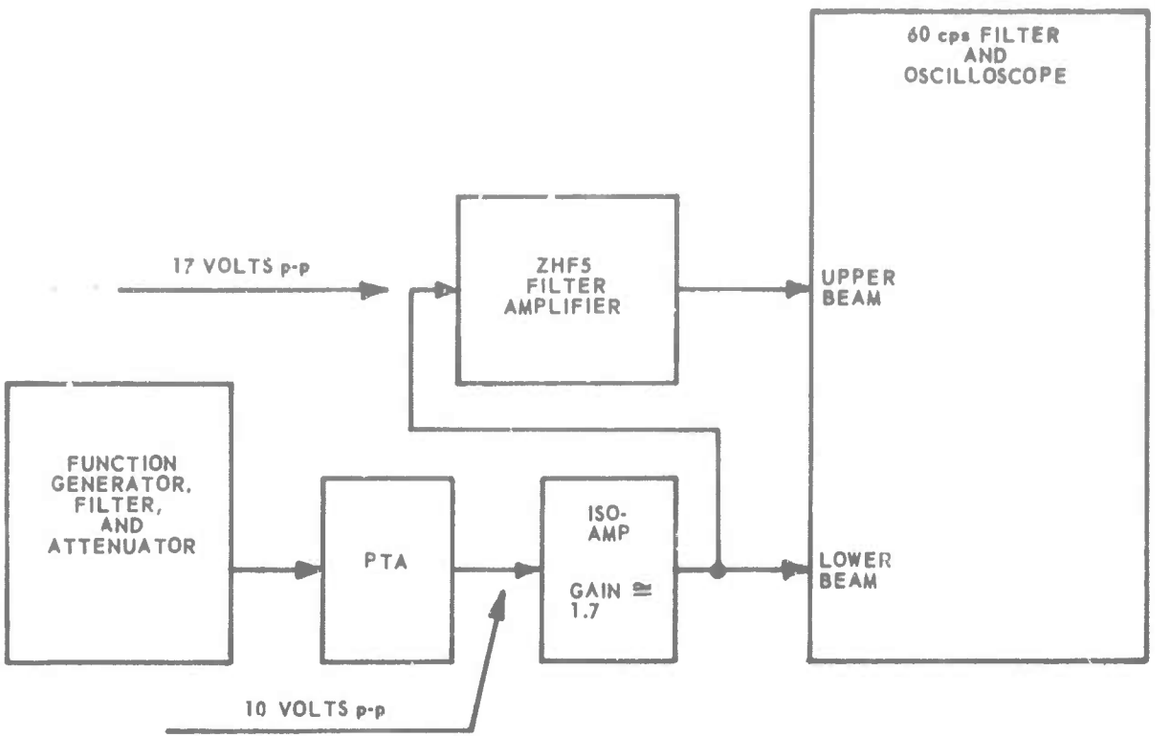

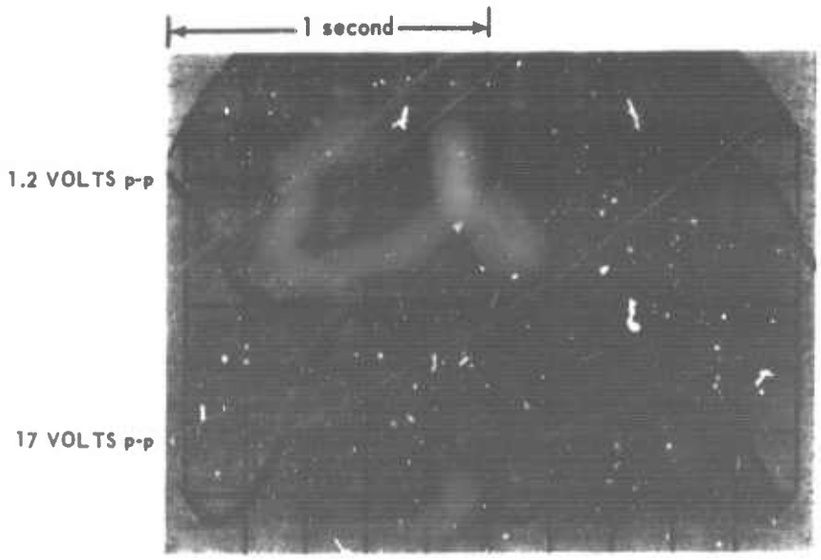

Figure 39. Block diagram and oscillogram for test of ZHF5 components with a PTA output level of 10 volts p-p

G 2589

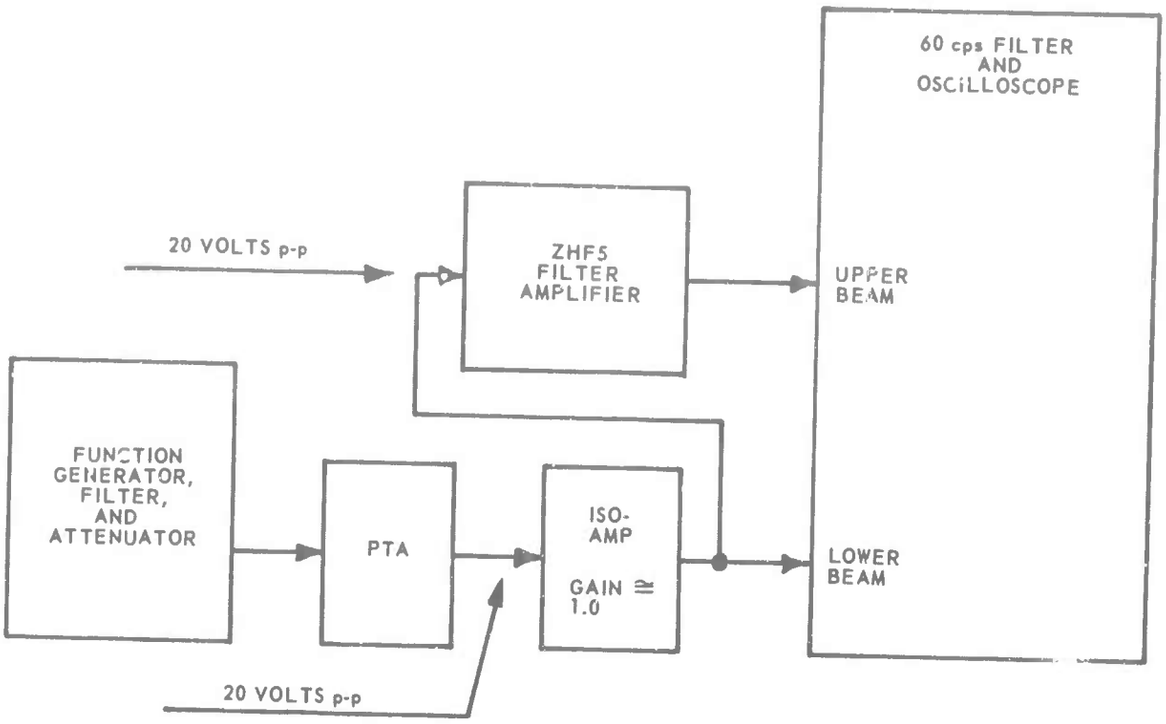

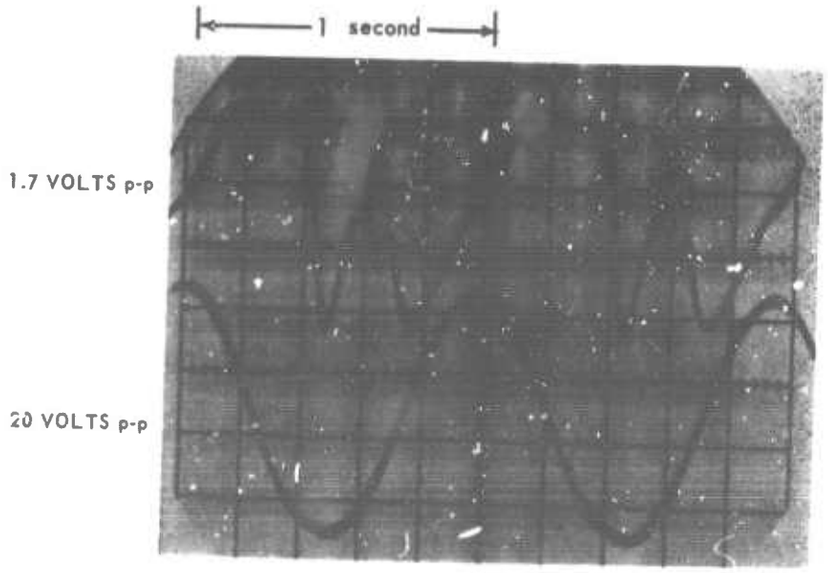

Figure 40. Block diagram and oscillogram test of ZHF5 components with a PTA output level of 20 volts p-p

G 2590

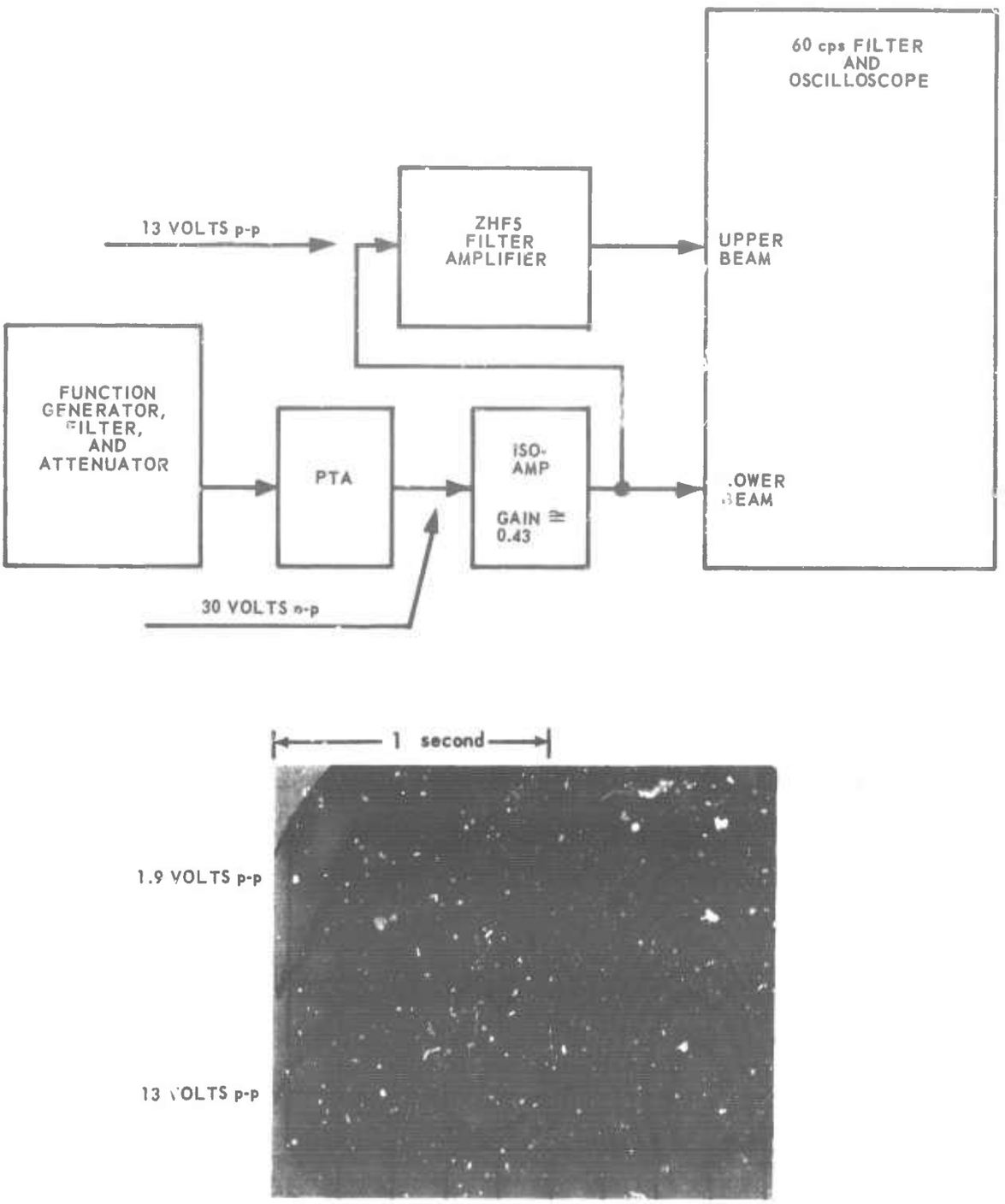

Figure 41. Block diagram and oscillogram for test of ZHF5 components with a PTA output level of 30 volts p-p G 2591

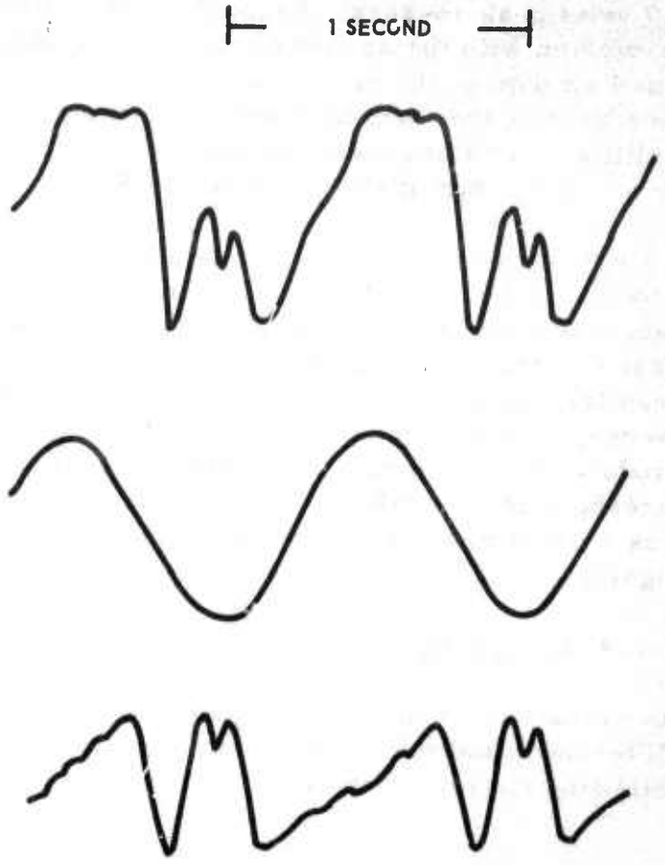

A. OUTPUT OF PTA (20 VOLTS p-p AT 1.0 cps) FILTERED BY THE ZHF5 FILTER AMPLIFIER

B. FUNDAMENTAL COMPONENT OF THE WAVEFORM SHOWN IN FIGURE 1A

C. HARMONIC DISTORTION COMPONENTS OF THE WAVEFORM SHOWN IN FIGURE 1A

D. APPROXIMATE PERCENTAGE DISTORTION AT THE OUTPUT OF A PTA

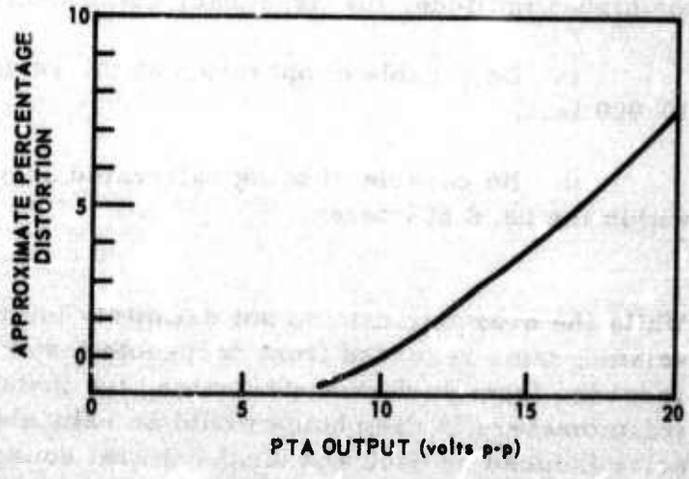

Figure 42. Output waveforms and approximate distortion curve for a short-period PTA G 2592

2.7 volts peak-to-peak). Although most of this distortion voltage was associated with the second harmonic frequency of the signal (2.5 cps), a small amount of the distortion voltage (at least 0.5 volts peak-to-peak) was generated at the third harmonic frequency (3.75 cps). Approximately 2 millimicrons of ground motion at 3.75 cps would be required to produce the same voltage at the output of the PTA.

A study of the P arrival from the LONG SHOT event, published in Appendix 3 to TR 66-54, indicated that the amplitudes of the signal components decreased with increasing frequency at a rate of at least 24 dB per octave. Based on this, any signal components in the vicinity of 3.75 cps would have been less than 2 millimicrons. At this frequency, the distortion voltage at the output of the PTA was greater than the voltage which would have been produced by the maximum expected signal. We determined that the distortion threshold of the ZHF3 system was approximately 225 millimicrons at 1.25 cps; this system was also driven into the distortion region by the LONG SHOT signal.

7.1.4 Evaluation

An evaluation of the high-frequency seismographs as they were operated at TFSO indicated that an adequate high-frequency system should have the following characteristics:

a. Have an increase in signal-to-system noise ratio of about 12 dB/octave in the frequency range from 3 to 10 cps;

b. Be much less susceptible to problems arising from distortion of the high-amplitude, low-frequency components of seismic signals;

c. Be capable of operation at the surface or at any depth up to 10,000 feet;

d. Be capable of being calibrated accurately at all frequencies within the band of interest.

While the available data do not definitely indicate that the high-frequency seismograms recorded from deep-hole instruments are superior to those recorded from surface instruments, the installation of high-frequency seismometers in deep holes would be valuable in reducing the effects of noise induced by wind and local cultural sources. In addition, it is possible that the high-frequency components of seismic signals might be detected best by buried seismometers.

7.1.5 Recommendation for Optimum System

The report of the investigation of the desired characteristics and instrumentation requirements for an improved high-frequency system were submitted to the Project Officer in P-624 on 15 April 1966. We stated that the most expeditious and economical approach to the design of a suitable seismometer would be to modify and/or to combine several available seismometers in order to obtain a seismometer with the required characteristics.

A memorandum describing the requirements of an improved high-frequency seismograph, the various tests on which these requirements were based, and a request for authority to build a high-frequency seismograph were submitted to the Project Officer in late October 1966. We concluded from these tests that eight Model GS-13V geophones, installed in a pressure case, would provide a satisfactory seismometer for an improved high- equency seismograph. These geophones are produced by Engineering Products Company of Tulsa, Oklahoma, and would each be modified to have a 0.453-kilogram mass and a 2,860-ohm data coil. An Ithaco amplifier was recommended for amplification of the output of this seismometer.

7.2 LONG-PERIOD SYSTEM TESTS

7.2.1 Tests of Standard Seismograph Systems

An evaluation of the standard TFSO long-period seismograph system was initiated early in the reporting period. A series of tests, the purpose of which was to improve the general response of the system, continued throughout the contract. Modifications resulting from these tests are discussed in section 3.10.1.

Tests include the following:

a. Installation of 110-second Harris galvanometers;

b. Installation of new cable between the seismometers and the PTA's;

c. Operation of a long-period PTA in the central recording building;

d. Evaluation of the effectiveness of convection shields installed over the seismometers and of the case heaters;

e. Operation of the system in a pressure-sealed pier room;

f. Operation of a seismograph in a buried metal near-surface tank vault.

Figures 43 through 46 are seismograms made during various tests of the standard long-period system. Note that the effective magnification of the horizontal components was increased by a factor of 10. Operation of the seismograph in the buried metal vault is still in progress. The surface long-period vault was installed by blasting into a surface granite outcrop approximately 1000 feet northwest of the walk-in-vault.

7.2.2 Tests of Experimental Seismograph

A modified Geotech Long-Period Seismometer, Model 8700C, was shipped to TFSO in May 1965 for testing. The tests conducted were designed to determine whether the Model 8700C long-period horizontal seismometer, modified by replacing the standard cross-ribbon flexure hinge system with a wire-flexure hinge system, afforded improved seismograph operational characteristics. The mast and boom assemblies of the standard Model 8700C seismometer and the modified seismometer are shown in figures 47 and 48, respectively.

7.2.2 1 Stability of Natural Period

The modified seismometer was adjusted so that its natural period was 20 seconds with the mass centered. The mass-position was then varied, and the natural period of the seismometer was checked at several different mass positions. The seismometer was then adjusted to a natural period of 30 seconds with the mass centered, and the process was repeated. The results of these tests are shown in figure 49. The maximum natural period changes observed were about 3.5 and 5.5 percent with the natural period of the seismometer set at 20 and 30 seconds, respectively. Figure 50 shows corresponding data for a typical standard Model 8700C seismometer.

7.2.2.2 Response of the Modified Seismometer to Vertical Forces

Data for table 11 were obtained by augmenting the inertial mass of the seismometer and recording the position of the seismometer mass before and after each weight change. These data indicate that the seismometer is relatively insensitive to vertically applied forces and, therefore, will be insensitive to the mass buoyancy forces caused by atmospheric pressure changes.

7.2.2.3 Determination of Open-Circuit Damping of the Modified Seismometer

The open-circuit damping of the modified seismometer was determined from an analog recording of the open-circuit natural period and the following formula:

$$\lambda = \sqrt{\frac{\alpha^2}{4\pi^2 + \alpha^2}}$$

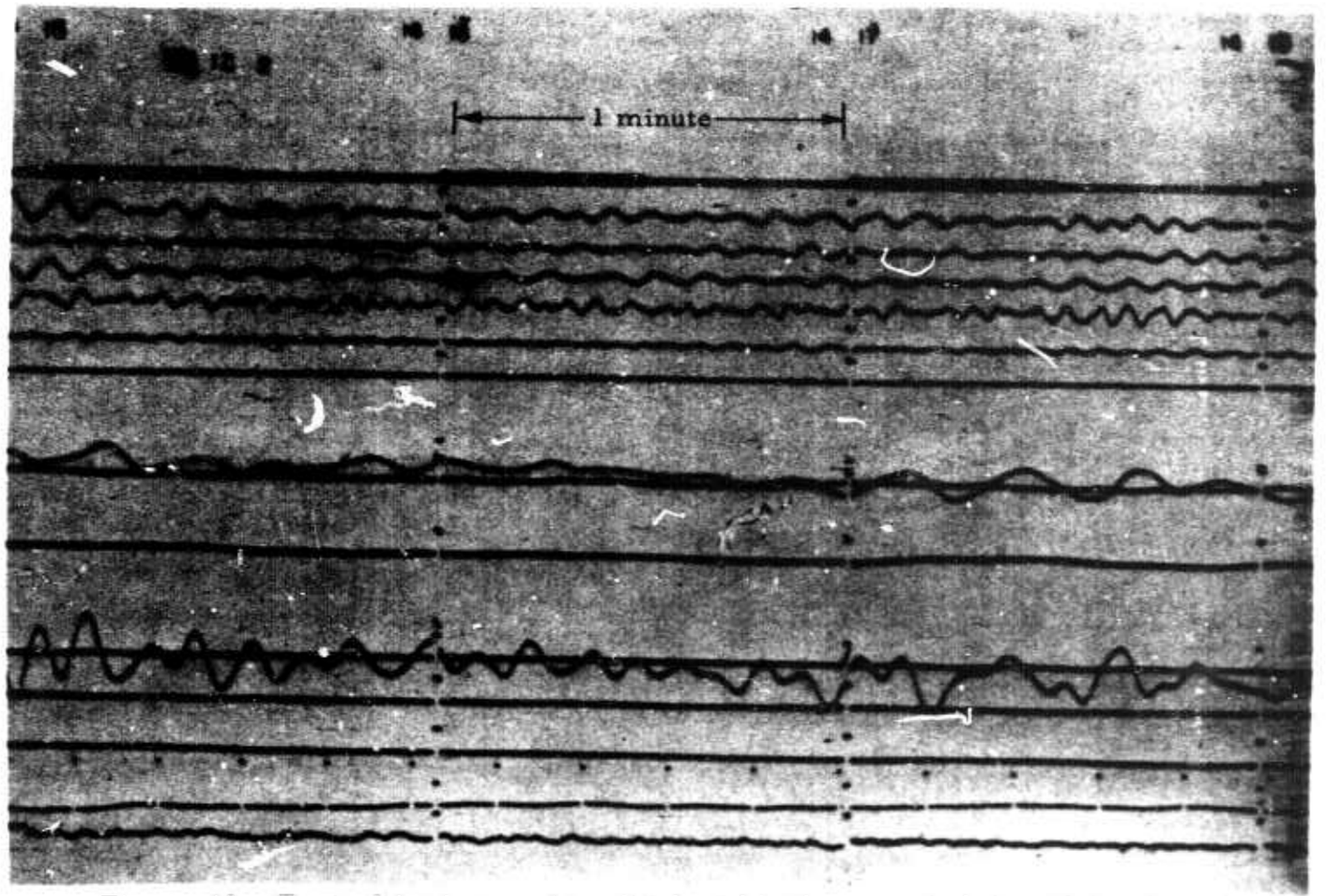

Figure 43. Typical background as displayed by long-period, broad-band, and intermediate band seismographs at TFSO near beginning of reporting period. Note magnifications of horizontal components of long-period system. (X10 view of 16-millimeter film)

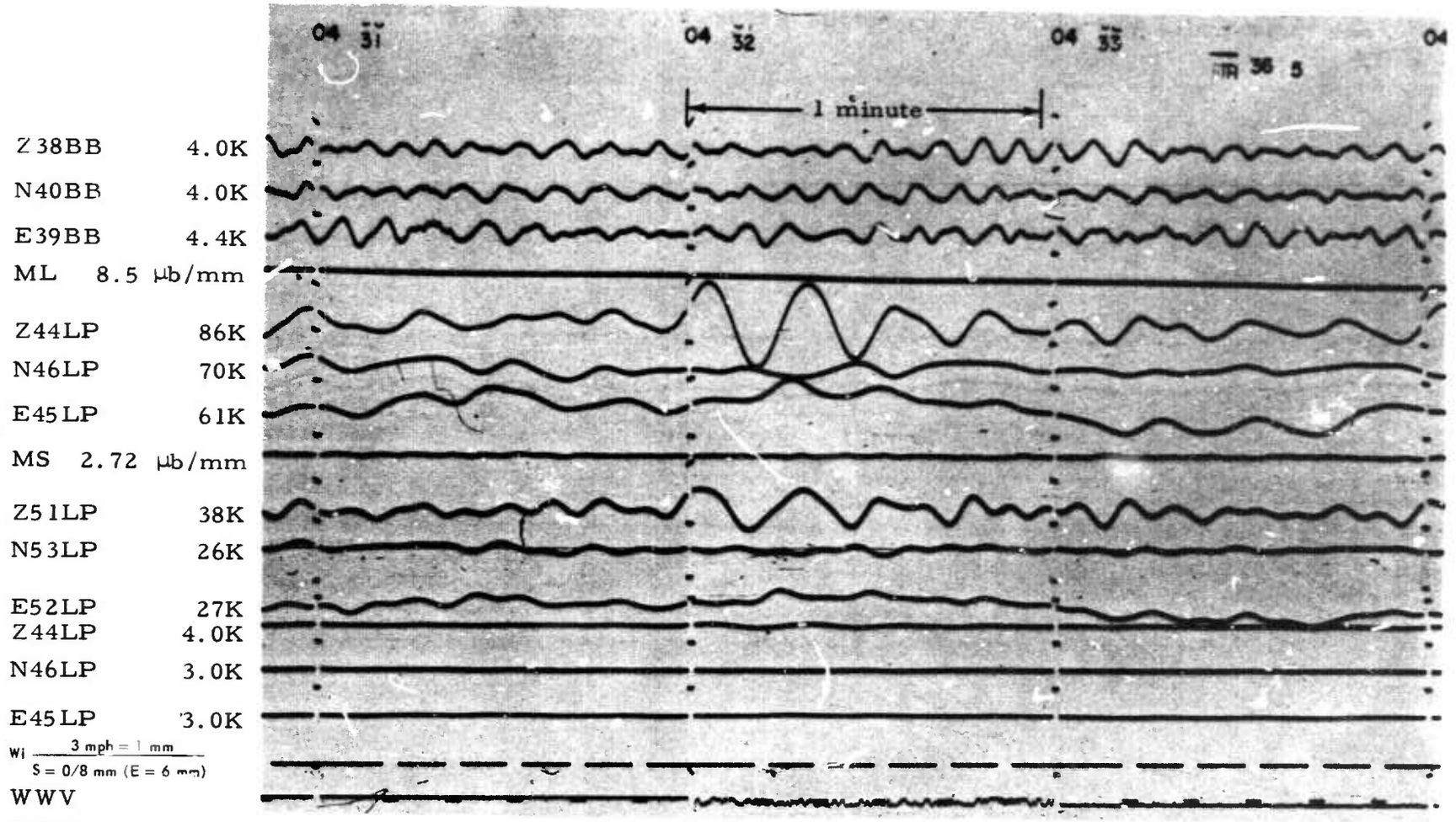

Figure 44. Typical background and weak surface waves as displayed by broad-band and long-period seismographs at TFSO at close of reporting period. (X10 view of 16-millimeter film)

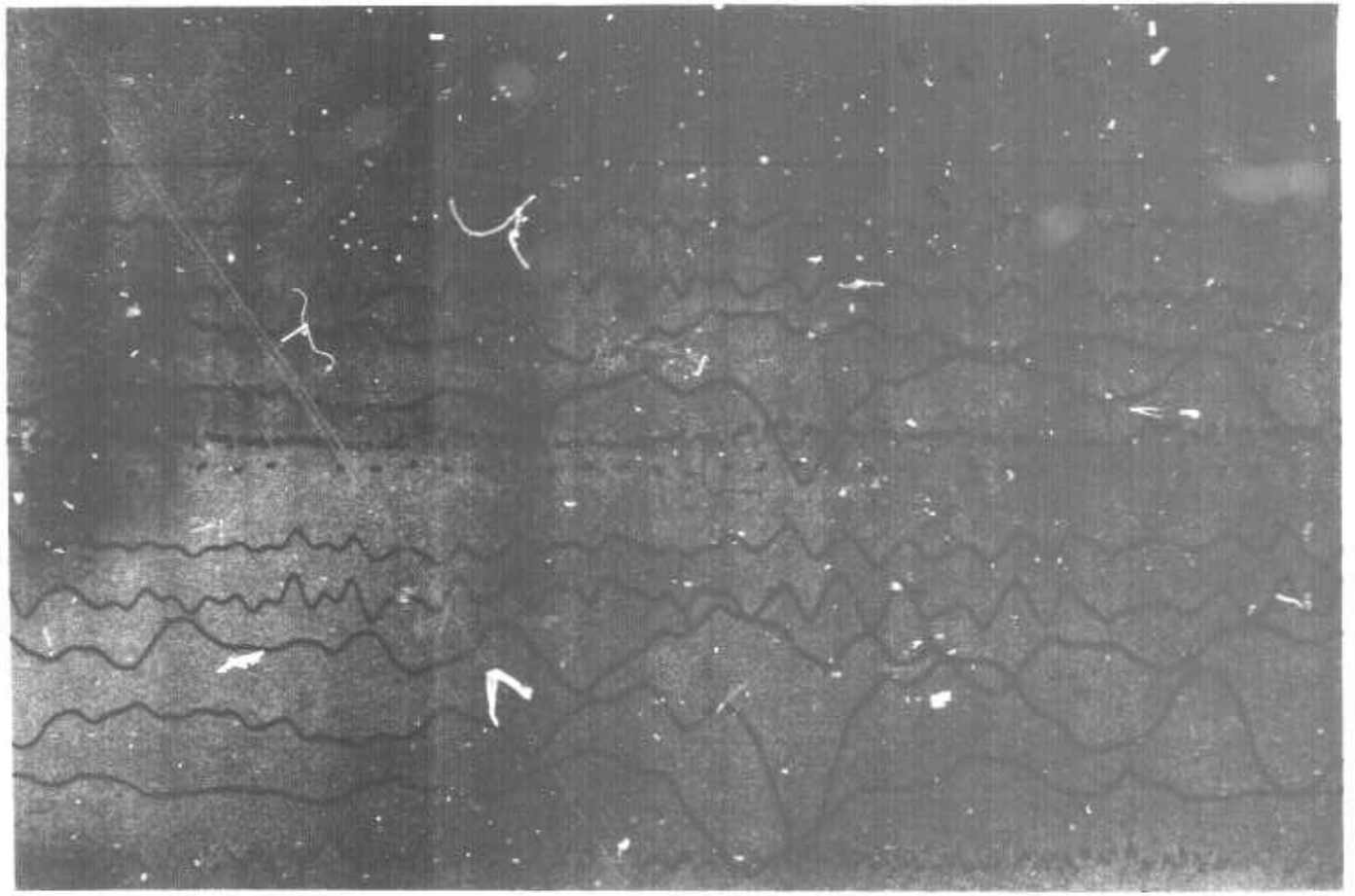

Figure 45. Long-period experimental seismogram comparing Z57LP and Z54LP (housed in a surface tank vault) to Z51LP and Z44LP (located in a large walk-in concrete vault) during period of pressure change. WI register at about 10 mph. (X10 view of 16-millimeter film)

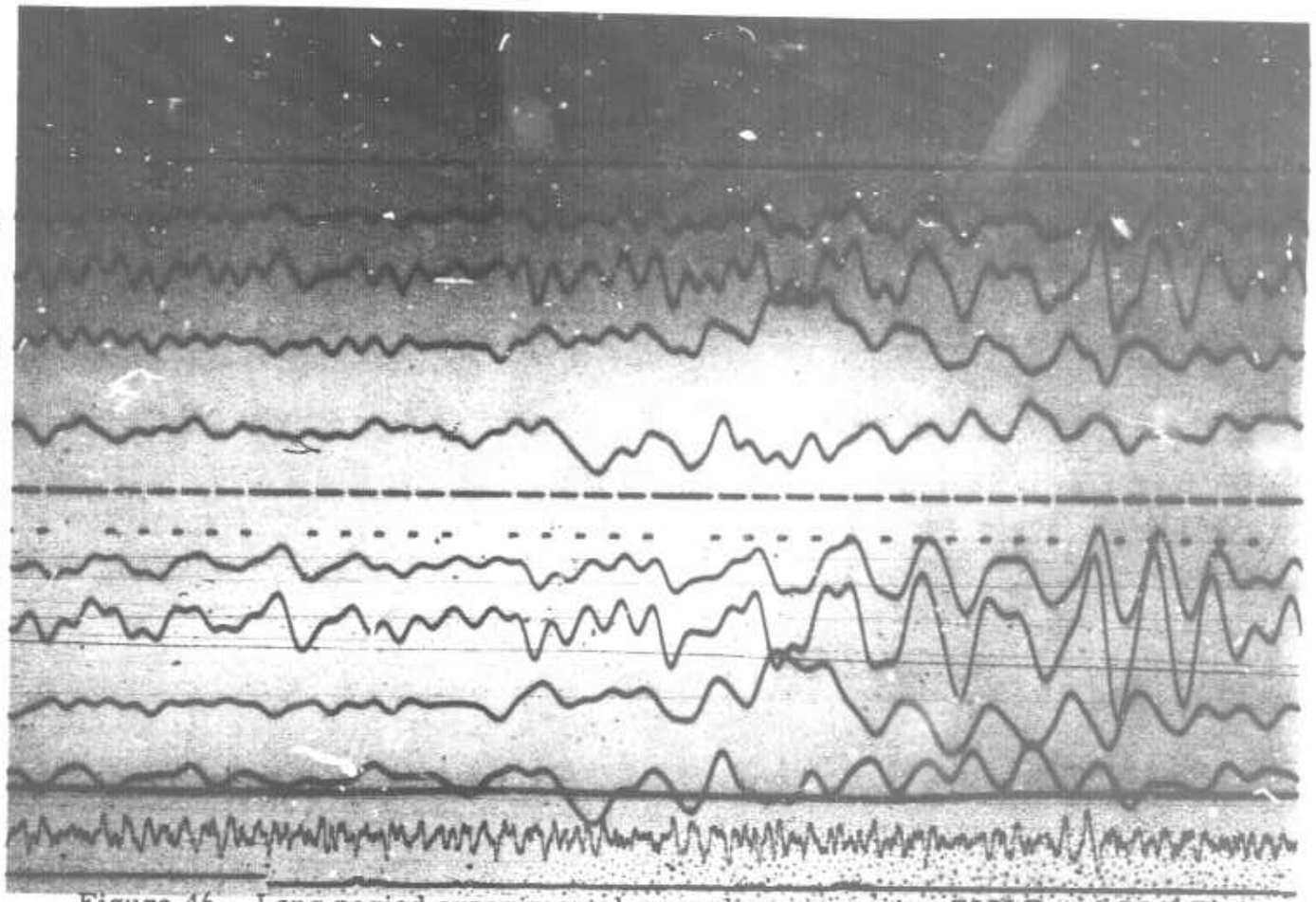

Figure 46. Long period experimental recording comparing Z57LP and Z54LP (notched) (housed in a surface tank vault) to Z51LP and Z44LP (located in a large walk-in concrete vault) during period of little pressure change. (X10 view of 16-millimeter film)

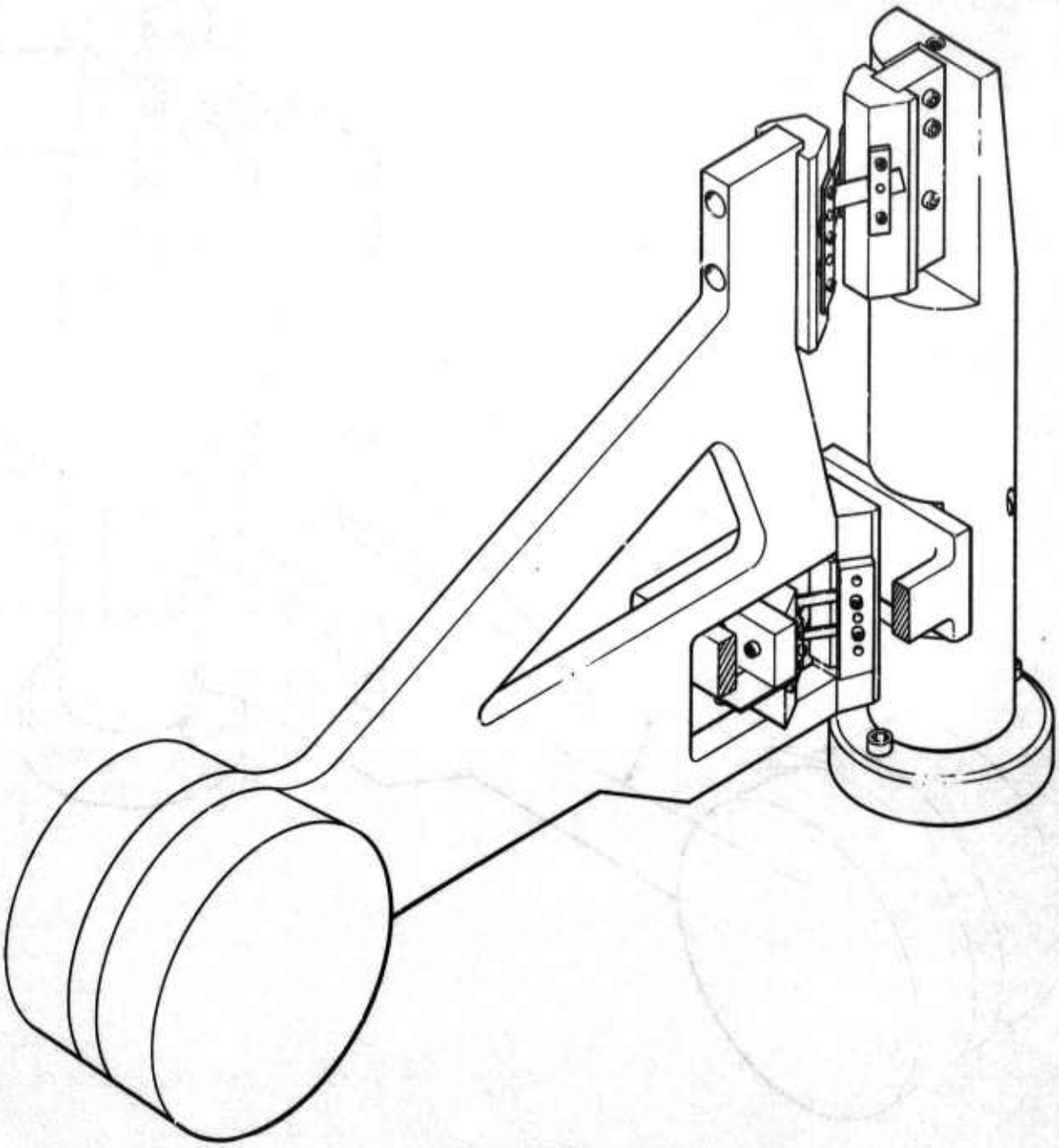

Figure 47. Suspension system of the Geotech Model 8700C seismometer equipped with cross-ribbon flexures G 2593

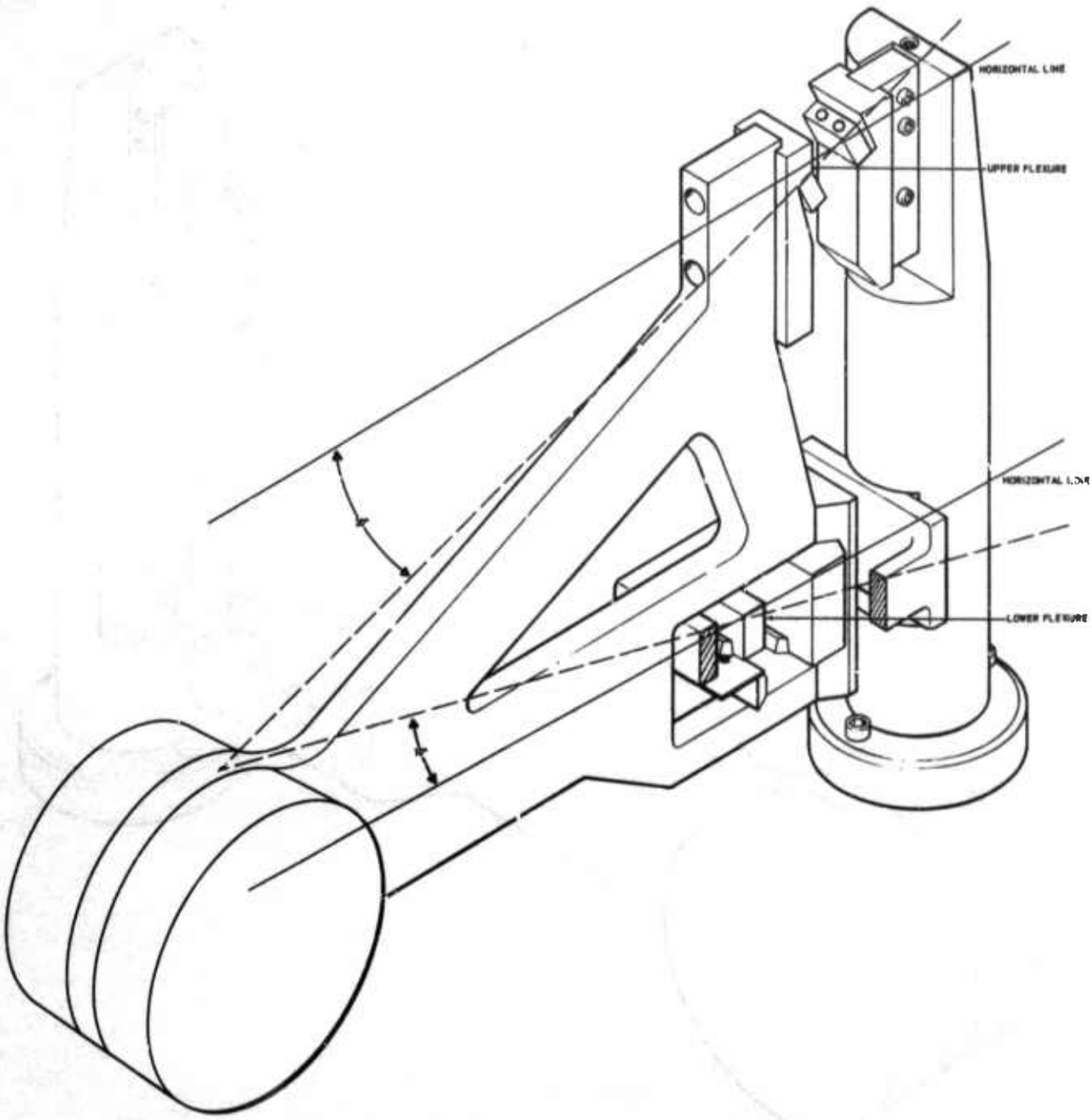

Figure 48. Suspension system of the Geotech Model 8700C long-period horizontal seismometer equipped with a wire hinge system. Dashed lines indicate the lines that contain the wire flexures. Dotted lines indicate actual location of flexures.

G 2594

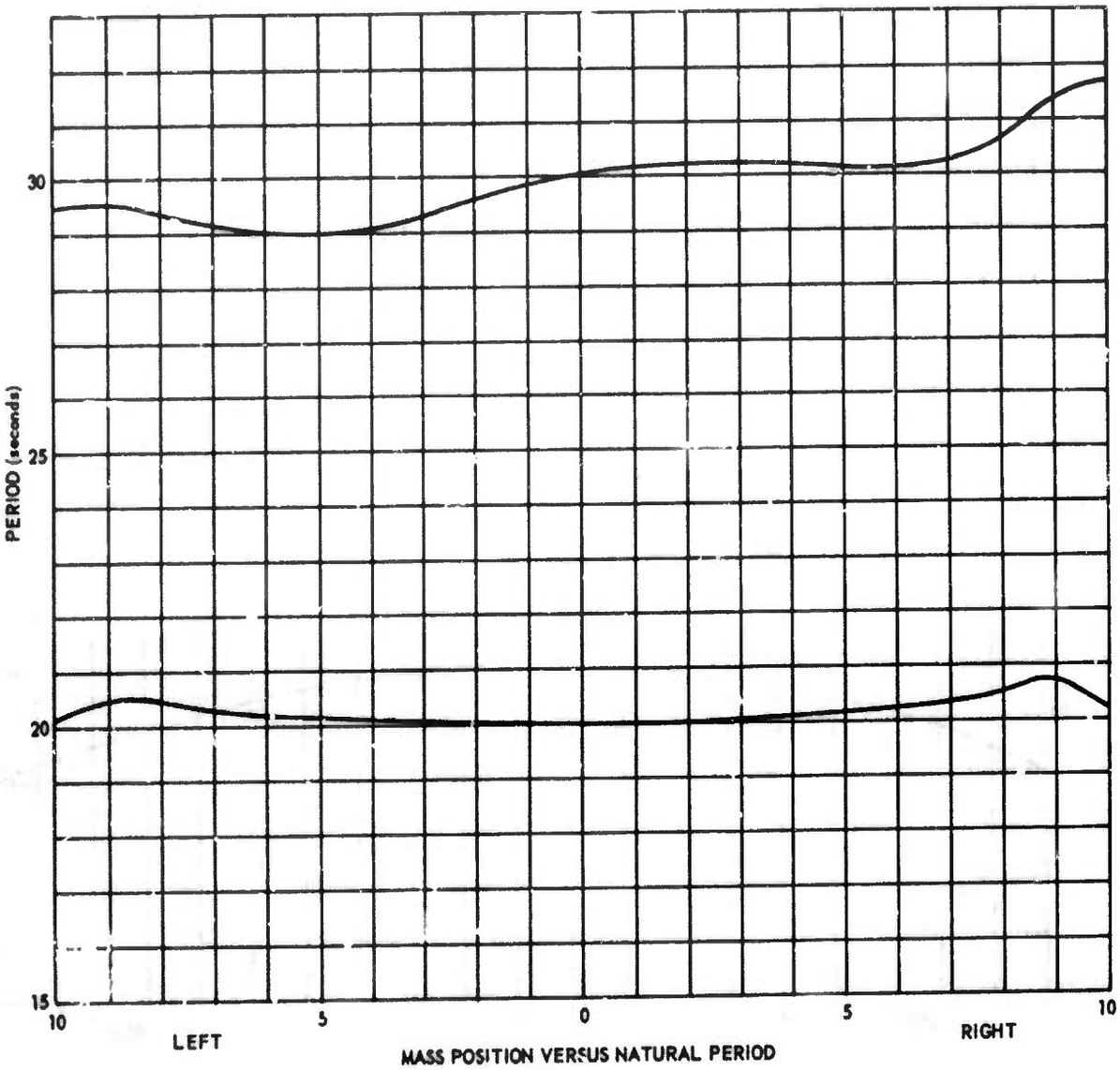

Figure 49. Mass position versus natural period for the Geotech Model 8700C seismometer equipped with wire flexures

G 2595

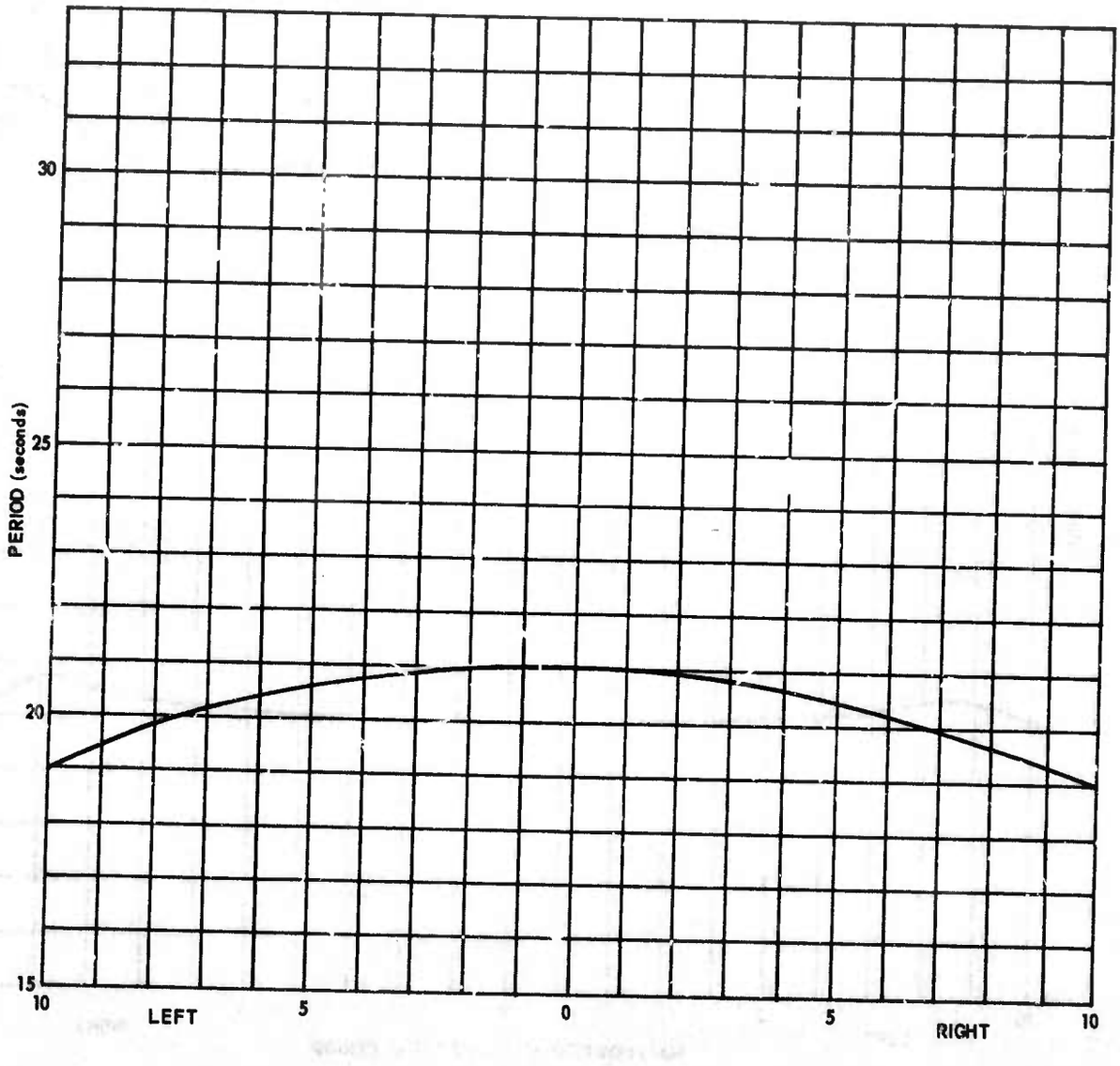

Figure 50. Typical natural period versus mass-position curve of the Geotech Model 8700C seismometer G 2596

Table 11. Response of Geotech Model 8700C seismometer (equipped with wire flexures) to the removal of test weights from the inertial mass

Mass of test weight grams	Initial rest position of mass (mm) (test wt on)	Final rest position (mm) (test wt off)	Change in rest mass position (mm)	Direction of mass movement
100	0.2 left	1.1 right	1.3	to right
100	0.4 right	1.1 right	0.7	to left
100	0.7 left	0.7 right	1.4	to right
100	1.6 left	0	1.6	to left
100	3.8 left	1.2 left	2.6	to right
50	0.5 left	0.1 right	0.6	to right
50	0.6 left	0	0.6	to left
50	0.4 left	0.1 right	0.5	to right

λ is the ratio of the external damping to critical damping and α is the natural logarithm of the ratio obtained from two successive maximum positive zero-to-peak amplitudes. The open-circuit damping was found to be 0.029. This degree of damping is about the degree of damping normally attributed to viscous effects of the air.

7.2.3 Operational Tests

The modified seismometer was subsequently installed in the sealed vault at TFSO on the same pier with the two Geotech Model 8700C long-period horizontal seismometers that are part of the TFSO system. The three seismometers were oriented north-south, and their parameters and responses were equalized.

7.2.3.1 Heat Cycling

Initially, the modified seismometer produced intermittent noise "spikes" (figure 51), and the position of its mass varied. No similar noise spikes or variations of mass position were observed on the control systems. The noise and mass-position instability observed on the modified seismograph were first attributed to either misalignment or damage of the wire flexures. The flexures were replaced; however, no apparent improvement resulted.

The modified seismometer was heat-cycled by alternately increasing and decreasing the temperature of the seismometer to relieve stresses in the mechanical parts of the instrument which might have been induced in shipment. The spikes were no longer observed on the seismograms after a second period of heat cycling which lasted for 72 hours.

7.2.3.2 Conclusions

After the noise spikes had been eliminated, the three seismometers were set to a magnification of 60K at 0.04 cps, and data were recorded for a 30-day period.

Little difference was noted in the character of the data produced by the three seismometers (see figures 52 and 53) when air convection currents within the seismometer vault were at a minimum. Some differences were noted among seismograms produced by the three seismometers during intervals in which convections were present. Figure 54 is a seismogram illustrating the differences attributed to air convections within the vault caused by changing atmospheric conditions.

The data in figures 49 and 50 show that the natural period of the modified seismometer varies less with mass position than that of the standard Model 8700C seismometer. Also, the natural period of the modified seismometer was more readily adjustable than that of the standard seismometer

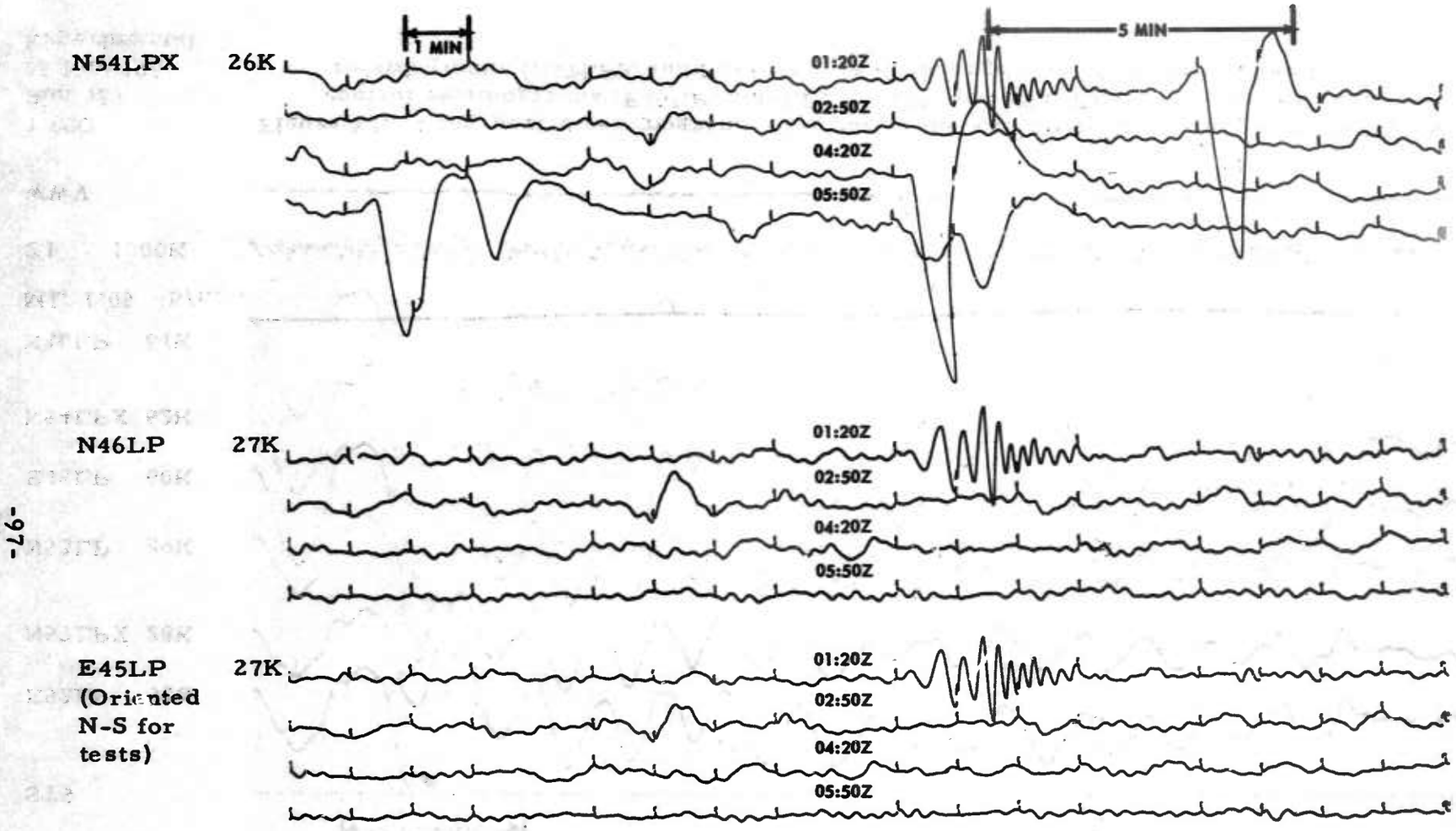

Figure 51. Long-period seismogram recorded at TFSO showing spikes on N54LPX. Note absence of spikes on control instruments N46LP and E45LP. Signal at 01:21, from unknown epicenter, is comparable on all instruments. (Direct print from Helicorder record)

TFSO
Exp LP Helicorder

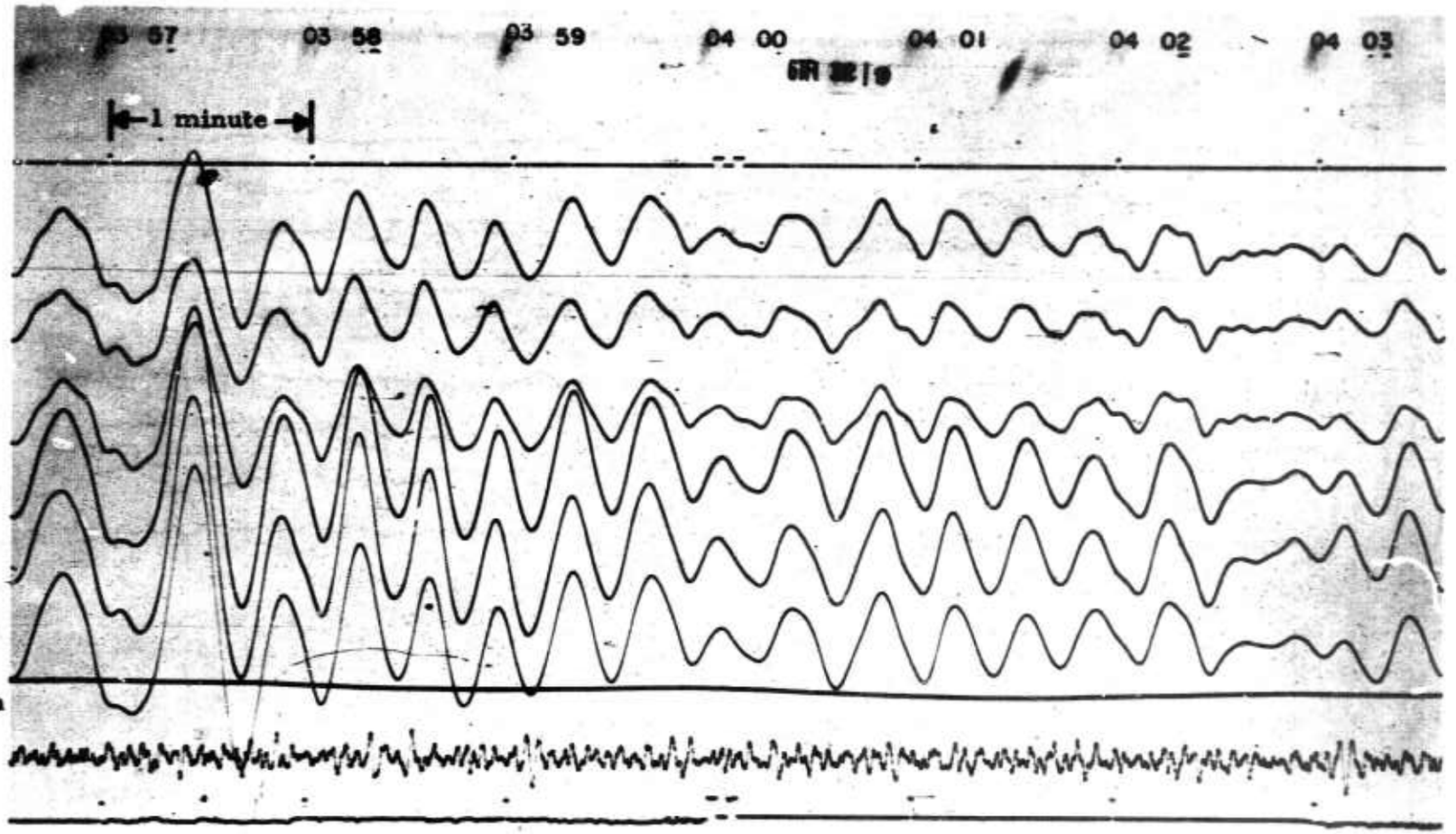

TFSO
Run 329
25 Nov 1966
Experimental

Figure 52. Long-period seismogram illustrating the similarity of the data recorded by the control seismographs (E45LP, N46LP, E52LP, and N53LP) and the experimental seismographs (N57LPX and N54LPX). (X10 Enlargement of 16-millimeter film)

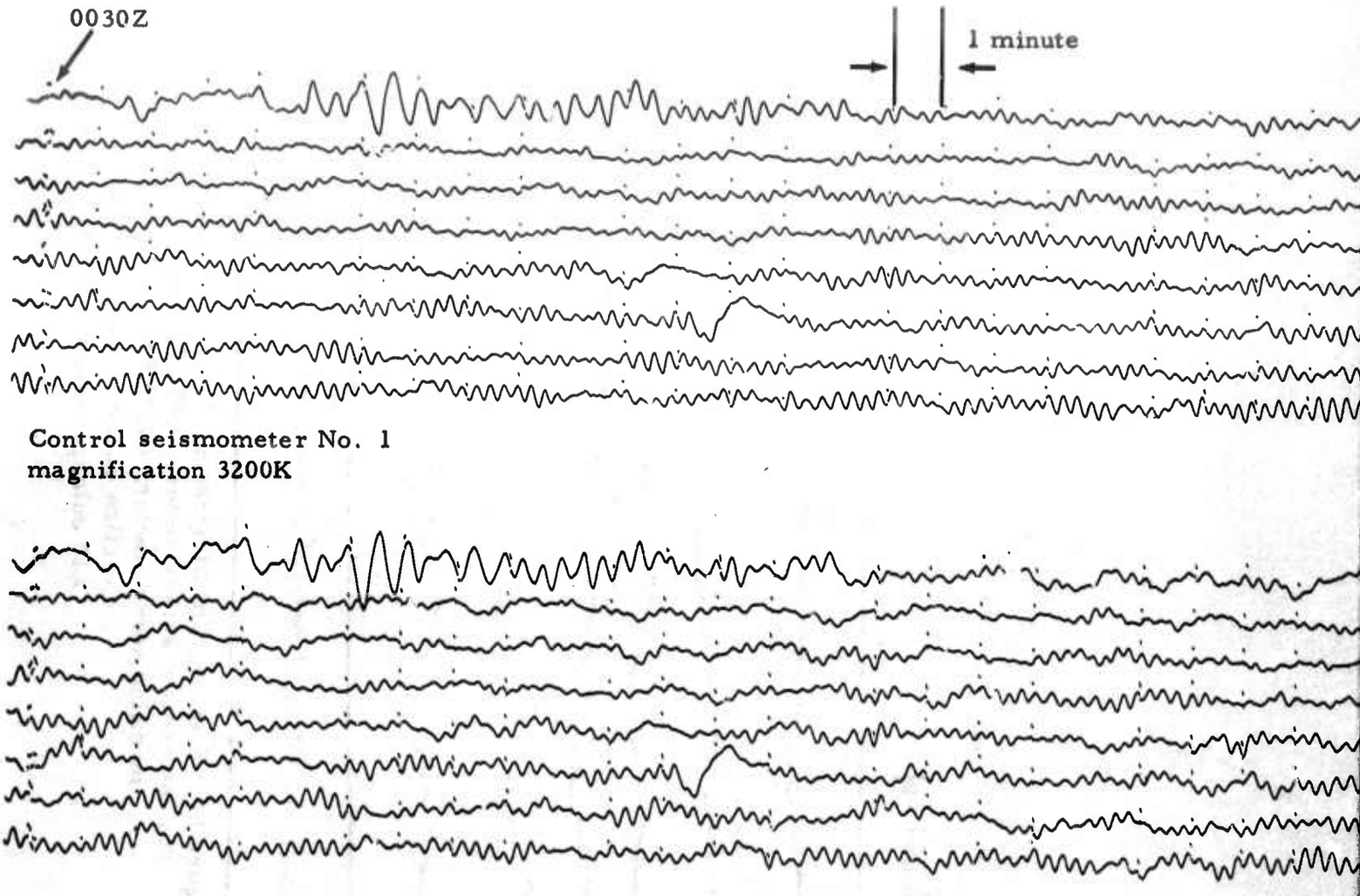

TFSO
Run 322
19 Nov 1966

Figure 53. Seismogram illustrating close correlation of data produced
seismometer (Control seismometer No. 1) and the Geotech Mod
equipped with wire flextures (modified seis

minute

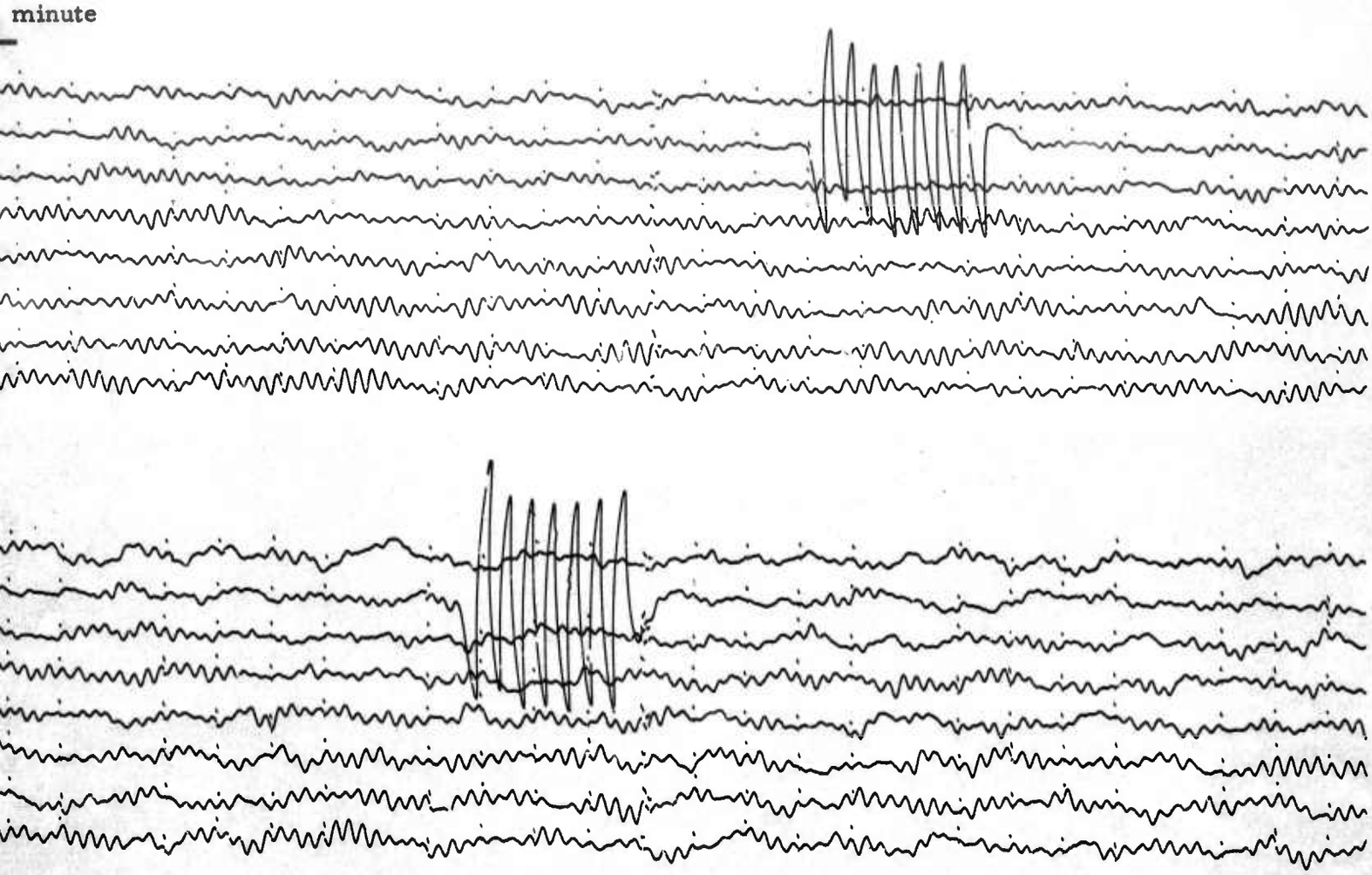

correlation of data produced by the Geotech Model 8700C
er No. 1) and the Geotech Model 8700C seismometer
wire flextures (modified seismometer)

because the modified seismometer requires only 2 adjustments; whereas, the standard seismometer requires 6 adjustments. Little difference was found in the character of the data produced by any of the seismometers during periods when convection currents within the vault where minimal. During periods of varying atmospheric conditions, however, greater differences were noted among the seismograms. In our opinion, the noise characteristics of the modified and standard seismometers are essentially equal. Based on the data in figure 49, the modified seismometer could probably be operated with a natural period greater than 20 seconds more effectively than could the standard seismometer.

7.3 EVALUATION OF THE FRENCH SEISMOGRAPH SYSTEM

The evaluation of the French seismograph system was reported in TR 66-53 and in a special letter report dated 3 October 1966.

Examples of signals recorded by the French seismograph and by standard TFSO seismographs are shown in figures 55, 56, and 57. The quarry blast shown in figure 55 is from San Manuel Magma at a distance of 1.5 degrees. The epicenter for the teleseismic event shown in figure 56 is southern Peru, a distance of approximately 64 degrees.

On 11 May, we began recording the output of the French seismograph on a short-period Develocorder so that these seismograms (ZFX) could be compared directly with those from the standard TFSO short-period systems. Signals recorded by the French seismograph and the standard short-period seismographs from three events are shown in figures 58 through 60. Frequency responses for the high-frequency seismographs (section 7.1), the French seismograph, and a standard short-period seismograph are shown in figure 61.

The film seismograms recorded by the French seismograph at TFSO were typically similar to the seismograms recorded by the standard TFSO short-period seismographs as shown in figures 55 through 60. In our opinion, two factors are responsible for this similarity:

a. The frequency responses of the French system and the TFSO short-period systems are similar in the range from 0.2 to 4.0 cps.

b. The seismic events studied produced very little energy at frequencies above 4.0 cps.

X1 reproduction of paper chart seismogram recorded by the French seismograph

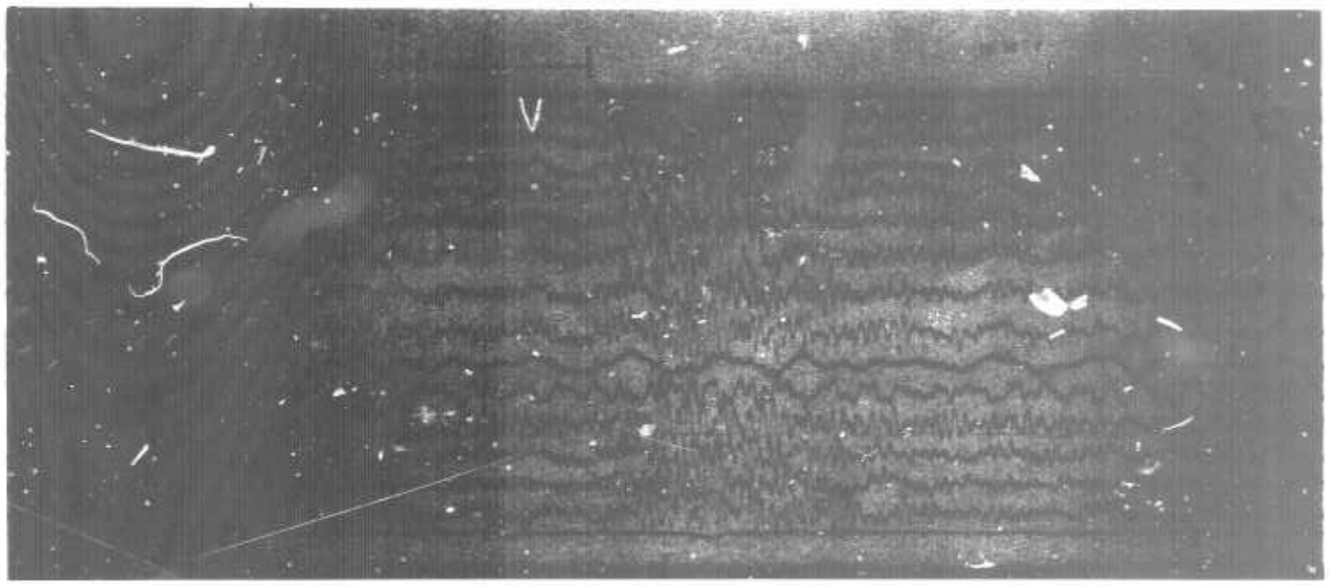

TCMDG	
Z31	600K
Z8	640K
Z2	600K
Z13	600K
Z16	620K
Z20	650K
Z4	650K
Z7	650K
ΣT	770K
ΣTF	3960K
ΣTFK	3960K
Z1	580K
N37SP	580K
E36SP	620K
WWV	

Figure 55. Seismograms of a quarry blast from San Manuel Magma at a distance of 1.5 degrees recorded by the French seismograph and by standard seismographs at TFSO. The time bases of these seismograms are approximately equal. The lower seismogram is a X6 enlargement of 16-millimeter film

TFSO
Run 117
27 April 1966
Data Group 7179

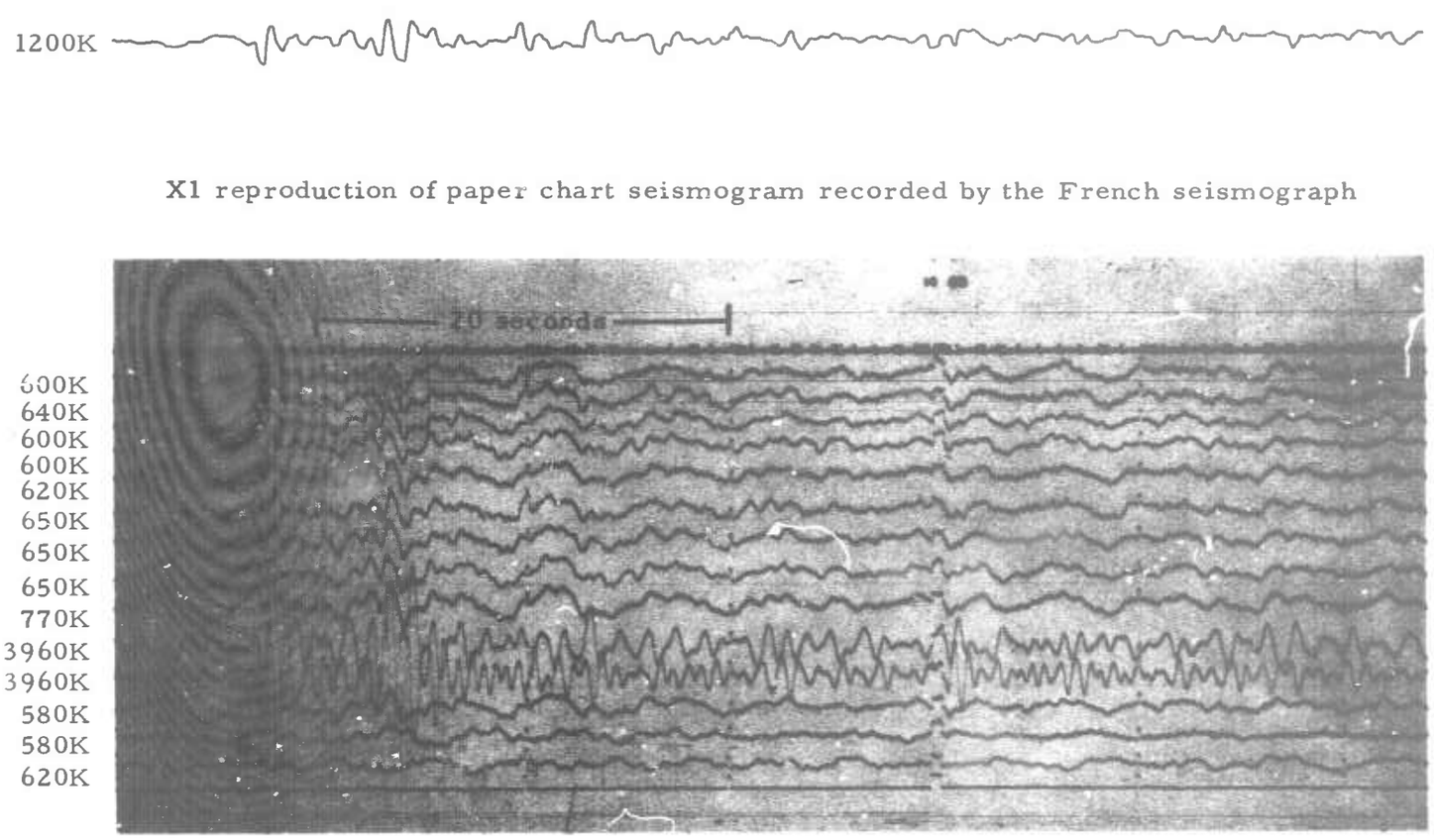

TFSO
Run 117
27 April 1966
Data Group 7179

Figure 56. Seismogram of a teleseismic event from southern Peru recorded by the French seismograph and by standard seismographs at TFSO. The time bases of these seismograms are approximately equal. The lower seismogram is a X6 enlargement of 16-millimeter film. Epicentral data 0 = 13:53:57.1 $\Delta \cong 63.9^{o}$, h ≅ 62 km, Azimuth = $\cong 136^{o}$, magnitude 45

X1 reproduction of paper chart seismogram recorded by the French seismograph

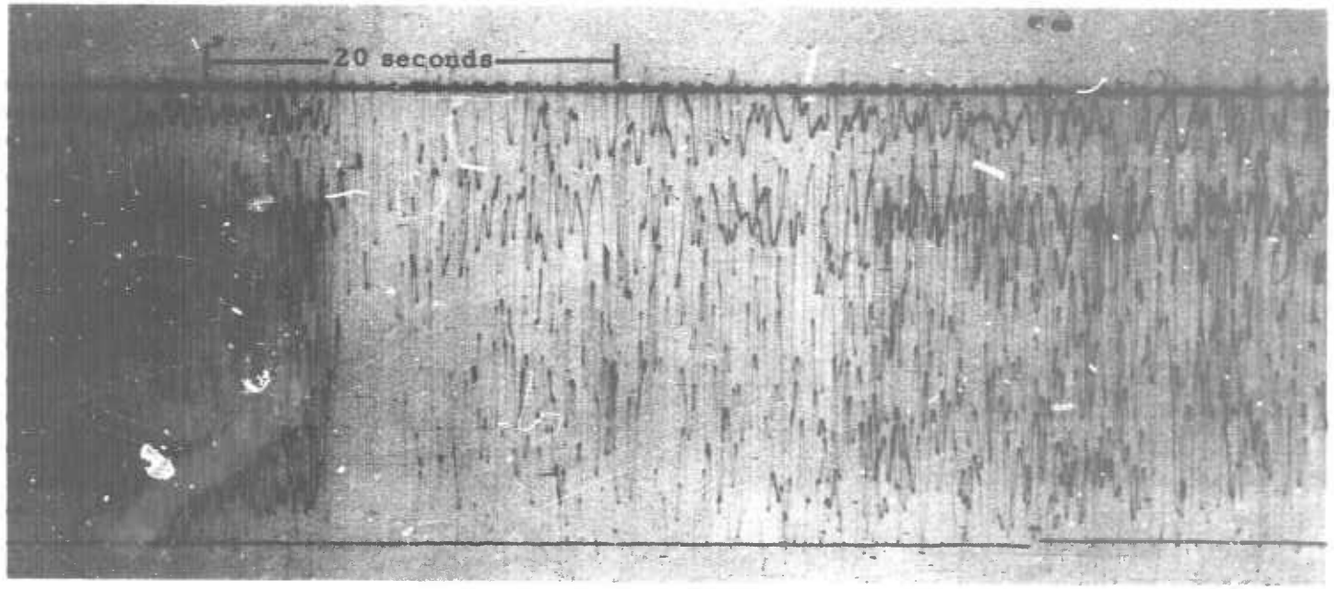

Figure 57. Seismograms of a near regional event (epicenter unknown) recorded by the French seismograph and by standard seismographs at TFSO. The time bases of these seismograms are approximately equal. The lower seismogram is a X6 enlargement of 16-millimeter film

TFSO
Run 115
25 April 1966
Data Group 7179

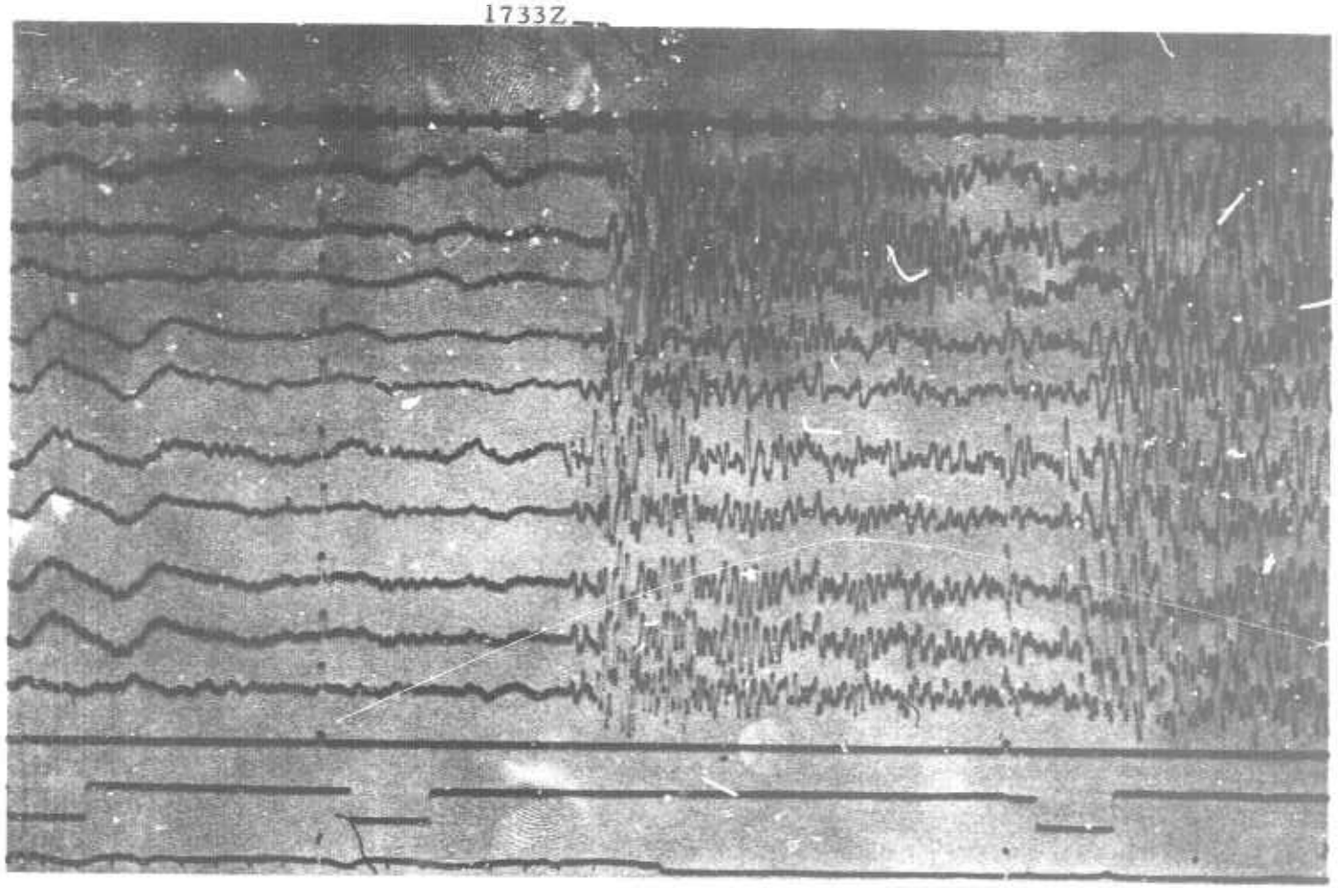

Figure 58. TFSO short-period seismogram showing a P arrival from eastern Arizona, $\Delta \simeq 1.0$ degrees. (X10 enlargement of 16-millimeter film)

TFSO
Run 196
15 July 1966
Data Group 7187

TCMDG

Z74	1000K
R80	1000K
T79	960K
Z10	960K
Z3	1040K
Z66	960K
Z100	1040K
Z102SG	960K
Z103SH	1000K
ZFX	1000K

MS 0.54 μb/mm

WI $\frac{3 \text{ mph} = 1 \text{ mm}}{S = 0/8 \text{ mm (E = 6 mm)}}$

WWV

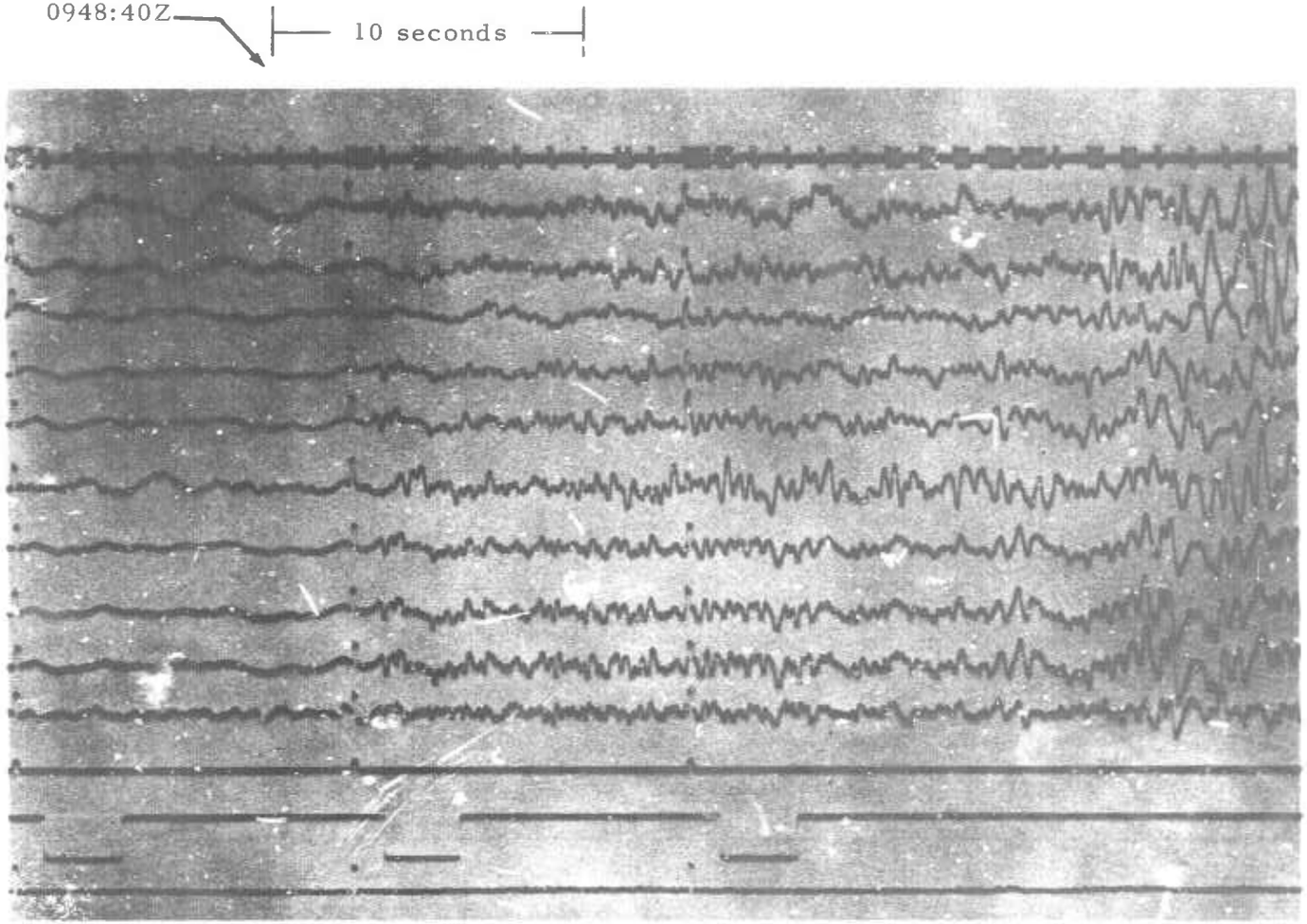

Figure 59. TFSO short-period seismogram showing a P arrival from southern California, $\Delta \simeq 5.8$ degrees. (X10 enlargement of 16-millimeter film)

TFSO
Run 196
15 July 1966
Data Group 7187

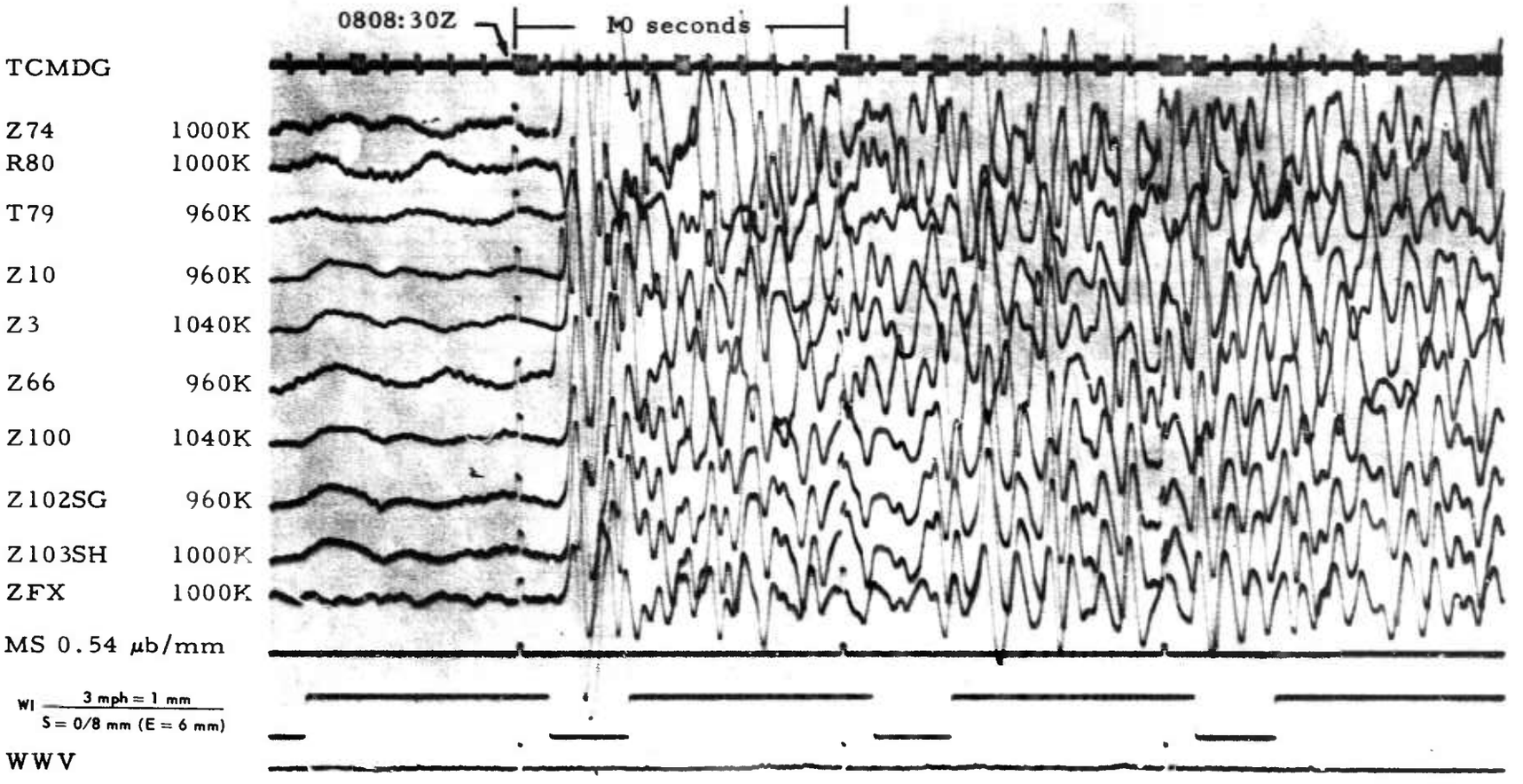

TFSO
Run 196
15 July 1966
Data Group 7187

Figure 60. TFSO short-period seismogram showing a P arrival from the Leeward Islands, $\Delta \simeq 47.6$ degrees, azimuth = 98°, h = 89 km, o = 08:00:00.7 m = 5.4 (C&GS) (X10 enlargement of 16-millimeter film)

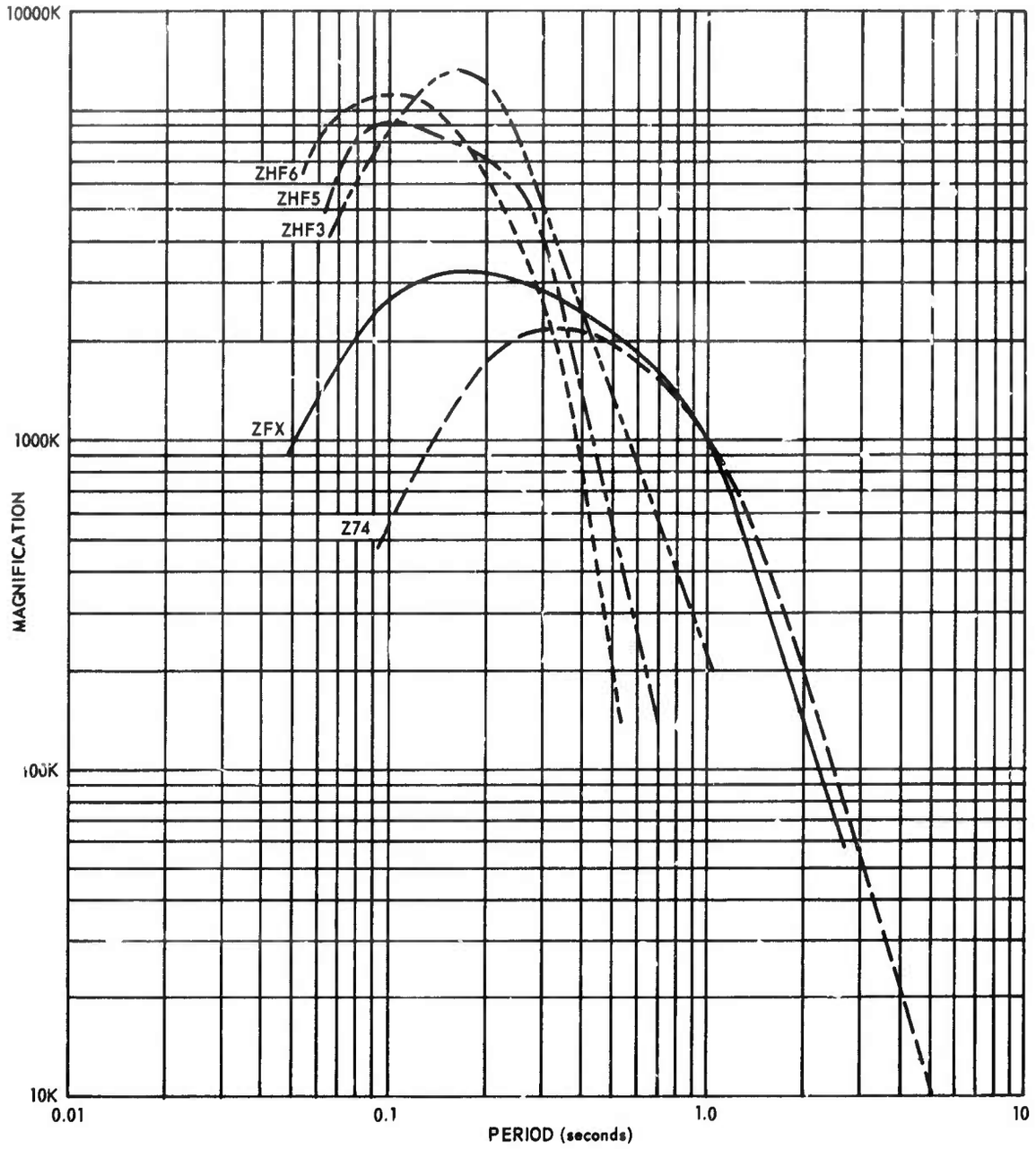

Figure 61. Frequency responses of the Z74, ZFX, ZHF5, and ZHF6 seismographs operated at TFSO G 2597

The seismograms from the TFSO high-frequency seismographs also showed little energy above 4.0 cps in teleseismic P-wave signals. Figure 35 is a typical seismogram from the TFSO high-frequency seismographs. The low-frequency response of the French seismograph is such that the high-amplitude, low-frequency components of seismic signals produce amplitudes on the seismograms that obscure any high-frequency components that might be present. Based on studies of the TFSO high-frequency magnetic-tape seismograms and spectrograms produced from these seismograms, we have concluded that the ratio of the seismic-signal level to the system-noise level of the TFSO systems was inadequate at frequencies above 5 cps. Also, we concluded that an adequate high-frequency seismograph must have a seismometer with a mass of approximately 4 kilograms and a natural frequency of about 8.0 cps. It is our opinion, therefore, that the characteristics of the seismometer used in the French seismograph system are more nearly ideal for recording signal components at frequencies below 5 cps.

The output of the French seismograph was recorded on a Develocorder during the period from 30 April to 29 July 1966. Except for periods of special attenuation, the magnification of this system was approximately 1200K at 1.0 cps. In late June, the amplifier developed a great deal of noise and the magnification dropped. The amplifier of the second system was used as a replacement unit. This unit also yielded low magnification. A malfunction was found in the attenuator at the high-gain setting. An attempt was not made to repair these units because spare parts and a manual were not available for the system. On 29 July, approval was given to discontinue the testing of the seismograph.

7.4 SHALLOW HOLE TESTS

7.4.1 General

In recent years, interest has developed in the use of shallow-hole seismometers and solid-state electronic amplifiers for seismometric applications. A number of seismometers and amplifiers have been tested, and several systems have been assembled and operated (Geotech, 1965). In October 1965, a program for the comparative field testing of two shallow-hole seismograph systems at TFSO was authorized by the Project VT/5055 Project Officer. TFSO was selected for the tests because of its excellent facilities and low microseismic background level.

One system tested employed the Geospace Model HS-10-1/ARPA seismometer in conjunction with the Texas Instruments Model RA-5 amplifier. The Model HS-10-1/ARPA seismometer and Model RA-5 amplifier were supplied as government furnished equipment (GFE). The second system employed the Geotech Model 20171 seismometer in conjunction

with the Geotech Model 23168-A amplifier. The Model 20171 seismometer and Model 23168-A amplifier were supplied by Geotech.

7.4.2 Description of Test Installation

The configuration of the field test installation is shown in figure 62. Both seismometers were equipped with holelocks and installed in the 200-foot cased hole near the experimental walk-in vault. A standard JM vertical seismometer was operated in the experimental vault as a control instrument.

Several components of the system were intentionally subjected to severe conditions. Both seismometers were operated under water which was present in the bottom of the shallow borehole. The low-level data were transmitted over 600 feet of cable which contained several connections in the field. Signal levels on these cables were on the order of 10^{-17} watts. The interface impedance was approximately 5 ohms for the 20171/23168-A combination and 50 ohms for the HS/RA-5 combination.

Because earlier tests had shown that the Model RA-5 amplifier was very susceptible to temperature changes and input power variations, the amplifiers were provided with stable power supplies and were installed in the underground experimental vault to provide a stable temperature environment.

The amplified analog signals were transmitted about a mile over spiral-four cable to the central recording building. Three electrode gas-filled capsules and solid-state diodes were used at each end of this cable to provide transient protection.

The data cable to the central recording building was terminated into a balanced operational amplifier network to block dc offset voltages and to attenuate common mode potentials. A single-pole filter with a high-frequency cutoff at 5 cps was also incorporated in this circuit. A second operational amplifier network was used to provide additional filtering.

From the filter network, signals were routed into standard data handling channels. The test systems were recorded on film at standard short period magnification (1000K at 1 cps). Data were also recorded on digital tape for computer analysis.

7.4.3 Initial Installation and Operation

The systems were assembled and checked at our Garland laboratory, shipped to TFSO, reassembled, and checked again, prior to final installation.

After installation, we found that a water leak was present in the Model HS-10-1/ARPA seismometer/cable assembly. This cable assembly had been used earlier in another program and had been successfully operated

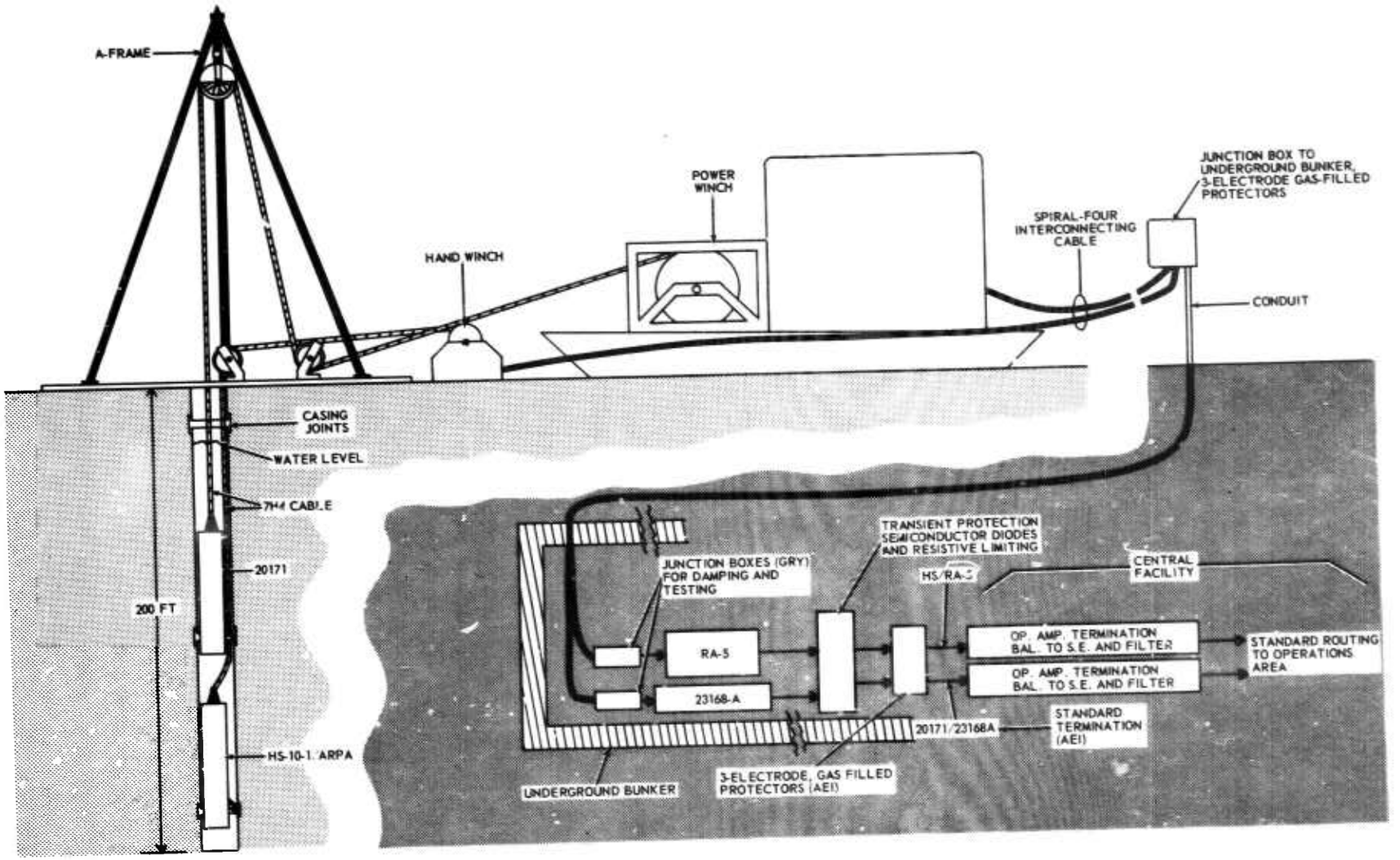

Figure 62. General configuration of test seismograph systems G 2598

under more than 100 feet of water. Apparently, the assembly had been weakened in transit. A second seismometer was installed after repairs to the water-damaged unit failed to return it to proper operating condition. Moisture trapped in the downhole cable caused leakage when the second seismometer was initially installed. Corrective measures were taken, and no leakage occurred during the remainder of the test period. No leakage problems were encountered with the Model 20171 seismometer.

Hole measurements were made on 27 April 1966 which showed a deviation from vertical of 2.5 degrees, at a depth of 70 feet. Temperatures measured at 40, 100, 190 feet below the water surface were 60, 59, and 55 degrees Fahrenheit, respectively.

7.4.4 Parameter Stability

Seismometer and amplifier parameters were measured several times during the period of the tests to provide data on the stability of the systems. Table 12 lists the nominal parameters of the two seismometer/amplifier combinations.

The natural period of the second Model HS-10-1/ARPA seismometer changed from 0.95 second to 1.25 seconds during installation in the hole. A change of this magnitude was not expected; however, after the second seismometer was installed, checks indicated that the unit was operating stably and linearly. The natural period of the Model 20171 seismometer changed from 1.24 seconds to 1.18 seconds during installation in the hole.

External damping resistors were installed in the coupling circuits to provide 0.64 damping at the measured downhole natural period, and both systems were operational by 22 January 1966. The natural periods were measured again on 24 February and found to be 1.23 seconds for the Model HS-10-1/ARPA seismometer and 1.16 seconds for the Model 20171 seismometer.

On 14 March, both seismometers were repositioned in the hole. After relocation, the natural period of the Model HS-10-1/ARPA seismometer was 1.28 seconds and that of the Model 20171 seismometer was 1.18 seconds. On 27 July, the Model HS-10-1/ARPA seismometer was damaged by lightning. Subsequently, both seismometers were returned to the engineering laboratory for inspection and maintenance.

7.4.5 Seismometer Removal and Reinstallation

The Model HS-10-1/ARPA and Model 20171 seismometers were removed from the hole on 2 August. The Model HS-10-1/ARPA unit had water under the RTV 108 silicone compound used to seal the top, but water had not leaked into the case. The RTV 108 compound originally formed a tight bond but

Table 12. Nominal parameter values of test seismometer/amplifier combinations

	HS-10-1/RA-5 (No. 1)	20171/23168A
Natural period (Tn, sec)	1.0	1.25 (adjustable, 0.95 to 1 33)
Generator constant (G, V/m/s)	1000	810
Internal damping (λ int, ratio to critical)	0.375	<0.05
Inertial mass (M, kg)	0.825	5
Coil resistance (Rc, ohms)	50 kΩ	10.7 kΩ
External resistance (Rx, ohms)	318 kΩ	9.77 kΩ
Total damping (λ, ratio to critical)	0.637	0.637
Seis efficiency (η, ratio)	0.865	0.477
Seis sensitivity (μV/mμ @ 1 cps)	4.3	2.8
Cal motor constant (G cal, newton/ampere)	0.0326 (1 mμ/μA @ 1 cps)	0.1975 (1 mμ/μA @ 1 cps)
Outer case test pressure (psi)	250	500
Outer case dimension (inches)	4.75" o.d. x 11.25" (without holelock)	3.75" o.d. x 40.63" (without holelock)
Amplifier gain (midband, 1 cps)	10,000	10,000
Amplified sensitivity (mV/mμ @ 1 cps)	43	28

had weakened during the 6-month period. The cable head assembly was left intact since it appeared to be sealed.

One of the data coil pig-tail connections inside the Model HS-10-1/ARPA seismometer was parted by the electrical impulse resulting from a lightning strike nearby. The Model 23168-A amplifier output stage in the Geotech seismograph was damaged by lightning at approximately the time of the HS-10-1/ARPA damage. The Model RA-5 amplifier was not damaged.

Both seismometers were reinstalled in the hole and were operated until 22 September. The natural period of the Model HS-10-1/ARPA seismometer remained within the 1.23- to 1.28-second range, and the natural period of the Model 20171 seismometer remained within the range between 1.250 and 1.257 seconds after damaged delta rods were replaced in August.

Variations in the frequency response; reflecting changes in the generator constant, motor constant, and amplifier gain; are summarized in figures 63 and 64. Figures 63 and 64 show combined plots of monthly operational seismograph responses taken during the test periods.

7.4.6 Lightning Damage

During the test period there was sufficient lightning activity to demonstrate that the sensitive input stages of both amplifiers could withstand high-level transients without permanent damage. The seismometer/amplifier interconnecting cables were located above ground and protected with AEI three-electrode, gas-filled capsules at the vault junction box. Broad-band noise pickup on the interconnecting field cables was approximately 2 millivolts, peak-to-peak, more than 1000 times greater than the lower signal voltages. The predominant noise pickup components were, in order of magnitude, 60 cps repetitive pulses associated with fluorescent lighting and ac-to-dc power supplies, 20,000 cps signals, thought to be from the ground pattern of Radio Station WWVL, located at Fort Collins, Colorado, and high-frequency signals associated with mobile radio transmitters.

Lightning did not damage the Model RA-5 amplifier but apparently did burn out an internal data coil lead in the Model HS-10-1/ARPA unit on 27 July. The operational amplifier networks at the CRB were not damaged.

On four occasions, 18 April, 30 June, 27 July, and 30 August, lightning damaged the Model 23168A amplifier output stage. In some cases, the unit was rendered completely inoperative; in others, it exhibited low gain or low clipping level due to damaged parts. This damage was considered to be due primarily to an inadequacy of the output stage. A Geotech Model 25220 amplifier with a more rugged output stage was received for testing in November 1966. This unit was subsequently tested with a JM seismometer.

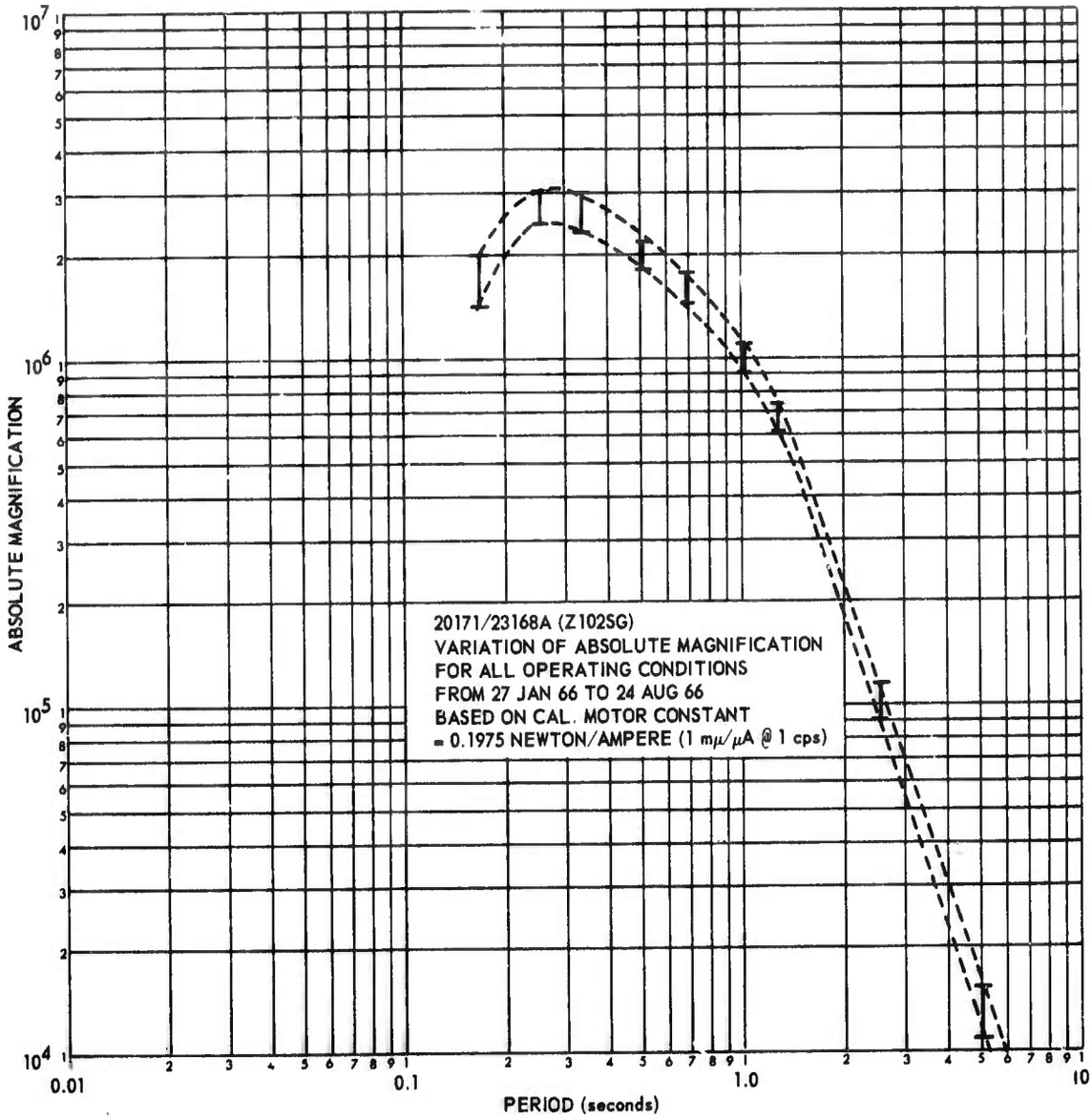

Figure 63. Spread in magnification during test period 20171/23168-A (Z102SG)

G 2599

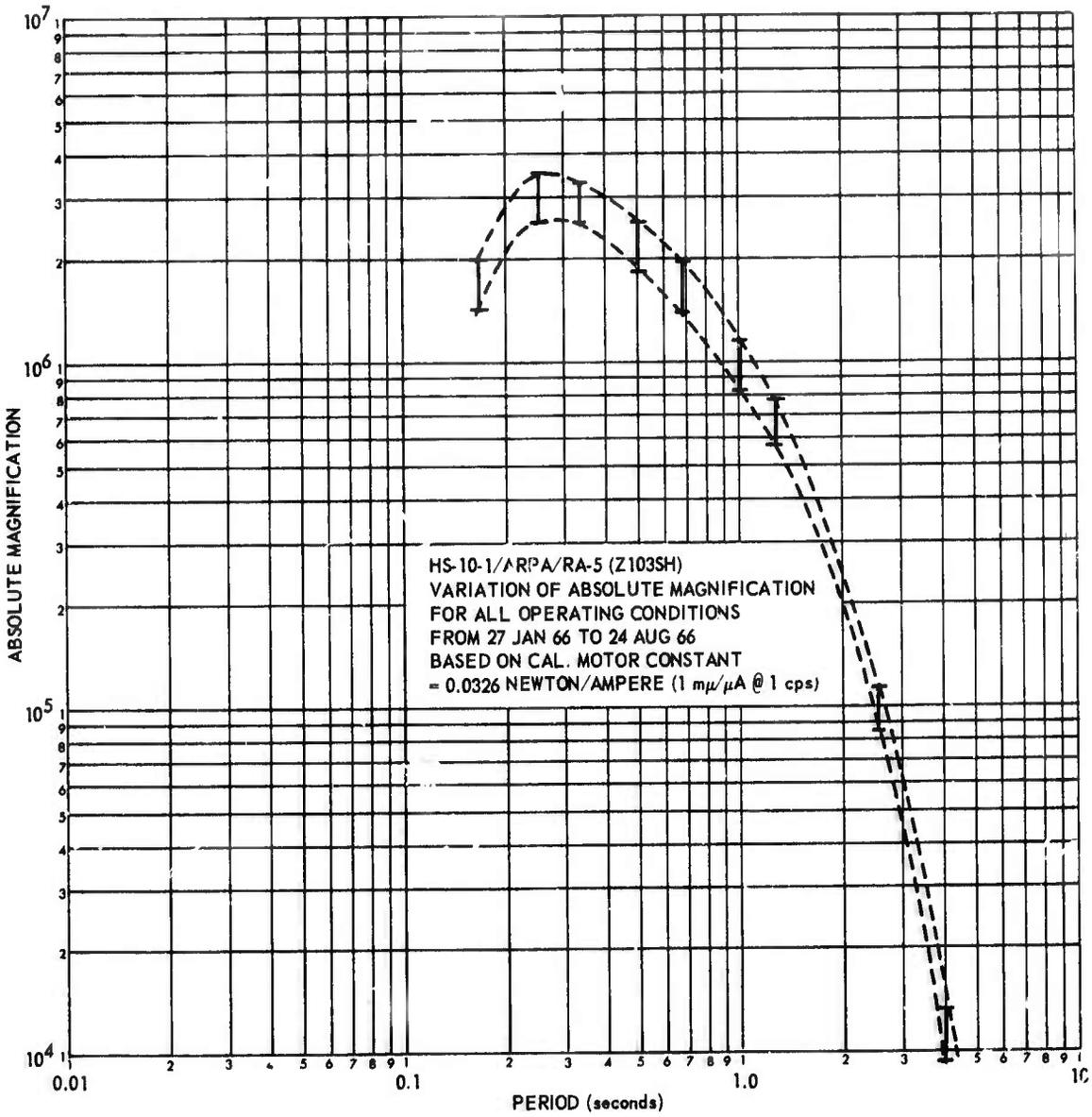

Figure 64. Spread in magnification during test period HS-10-1/ARPA/RA-5 (Z103SH) G 2600

7.4.7 Cable Leakage

System noise, caused by leakage to ground in the data cables, was observed several times on both systems and was remedied by working on the surface end of the seismometer cables. Leakage was frequently due to water condensing in the plastic covering over the cable connections. Drying the cable usually eliminated the leakage, but on 21 January, it was necessary to strip and reterminate the cable. On 7 February, the cable terminations were dried, and plastic bags with desiccant were placed over the connections and sealed with Kearney compound. This arrangement was very effective in keeping water out and maintaining the leakage resistance at an acceptable level.

7.4.8 General Performance

Data from the early tests indicated that both systems were capable of operation at a magnification of 1000K at 1 cps. Figures 35 and 36 and figures 65 and 66 show seismograms for the two test systems and the control system. The 20171/23168-A system is designated Z102SG, the HS/RA-5 system is designated Z102SH, and the control standard is designated Z100. At the time these data were taken, the Model 20171 seismometer was operating at a depth of approximately 180 feet, under 140 feet of water. The Model HS-10-1/ARPA seismometer was operating at a depth of approximately 160 feet, under 120 feet of water.

7.4.9 Noise Characteristics

Special test data were recorded on digital magnetic tape and processed at our Garland laboratory to calculate power spectral estimates of the seismic background at TFSO during periods of low microseismic activity and the system noise of the test seismographs. In figures 67 and 68 all power spectra have been corrected for system response and have been plotted in terms of mean square earth displacement per cps in decibels relative to $1\ (m\mu)^2/cps$.

The first data to be analyzed were recorded on 27 July, just prior to the lightning damage. In processing these data, we found that the noise level of the Model 23168-A amplifier was significantly different than it had been for the seismograms shown in figures 35 and 36 and figures 65 and 66 recorded on 25 January. Figure 69 shows a time series recorded by the 20171/23168-A (Z102SG) system on 27 July. We assumed that a power spectral estimate for this time series would not provide meaningful information because of the high-amplitude noise pulses that are present. Power spectra were computed from later data taken from the Model 25220 amplifier/JM seismometer seismograph.

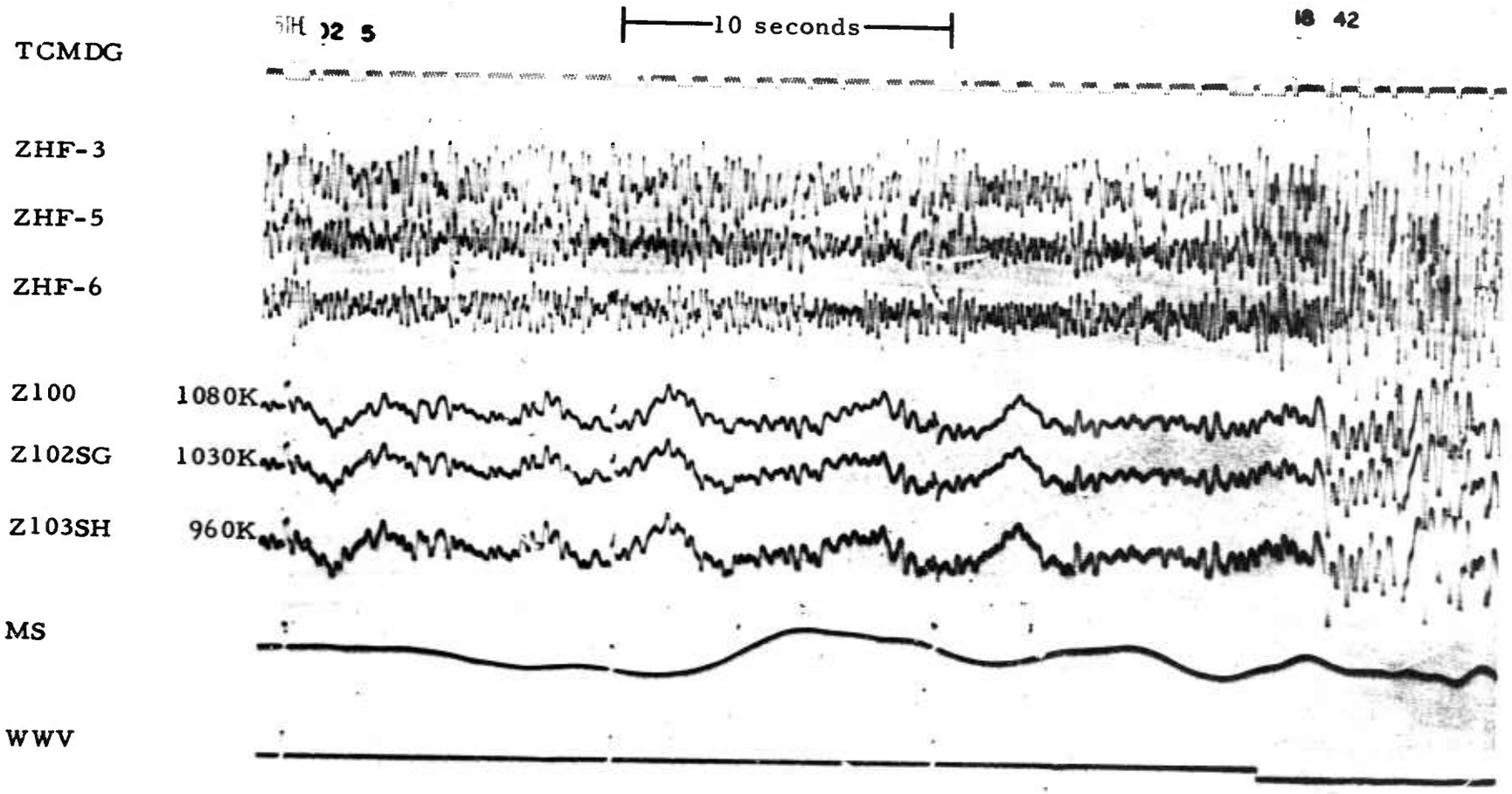

Run 025
25 Jan 1966
Data Group 7178

Figure 66. Short-period recording exhibiting response of shallow-well seismometers and the JMZ to a near-regional event from northwest New Mexico $\Delta \cong 4.0$, azimuth $\cong 56^{\circ}$. (X10 enlargement of 16-millimeter film)

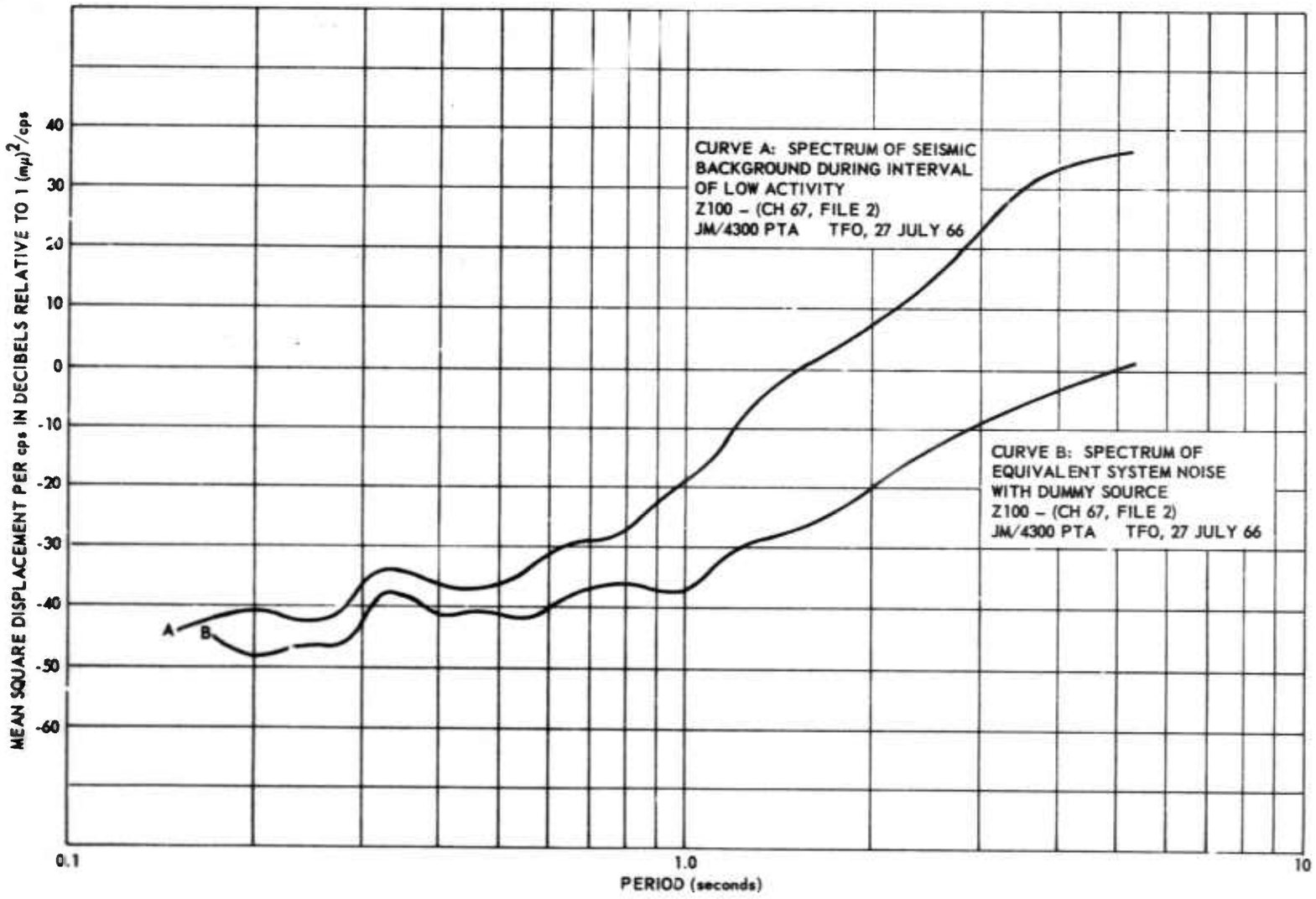

Figure 67. Spectral relations of low level seismic background and system noise
Z100 - CH 67, JM/4300 PTA G 2601

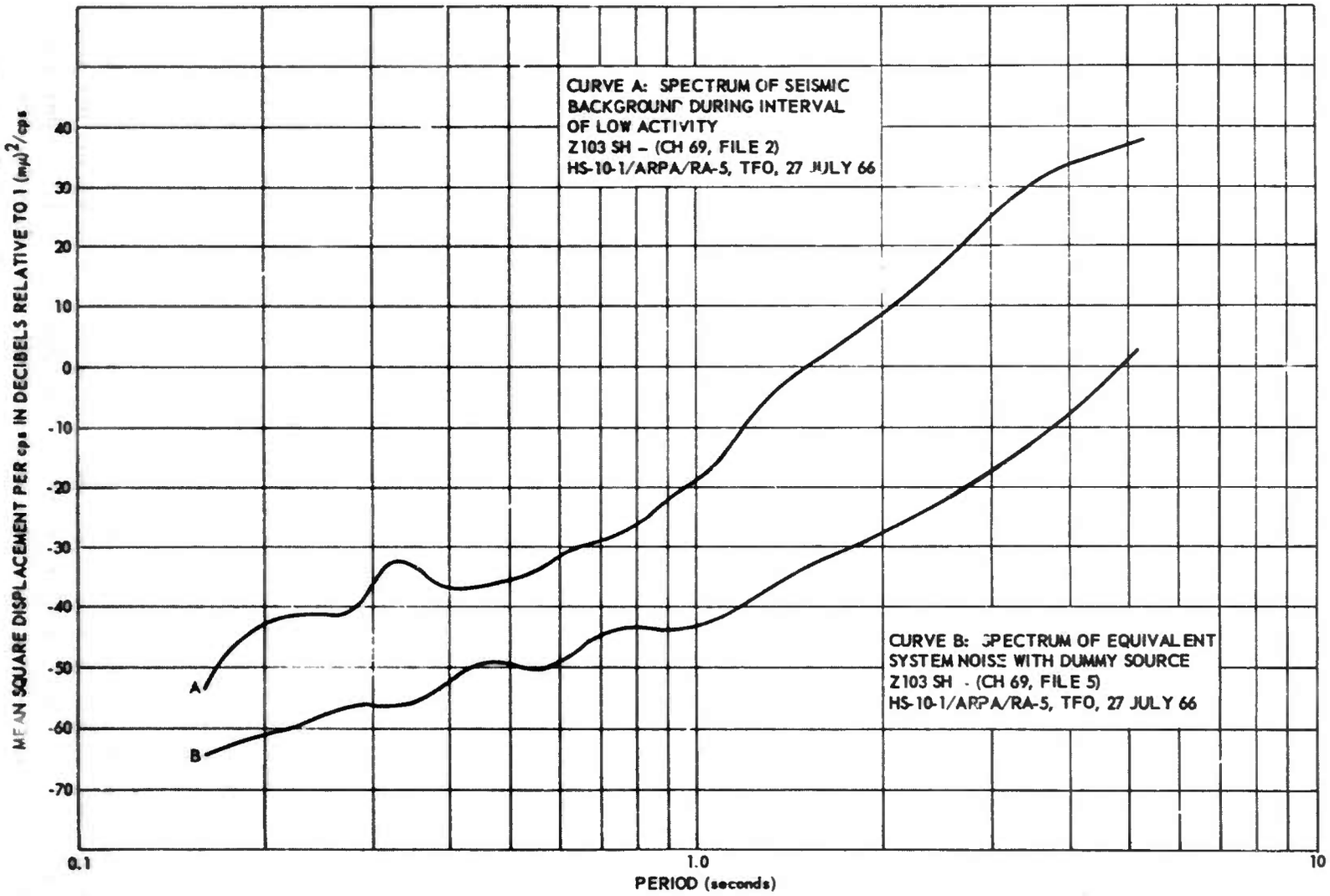

Figure 68. Spectral relations of low level seismic background and system noise Z103SH - CH 69 HS-10-1/ARPA/RA-5

G 2602

The source of the noise shown in figure 69 was not isolated because lightning damaged the amplifier on 27 July. The test history of the Model 23168-A amplifier indicated that either a weakened output stage or cable leakage was the most probable cause of the noise. Static potentials developed by the oncoming storm could also have been a contributing factor.

Figure 67 shows power spectra of seismic background (curve A) and system noise with dummy source (curve B) for the control seismograph, Z100. The seismic background was significantly below the minimum level indicated by the Brune and Oliver curves reported by Byrne (1961). Thus, the separation between the seismic background and the system noise levels at periods above 1 second are below those which had been expected. For the same time interval, the seismic background (figure 68) computed for the HS-10-1/ARPA/RA-5(Z103SH) system was essentially the same as the Z100 seismic background spectrum. The Z103SH noise spectrum was somewhat lower than the Z100 noise spectrum, as was expected, since the Z103SH was operated in the direct-coupled mode and the Z100 was operated with 12 dB attenuation between seismometer and amplifier.

Power spectral estimates calculated from data recorded on 8 December are shown in figure 70. These data were corrected for system response.

Curves A and B of figure 70 represent the power spectral estimates of seismic background and system noise (with dummy source resistor), respectively, for the Z74 control seismograph. The system noise for Z74 was not greatly different from that observed on the Z100 system on 27 July. The seismic background levels at periods greater than 1 second were approximately equal in the two samples, whereas, at periods less than 1 second, the 8 December sample exhibited a higher level. The separation between seismic background and system noise was less than 20 dB at periods less than 1 second for the Z74 data which were recorded with 12 dB attenuation between the seismometer and the amplifier.

Figure 71 compares the Z74 seismic background with the JM/25220 (Z102) seismic background for the same time interval. The difference in the 0.63 second region could have been caused by differences in the surface noise at the two locations and by estimating error. Power spectra were computed at a confidence level of 80 percent and with an accuracy of approximately 3 dB.

Figure 72 shows power spectra of seismic background (curve A) and system noise with dummy source (curve B) recorded with the Z74 seismometer and amplifier directly coupled. For the time series from which these spectral estimates were made, the system noise was more than 20 dB below the seismic background. The background spectrum of the Z102 and Z74 seismograms during this time interval are in close agreement, as shown in

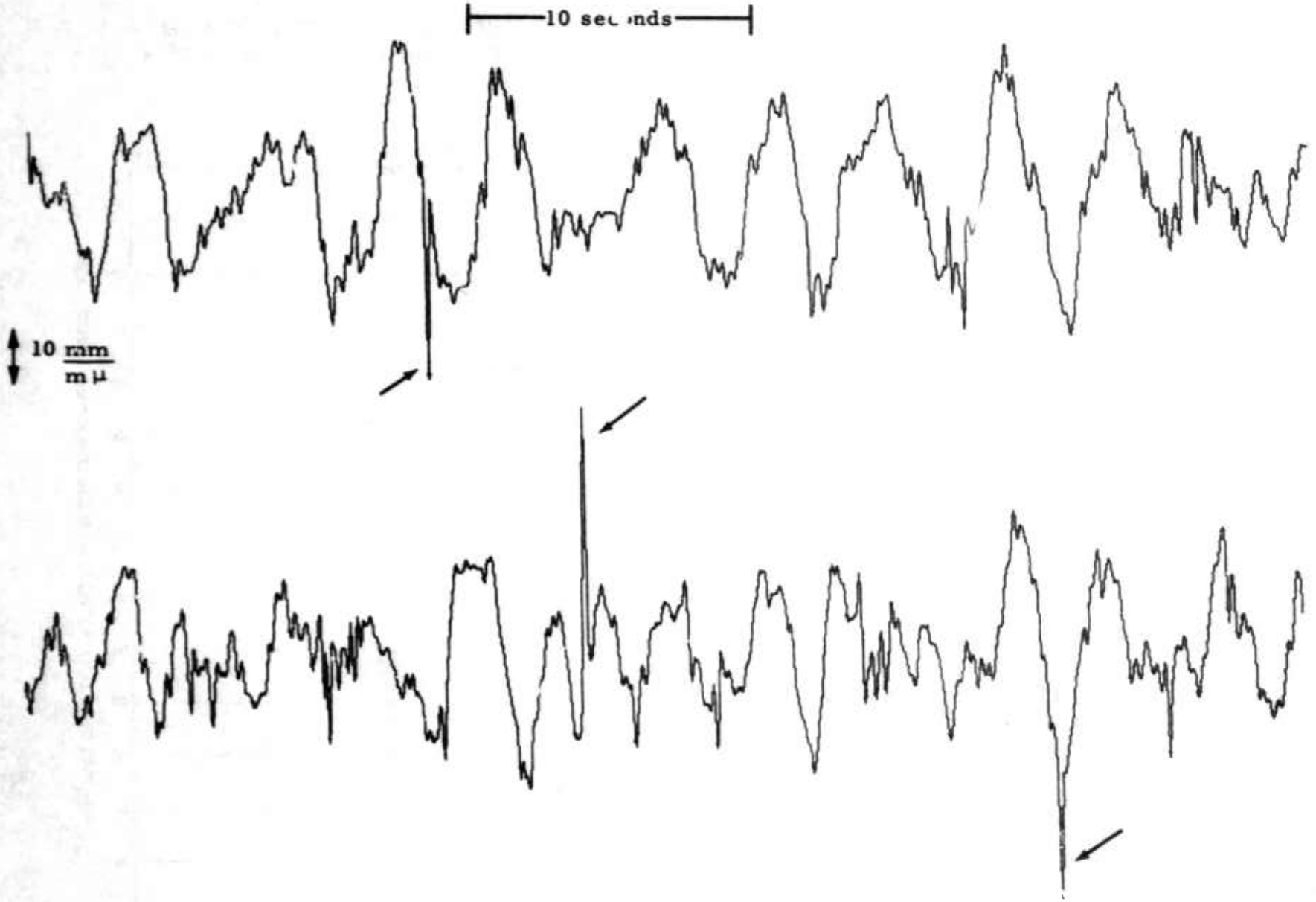

Figure 69. Noise pulses (arrows) on Z102SG during interval of low seismic background (magnification approximately 10,000K)at 1 cps (Analog conversion of digital-tape seismogram)

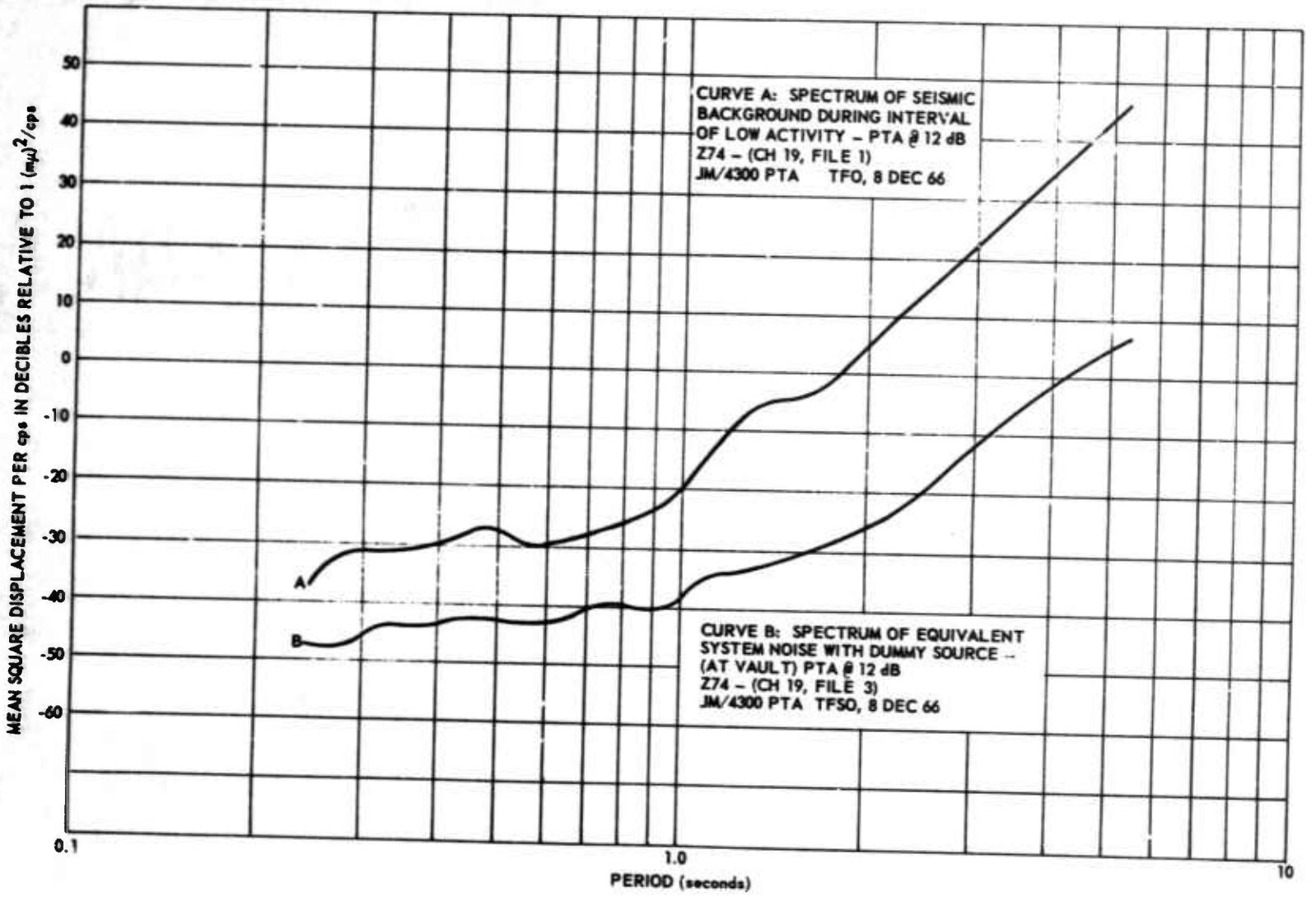

Figure 70. Spectral relations of low level seismic background and system noise PTA at 12 dB TFO Z74 - (Astrodata CH 19) JM/4300 PTA TFO, 8 Dec 1966

G 2603

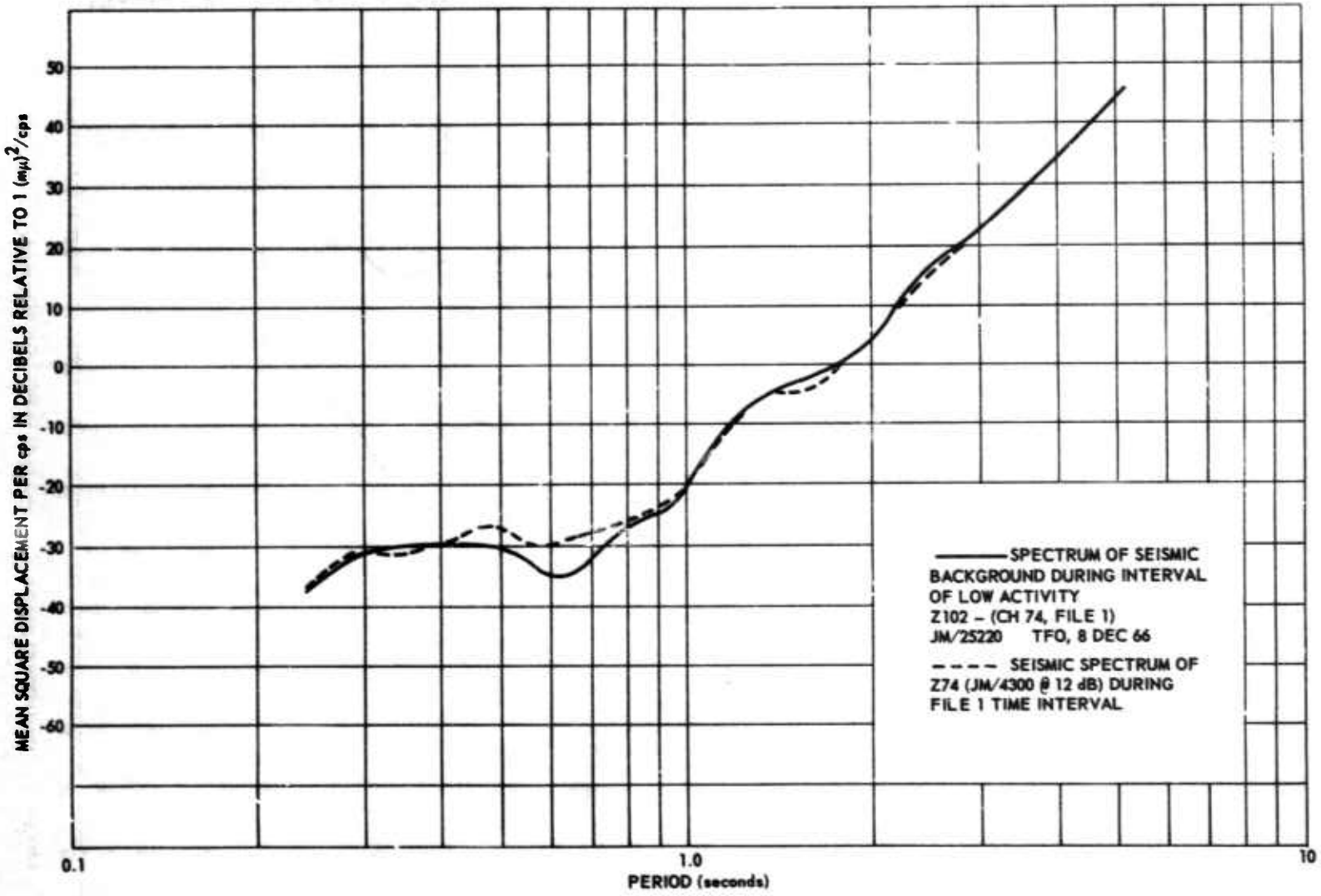

Figure 71. Spectrum of seismic background during interval of low activity Z102 - (CH 74, File 1) JM/25220 TFO, 8 Dec 66 G 2604

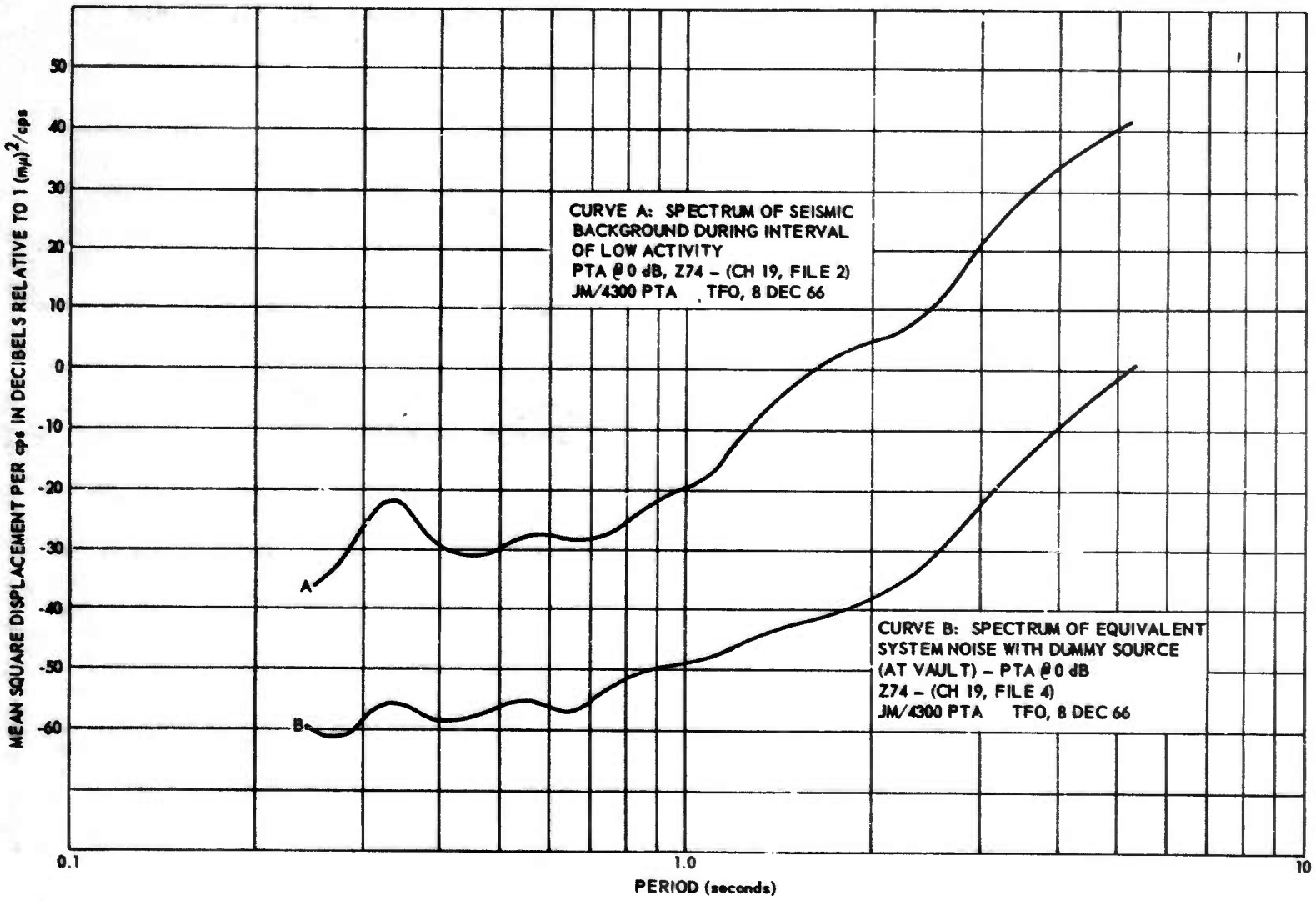

Figure 72. Spectral relations of low level seismic background and system noise PTA at 0 dB TFO Z74 - (Astrodata CH 19) JM/4300 PTA TFO, 8 Dec 66

G 2605

figure 73. A slight difference between the two spectra is to be expected since the difference between the direct-coupled Z74 response and the loosely coupled Z74 response was not taken into account.

7.4.10 Z102 System Noise

System noise with a dummy source for the Z102 seismograph, which utilized a Model 25220 amplifier and JM seismometer, was recorded on 8 December. When we processed these noise data, we discovered that the system noise of the seismograph was below the digitizing threshold of the Astrodata Data Acquisition System, as operated during most of the recording interval. Figures 74 and 75 show time series for the Z74 seismograph with 12 dB attenuation and the Z102 seismograph at the same magnification. Figures 70, 74, and 75 indicate that the system noise of the Z102 seismograph must be less than curve B of figure 70 but greater than curve B of figure 72. That is, the system noise spectrum of the JM/25220 combination would be approximately the same as that of a standard TFSO seismograph operated with 6 dB attenuation.

Although a power spectrum of the system noise with dummy source could not be computed for the Z102 seismograph because the system noise was below the digitizing threshold most of the time, the data in figures 72 and 73 specify the JM/25220 noise characteristics with good accuracy.

7.4.11 Theoretical Consideration of System Noise

In the past, we have assumed that a noise test in which a dummy source resistance equal to the seismometer coil resistance is substituted into the seismograph system, provides a valid estimate of the system noise. This assumption is adequate when testing seismograph systems employing galvanometer-input amplifiers (PTA's).

Accurate determination of system noise requires that the actual dynamic impedance of the seismometer be substituted for the seismometer. In the case of the (current-sensing) galvanometer input, substitution of a dummy source equal to the seismometer coil resistance maintains the system frequency response and results in "worse case" noise current through the galvanometer.

In the case of the high-input impedance, voltage-sensitive amplifier, substitution of a resistance equal to the coil resistance results in less than minimum noise voltage at the amplifier input over the band of interest.

Curves showing the theoretical equivalent earth-displacement spectrum of system noise, considering only the seismometer thermal noise (for example, noiseless voltage-sensitive amplifier), for the HS 10-1/ARPA and 20171-A/ seismometers are shown in figure 76. A comparison of the thermal noise

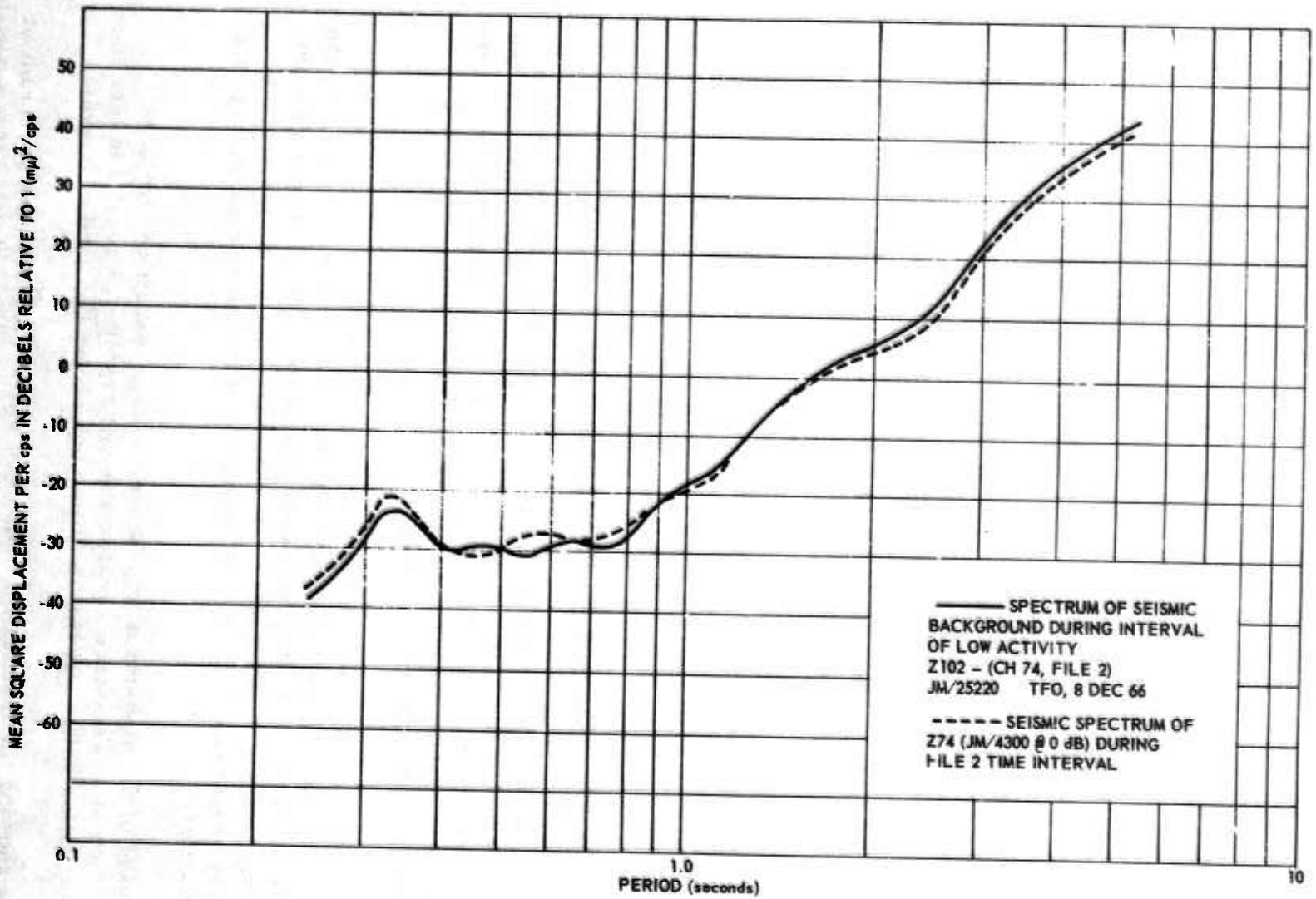

Figure 73. Spectrum of seismic background during interval of low activity Z102 - (CH 74, File 2) JM/25220 TFO, 8 Dec 66 G 2606

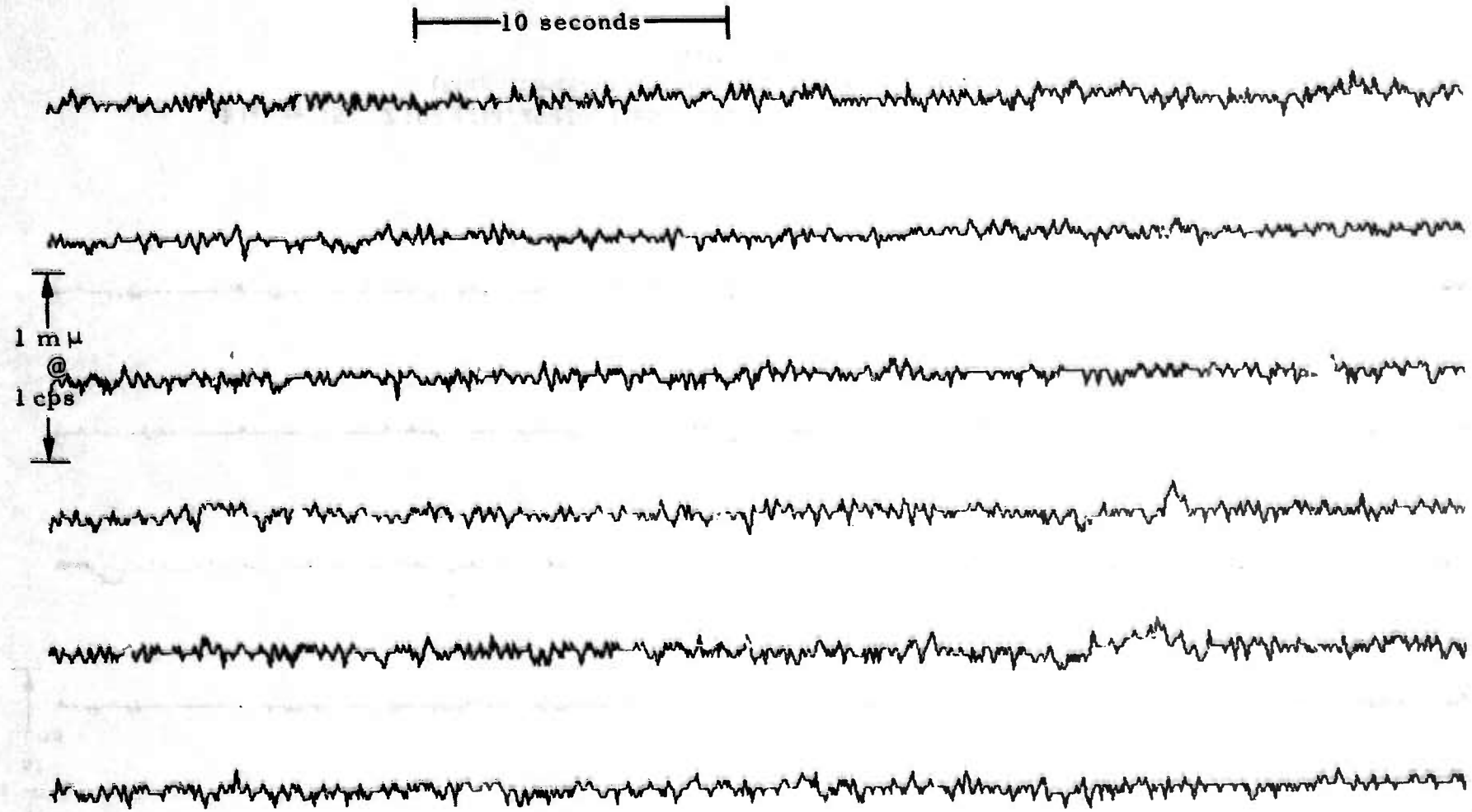

Figure 74. Z74 time series used for computing noise spectrum of system with dummy source (PTA at 12 dB, magnification = 32,000K at 1 cps) (Analog conversion of digital-tape seismogram)

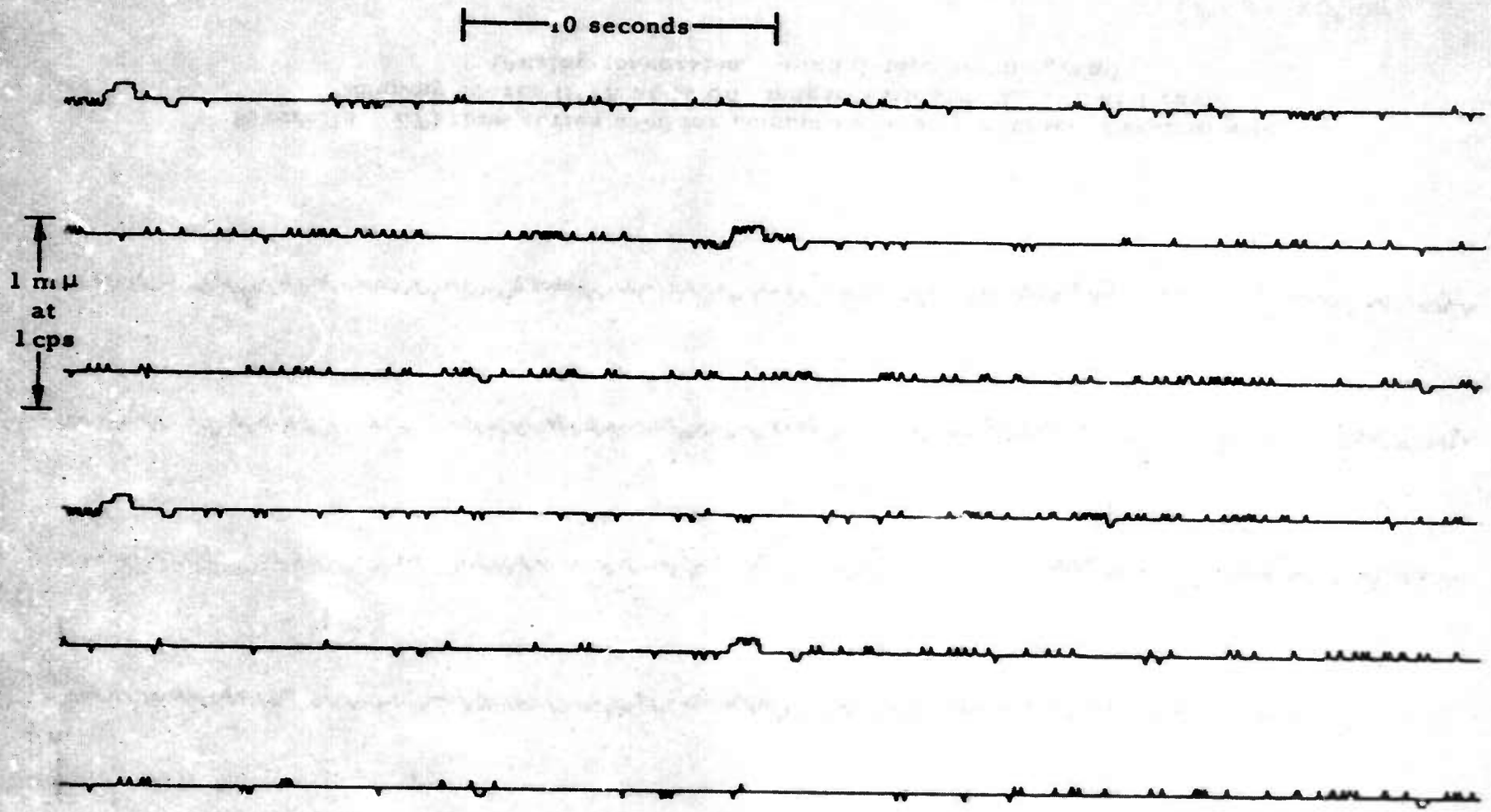

Figure 75. Z102 (JM/25220) time series of system noise with dummy source (Magnification = 32000K at 1 cps) (Analog conversion of digital-tape seismogram)

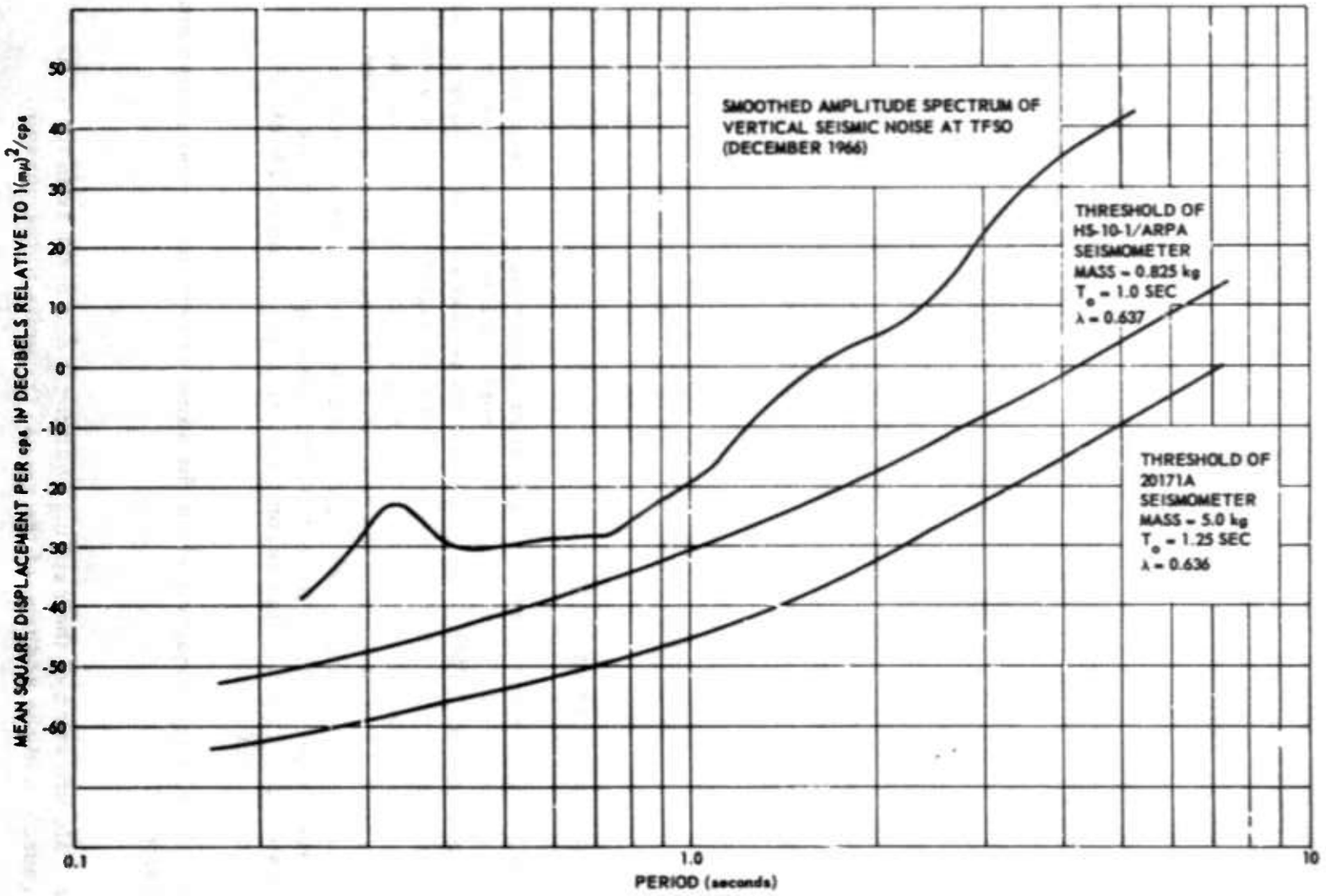

Figure 76. Comparison of representative TFSO seismic background level with minimum thermal noise levels of the HS-10-1/ARPA and 20171-A seismographs (with noiseless amplifiers) G 2607

curve for the HS-10-1/ARPA seismometer with curve B of figure 68, which represents the equivalent system noise of the HS-10-1/RA-5 combination with dummy source, shows that the dummy-source tests of this system yielded misleading results. The maximum error in the dummy-source tests occurred at the natural frequency of the seismometer (1 cps) and is in excess of 10 dB.

Also shown in figure 76 is a smoothed spectrum of the TFSO seismic noise recorded by a direct-coupled galvanometer-input seismograph. The thermal noise levels of each of the systems tested is below the level of the TFSO seismic noise. However, the HS-10-1/ARPA seismograph is marginal because at about 1.3 cps, the separation between the seismic noise and thermal noise is less than 8 dB, and between about 2 cps and 0.8 cps, the separation is less than 20 dB. The thermal noise level of the Model 20171-A seismograph is between 10 and 16 dB lower than that of the HS-10-1/ARPA system and is, therefore, more than 20 dB below the seismic noise level throughout the band of interest. These data show that for a seismic background level comparable to that of TFSO, an effective seismograph should have a seismometer with a mass of at least 5 kilogram.

8. DEVELOPMENTAL FUNCTION

8.1 AUTOMATIC CALIBRATION

Considerable effort is required for the routine calibration and frequency response tests of the more than 60 short-period and long-period seismographs in operation at TFSO. The effort for these tasks could be substantially reduced, and the accuracy of calibrations could be significantly improved through the elimination of human error by using an automatic calibration system. Based on discussions of the desirable features of such a system with the Project Officer and TFSO engineering personnel, we submitted a request to the Project Officer for authority to develop an automatic calibration system for TFSO. This recommendation was made in TR 66-85, dated 7 October 1966.

Two basic plans, each requiring about the same amount of special equipment were considered.

a. Modification of the existing equipment and circuits in the calibration console and the addition of the necessary units to the console;

b. Development of an independent automatic calibration system, maintaining the calibration console in its present configuration.

The second plan was recommended because it retains the usefulness of the calibration console, because the independent automatic calibration system could be more easily upgraded and adapted to future requirements, and because fewer installation problems would be encountered.

A block diagram of the calibration system planned is shown in figure 77. The system could accommodate seismograph systems with as many as 98 individual elements and as many as 6 major summations. The automatic calibrator would facilitate automatic routine calibration and frequency response determination by providing the following:

a. Sequential switching of the calibration current among seismographs according to a predetermined program;

b. Control of the amplitude, frequency, and duration of the calibration current applied to each seismograph;

c. Provide a permanent monitor record of the calibration current supplied to each of the seismographs.

Automatic monitoring of the outputs of the seismographs during calibration and removal of individual seismographs from summation during calibration could be readily accomplished by installing additional components in the system, if experience indicates that these functions are desirable.

In our opinion, an automatic calibration system would be a valuable asset to the TFSO system and would provide increased accuracy of calibration resulting in increased confidence in the recorded data.

8.2 IMPROVED HIGH-FREQUENCY SEISMOGRAPH SYSTEM

A memorandum describing the requirements of an improved high-frequency seismograph, the various tests on which these requirements were based, and a request for authority to build a high-frequency seismograph were submitted to the Project Officer in late October 1966. The conclusions of these tests were that eight Model GS-13V geophones, installed in a pressure case, would provide a satisfactory seismometer for the improved high-frequency seismograph. These geophones, produced by the Engineering Products Company of Tulsa, Oklahoma, would each be modified to have a 0.453 kilogram mass and a 2,860-ohm data coil. An Ithaco amplifier was recommended for amplification of the output of this seismometer.

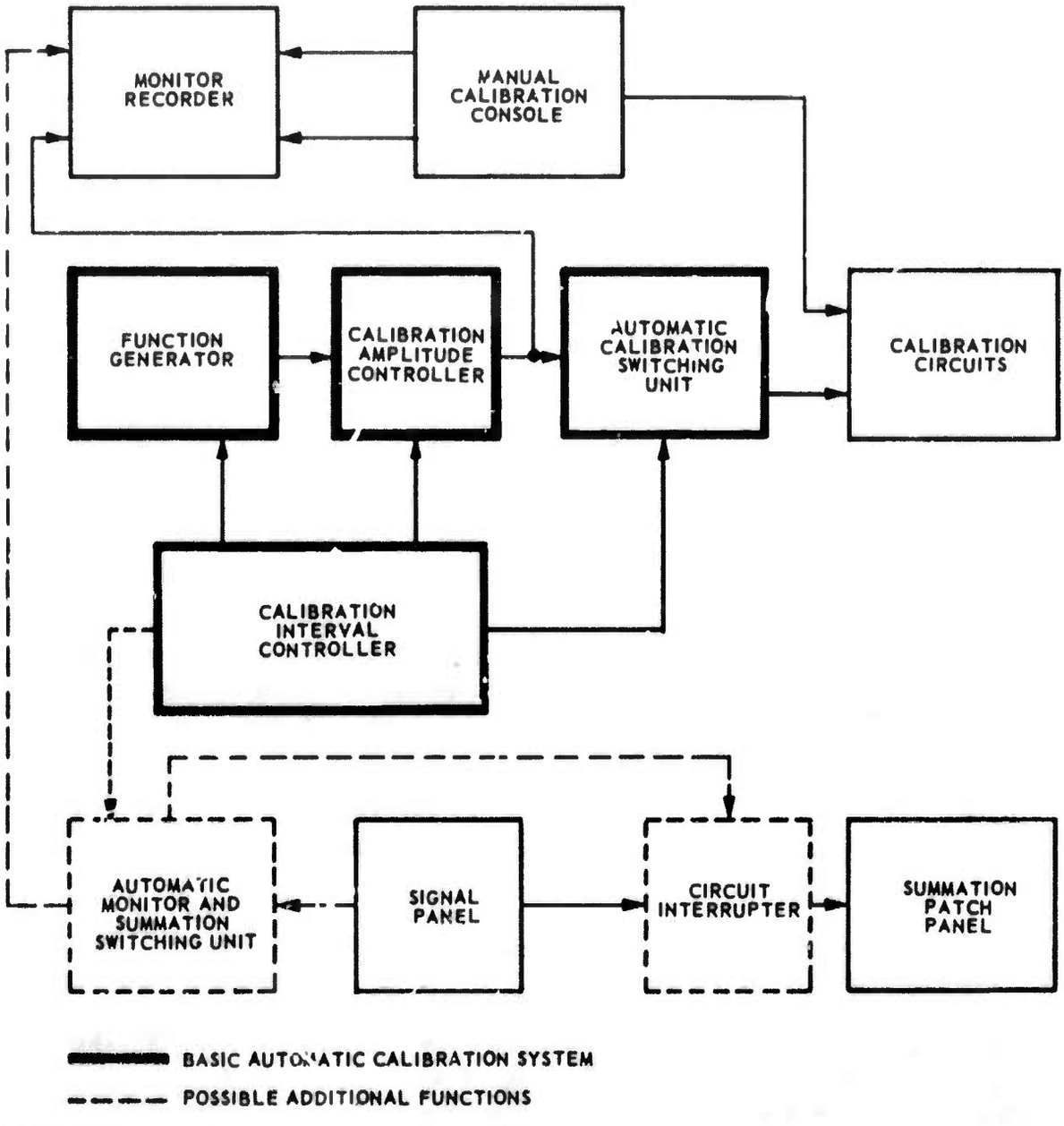

Figure 77. Block diagram of existing calibration equipment and the basic components of the automatic calibration system planned for TFSO G 1419

9. ASSISTANCE PROVIDED TO OTHER GROUPS

Throughout the term of Project VT/5055, the TFSO facilities and accompanying technical assistance were made available to other organizations and individuals as approved or requested by the Project Officer. Also, several civic, high school, and university groups toured the observatory on a noninterference basis. The following are among the groups using the TFSO facilities during the contract:

a. Dr. R. A. Haubrich, University of California, used the TFSO facilities from 1 June to 17 September 1965 to operate an Ambilog-200 computer system, on site. Thirty-two channels of data were provided to the University for "on line" processing.

b. Special recording for Texas Instruments was accomplished using the Astrodata digital data acquisition system. High-gain and low-gain recordings were made from both short-period and long-period instruments. Selected systems from the TFSO array and from eight LRSM vans made up the recording format.

The digital recording was conducted on a 24-hour-a-day basis between 16 August and 30 October. Two Texas Instruments (TI) representatives were at TFSO during this interval. The engineering laboratory was temporarily converted to a "clean room" to ensure the best possible recordings. Also, the Astrodata equipment was modified by changing the packing density from 800 bpi to 556 bpi and by installing operational amplifiers and filters.

c. Recordings were made for Dr. Stewart Smith and sent to the California Institute of Technology routinely during this reporting period. Data from three FM magnetic-tape recorders and one Develocorder were sent until 6 July 1966; one Develocorder seismogram has been supplied to Dr. Smith, daily, since July.

Dr. Smith has indicated that his group would like to receive magnetic-tape seismograms again in the future; however, no date has been established for the resumption of magnetic-tape recording for them.

d. Between 1 May and 1 July 1965, the Astrodata seismic digital recording equipment was used to gather data for MIT. Also, during this interval, eleven channels of TFSO and LRSM van data were telemetered from the observatory to Lincoln Laboratory, MIT, over a leased telephone circuit. On 21 October 1965, the 11-channel system was replaced by an 8-channel system. Seven channels of data have transmitted continuously since that time.

During periods of seismograph attenuation and special tests, MIT was notified whenever possible.

e. On several occasions during Project VT/5055, the facilities were toured and brief lectures were given on seismology to groups of college students and instructors. Most of the groups consisted of elementary education students from Arizona State University. A total of 815 college students visited the observatory.

Also, a few groups of high school science students from Phoenix high schools and elementary school students from the Payson-Pine area toured the observatory. During the term of the contract, 54 high school students and 94 elementary school students visited TFSO.

f. On 17 September 1965, 56 members of the Intercities Relations Committee of the Phoenix Chamber of Commerce toured the observatory. This committee had previously selected the observatory as the most interesting industry in the Payson area.

g. Dr. Harold Kirvoy of the Astrogeological Department of the United States Geological Survey (USGS) in Flagstaff, Arizona, requested and has received cooperation from TFSO in providing periodic information on specified events as requested by them.

10. RESEARCH INVESTIGATIONS

10.1 SIGNAL CLASSIFICATION STUDY

A cascading classification of earthquake signals, anagolous to biological or fingerprint classification, based on visual characteristics of longitudinal waves (typically P or PKP) as recorded on summation seismograms is being developed. During this reporting period, approximately 150 earthquakes of magnitude 5.0 or above were selected for initial study. Signals recorded at TFSO, UBSO, and WMSO are used in the study. A composite film seismogram of these events is being prepared. This seismogram will contain all recorded signals from the control epicenters. The signals are coded to reflect the receiving station and the epicenter. Several experienced analysts will be asked to classify the signals according to instructions being prepared, which will accompany the film to the observatory. The classification of signatures is based on the number, relative position, relative amplitude, and rate of decay of energy pulses in the first 20 seconds of the signals. Classifications assigned by observatory analysts

will be checked against classification assigned by Garland-based analysts to determine the effectiveness and repeatability of the classification system.

10.2 SHORT-PERIOD ARRAY RECOMMENDATION

10.2.1 General

Under Project VT/5055, we undertook a study to determine how the ratio of the teleseismic signal to ambient noise level at TFSO could be improved. We reviewed the available data regarding the characteristics of the ambient noise field at TFSO and considered the potential effectiveness of several array configurations in attaining our goal. The results of this study were reported, and a configuration for the redesign of the TFSO array was recommended in our Project Recommendation P-688 which was submitted to the Project Officer on 7 September 1966.

The beam-steered output of the recommended array is expected to provide an improvement in signal-to-noise ratio (S/N) of between 8 and 12 dB relative to the existing 31-element array at frequencies at which we expect teleseismic P waves. In addition, a 19-element minor array (composed of selected elements of the existing array) will be operated to maintain the detection capability of the observatory during part of the installation of the expanded array.

10.2.2 Proposed Arrays

10.2.2.1 Minor Array

We recommended that 19 selected elements from the existing array be left in place to form the minor array. The elements of this array will be uniformly spaced at distances of about 0.61 kilometers in a hexagonal pattern; the maximum dimension of the minor array will be about 2.5 kilometers. A diagram of this array is shown in figure 78 and the $\vec{k}$ plane response of the array is shown in figure 79.

We expect the unprocessed summation of the outputs of the 19-element array to provide an on-line detection capability comparable to that of the existing 31-element array. Figure 80 shows cross-sections through the principal lobes of the $\vec{k}$ plane responses of the existing array and the proposed 19-element array. The observed S/N improvement obtained by summing the outputs of the existing array and the theoretical S/N improvement obtained by summing the outputs of the proposed minor array are compared in figure 81. Based on the fact that the S/N improvement at frequencies above about 1.5 cps obtained by summing the elements of the existing array is about 2.5 dB less than the predicted increase, we expect a similar difference to be observed for the 19-element array. Therefore,

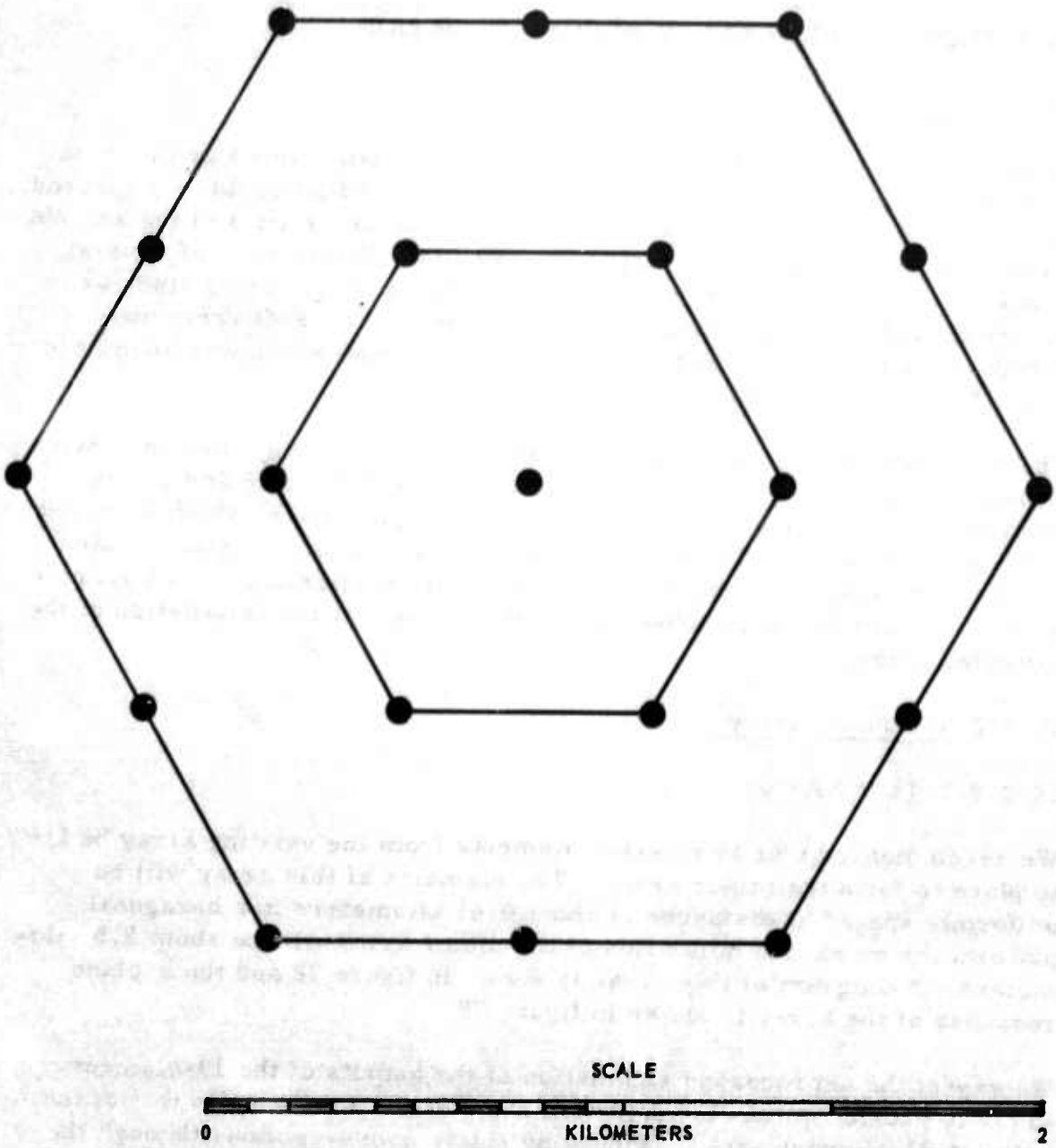

Figure 78. Proposed 19-element array at TFSO

G 2072

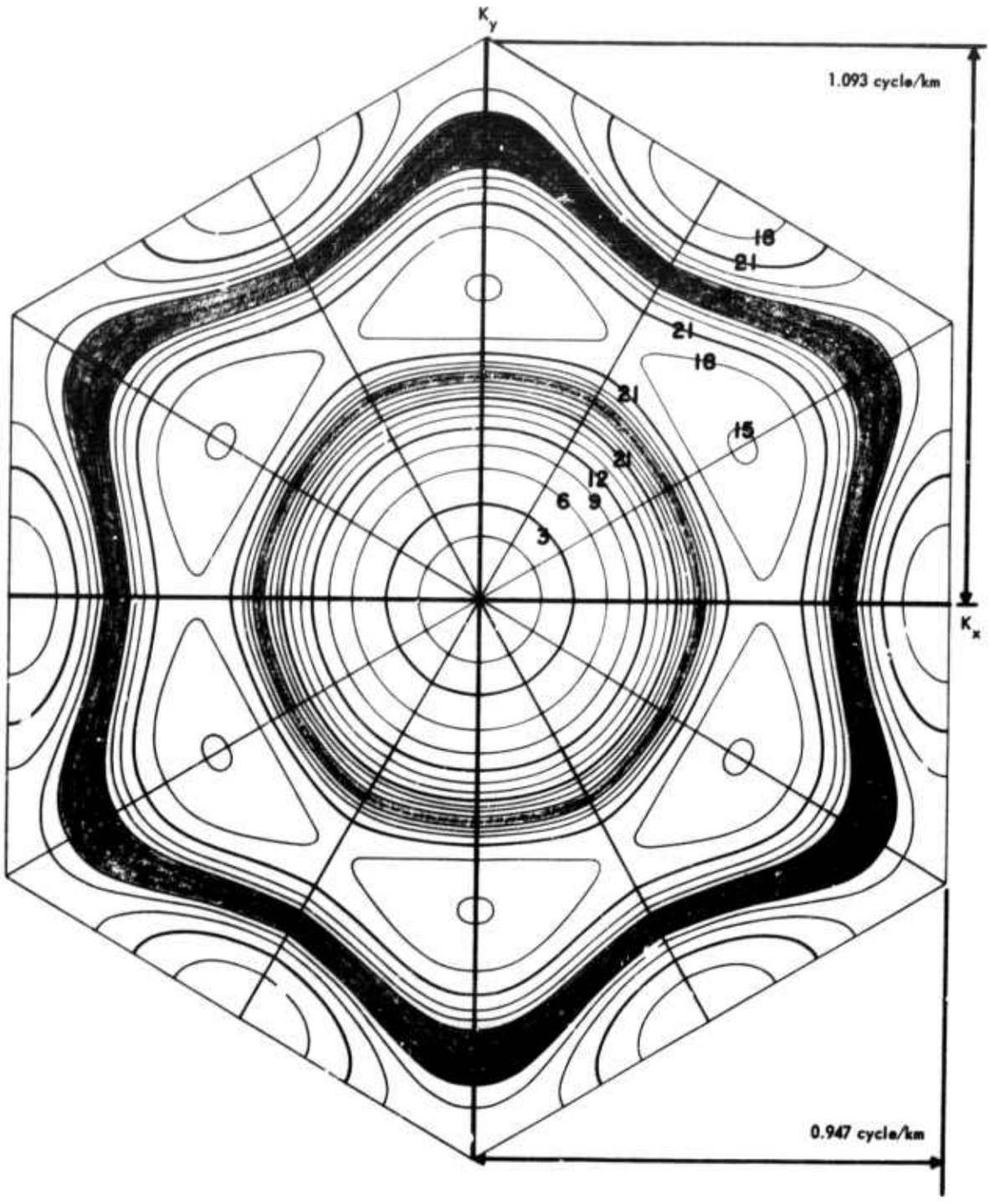

Figure 79. $\vec{k}$ Plane response for equally weighted 19 seismometer hexagonal array with seismometer spacing d (from TI-1961

G 2073

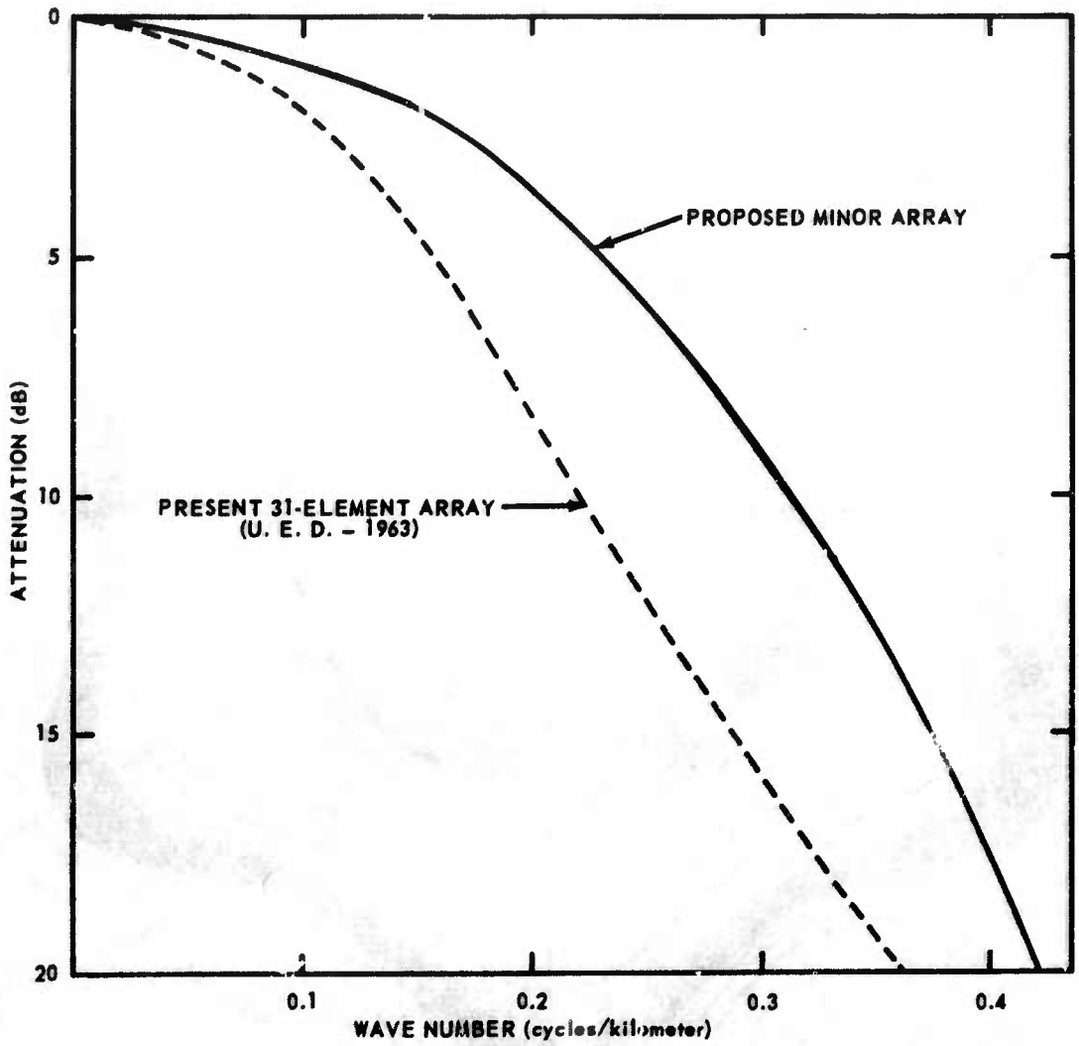

Figure 80. Comparison of the principles lobes of the present 31-element array and the proposed minor array

G 2074

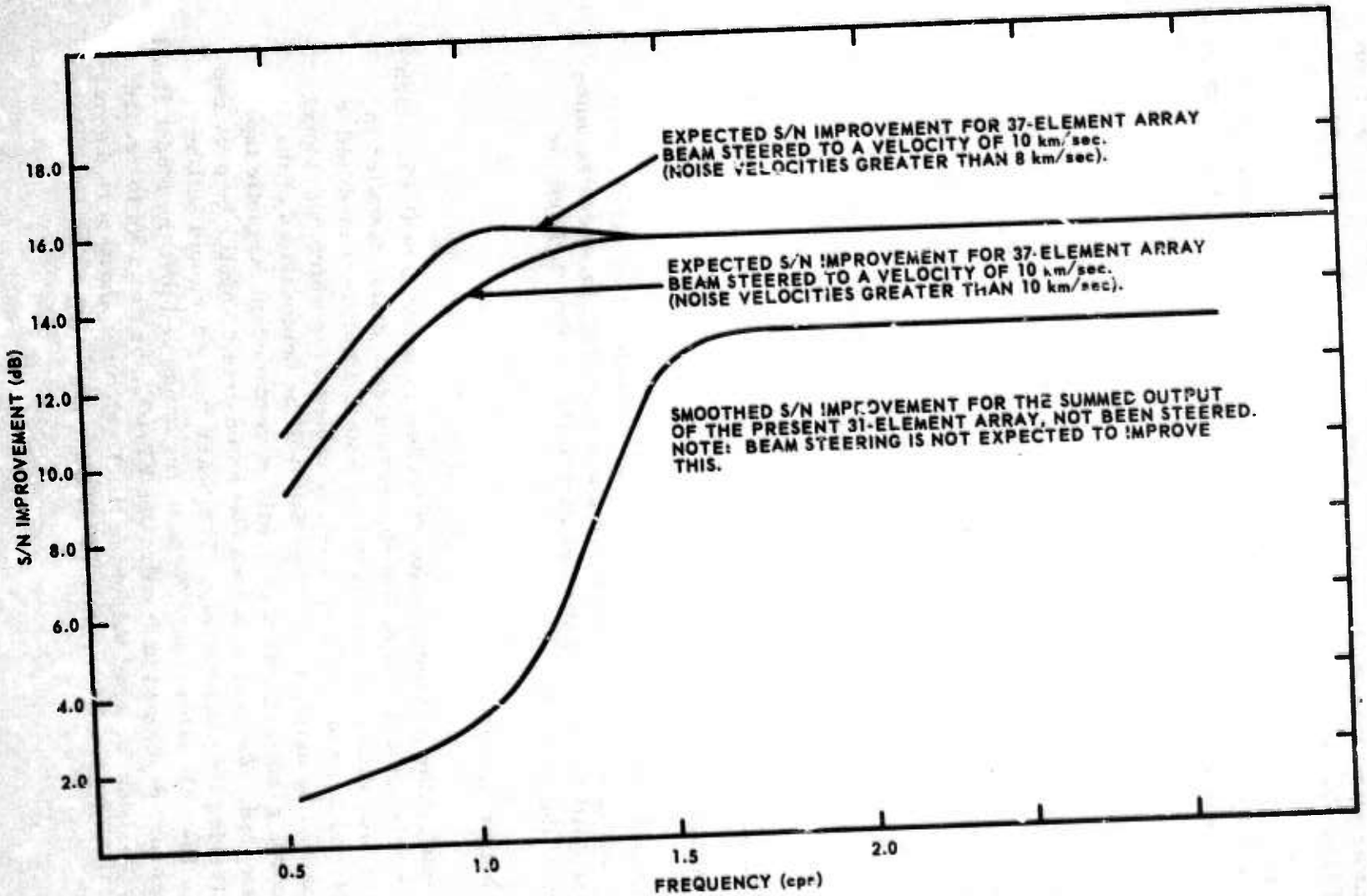

Figure 81. Comparison of S/N improvement for the summed output of the present 31-element array and the beam-steered output of the proposed 37-element array

G 2075

the actual improvement of S/N obtained at frequencies above 1.5 cps from the minor array will probably be about 2 dB less than the improvement obtained from the existing array.

In order to utilize the reusable cable from the minor array in the major array, the elements of the minor array will be redistributed and incorporated into the major array, after 18 of the elements of the major array have been installed.

10.2.2.2 Major Array

We recommended installation of a 37-element array of short-period vertical seismographs. The elements of this array are to be uniformly spaced at distances of 5 kilometers in a pattern of three concentric hexagons (see figure 82). The $\bar{k}$ plane response of this array is shown in figure 83.

We expect the beam-steered outputs of this array to provide an improvement in S/N for teleseismic P-wave signals of between 8 and 12 dB relative to the summed output of the existing 31-element array at frequencies below about 1 cps.

10.2.3 Instrumentation

10.2.3.1 Minor Array

We plan to use 19 elements of the present 31-element array for the minor array. No changes are required in the instrumentation for these seismographs which will be operated through part of the period required for installation of the major array.

10.2.3.2 Major Array

We plan to install the instrumentation described in option 3 of P-688 which includes JM seismometers with high-impedance data coils, installed in near-surface tank vaults; Model 25220 solid-state amplifiers modified to provide FM outputs; and single spiral-four cables over which both power and FM data will be multiplexed. The data will be demodulated at the central recording building where they will be recorded on magnetic tape and beam steered. We recommended that an on-line computer be provided for beam steering the major array. The beam steered outputs will be recorded on 16-millimeter film. We also recommended that the Model 18621 array processor, developed under Project VT/072, be provided to record and display the beam steered outputs of the 37-element short-period array on a single 16-millimeter film with X20 display capability.

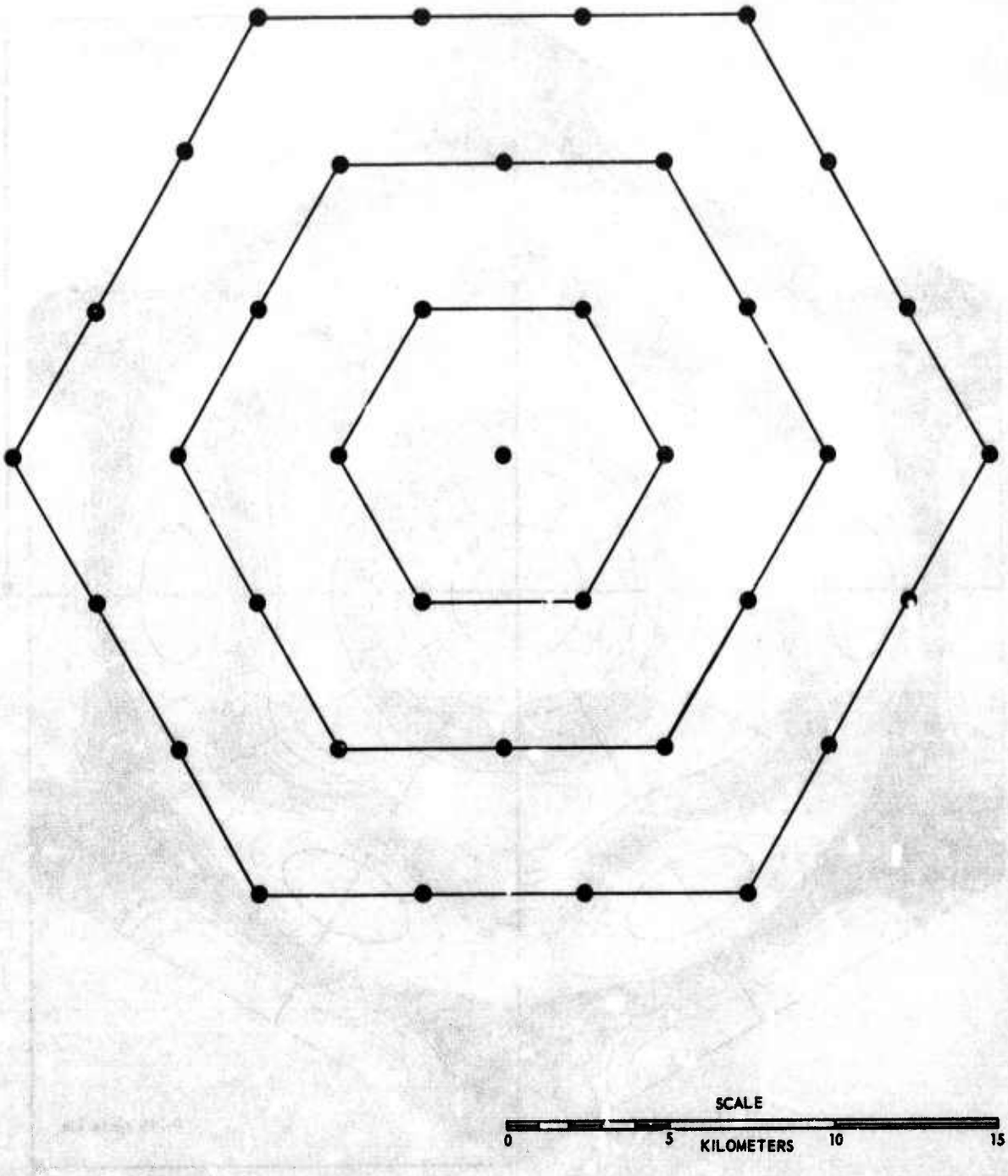

Figure 82. Proposed 37-element array at TFSO

G 2076

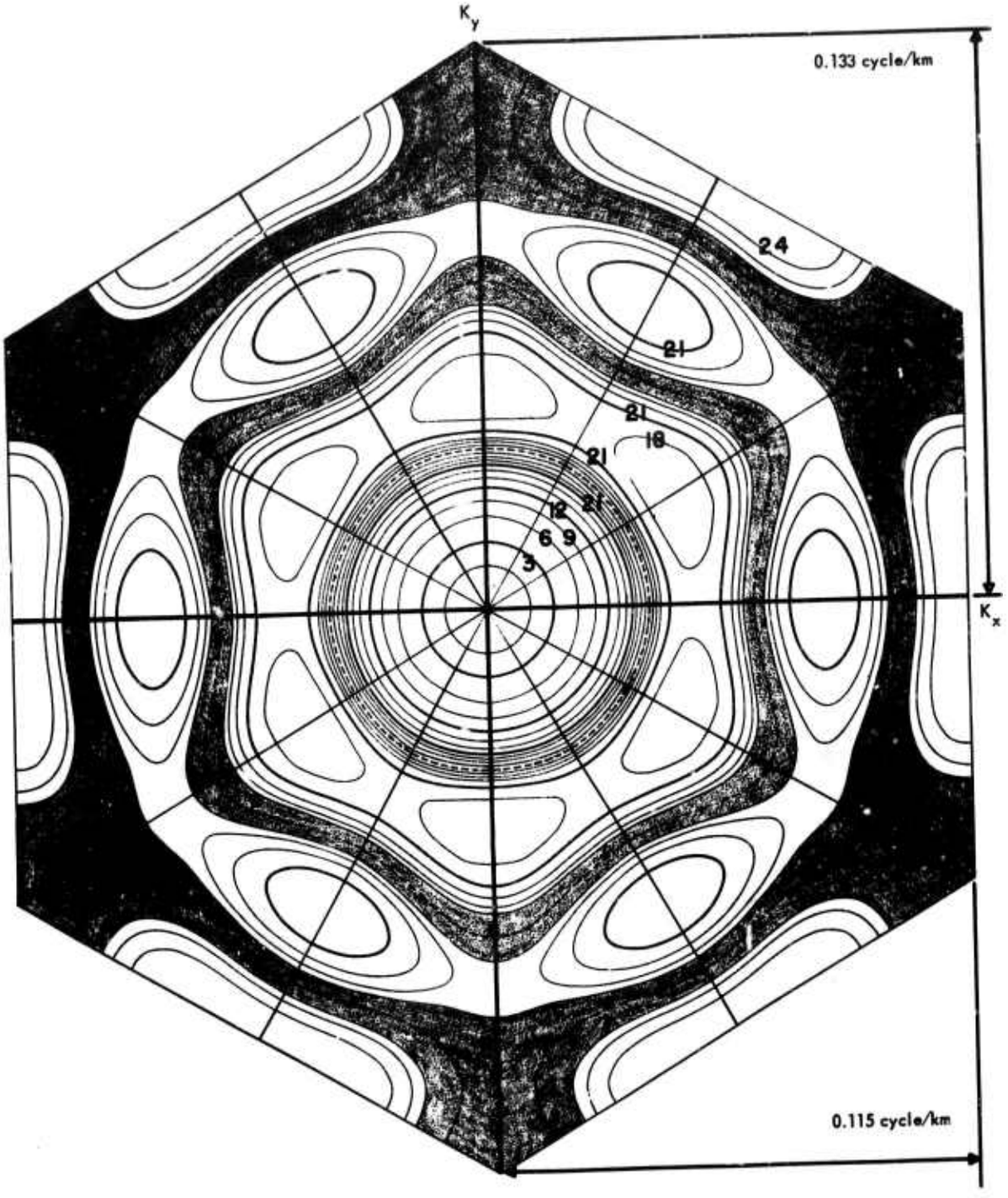

Figure 83. $\vec{k}$ Plane response for equally weighted 37 seismometer hexagonal array with seismometer spacing of 5 km (from TI-1961)

G 2077

Initially, we plan to steer 30 beams "tuned" to velocities and azimuths adequate to achieve global coverage with minimum attenuation for 1 cps teleseismic P-wave signals from hypocenters located at least 25 degrees from TFSO. Figures 84, 85, and 86 are the composite $\hat{k}$ responses for the 30 beams that we propose to steer initially for 0.67 cps, 1.0 cps, and 1.5 cps signals, respectively. These initial beams will be tuned as follows:

a. Twelve beams tuned to 12.5 kilometers/second in azimuthal increments of 30 degrees;

b. Twelve beams tuned to 19.2 kilometers/second in azimuthal increments of 30 degrees;

c. Six beams tuned to 47.6 kilometers/second in azimuthal increments of 60 degrees.

The effectiveness of these beams will be evaluated and, based on this evaluation, it may be desirable to test the effectiveness of more beams (up to 50) and/or beams steered to different velocities. In addition, it is our opinion that TFSO should have on-line processing capability in excess of that required for beam steering to facilitate on-line evaluation of other processes that are shown to be potentially useful by off-line testing.

10.3 LONG-PERIOD ARRAY RECOMMENDATION

10.3.1 General

In the past, much of the effort expended in seismological research and instrument development has been directed toward the improvement of short-period seismographs and toward studies of the applications of array theory to the reduction of short-period noise. Because of this, the detection threshold of short-period P-phase arrivals has been lowered appreciably, and is currently well below the threshold of long-period body and surface wave detection. Although short-period seismograph systems are considered to be the principal P-phase seismic event detection systems, the increasing importance of the role of long-period seismometric data in source discrimination and identification warrants the development of arrays of long-period seismographs designed to suppress long-period noise, thereby enhancing long-period signals and lowering the threshold of long-period body and surface waves. Decreasing the long-period body and surface-wave detection threshold can be expected to facilitate refinement of existing source discriminations and identification techniques and might yield data upon which new techniques could be based. Because long-period seismographs are better detectors of shear phases than are short-period seismographs,

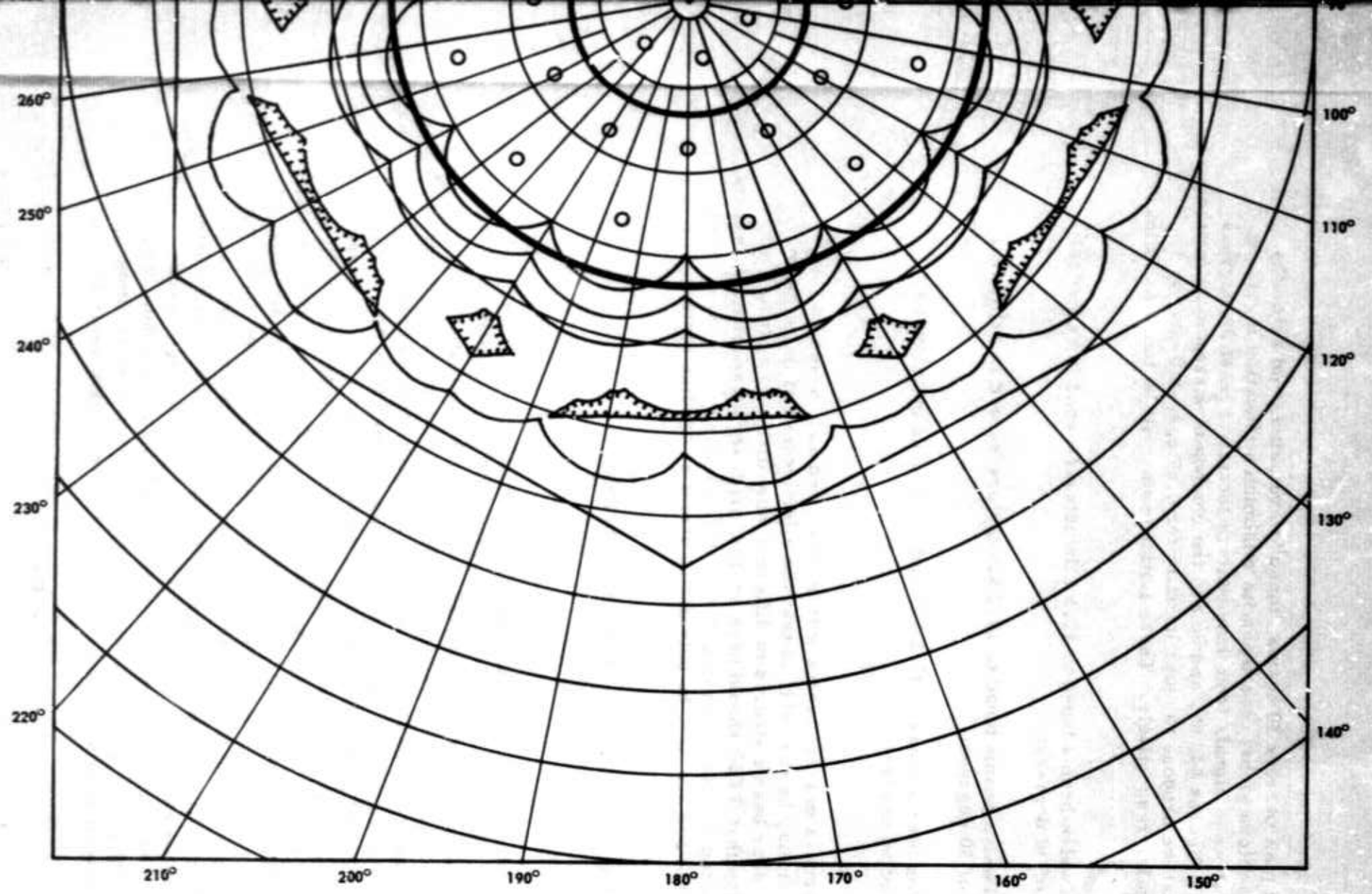

Figure 84. Composite $\vec{k}$ response for 30 beams of 37-element array

G 2078

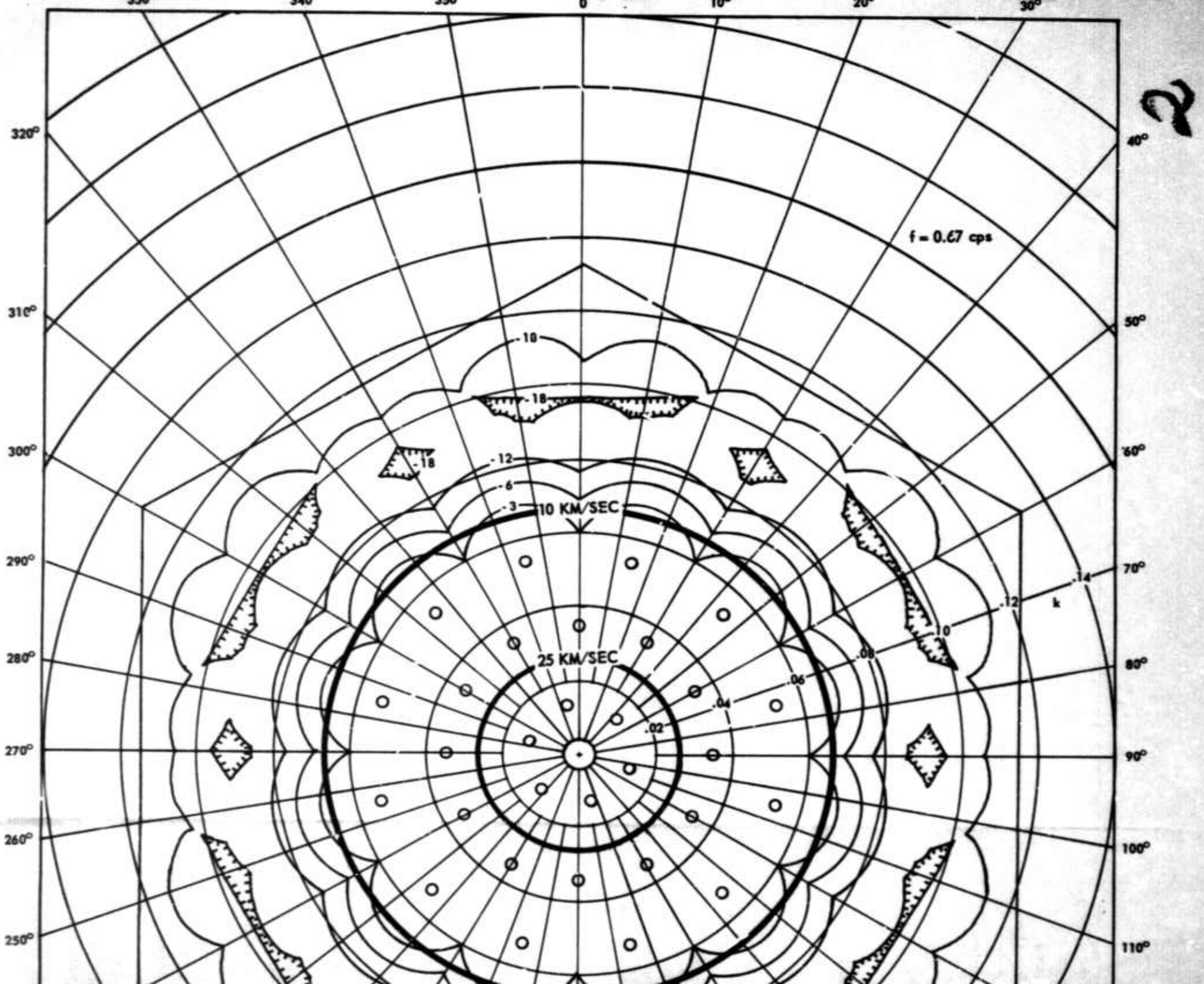
f = 0.67 cps
10 KM/SEC
25 KM/SEC
k
.02
.04
.06
.08
.10
.12
.14
3
6
12
18
18
18
320°
310°
300°
290°
280°
270°
260°
250°
40°
50°
60°
70°
80°
90°
100°
110°

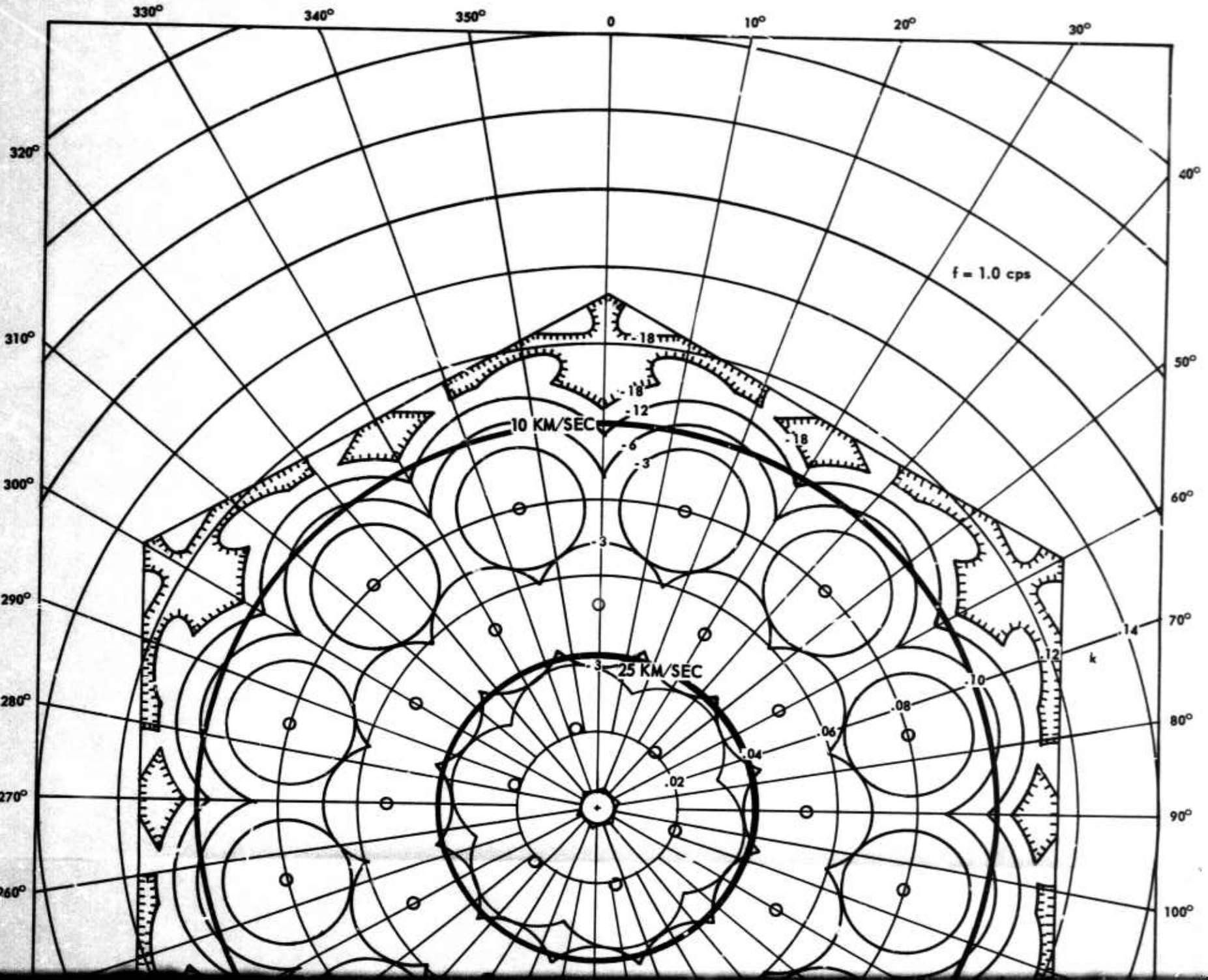
330°
340°
350°
0
10°
20°
30°
320°
40°
310°
50°
300°
60°
290°
70°
280°
80°
270°
90°
260°
100°
f = 1.0 cps
10 KM/SEC
25 KM/SEC
k
.18
.12
.6
.3
.14
.10
.08
.06
.04
.02

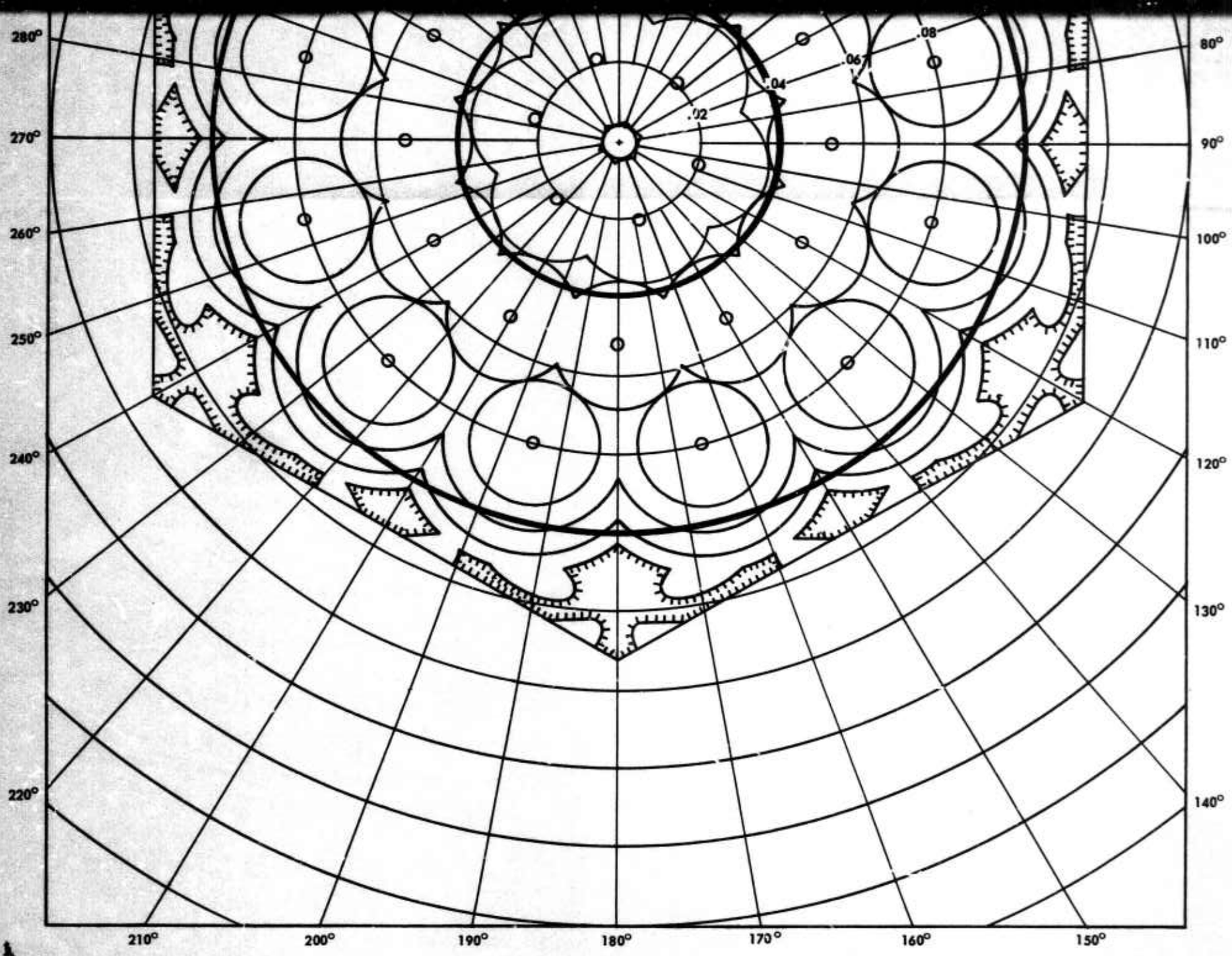

Figure 85. Composite $\vec{k}$ response of 30 beams of 37-element array

G 2079

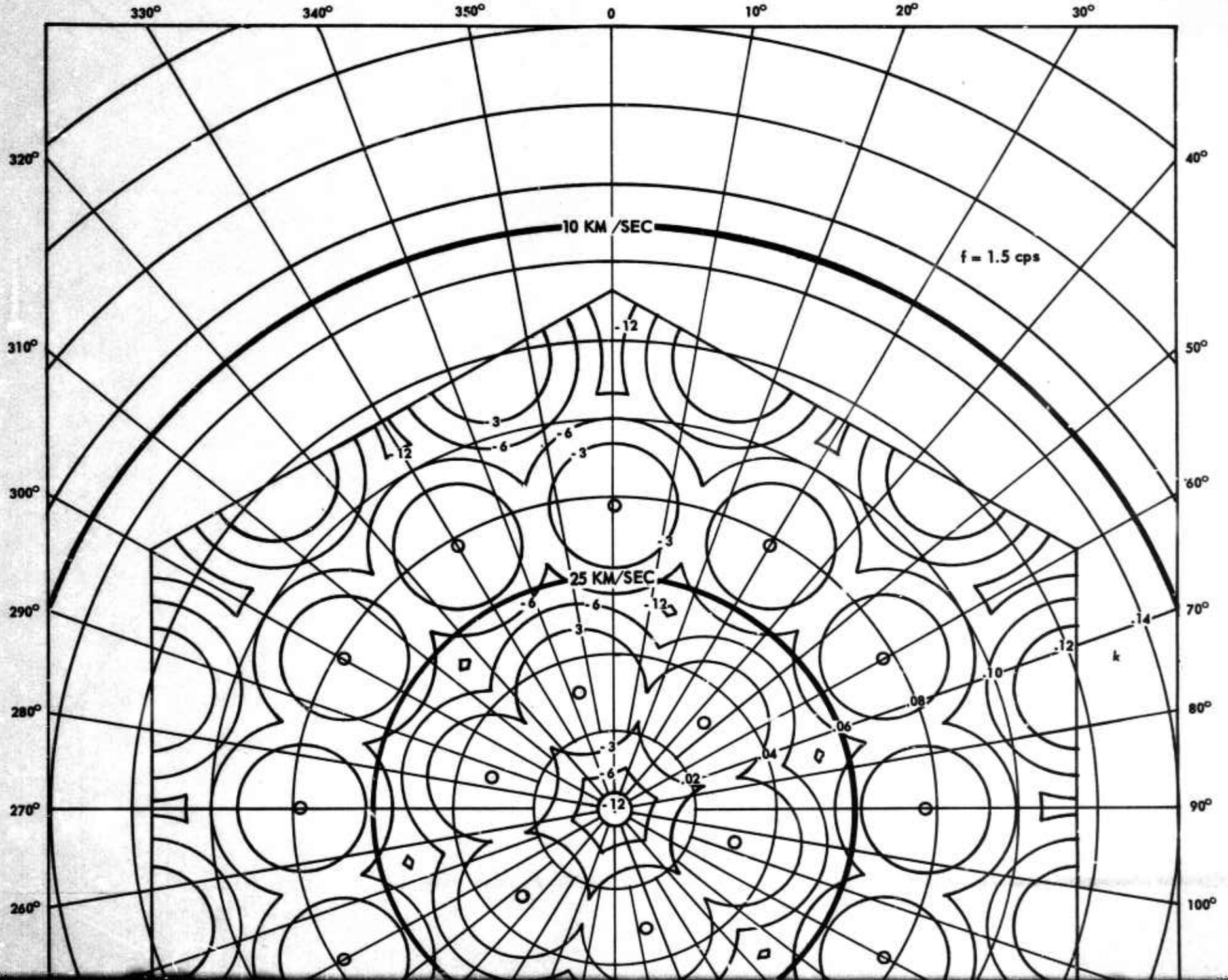
330°
340°
350°
0
10°
20°
30°
320°
40°
310°
50°
300°
60°
290°
70°
280°
80°
270°
90°
260°
100°
10 KM /SEC
25 KM/SEC
f = 1.5 cps
-12
-3
-6
-12
-3
-6
-6
-3
-6
-12
3
-3
-6
-12
3
-3
-6
-12
.14
.12
.10
.08
.06
.04
.02
k

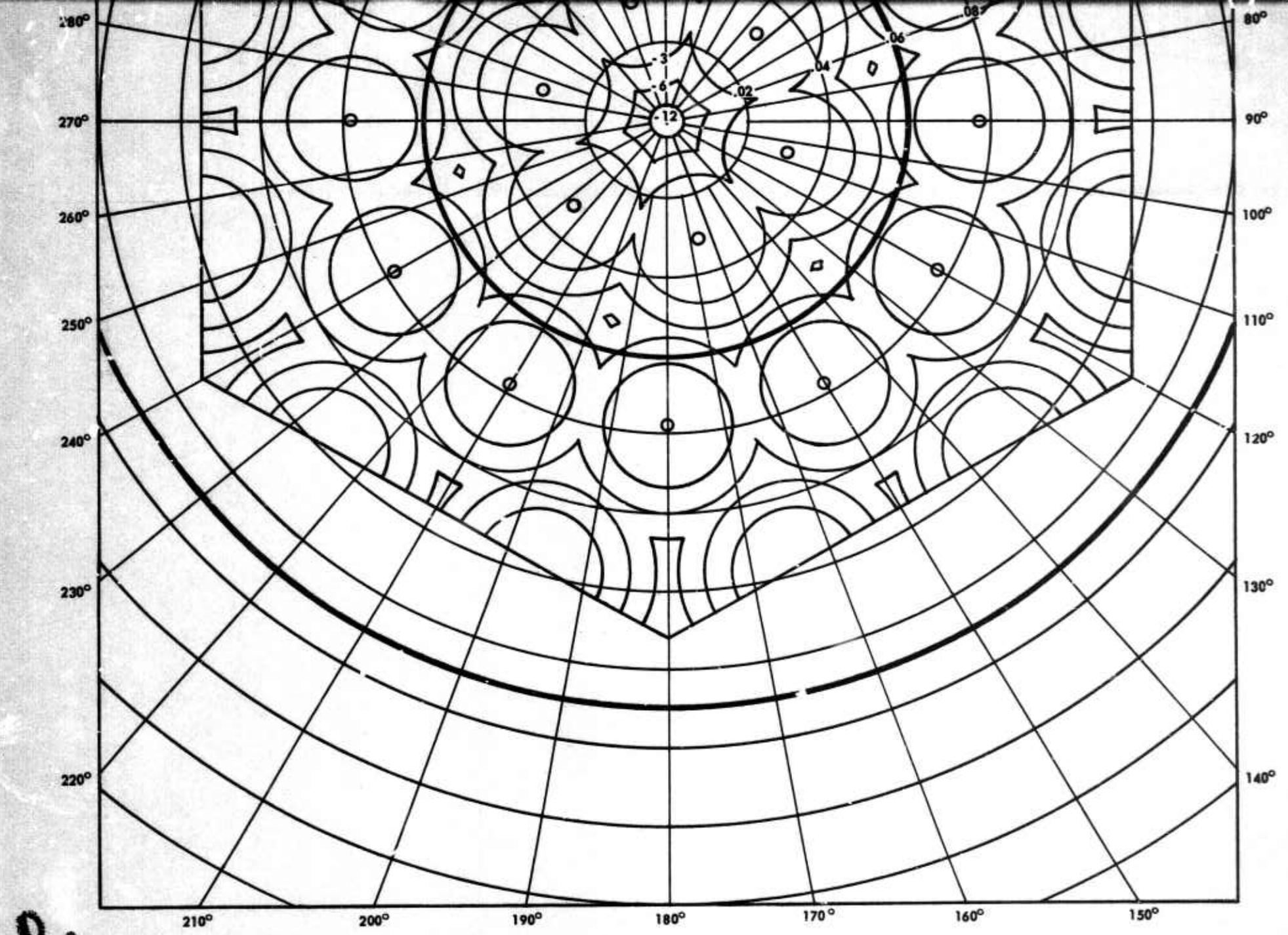

Figure 86. Composite $\vec{k}$ response for 30 beams of 37-element array

G 2080

and because shear phase data are important in source discrimination, it is judicious to consider the design of an array to enhance both the vertical and horizontal components of long-period body and surface waves.

To design an array for maximum effectiveness in increasing the S/N of long-period seismograms, detailed data on noise and signal coherency, noise stationarity, and noise and signal spectra must be considered. To date, only data adequate for very preliminary estimation of noise coherency and stationarity at TFSO are available; however, more data exist regarding noise and signal spectra and signal coherency. Based on the available data, the preliminary analysis of long-period noise and signals at TFSO conducted by Texas Instruments (1966a), and general characteristics of long-period microseismic noise (Kovach, 1965, Haubrich, 1965, and Oliver, 1963), we designed and recommended a 13-element array, each element of which is comprised of a three-component long-period seismograph, for installation at TFSO.

We reviewed our recommendation with a group of interested client-personnel during meetings at the VELA Seismological Center on 3 and 4 November 1966. During these meetings, we discussed the fact that the recommended long-period array design was based on reasonable (but assumed) characteristics of the long-period microseismic noise, and that more detailed noise data would assure greater confidence in the effectiveness of the array designed and would facilitate more propitious distribution of elements.

10.3.2 Assumed TFSO Long-Period Noise

The power density spectral estimates for several different long-period noise samples recorded at TFSO (figures 87 through 90) show that the noise power is concentrated in two predominant period ranges, one between 5 and 9 seconds and the second between 12 and 20 seconds, and that the power peak in each of these ranges is at about 8 and 16 seconds, respectively. Because the effects of the seismograph frequency responses have not been removed from these spectral data, the dominant noise power appears to be concentrated in the 15- to 20-second period band; this, however, is misleading; the actual noise power peak is in the 5- to 9-second period band. Noise data from the TFSO extended array operated under the LRSM program were found by TI to show that the power spectra for the vertical seismograph components are essentially independent of position over large distances (figure 87). The apparent variability in the level of the horizontal-component spectra may be the result of the fact that the orientations of the horizontal seismometers differed as much as 30 degrees from site to site.

In 1965, TI found that the velocity of 6-second microseismic noise recorded by the TFSO short-period seismographs was about 3.4 kilometers per second.

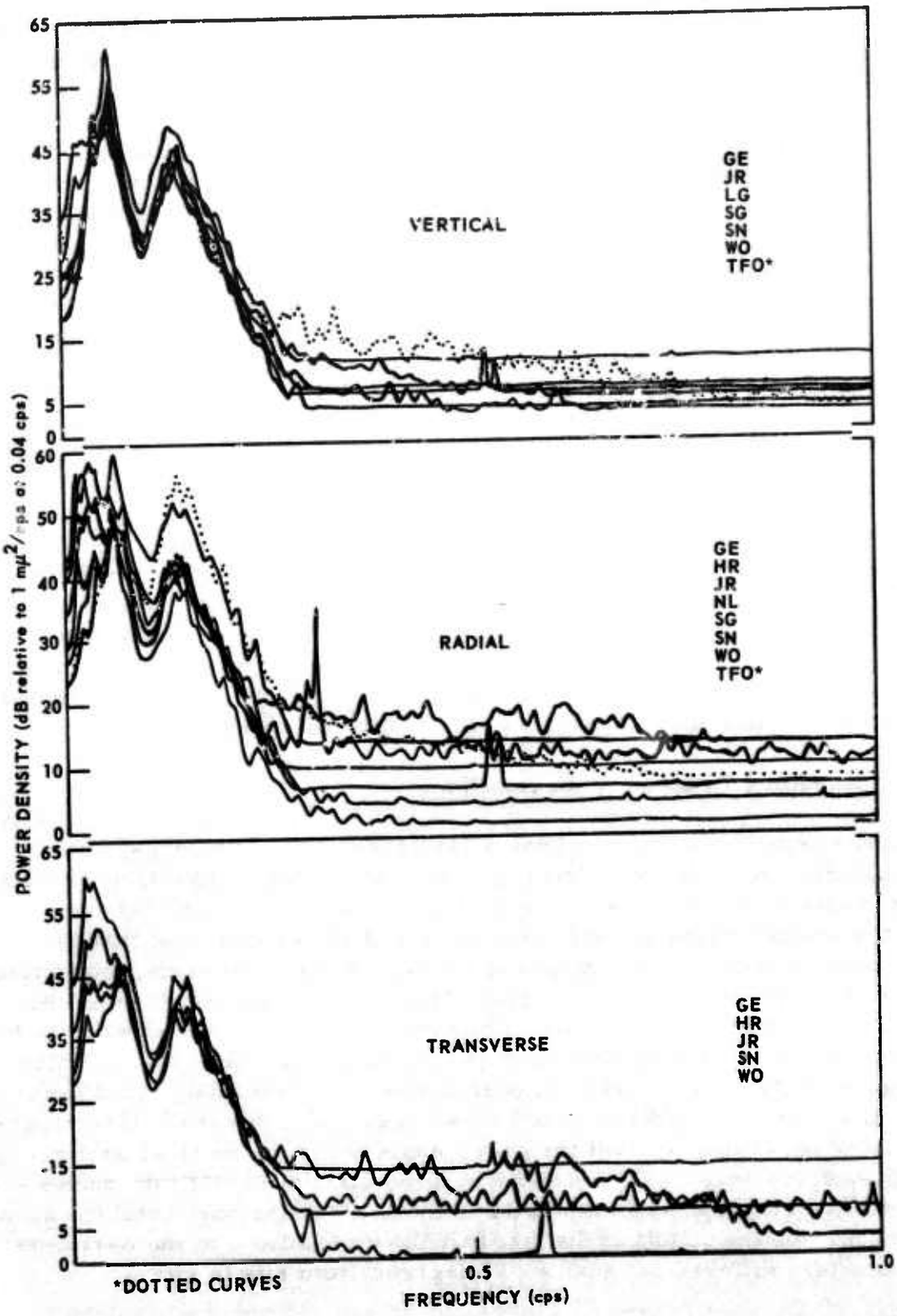

Figure 87. Power density spectra of long-period noise sample 3 for vertical, radial, and transverse components (1 cps bandwidth) of TFSO and extended array seismographs (from TI 1966a)

© 2081

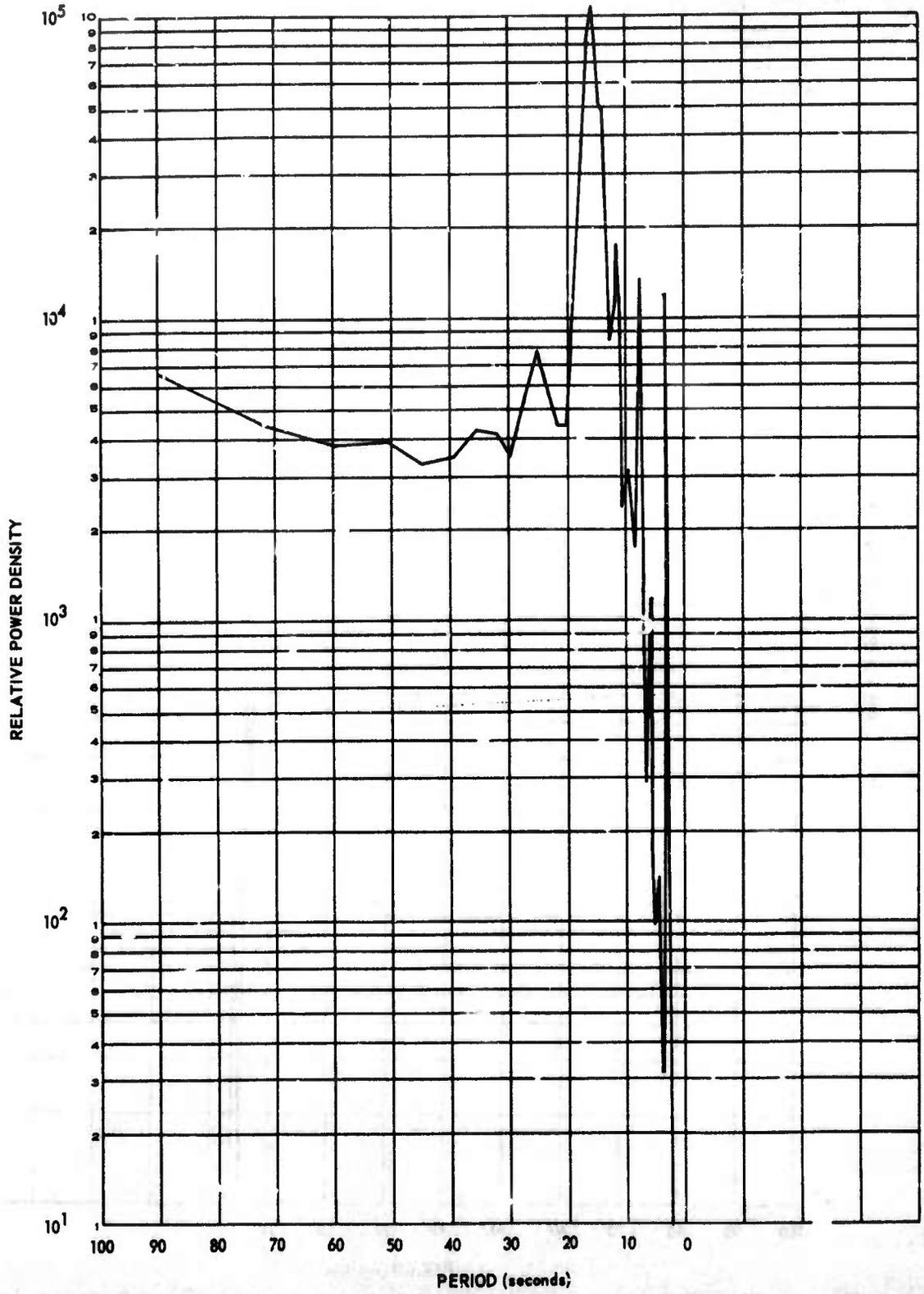

Figure 88. Relative power density spectral estimate of long-period noise for TFSO vertical component (not corrected for seismograph response)

3 2082

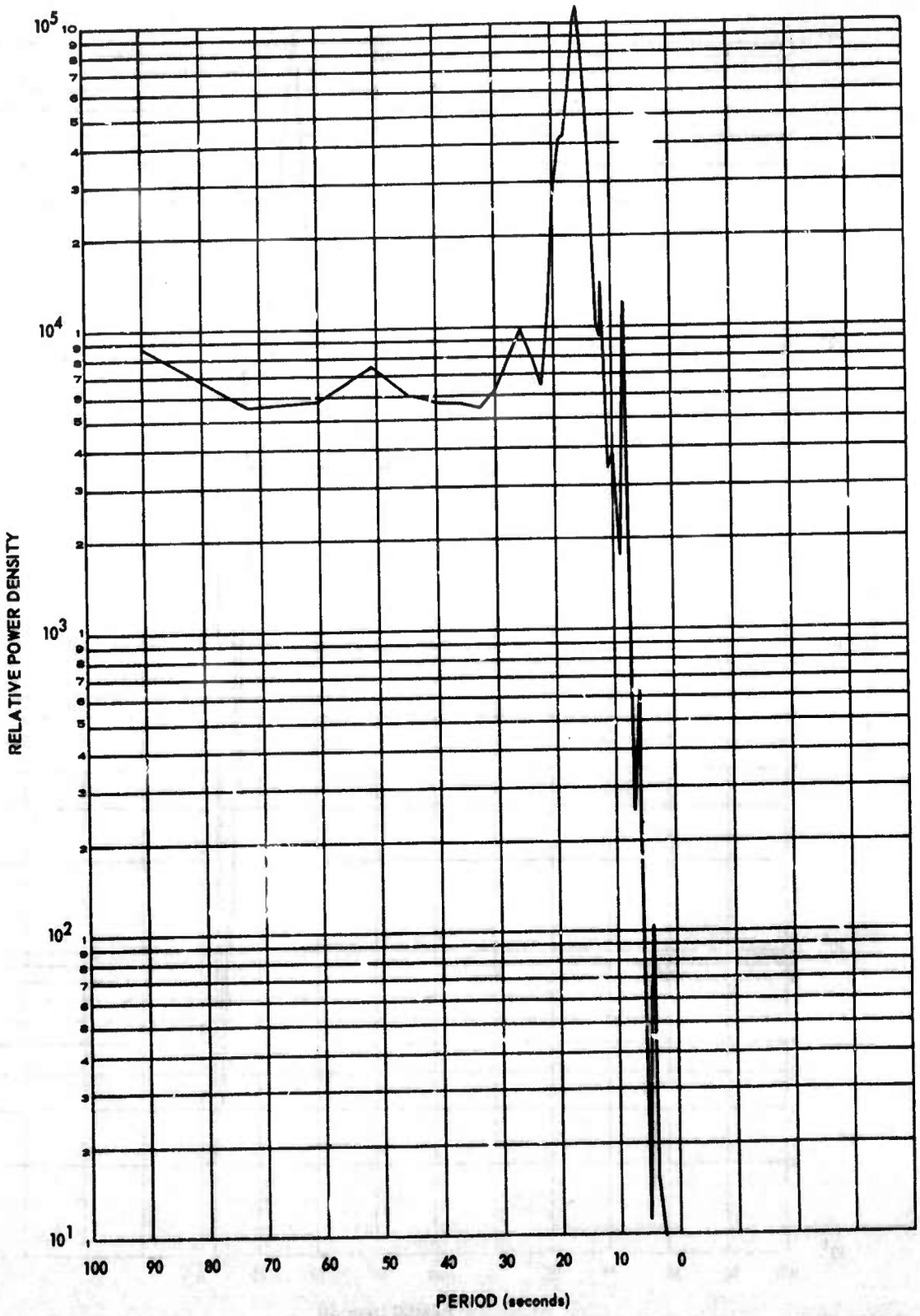

Figure 89. Relative power density spectral estimate of long-period noise for TFSO vertical component (not corrected for seismograph response)

G 2083

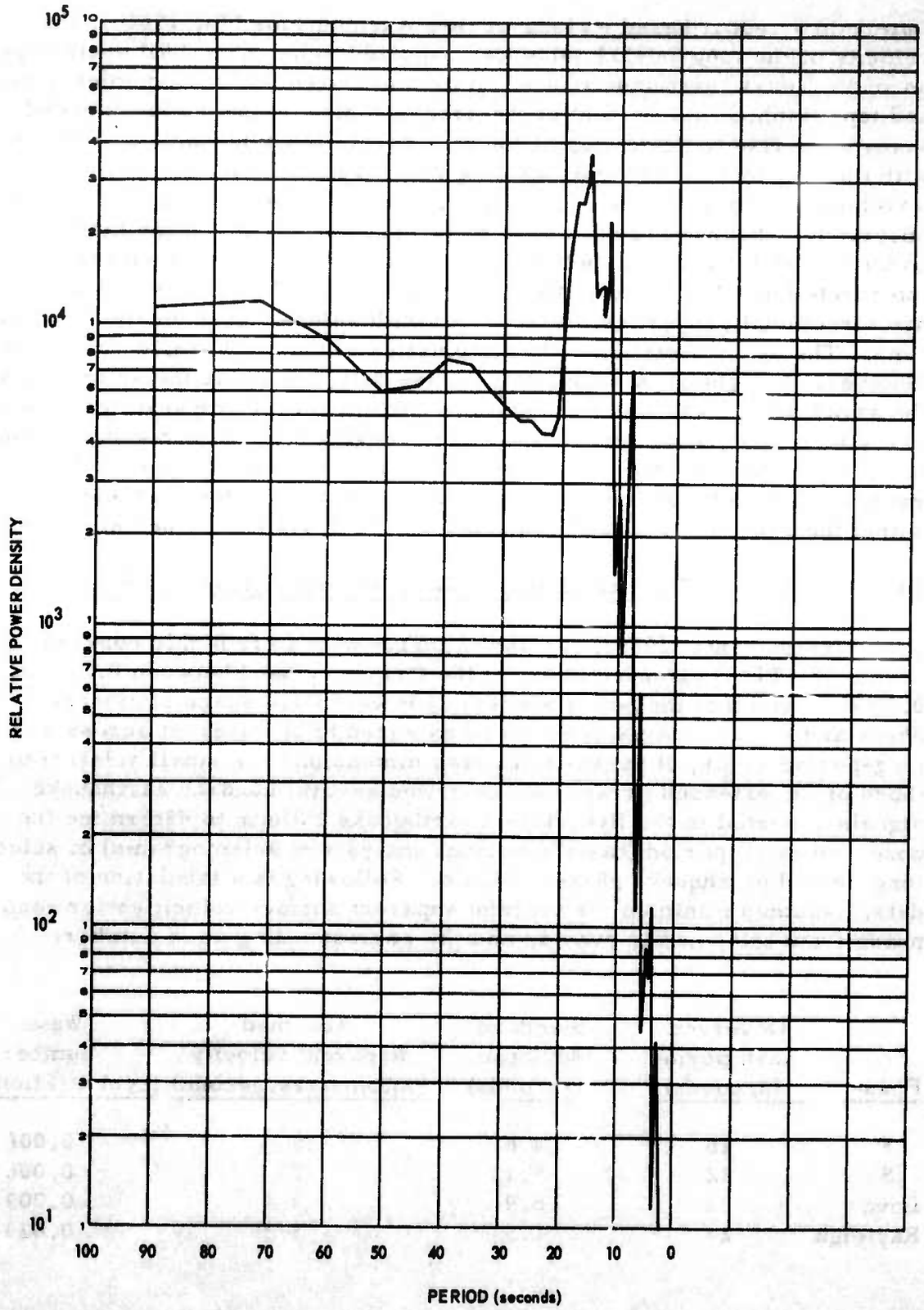

Figure 90. Relative power density spectral estimate of long-period noise for TFSO vertical component (not corrected for seismograph response)

G 2084

Later, in a report based on long-period seismograms (TI, 1966a), the velocity of the long-period noise was reported to be about 3 kilometers per second. Texas Instruments found limited evidence that the complex geologic and topographic environment of the area occupied by the TFSO extended array gave rise to scattering of the microseismic noise, which, when coupled with the fact that the detector spacing was large, relative to the microseismic wavelengths, could at least partially explain the relatively low coherences observed. Observed variations in the frequencies at which the highest coherence was observed, both from detector to detector and with time, were interpreted by TI to indicate that the noise recorded by the extended array had directional properties which varied with seismometer location and with time. The exact directional characteristics of the TFSO noise are not known, however. In light of these available noise data, the noise model on which the array design was based consists of surface waves propagating across the array in varying directions at velocities ranging between 2.8 and 3.4 kilometers per second, with the values of their wave numbers fixed within the ranges 0.015 to 0.027 and 0.033 to 0.071 cycles per kilometer and peaking within the ranges 0.018 to 0.023 and 0.037 to 0.045 cycles per kilometer.

10.3.3 Observed Characteristics of Long-Period Signals at TFSO

Texas Instruments (1966a) has shown that P waves are highly coherent across the TFSO extended array in the frequency band between 0.04 and 0.09 cps, and that the power spectra of P waves are space stationary. Shear and surface waves can also be expected to be coherent across a long-period array, if the overall array dimensions are small relative to those of the extended array. We reviewed several hundred earthquake signals reported in the five-station earthquake bulletin to determine the observed mean period (based on visual analysis of seismograms) of selected long-period earthquake phase arrivals. Following is a tabulation of these data, assumed minimum or average apparent surface velocities for each phase from teleseismic events, and the corresponding wave number:

Phase	Observed mean period (seconds)	Standard deviation (seconds)	Assumed apparent velocity (kilometers/second)	Wave number (cycles/kilometer)
P	16	4.6	10	0.006
S	22	5.1	7	0.006
Love	32	6.9	3.4	0.009
Rayleigh	23	4.5	3.2	0.013

By comparing the wave numbers shown in this table with those of the microseismic noise bands assumed in the noise model, it is apparent that with the exception of Rayleigh waves, the signal wave numbers of interest are

well separated from the wave numbers of the predominant microseismic noise, a condition well suited to signal enhancement by wave-number filtering.

10.3.4 Characteristics of the Recommended Array

Because much of the long-period microseismic noise energy is concentrated in two distinct frequency bands and, in our opinion, an attempt should be made to attenuate the noise in both of these bands to investigate the possibility of the presence of body wave signals being masked by this noise, and to provide a mechanism for the enhancement of surface wave signals through beam steering, we have designed an array for suppression of noise in each of these bands by direct summation. The recommended array consists of 13 three-component elements arranged in 2 concentric hexagonal rings with a common center element (figure 91). Elements of the outer ring, which is designed to suppress noise in the period band between 12 and 20 seconds, are spaced at intervals of 23.3 kilometers, and the elements of the inner ring are spaced 10.8 kilometers apart to suppress the noise in the 5- to 9-second band. To provide for maximum attainable suppression of microseismic noise in both bands from the overall array, if overall summation of the like components of each of the 13-elements is desired, the inner hexagon is rotated 30 degrees with respect to the outer hexagon.

10.3.4.1 Response of the Outer Ring

Figure 92 is the $\vec{k}$-plane response of the outer ring plus the center element of the recommended array showing the microseismic noise wave-number bands. Note that the 12- to 20-second noise is attenuated at least 11 dB relative to a single detector, and the noise in the range corresponding to the 16-second peak is attenuated more than 18 dB. Aliasing of microseisms in the 5- to 9-second period band will be a problem for noise propagated from some directions. To eliminate the potentially deleterious effects of the 5- to 9-second microseisms, the responses of the seismographs of the outer ring will be notch filtered.

Assuming signal wave numbers given in the tabulation in section 10.3.3 are representative, the response of the elements of the outer ring and the center of the array can be expected to attenuate body waves no more than 2 dB and surface waves about 8 dB. It is reasonable to anticipate that direct summation of the elements of the outer ring and center of the array will provide a minimum improvement in body wave S/N of about 9 dB over the period band between 12 and 20 seconds. It is probable that the S/N of surface waves can be improved more than the indicated 3 to 10 dB by beam steering, and that additional improvement in the body wave S/N might also be obtained. Because of the limited data available regarding the spectrum, velocities, directional properties, and coherence of the 12- to 20-second noise, no reasonable estimate of the extent to which beam steering will improve S/N

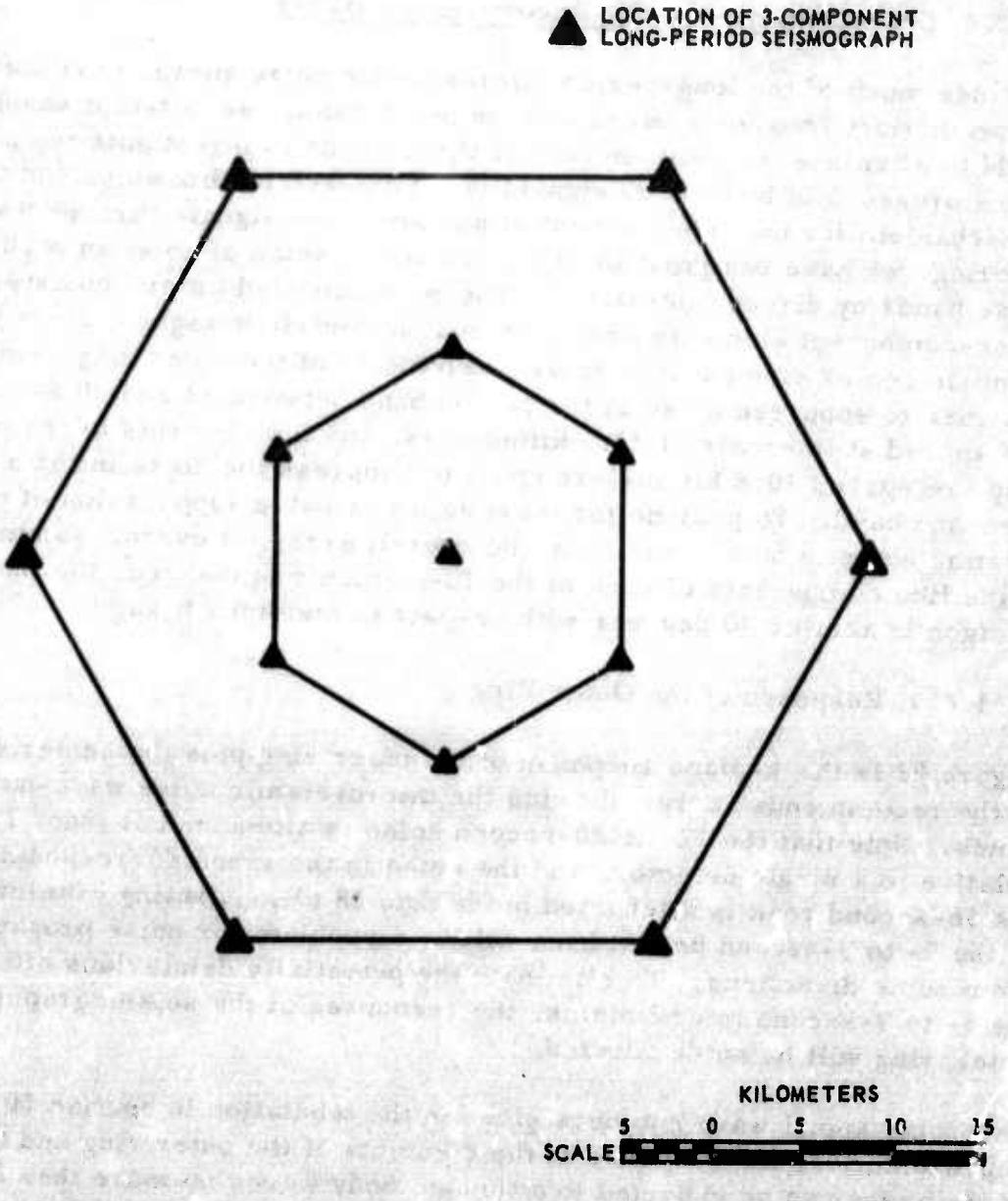

Figure 91. Recommended configuration of TFSO long-period array

G 2085

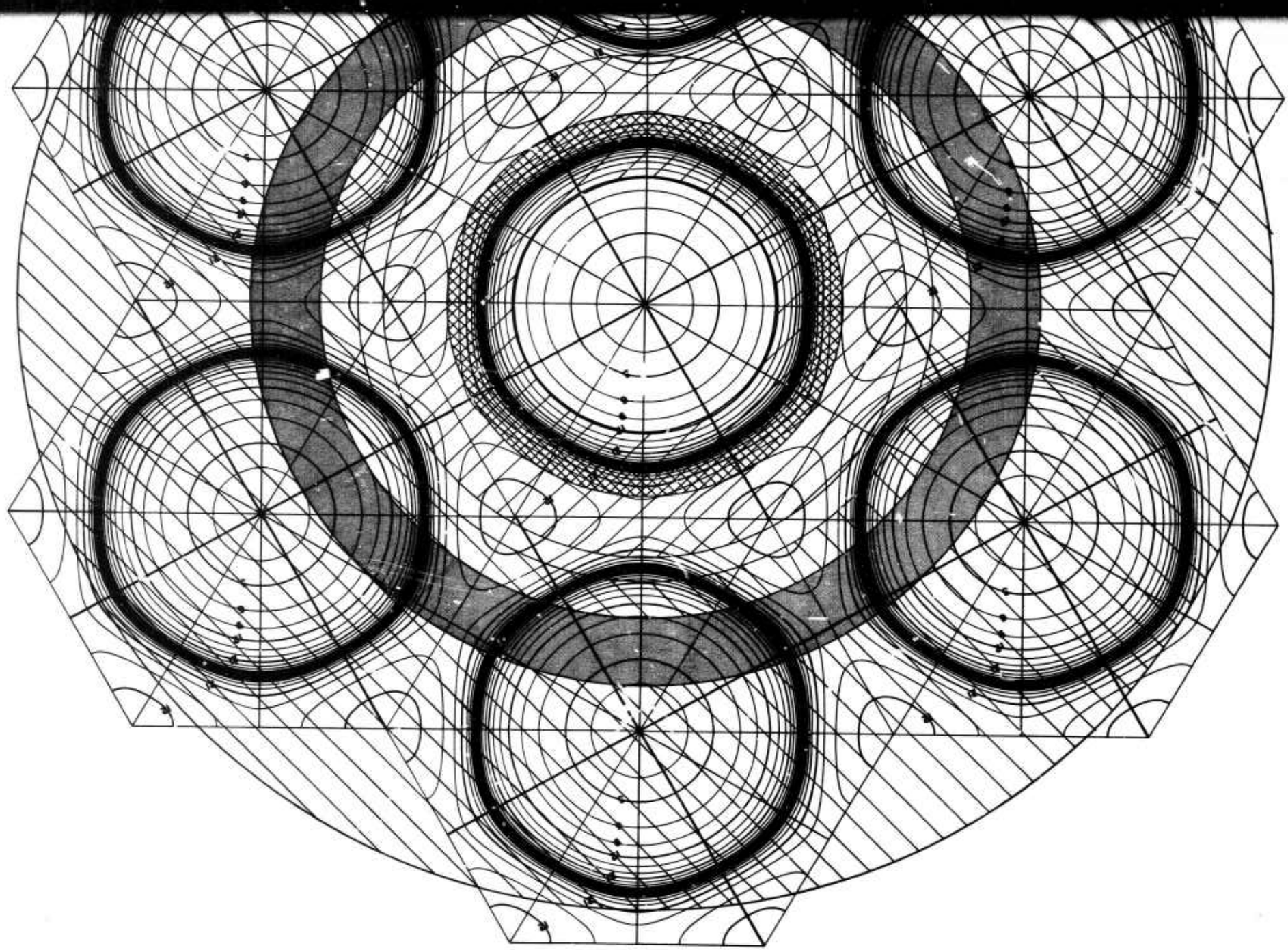

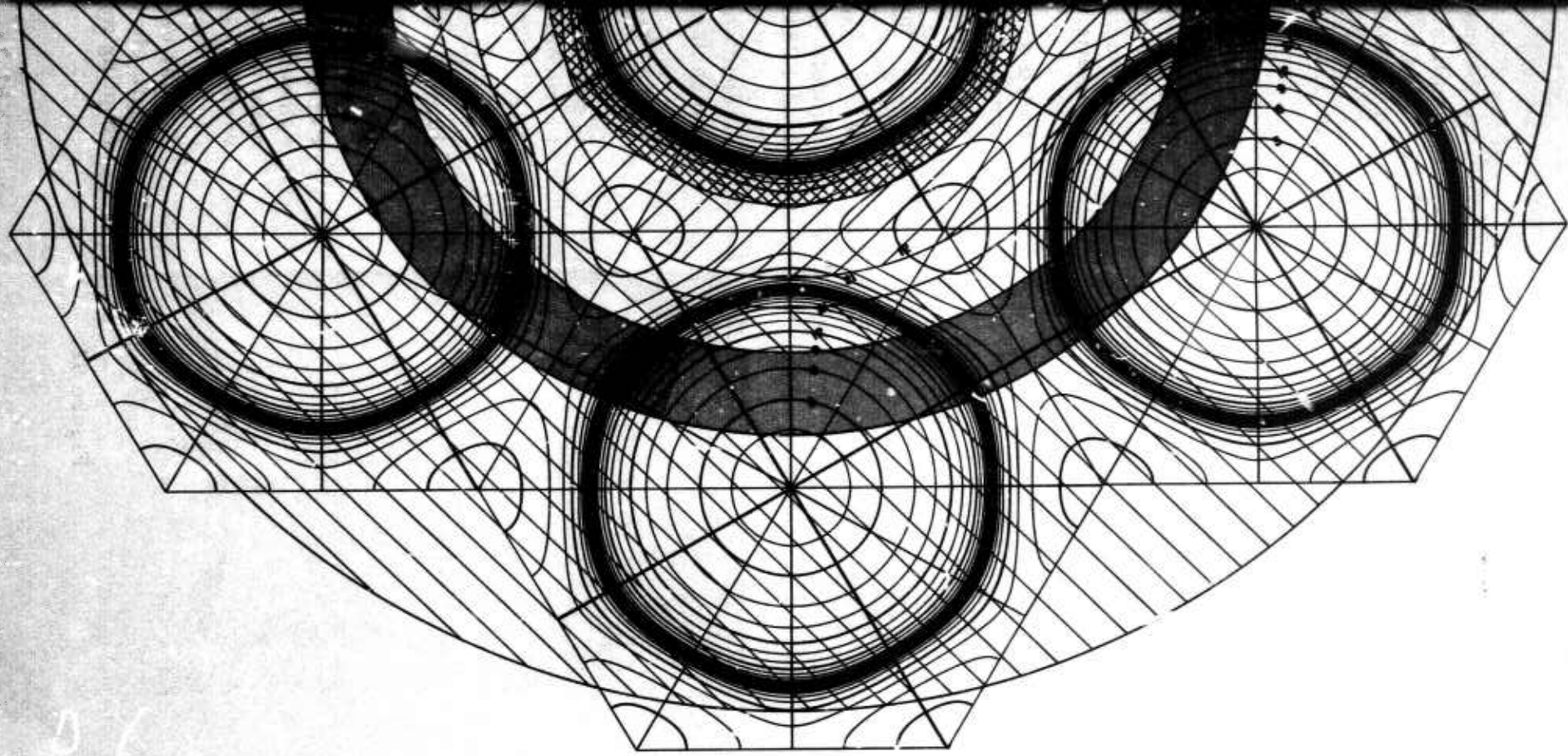

Figure 92. $\vec{k}$ space response for equally weighted 7-element hexagonal array with seismometer spacing of 23.3 kilometers (outer ring plus center element of recommended array) showing predominant microseismic noise wave-number bands

G 2086

can be made at this time. Also, it is possible that dispersion may complicate the enhancement of Rayleigh and Love waves by summation. In this case, we will develop off-line processing techniques to reduce the adverse dispersive effects.

10.3.4.2 Response of the Inner Ring

The $\vec{k}$-plane response of the six elements of the inner ring and the center element is shown in figure 93. Also shown in figure 93 are the predominant microseismic noise wave-number bands. The noise in the 5- to 9-second period band will be attenuated at least 11 dB, and the 8-second noise will be attenuated at least 21 dB. We expect the long-period noise which peaks at 16 seconds to be attenuated about 5 dB and the noise nearer to 20 seconds to be attenuated less.

Based on the representative signal wave numbers discussed previously, the predicted attenuation of body- and surface-wave signals by the inner ring of elements is less than 1 dB.

10.3.5 Instrumentation and Installation

We recommended using Geotech advanced long-period seismometers (Models 7505A and 8700C) and Geotech Long-Period, Solid-State Amplifiers, Model 28450-3, in the seismographs of the long-period array. One unnotched response will be provided from each element of the inner ring, while both a notched and an unnotched response will be provided from the center element and each element of the outer ring.

10.3.6 Data Recording Equipment

In order to provide comprehensive data displays for routine on-line analysis, we recommended that the individual outputs, summations, and beam-steered outputs from the long-period array be recorded on six Develocorders.

10.4 ARRAY COUPLING STUDY

10.4.1 Introduction

Previous studies (Taylor, 1964, and Rugg, 1965) based on events from two epicentral regions indicated that significant differences in amplitude response exist among the elements of the TFSO array, and that the pattern of amplitude variation is approximately the same for the two epicentral regions studied.

A study using data from more regions was undertaken to determine if amplitude variations can be attributed to local site effects, such as vault coupling to the ground, rock type on which the vault is situated, and relative

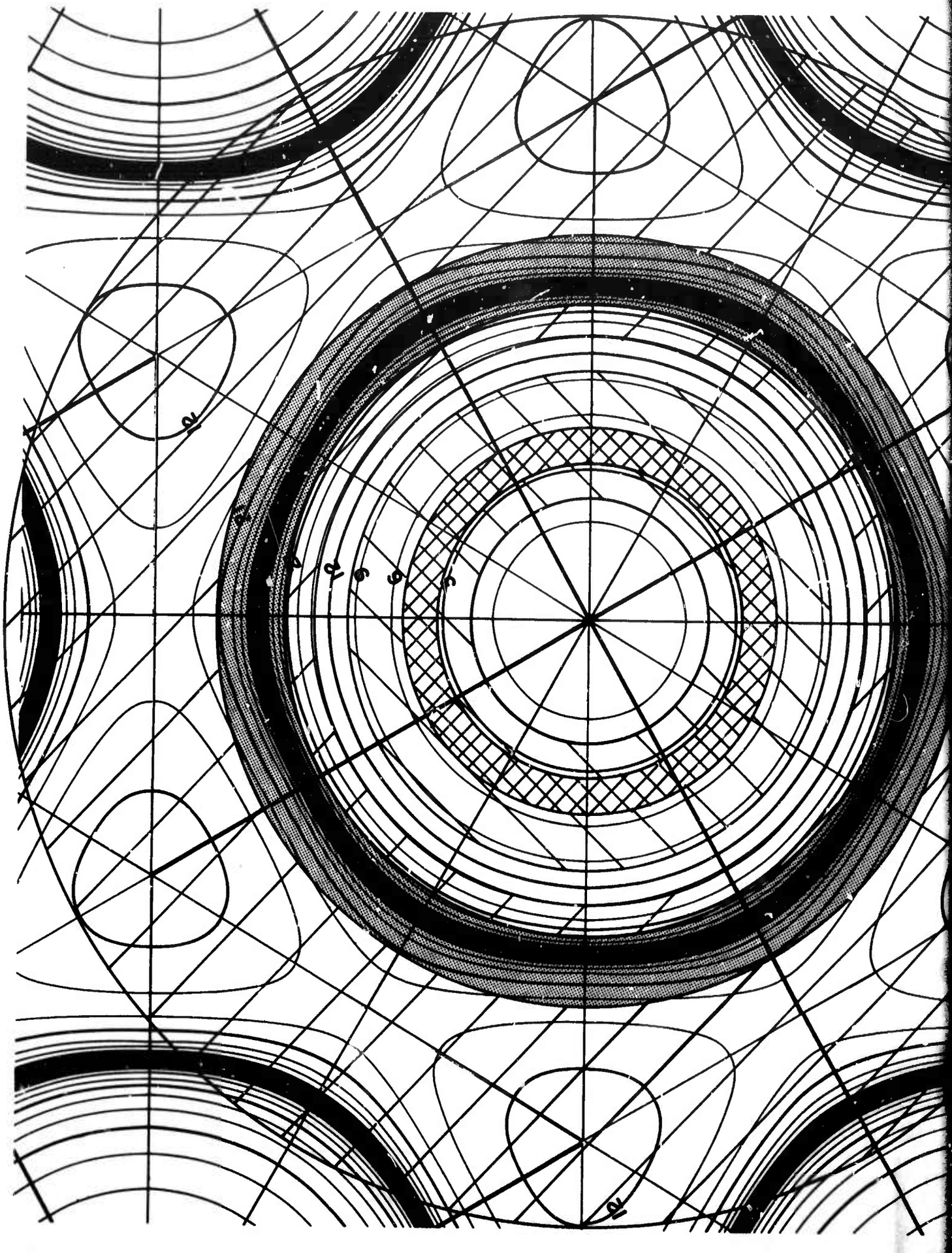

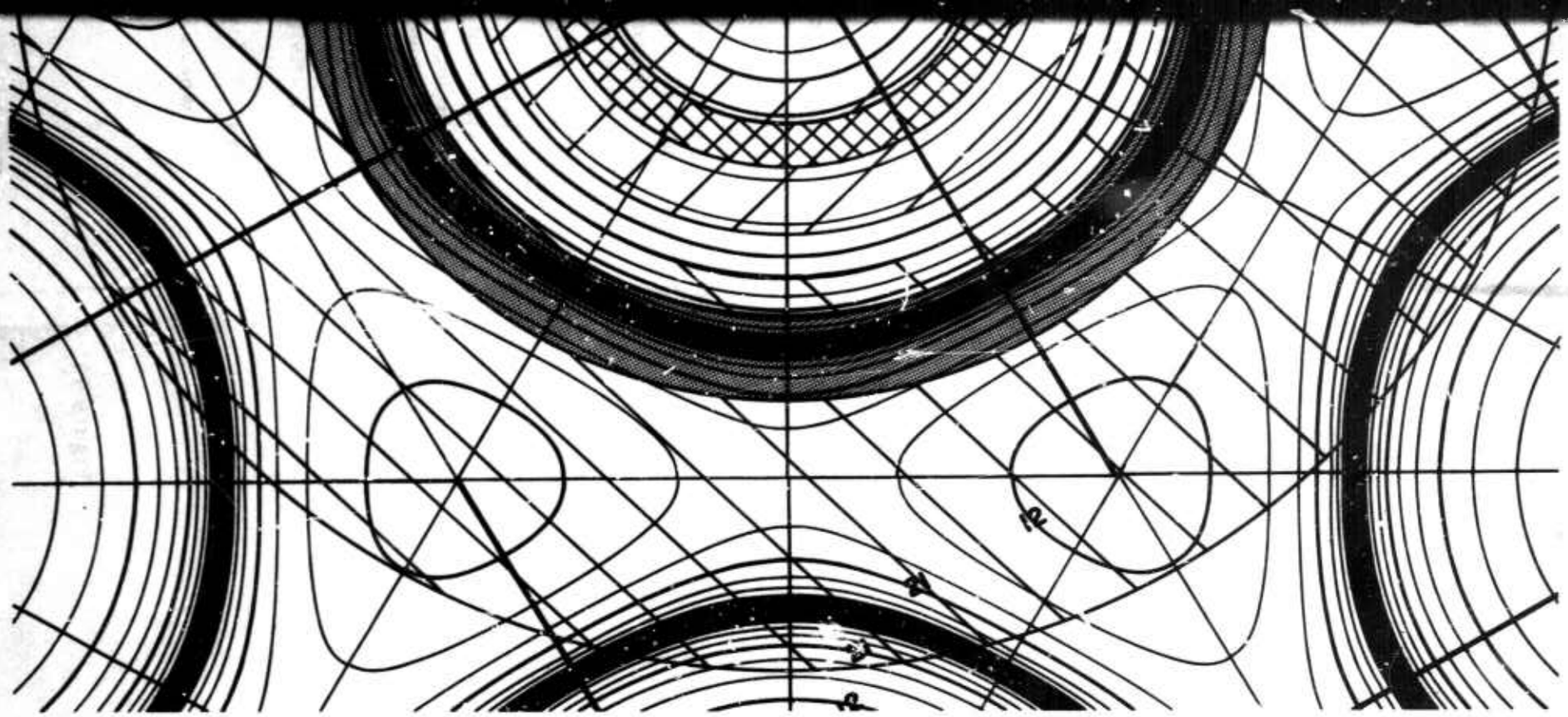

Figure 93. $\vec{k}$ space response for equally weighted 7-element hexagonal array with seismometer spacing of 10.8 kilometers (inner ring plus center element of recommended array) showing predominant microseismic noise wave-number bands

G 2067

position within the TFSO array, and to deter nine if there are significant differences in patterns of amplitude variation for earthquakes from different epicentral regions.

10.4.2 Data Selection and Reduction

Data used in this study were selected from data recorded routinely at TFSO during the period November 1965 through July 1966. Ten epicentral regions were selected from which at least five earthquake signals were recorded during the sampling period. The regions were chosen to be as small as possible to minimize the effects of differences in travel path among events from the same region. To minimize the effect of background noise, only those signals whose amplitudes were equal to or greater than 6 millimeters peak-to-peak at X10 view (at a gain of 1000K) were used in the study. For those regions with more than 5 earthquakes that satisfied the amplitude criterion, those 5 events whose epicenters were most nearly the same were selected. The epicentral regions selected are shown as a function of epicentral distance and azimuth from TFSO in figure 94. A more symmetrical distribution of epicentral regions with respect to azimuth could not be found in the data sample examined without relaxing the qualifying criteria.

For each event used in the study, amplitude and period measurements were made and ground displacement (center-to-peak) was computed from the output of each of 23 elements of the TFSO array. Because the distribution of amplitudes was expected to be log normal rather than normal, amplitude deviations for a given event were computed as ratios to the geometric mean amplitude for that event. Of the seismographs selected for this study, 14 of the seismometer vaults are located on granite; 1 is on basalt, and 8 are located on approximately 200 feet of limestone underlain by granite. (The seismometer vaults for this study are identified with designators used prior to 9 December 1966.)

10.4.3 Statistical Model

In order to develop an additive model for statistical analysis, the amplitude deviation of a given detector for a given event was defined as the difference of the logarithm of the ground displacement computed for the given detector and the mean logarithmic amplitude (averaged over detectors) for the given event. The estimates of the seismometer and region effects were reconverted to ratio form after the statistical analysis had been carried out.

The statistical model used in the study follows:

$$Z_{ijm} = Y_{ijm} - \overline{Y}_{i \cdot m} = \beta_j + \gamma_{ij} + e_{ijm}$$

where

Y_{ijm} = $\log_{10}$ amplitude (in mμ) recorded on seismometer j from the m'th event with epicenter in region i

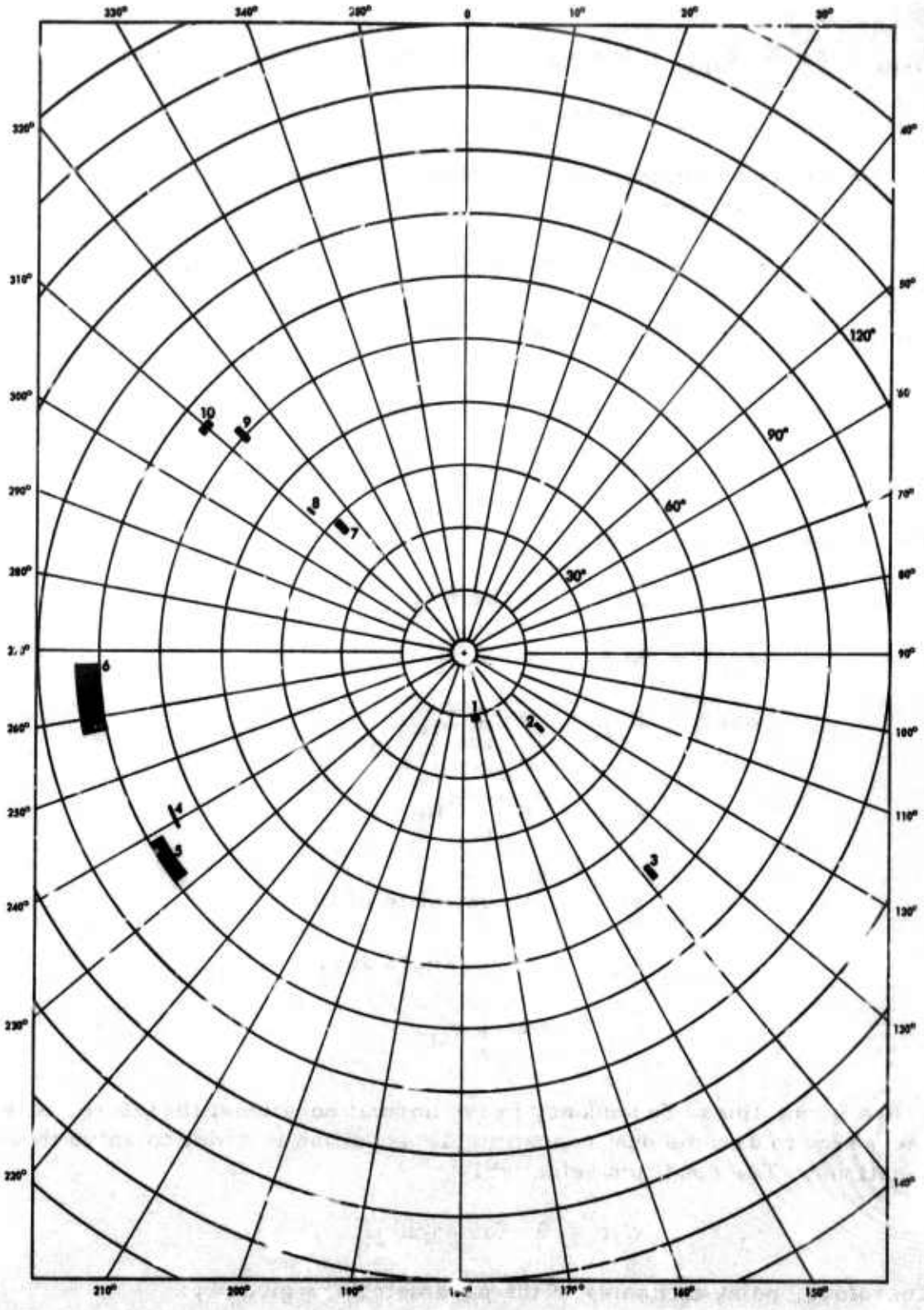

Figure 94. Epicentral regions considered, as a function of distance and azimuth from TFSO G 2608

$\bar{Y}_{i.m} = \frac{1}{23} \sum_{J=1}^{23} Y_{ijm}$: Average logarithmic amplitude of m'th event from region i

β_j = effect of seismometer coupling, rock type, and location of seismometer j

γ_{ij} = effect of region i on the pattern of amplitude variation.

e_{ijm} = error of m'th observation in cell ij.

i = 1, I	I = 10
j = 1, J	J = 23
m = 1, M	M = 5

The normal equations are:

$$Z_{.j.} = IM\ \hat{\beta}_j + M\ \hat{\gamma}_{.ij}$$

$$Z_{ij.} = M\ \hat{\beta}_j + M\ \hat{\gamma}_{ij}$$

where $Z_{.j.} = \sum_{im} Z_{ijm}$

$Z_{ij.} = \sum_{m} Z_{ijm}$

$\hat{\beta}_j$ = estimate of β_j

$\hat{\gamma}_{ij}$ = estimate of γ_j

$\hat{\gamma}_{.j} = \sum_{i} \hat{\gamma}_{ij}$

There is one linear dependency in the normal equations; therefore, it is necessary to assume one nonestimable condition in order to solve these equations. The condition selected is:

$$\hat{\gamma}_{.j} = 0 \quad \text{for each } j.$$

Therefore, point estimates of the parameter are given by:

$$\hat{\beta}_j = \frac{1}{IM} Z_{.j.}$$

$$\hat{\gamma}_{ij} = \frac{1}{M} Z_{ij.} - \frac{1}{IM} Z_{.j.}$$

Point estimates of the parameters, expressed as antilogarithms of the $\hat{\beta}_j$ and $\hat{\gamma}_{ij}$, are listed in table 13.

The null hypotheses tested are

1. $\hat{\gamma}_{ij} = 0$ for all i and j
2. $\hat{\beta}_j = 0$ for all j.

The sums of squares and degrees of freedom for testing these hypotheses are as follows:

$$TSS = \sum_{ijm} Z^2_{ijm}$$

$$TDF = IJM - 1; \text{ since } Z_{...} = 0$$

$$\beta SS = \frac{1}{IM} \sum_{j} Z^2_{.j.}$$

$$\beta DF = J - 1; \text{ since } \hat{\beta}_{.} = 0 \text{ (because } Z_{...} = 0)$$

$$\gamma SS_{adj} = \frac{1}{M} \sum_{ij} Z^2_{ij.} - \frac{1}{IM} \sum_{j} Z^2_{i.j.}$$

$$\gamma DF = (I - 1) J; \text{ since } \hat{\gamma}_{.j} = 0$$

$$ErrSS = \sum_{ijm} Z^2_{ijm} - \frac{1}{M} \sum_{ij} Z^2_{ij.}$$

$$ErrDF = IJ\ (M - 1)$$

The analysis of variance is given in table 14.

10.4.4 Discussion

The analysis of variance indicates that highly significant differences exist both among the β_j and among the γ_{ij}; therefore, both null hypotheses must be rejected.

Estimates of the seismometer effects, expressed as antilogarithms of the $\hat{\beta}_j$, are shown as a function of seismometer location in figure 95. These seismometer effects are interpreted to be due to a combination of vault coupling, rock type, and relative position within the array. No attempt has been made to separate these different types of seismometer effects.

Table 13. Estimates of seismometer effect ($\hat{\beta}_j$) and region-seismometer interaction effect ($\hat{\gamma}_{ij}$)

Seismometer	j	$\hat{\beta}_j$	$\hat{\gamma}_{1j}$	$\hat{\gamma}_{2j}$	$\hat{\gamma}_{3j}$	$\hat{\gamma}_{4j}$	$\hat{\gamma}_{5j}$	$\hat{\gamma}_{6j}$	$\hat{\gamma}_{7j}$	$\hat{\gamma}_{3j}$	$\hat{\gamma}_{9j}$	$\hat{\gamma}_{10j}$
Z31	1	1.04	1.07	1.04	0.93	1.04	0.99	1.02	1.02	0.98	0.93	0.99
Z13	2	1.01	0.97	1.10	1.05	1.03	1.00	0.85	0.99	1.07	0.93	1.04
Z2	3	1.01	1.13	1.01	1.05	1.07	0.99	0.92	0.95	1.06	0.96	0.88
Z1	4	1.01	1.11	1.00	1.00	1.11	1.00	0.99	0.96	1.01	0.98	0.88
Z74	5	1.11	0.86	0.91	0.95	0.92	1.08	1.06	1.05	1.04	1.09	1.09
Z67	6	1.04	1.13	1.16	1.13	0.77	0.94	1.02	1.14	1.04	0.85	0.91
Z70	7	1.00	0.90	0.82	0.92	1.03	1.04	1.02	1.05	1.18	1.13	0.96
Z63	8	1.06	0.91	1.18	1.02	1.08	1.06	1.06	0.94	0.95	0.92	0.92
Z15	9	0.97	0.98	0.97	1.00	1.03	1.02	0.99	1.02	0.96	1.00	1.04
Z27	10	0.95	1.05	0.95	0.89	1.05	1.01	1.02	1.07	0.94	1.01	1.03
Z17	11	0.99	1.04	0.97	1.00	0.99	0.97	1.03	1.04	0.91	0.97	1.08
Z25	12	0.97	0.92	0.86	0.99	1.06	1.05	0.95	1.05	0.94	1.09	1.13
Z61	13	0.95	0.99	1.12	1.02	1.03	1.10	1.00	0.95	0.97	0.96	0.89
Z72	14	1.08	0.87	0.87	0.97	1.06	0.97	1.06	0.92	1.07	1.08	1.15
Z68	15	1.01	0.84	0.93	0.95	1.04	1.13	0.97	1.08	1.01	1.05	1.02
Z65	16	1.04	1.16	1.07	0.99	0.88	0.96	0.95	1.03	0.97	1.03	0.99
Z8	17	0.97	1.03	1.04	1.00	1.06	0.97	1.07	0.98	0.98	0.95	0.93
Z16	18	0.88	1.09	1.00	1.04	0.92	0.94	0.99	0.99	1.04	0.99	1.02
Z19	19	1.01	0.95	0.85	1.03	1.05	0.99	1.04	1.02	0.99	1.03	1.07
Z24	20	1.01	1.09	1.09	1.01	0.92	0.93	0.99	0.88	0.96	1.08	1.08
Z29	21	1.02	1.05	1.01	1.02	0.89	0.95	1.07	0.96	1.04	1.01	1.00
Z99	22	0.93	1.00	1.09	1.03	1.01	0.97	1.03	0.96	0.97	1.00	0.95
Z5	23	0.97	0.97	1.05	1.05	1.03	0.98	0.95	0.99	0.96	1.01	1.01

Table 14. Analysis of variance

SV	DF	SS	MS	F	0.99 significance
Total	1149	4.4239			
β	22	0.5137	0.0234	7.59	yes
γ adj	207	1.0786	0.0052	1.69	yes
Err	920	2.8316	0.0031		

Estimates of the interaction effect of epicentral region and seismometer location, expressed as antilogarithms of the $\hat{\gamma}_{ij}$, are presented as a function of seismometer position in figures 96 through 105. The arrows in each figure indicate the range of directions in which the wave-fronts were moving across the array for earthquake signals from the indicated region. It can be seen from these figures that, in general, amplitudes decrease across the array in the direction in which the wave is moving. Region 10 (Honshu, Japan) is an exception to this pattern. The effects of epicentral region, therefore, may possibly be interpreted as a simple attenuation effect, because of differences among the seismometers in distance from the epicenter. For the distance differences involved in this study (about 10 kilometers maximum), the amplitude attenuation to be expected as a function of epicentral distance (as embodied, for example, in magnitude correction factors) is not known accurately enough to test this interpretation of the region effect.

10.5 SIGNAL AMPLITUDE STUDY

A preliminary study designed to determine whether signal amplitudes recorded on the short-period seismograms were dependent on vault type was completed in April 1966. The amplitudes of 28 teleseismic signals, with periods ranging between 0.7 and 2.0 seconds, recorded by the Z1 and Z60 seismographs were compared with the amplitudes of the same signals recorded by the Z99 and Z100 seismographs, respectively. The Z1 seismometer is housed in a tank-type vault located about 70 feet northeast of Z99 which is housed in the northwest pier room of the walk-in-type long-period vault. Similarly, the Z60 seismometer is housed in a tank-type vault located about 1800 feet northwest of Z100 which is housed in the walk-in-type experimental vault. The locations of these vaults are shown in figure 106. The algebraic differences in recorded amplitude of each of the signals between each of the seismograph pairs was averaged to determine whether significant differences were present. No difference was found between the amplitudes recorded by the Z60-Z100 seismograph pair. We found that the amplitudes recorded by Z1 averaged about 7 percent higher

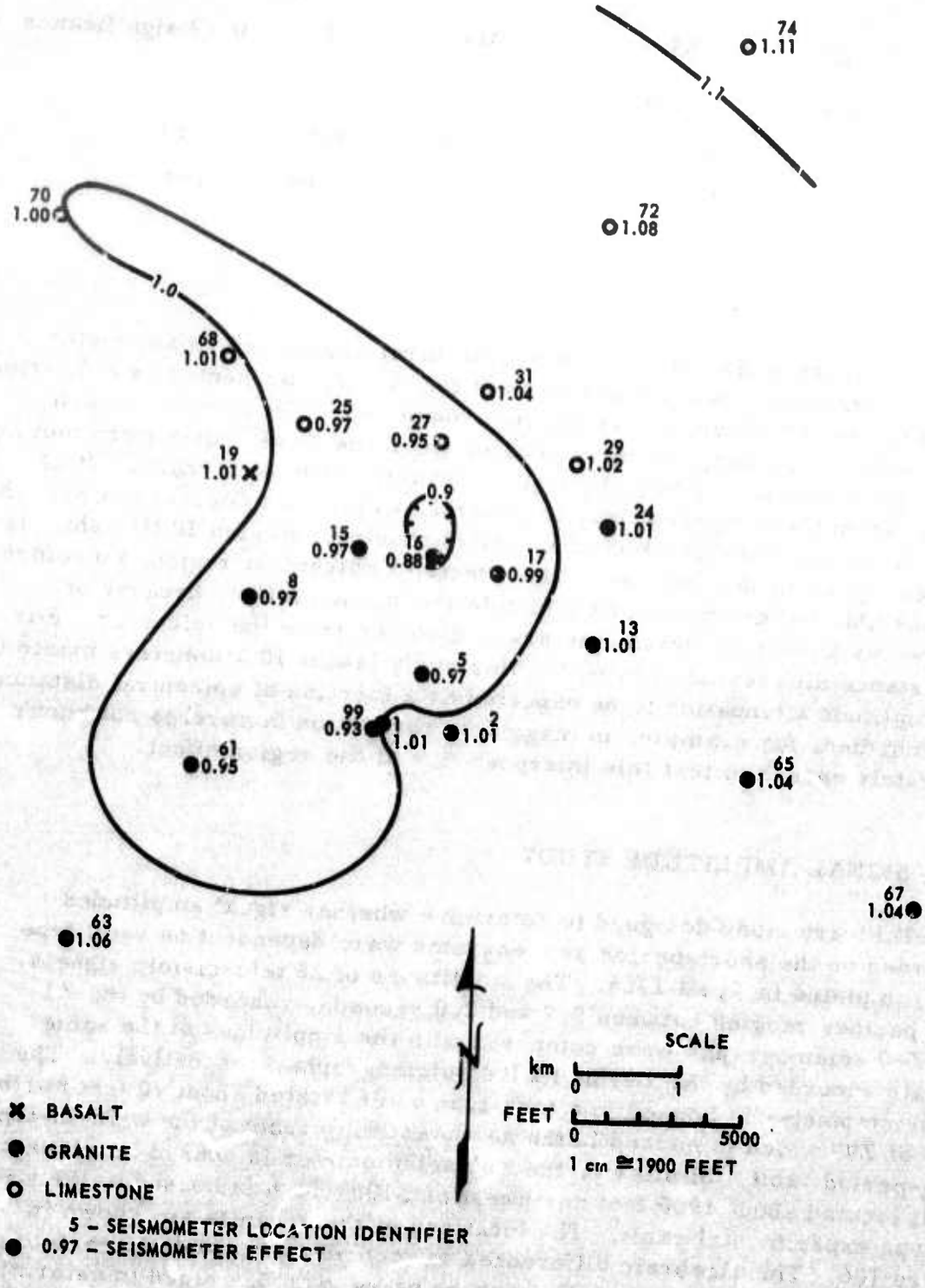

Figure 95. Estimates of seismometer effect ($\hat{\beta}_j$)

G 2609

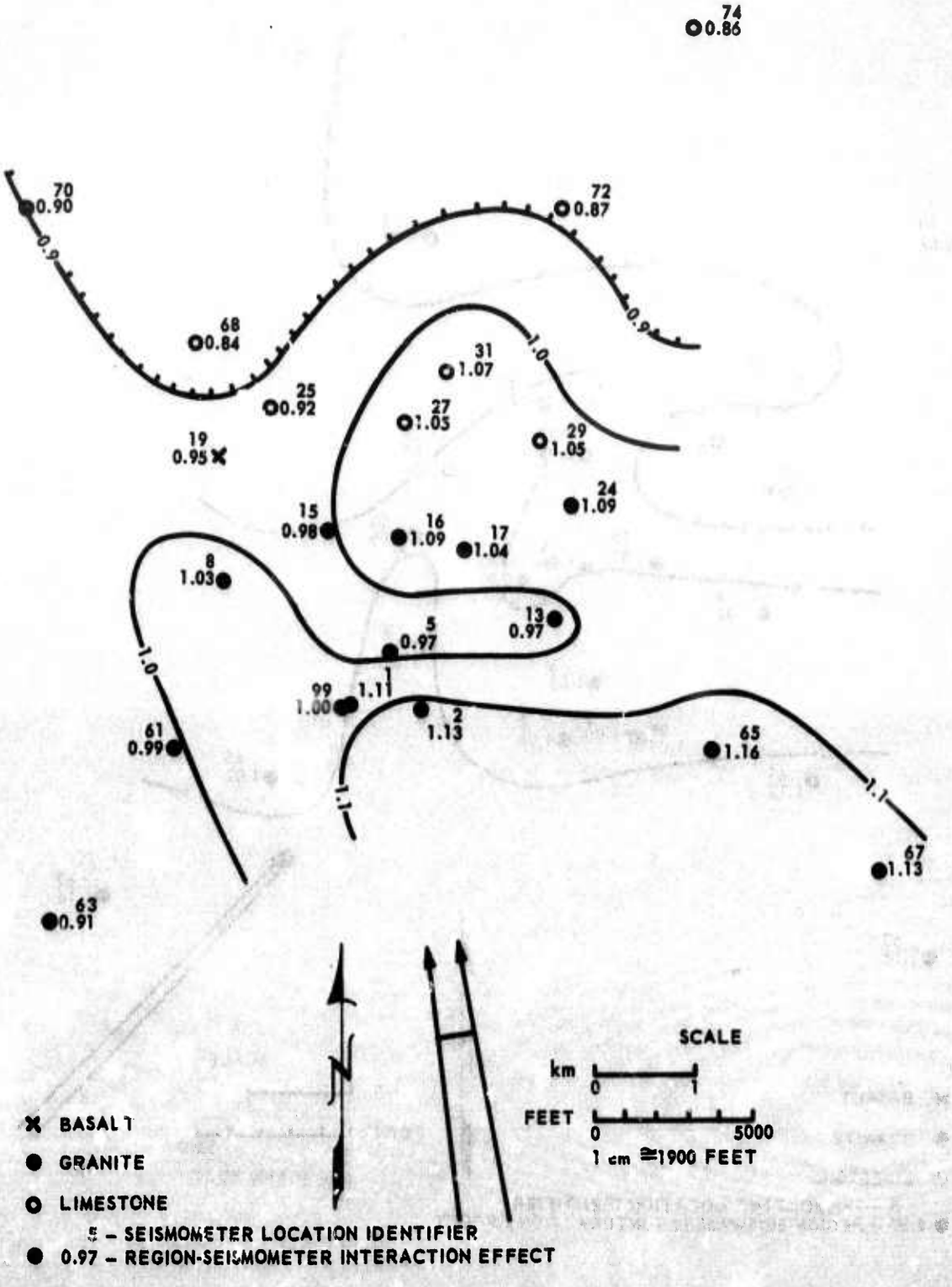

Figure 96. Estimates of region-seismometer interaction effect for Region 1 ($\hat{\gamma}_{ij}$)

G 2610

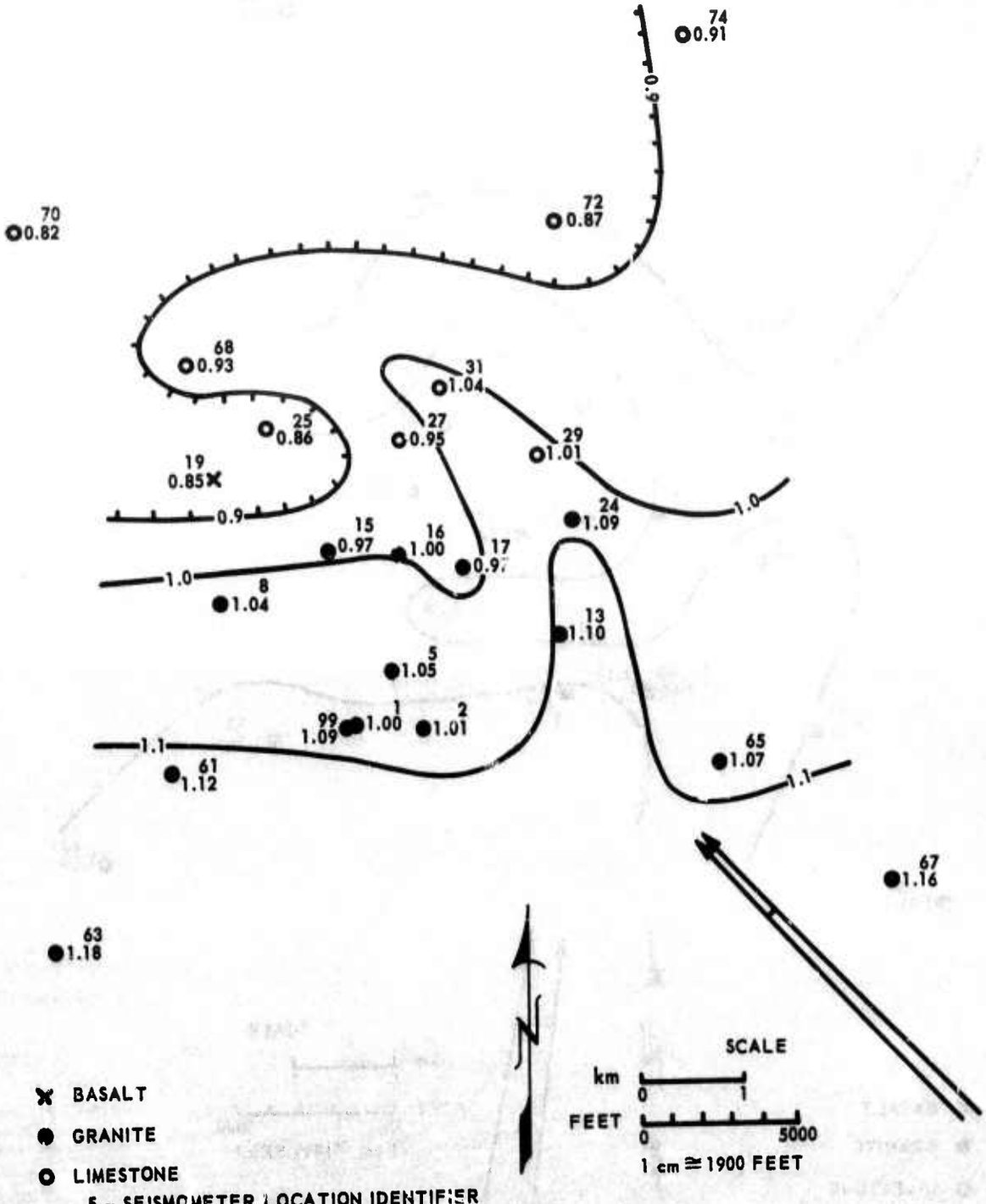

Figure 97. Estimates of region-seismometer interaction effect for Region 2 ($\hat{Y}_{2j}$)

G 2611

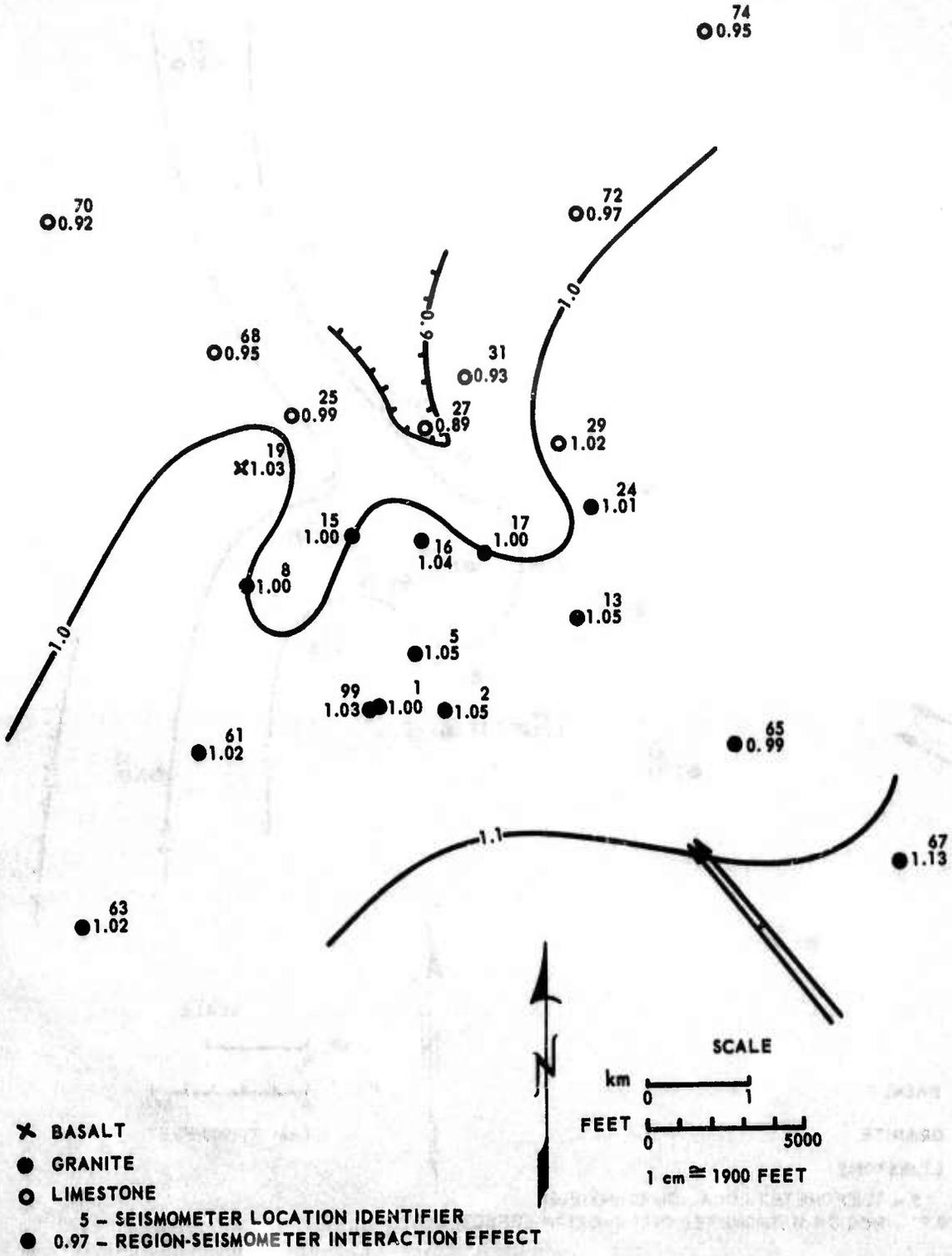

Figure 98. Estimates of region-seismometer interaction effect for Region 3 ($\hat{\gamma}_{3j}$)

G 2612

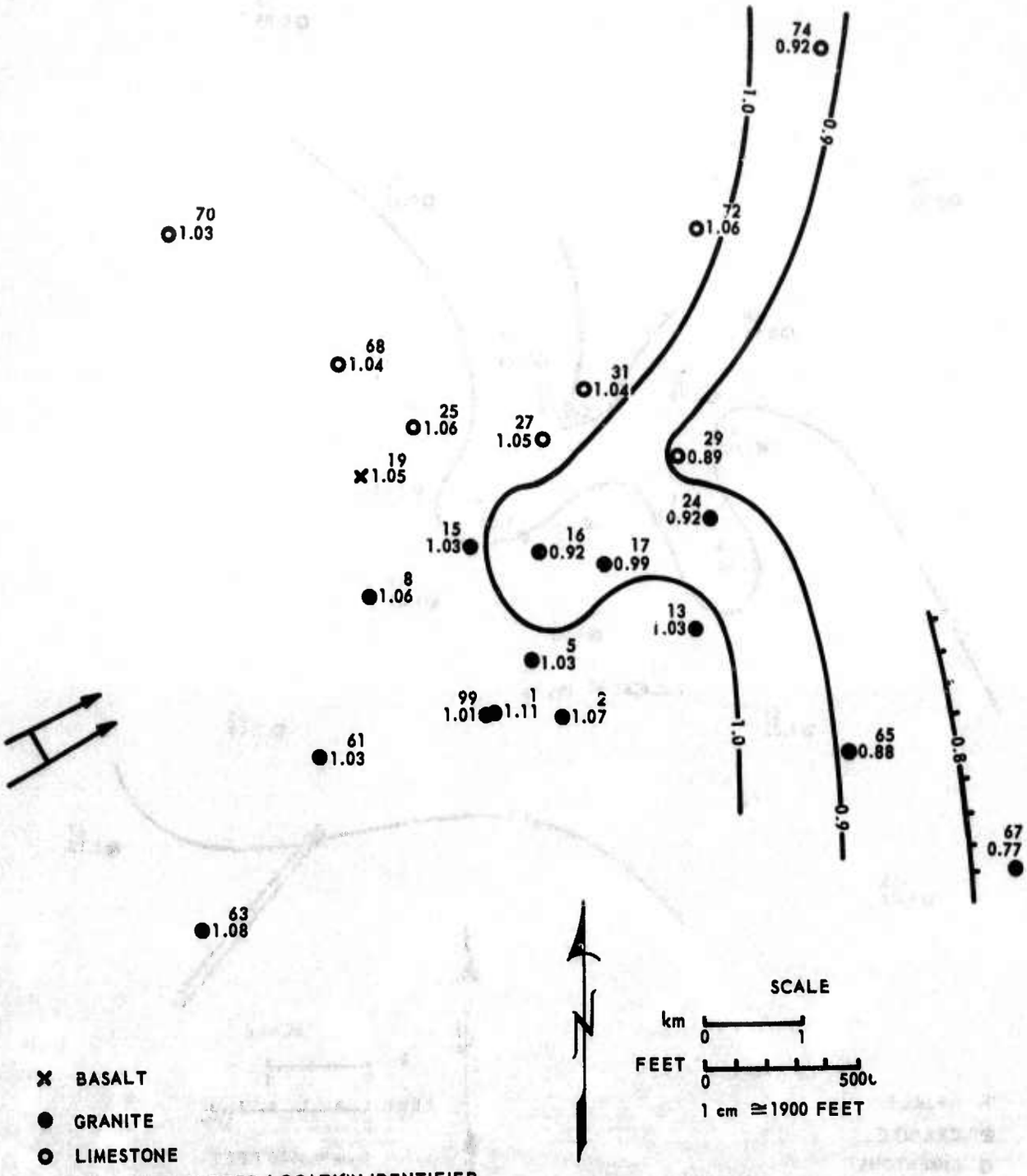

Figure 99. Estimates of region-seismometer interaction effect for Region 4 ($\hat{Y}_{4j}$)

G 2613

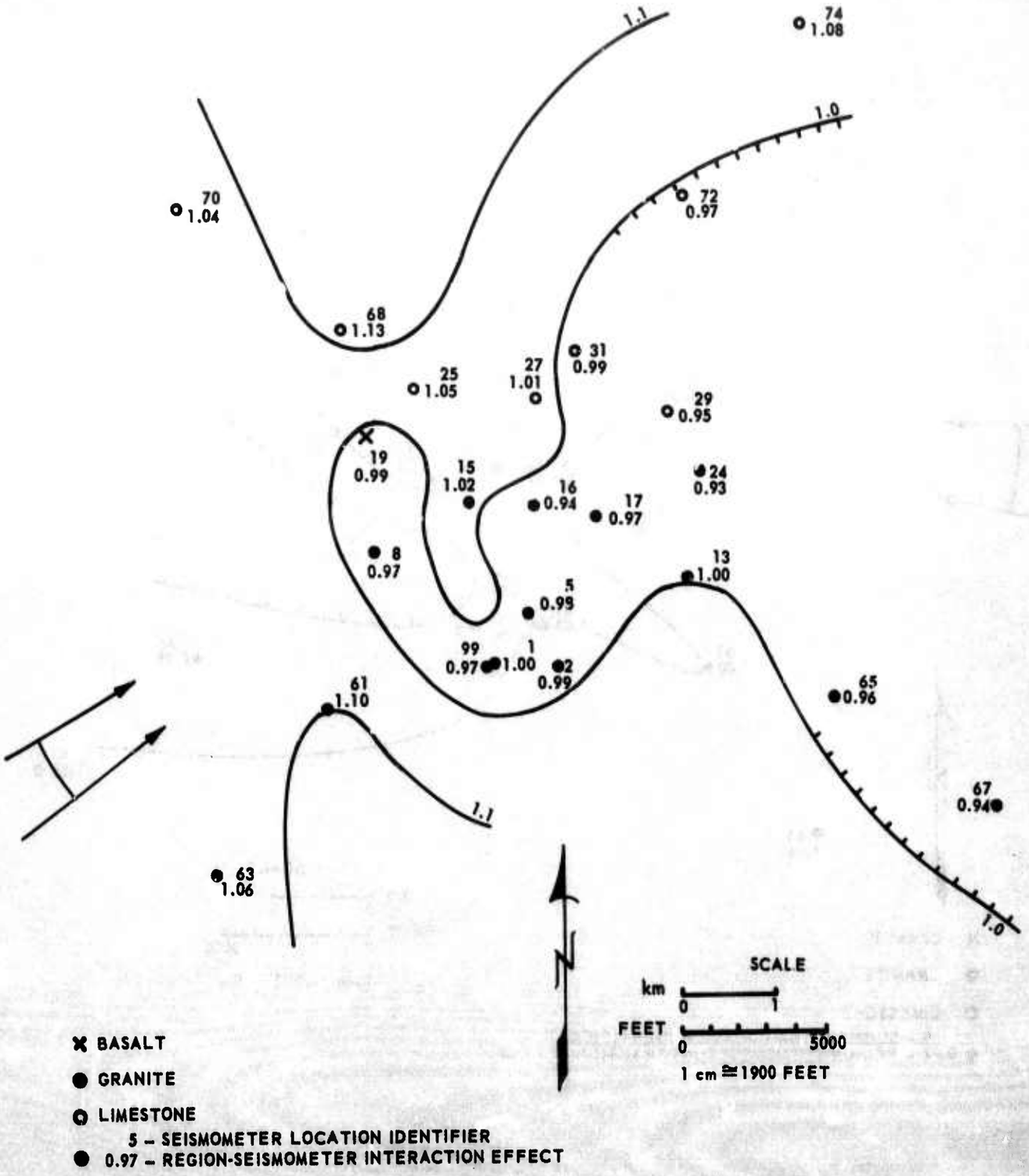

Figure 100. Estimates of region-seismometer interaction effect for Region 5 ($\hat{Y}_{5j}$)

G 2614

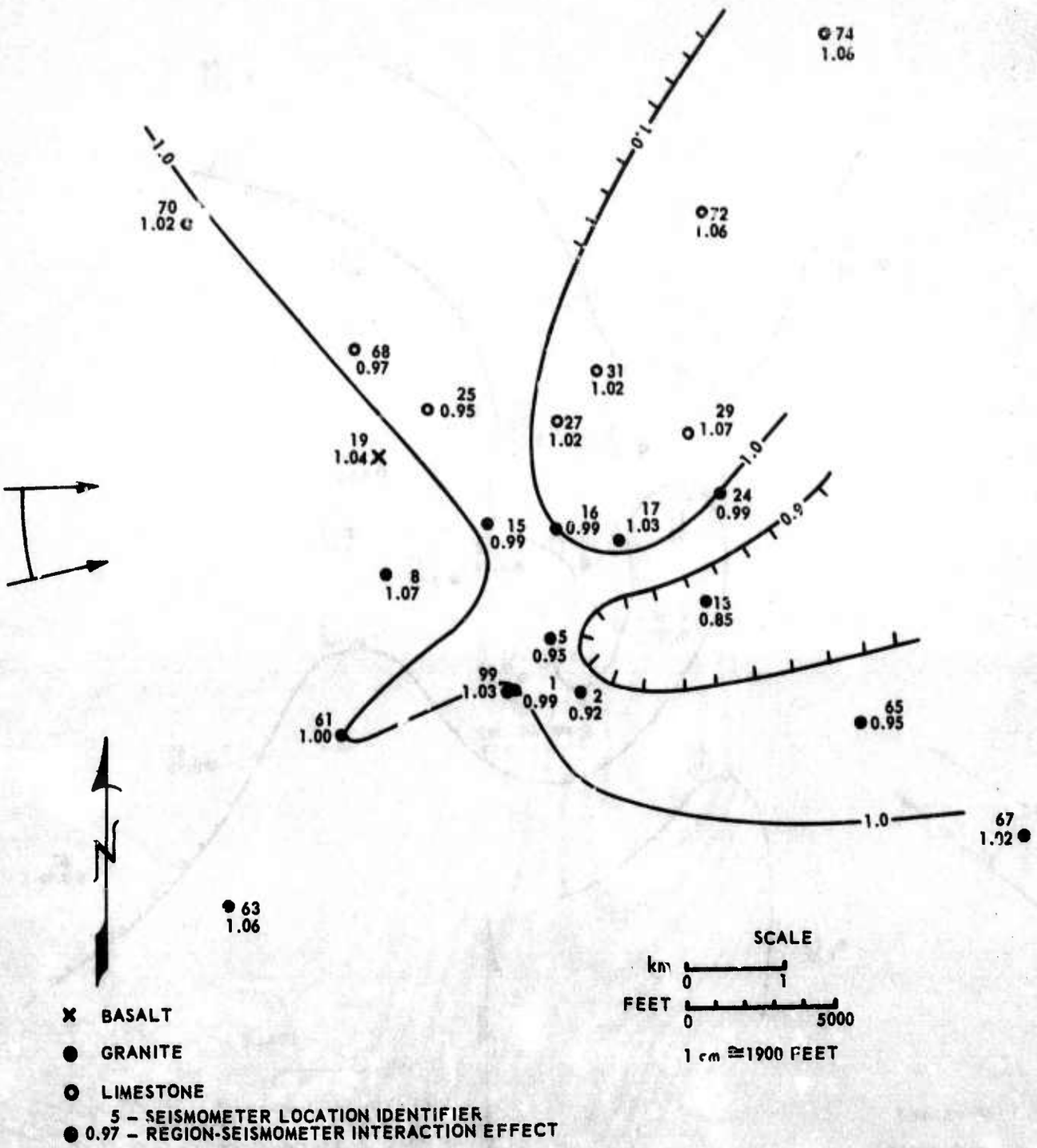

Figure 101. Estimates of region-seismometer interaction effect for Region 6 ($\hat{\gamma}_{6j}$) G 2615

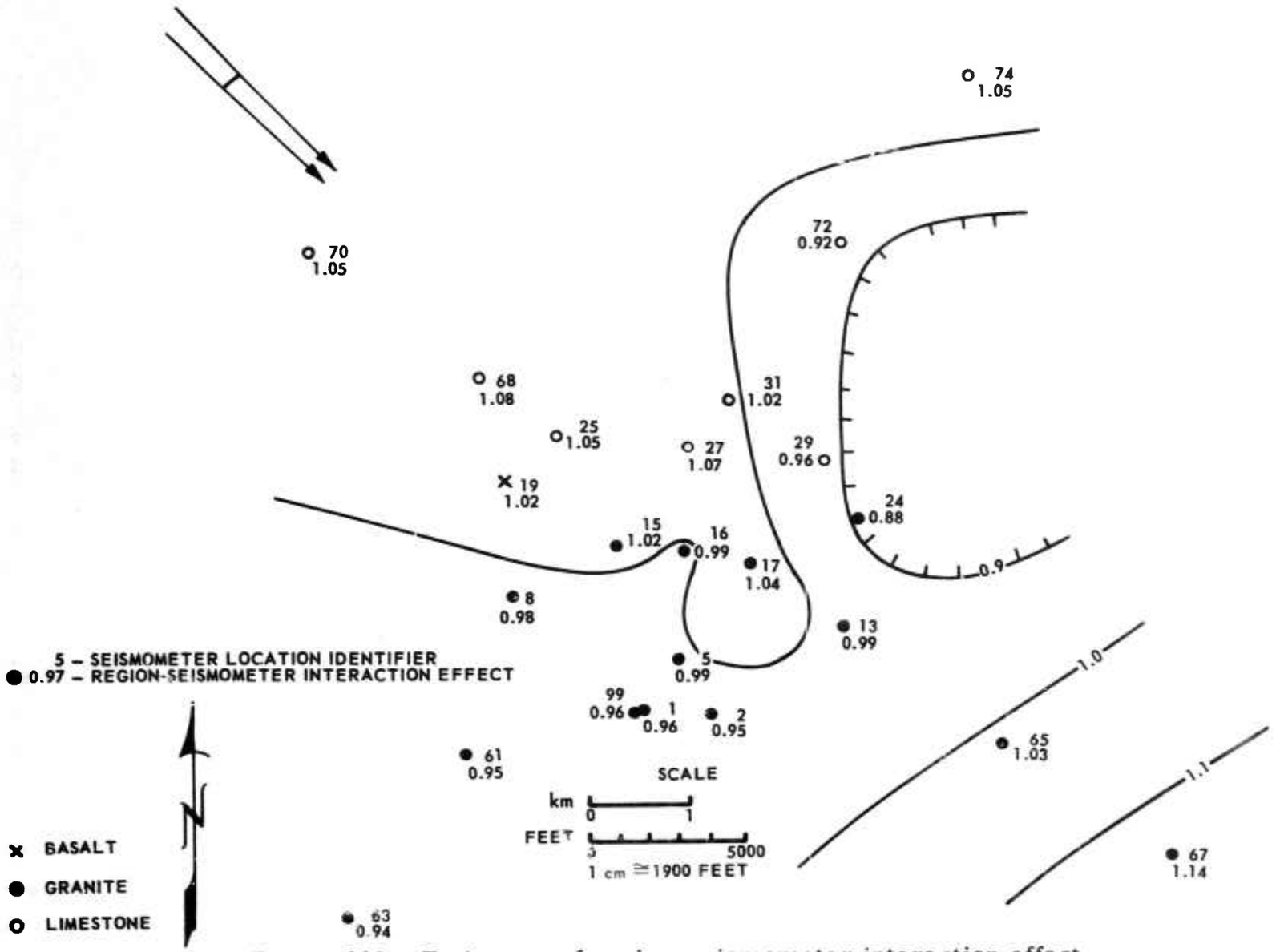

Figure 102. Estimates of region-seismometer interaction effect for Region 7 ($\hat{\gamma}_{7j}$)

G 2616

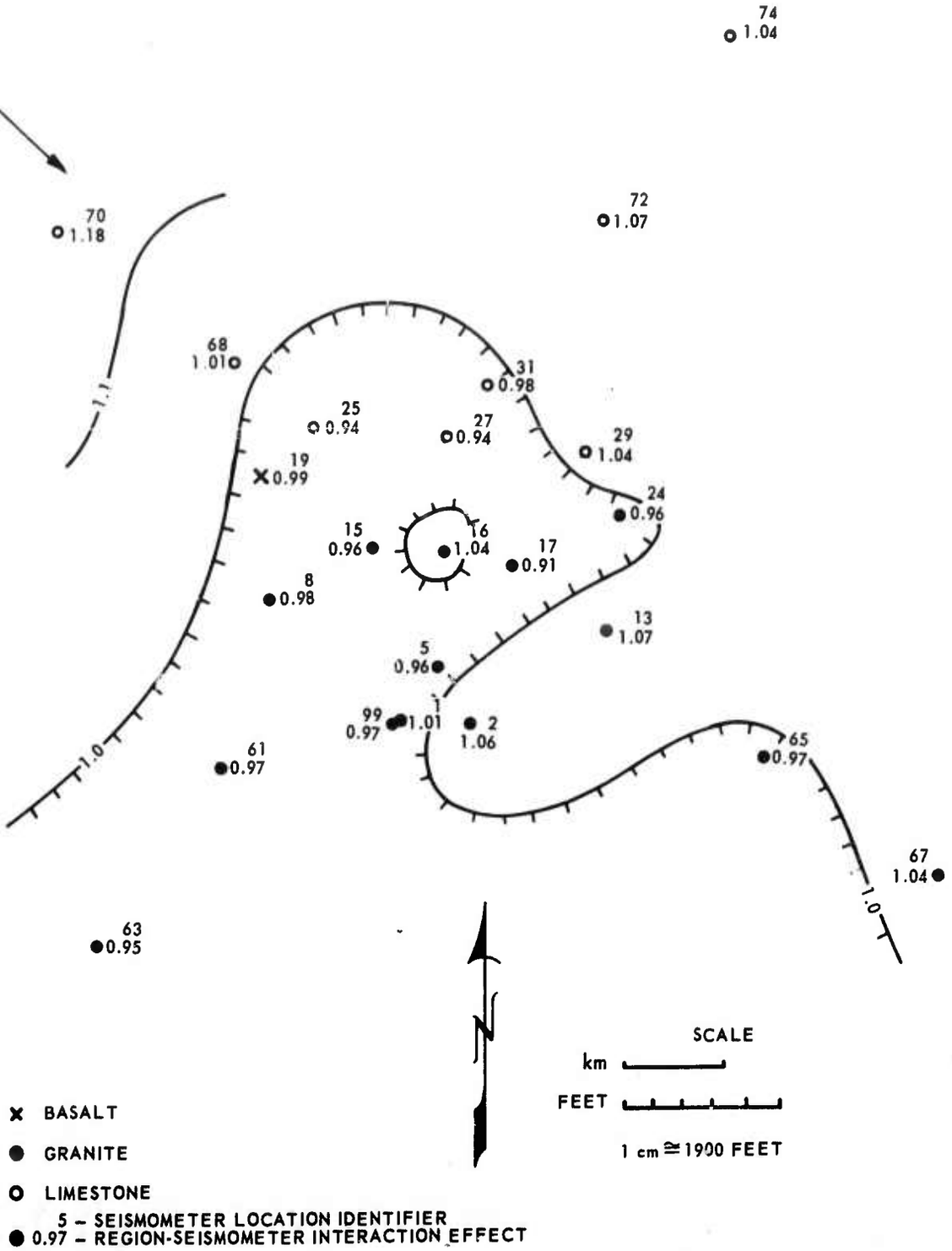

Figure 103. Estimates of region-seismometer interaction effect for Region 8 ($\hat{Y}_{8j}$) G 2617

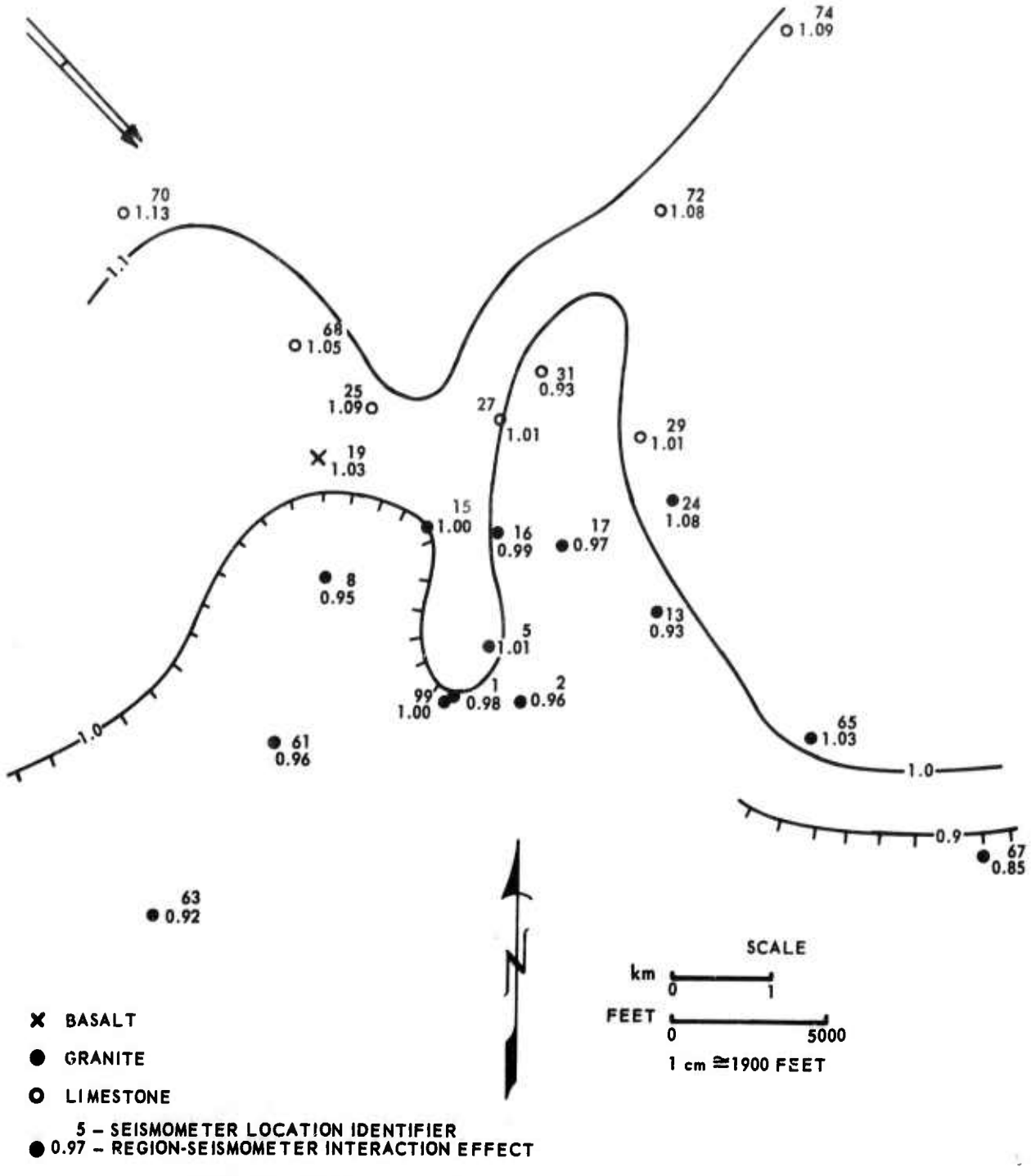

Figure 104. Estimates of region-seismometer interaction effect for Region 9 ($\hat{\gamma}_{9j}$) G 2618

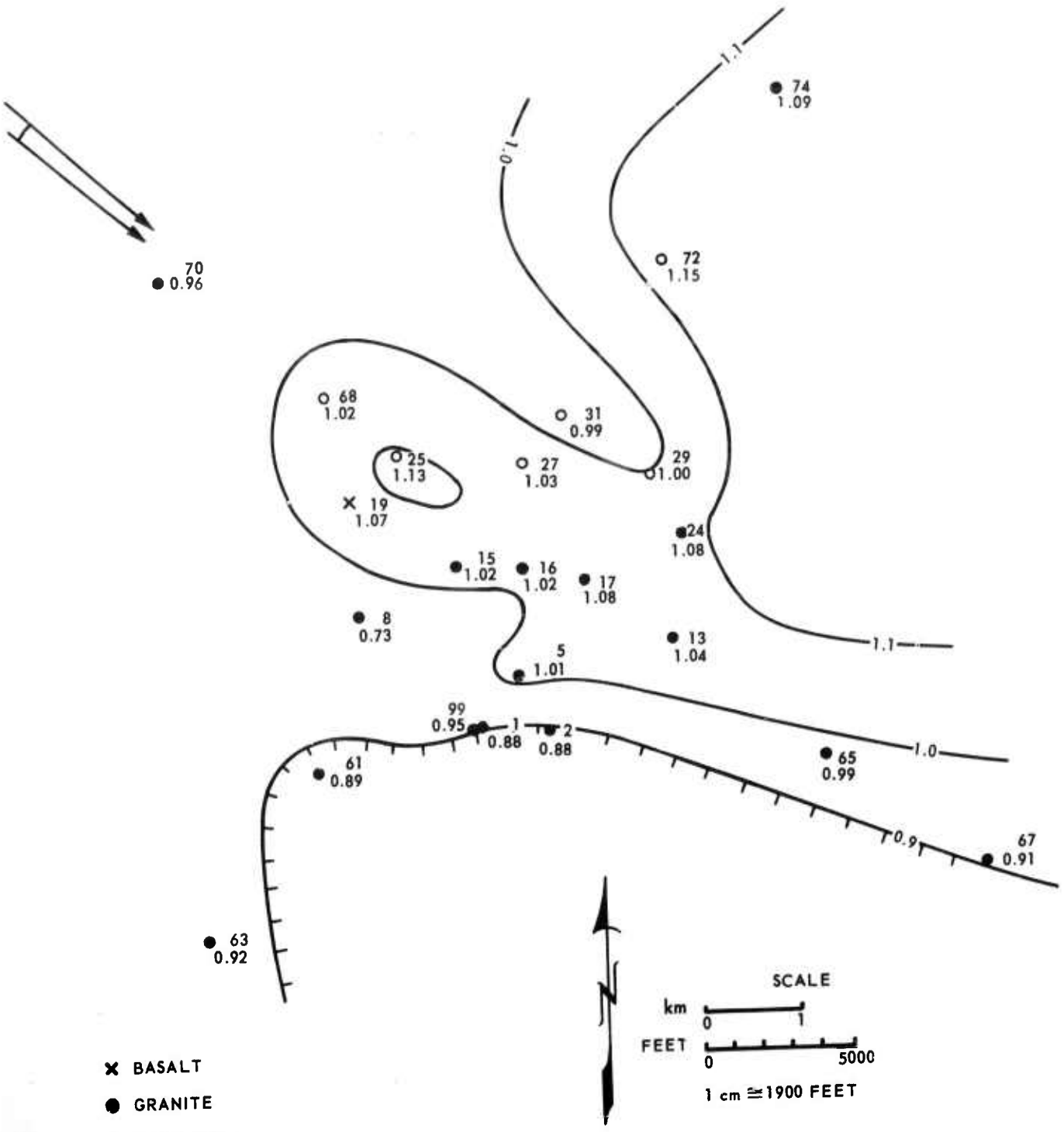

Figure 105. Estimates of region-seismometer interaction effect for Region 10 ($\hat{Y}_{10\,j}$)

G 2619

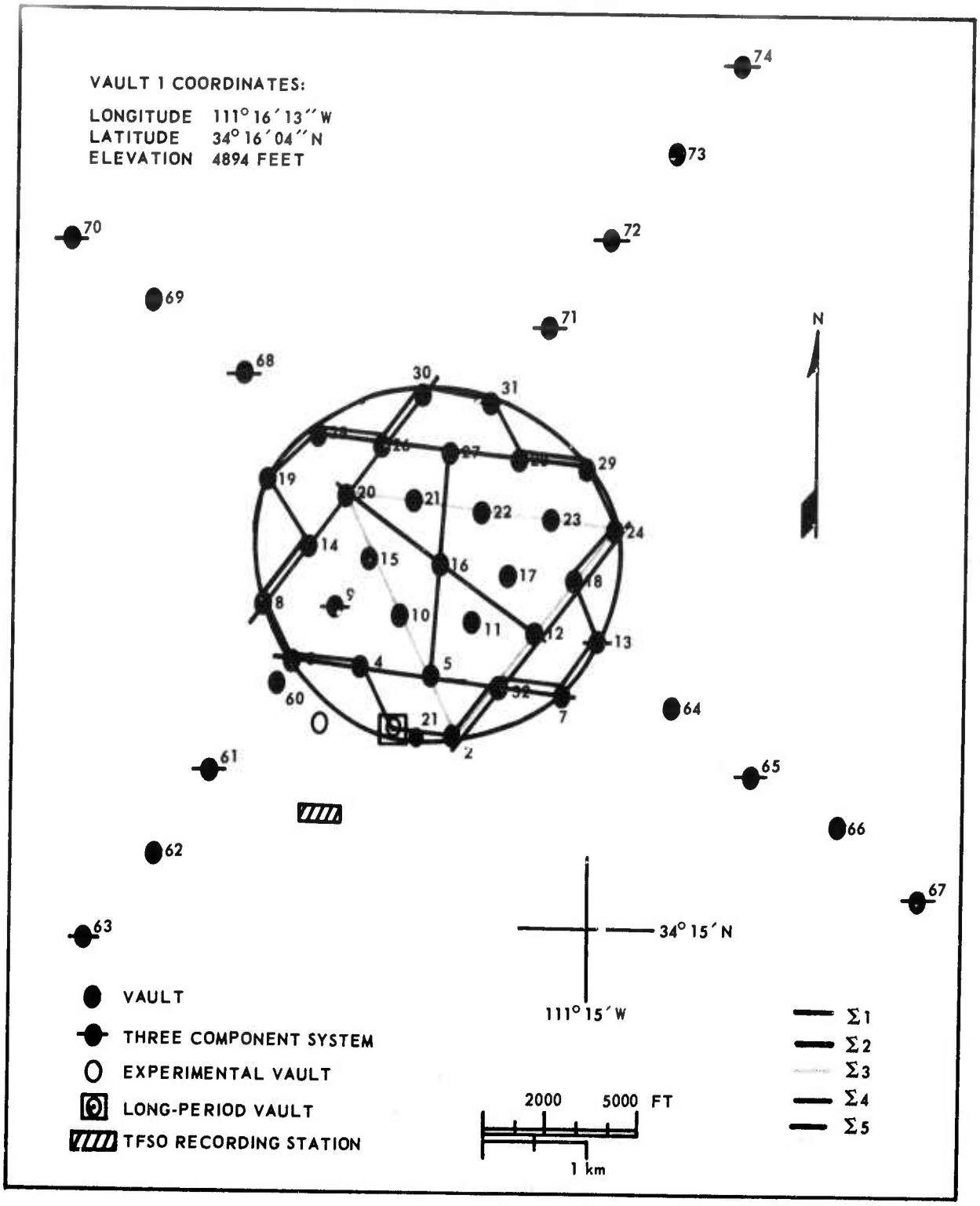

Figure 106. Tonto Forest Seismological Observatory vault locations

G 654

than the amplitudes recorded by Z99. The frequency responses of the Z1 and Z99 seismographs were matched and their calibrator motor constants differed by less than 1 percent.

In addition, the amplitudes of the signals recorded by Z1 were greater than the amplitudes recorded by the Z60-Z100 seismograph pair. The local surface geology within the area encompassing these instruments is generally uniform, and vault type does not appear to influence the amplitude with which teleseismic signals are recorded.

If the 7 percent amplitude difference observed between Z1 and Z99 is significant, the difference probably can be explained best as the result of differences in the degree to which the piers on which the seismometers are operated are coupled to the bedrock (see section 10.4).

10.6 WIND NOISE STUDY

A study to determine the effects of wind-generated noise on the short-period seismographs of the TFSO array was conducted in the fall and winter of 1965-66. Figure 107 is a graph showing trace amplitude, in millimeters at X10 view of 16-millimeter film, as a function of wind velocity for eight of the seismographs of the 31-element array. In general, wind speeds up to 10 to 15 mph do not have a degrading effect on TFSO data.

Six vertical seismograph systems, Z8, Z12, Z24, Z26, and Z28, exhibiting the lowest amplitude response to wind, were selected to form summation "Q" (ΣQ). This summation was recorded and evaluated for approximately 45 days. During this time, on only one occasion did the wind velocity reach 15-25 mph. The high wind lasted for a period of approximately 20 hours, on 22 December 1965. Figure 108 is a short-period experimental recording showing the response of ΣQ, ΣT, Z1, and various other experimental summations to wind-generated noise. As seen in this figure, ΣQ shows no less response to wind than does ΣT; in fact, the shorter period noise is of a slightly higher amplitude. We conclude that ΣQ adds nothing to the TFSO detection capability during windy periods, the random cancellation effect of the summation of 31 vertical seismographs (ΣT) having a greater effect.

10.7 EVALUATE VARIOUS SUMMATION SEISMOGRAPH

Various combinations of vertical elements within the 31-instrument array at TFSO were selected for an array-pattern study. The purpose of this study was twofold:

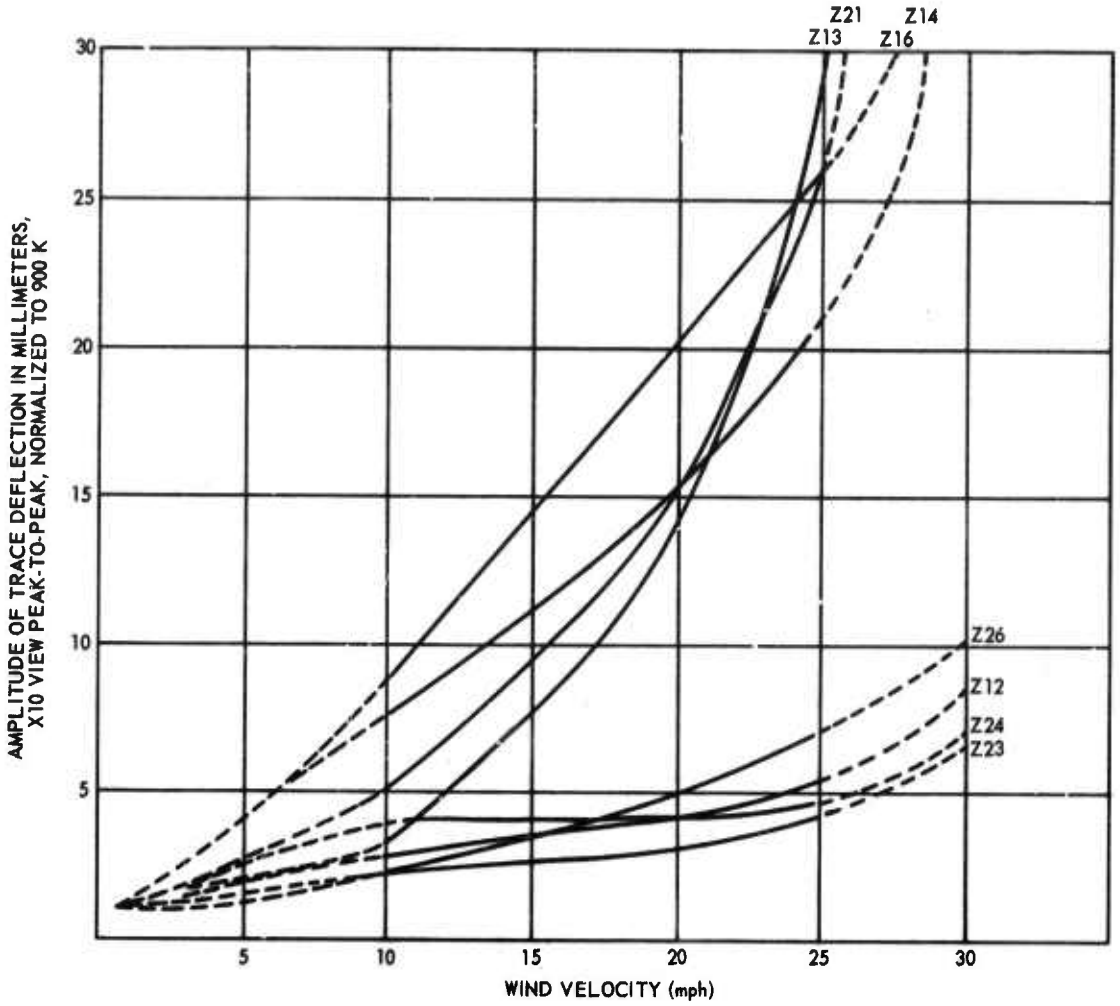

Figure 107. Response of four quietest and four noisiest short-period vertical seismographs selected from 19 seismographs of the 31 element array

G 2620

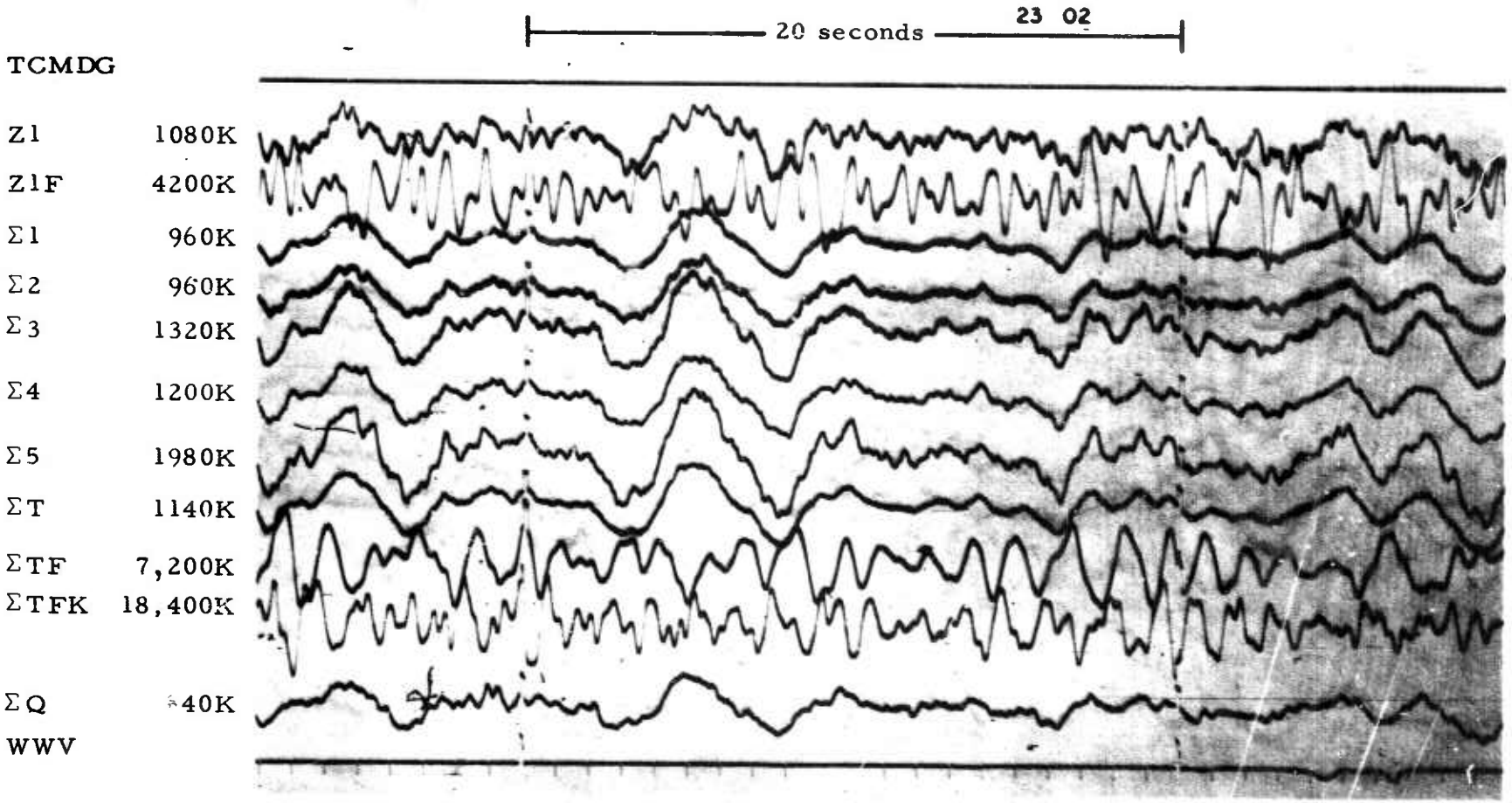

TFSO
Run 356
22 Dec 1965

Figure 108. Short-period recording exhibiting response of experimental summation and ΣT to wind noise during wind with velocities of 25 mph. (X10 enlargement of 16-millimeter film)

a. To determine whether a more effective pattern could be found that would enhance signal-to-noise ratios;

b. To determine whether the number of elements in the summation could be decreased from 31 without significantly affecting the effectiveness of the summation seismograph.

Five summations were formed and recorded side by side with ΣT. These experimental "arrays" are shown in figure 106 and are as follows:

$\Sigma 1$ - Pattern of array is an indented circle and is comprised of 19 vertical elements;

$\Sigma 2$ - Pattern of array is a circle and is comprised of 12 vertical elements;

$\Sigma 3$ - Pattern of array is a triangle and is comprised of 12 vertical elements;

$\Sigma 4$ - Pattern of array is an "H" oriented NE-SW and is comprised of 11 vertical elements;

$\Sigma 5$ - Pattern of array 13 is an "H" oriented WNW-ESE and is comprised of 11 vertical elements.

The predominant short-period microseisms recorded at TFSO are in three period ranges: 0.2 to 0.6 second, 1.1 to 1.6 seconds, and 2.0 to 4.0 seconds. The arrays $\Sigma 1$, $\Sigma 2$, and $\Sigma 3$ were compared to ΣT in cancelling the shortest period microseisms. During intervals when the background level is lower than normal, there is no significant difference in the response of any of these four summations, and during intervals of normal background level, there is no significant difference in the response of $\Sigma 1$, $\Sigma 2$, and ΣT. The "H" arrays and $\Sigma 3$ (triangle) response to high-frequency microseisms are all about equal.

Figures 109 and 110 are short-period experimental recordings showing the response of the various summations to different background levels.

The microseisms in the period range of 1.1 to 1.6 seconds are those most detrimental to the detection of signals at TFSO. These microseisms appear to be directional, arriving generally from the west. The "H" arrays proved to be ineffective in cancelling the microseisms in the period range of 1.1 to 1.6 seconds mainly because of their apparent high velocity which approaches that of P waves.

The ΣT (31 elements) is the most effective array, overall; however, it appears that any random pattern of approximately 18 to 25 elements would have about the same detection capability.

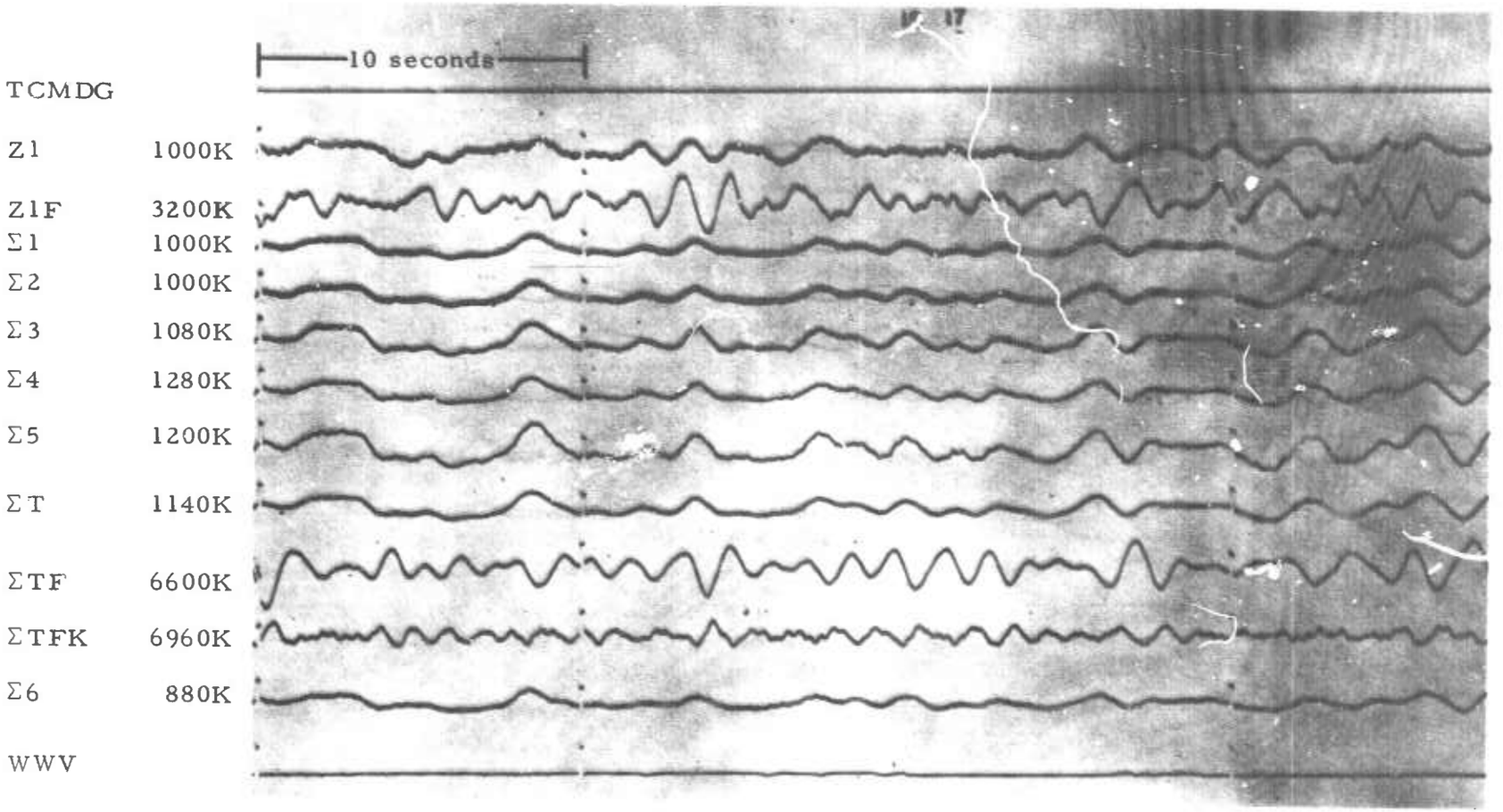

TFSO
Run 348
14 Dec 1965

Figure 109. Short-period experimental recording exhibiting response of experimental summations and ΣT to microseisms during interval when background level is unusually low. (X10 enlargement of 16-millimeter film)

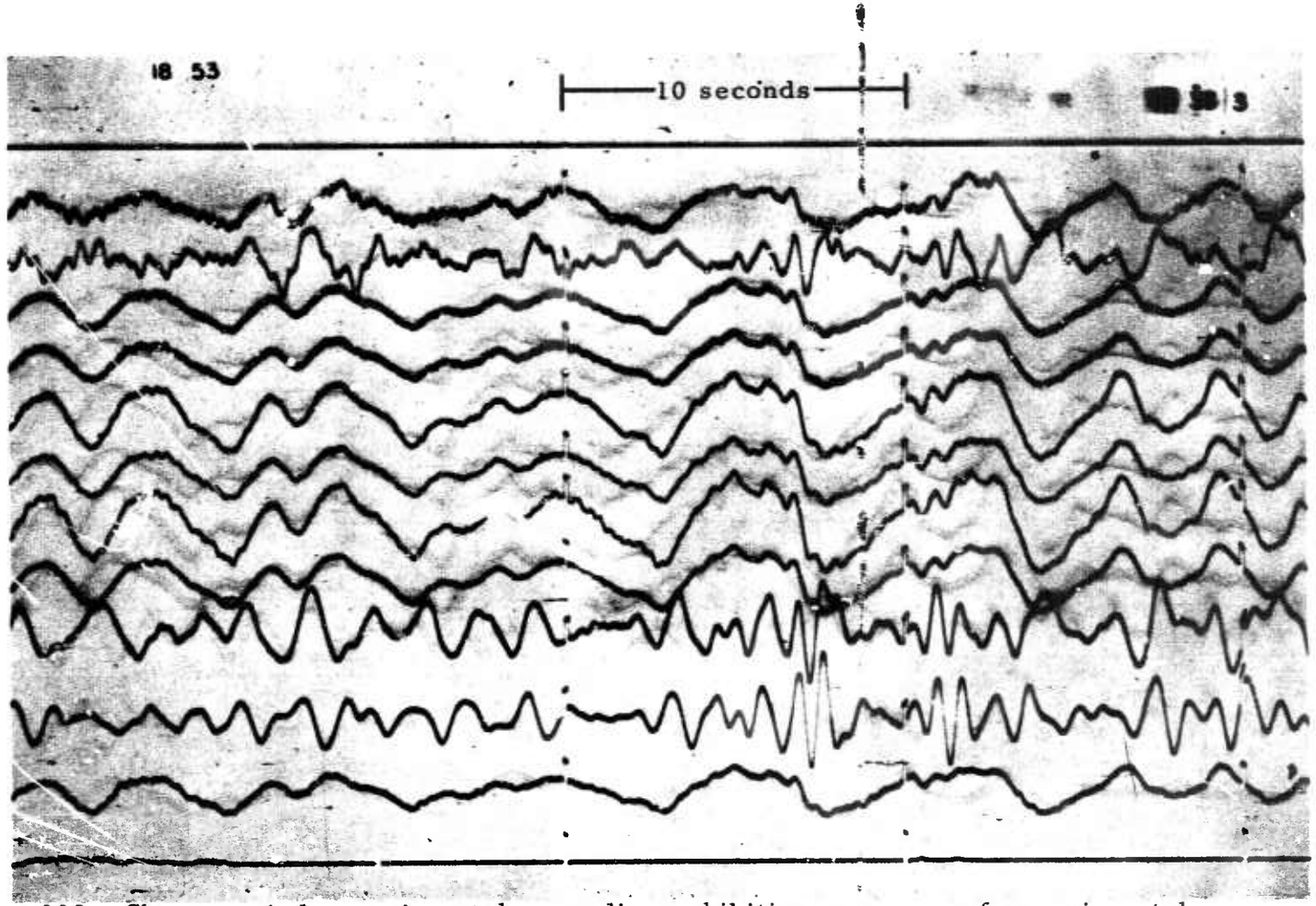

Figure 110. Short-period experimental recording exhibiting response of experimental summations and ΣT to microseism during period of typical background level.
(Note: Teleseismic signal from Solomon Islands, Δ = 96.8°,
Azimuth = 267°, h = 68 km, o = 18:39:47.2, m = 5.4)
(X10 enlargement of 16-millimeter film)

TFSO
Run 363
29 Dec 1965

10.8 EVALUATION OF THE EFFECTIVENESS OF VARIOUS BANDPASS FILTERS

10.8.1 Filtered Summations Seismographs

The response of the filtered summation ΣTF at TFSO does not provide optimum effectiveness. This filter, manufactured by United Electro-Dynamics, Inc., is set at a cutoff of 1.755 cps (0.57 second) with a slope of 12 dB per octave at the high end and at 0.7 cps (1.43 seconds) with a slope of 24 dB per octave on the low end.

Using a Krohn-Hite Model 330A filter, recordings were made with various bandpass settings to compare with ΣTF. This system was designated ΣTFK. The frequency response of ΣTF and two of the experimental ΣTFK systems are shown in figure 111. The response of ΣTF does enhance the shorter period teleseismic signal; however, this was not effective in improving the detection capability because microseisms in the period range of 0.6 and 1.1 seconds were also enhanced. The ΣTFK seismograms produced when the filter was set at 3.0 cps (0.3 second) and 0.8 cps (1.25 seconds) with 24 dB per octave slope responded very well to the shorter period signals and less to the longer period energy (see figure 112).

Figures 113 and 114 show the response of both filters to low-level events having periods of 0.6 and 0.9 second, respectively. ΣTFK was also set with the low cutoff at 1.0 cps and proved to be almost as effective as when set at 0.8 cps. Figures 115 and 116 show this response to signals having periods of 0.8 and 1.1.

We conclude that no single response provided the optimum filtered seismogram for a flag trace; however, by using two filtered summation seismograms in conjunction with primary data, the analysis was aided significantly.

10.9 MAGNITUDE STUDIES

Magnitude studies to develop station magnitude corrections for BMSO, CPSO, TFSO, UBSO, and WMSO and refined distance-depth magnitude correction factors were conducted jointly under Projects VT/5054 and VT/5055. Results of these studies were published in Technical Report No. 66-73, Magnitude Studies Conducted under Projects VT/5054 and VT/5055, 20 July 1966.

Magnitude station corrections determined from a statistical model and from magnitude frequency distributions agreed within 0.06 magnitude unit. The station corrections determined from the statistical model are presented in table 15.

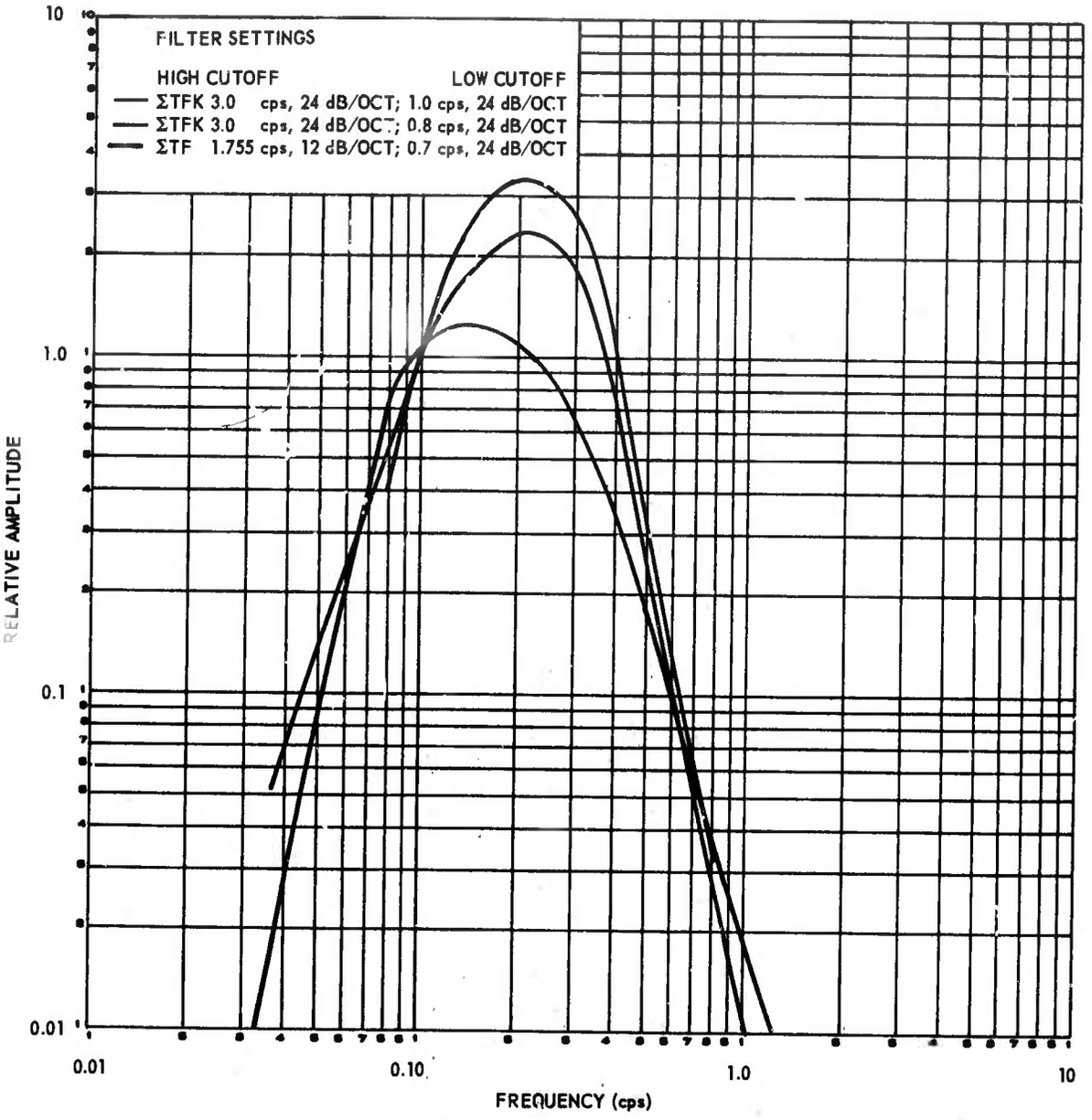

Figure 111. Frequency response of filtered summation systems TFSO

G 655

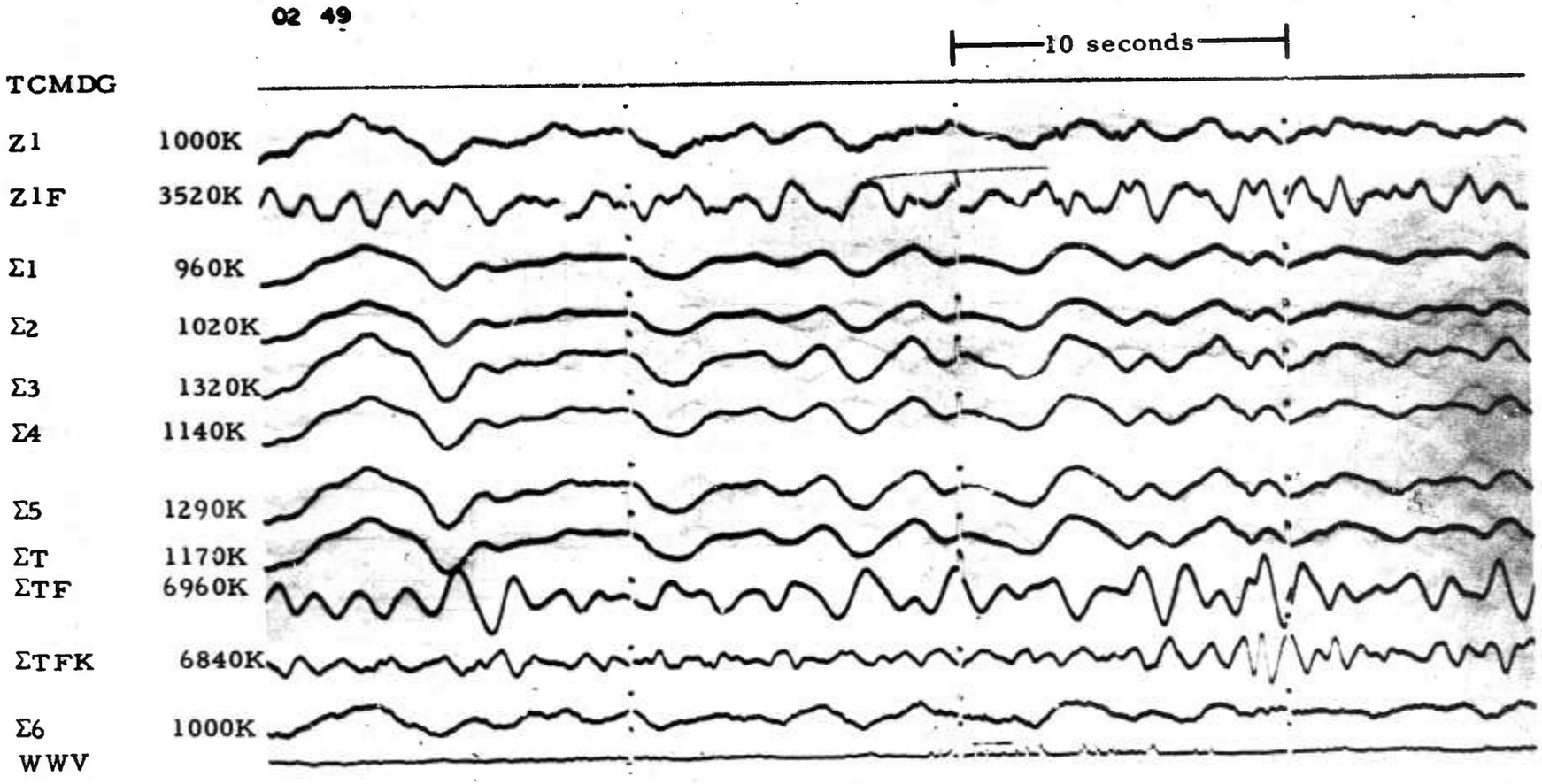

Figure 112. Short-period experimental seismogram exhibiting response of ΣTF and ΣTFK to a low-level teleseismic signal from the Aleutian Islands with period of 0.8 sec.

TFSO
Run 344
10 Dec 1965

Filter settings are:

	High cutoff	Low cutoff
ΣTF	1.755 cps 12 dB/oct	0.7 cps 24 dB/oct
ΣTFK	3.0 cps 24 dB/oct	0.8 cps 24 dB/oct

(Hypocentral data: Δ = 56.1°, Azimuth = 315°, h = 33 km, o = 02:39:50.0, m = 3.9)

(X10 enlargement of 16 millimeter film)

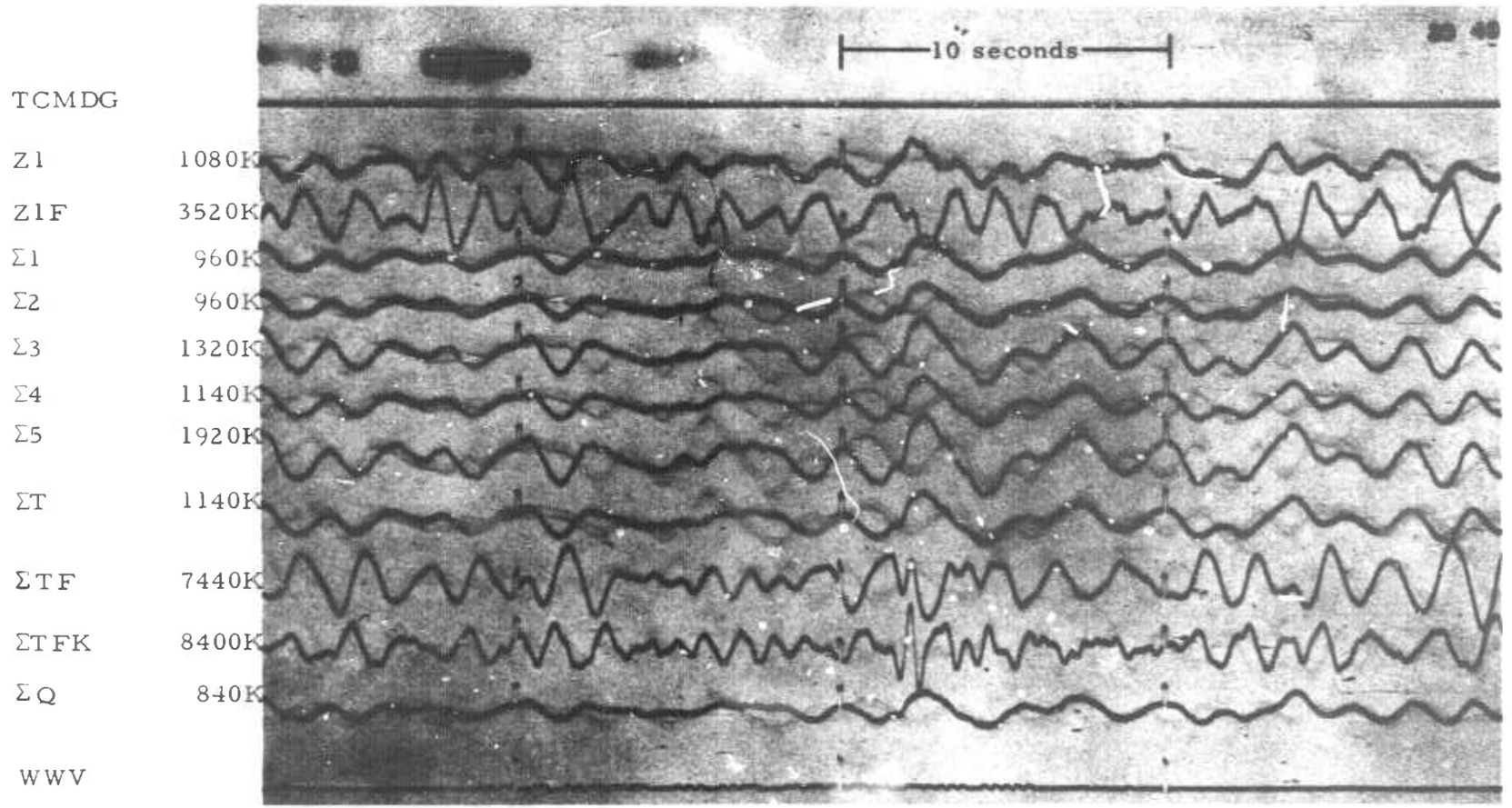

Figure 113. Short-period experimental recording exhibiting response of ΣTF and ΣTFK to a low-level teleseismic event from unknown epicenter having period of 0.6 sec at the following filter settings. (X10 enlargement of 16-millimeter film)

TFSO		High cutoff	Low cutoff
Run 350	ΣTF	1.755 cps 12 dB/oct	0.7 cps 24 dB/oct
16 Dec 1965	ΣTFK	3.0 cps 24 dB/oct	0.8 cps 24 dB/oct

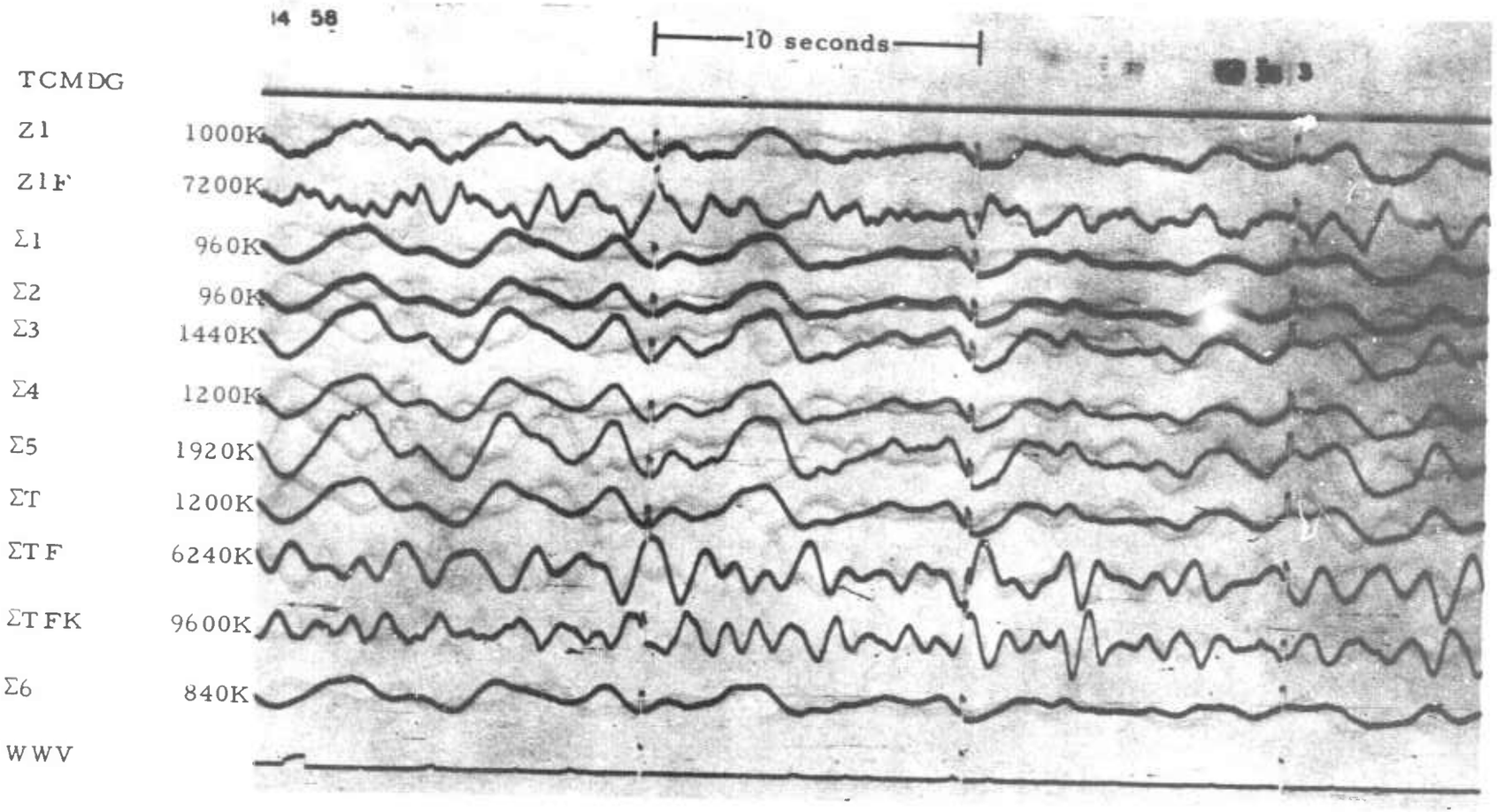

Figure 114. Short-period experimental seismogram exhibiting response of ΣTF and ΣTFK to a low-level teleseismic event having a period of 0.9 sec. Filter settings are:

TFSO
Run 353
19 Dec 1965

	High cutoff	Low cutoff
ΣTF	1.755 cps 12 dB/oct	0.7 cps 24 dB/oct
ΣTFK	3.0 cps 24 dB/oct	0.8 cps 24 dB/oct

Epicenter unknown. (X10 view of 16-millimeter film)

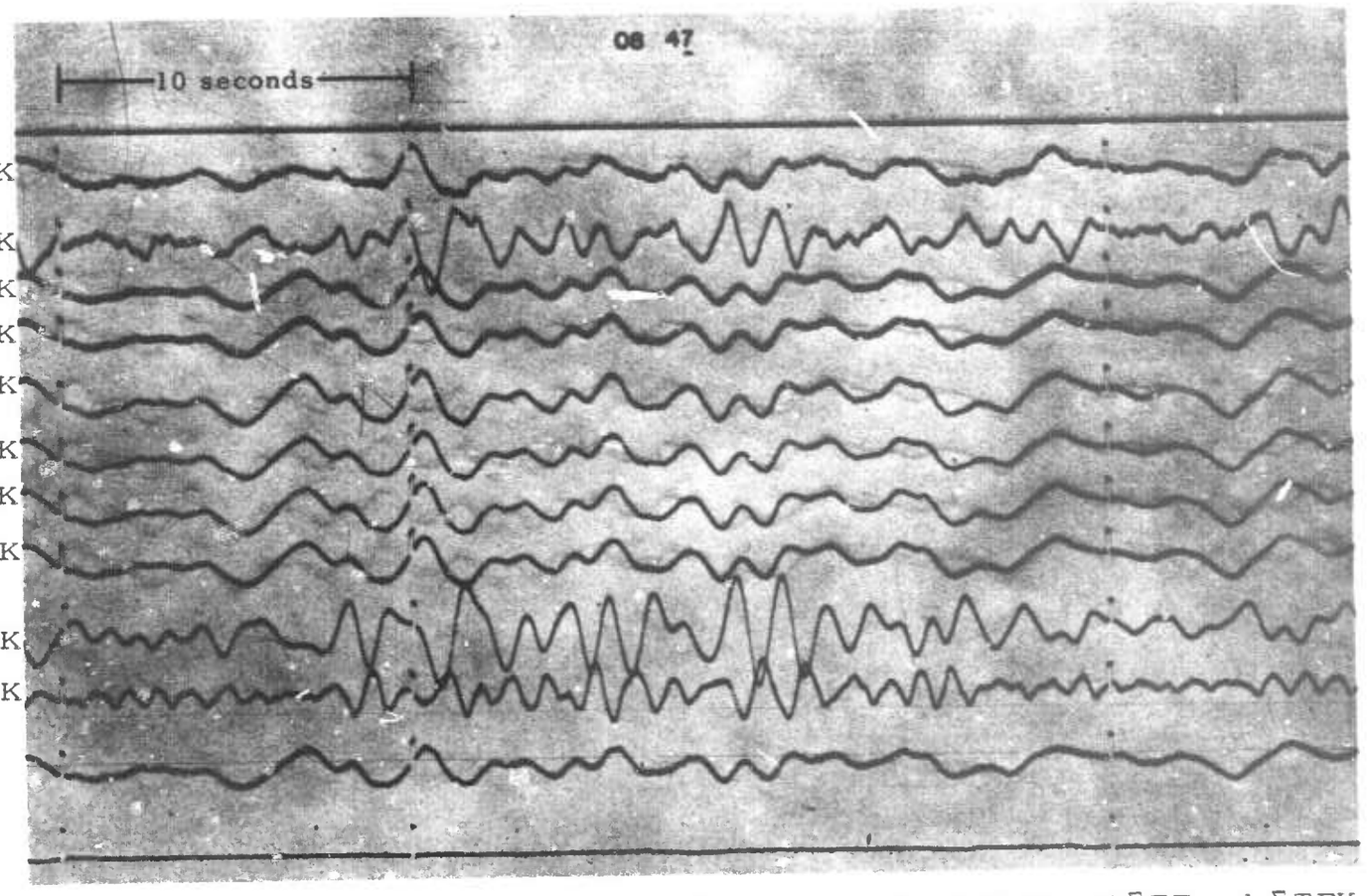

Figure 115. Short-period experimental recording showing the response of ΣTF and ΣTFK to a teleseismic signal having a period of 1.1 sec. Filter settings are:

	High cutoff	Low cutoff
ΣTF	1.755 cps 12 dB/oct	0.7 cps 24 dB/oct
ΣTFK	3.0 cps 24 dB/oct	1.0 cps 24 dB/oct

Epicenter unknown. (X10 enlargement of 16 millimeter film)

TFSO
Run 015
15 Jan 1966

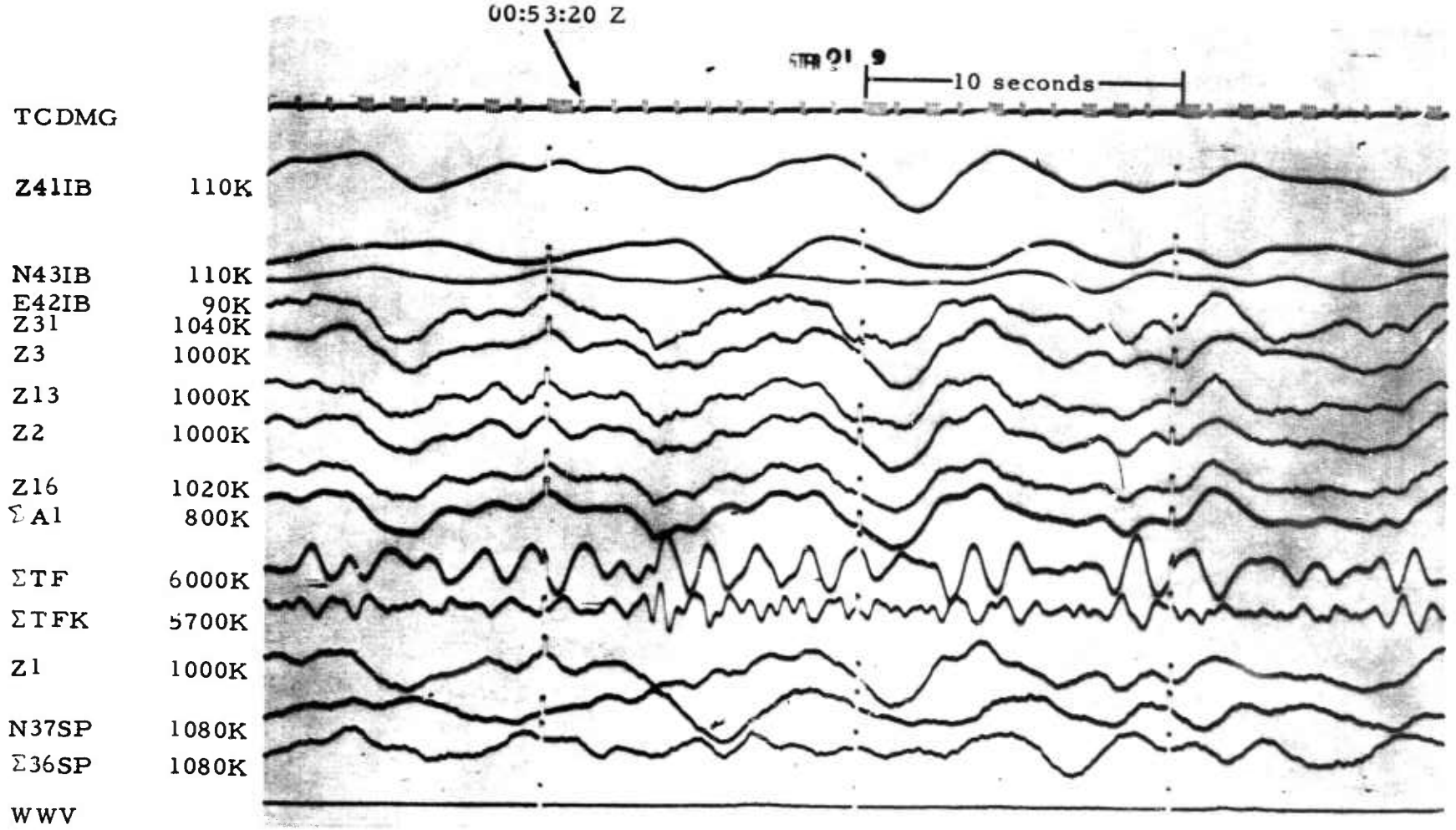

Figure 116. Short-period recording of primary data exhibiting the effectiveness of an experimental summation (ΣTFK) in detecting low-level signal having a period of 0.8 sec. Filter settings are:

	High cutoff	Low cutoff
ΣTF	1.755 cps 12 dB/oct	0.7 cps 24 dB/oct
ΣTFK	3.0 cps 24 dB/oct	1.0 cps 24 dB/oct

Epicenter unknown (X10 enlargement of 16 millimeter film)

TFSO
Run 019
19 Jan 1966
Data Group 7149

Table 15. Station magnitude corrections (S) for BMSO, CPSO, TFSO, UBSO, and WMSO

Observatory	S (mag units)
BMSO	+0.17
CPSO	-0.08
TFSO	+0.24
UBSO	-0.05
WMSO	-0.03

Little error was found in the standard distance-depth correction factors $(Q_p)(\Delta, h)$ except for distances less than 15 degrees, for which Q_p is too large, and for distances greater than 100 degrees, for which Q_p is too small. The sample of earthquakes studied was adequate only for depths less than 200 kilometers for distances between 20 and 90 degrees, and for depths less than 50 kilometers for distances between 0 and 110 degrees. The estimated error $(\hat{\alpha})$ in Q_p (Δ, h) for those values of epicentral distance and hypocentral depth for which there were at least ten observations is presented in figure 117.

10.10 LONG-PERIOD NOISE STUDY

Following the November meeting at VSC, the Project VT/5055 Project Officer notified us that the five portable seismograph systems operated under the LRSM program (Project VT/6703) would be available for a period of about 10 weeks following the Project STERLING experiment. The Project Officer requested that we recommend a configuration for a long-period array based on the use of the five LRSM portable systems. We attempted to design the test array so that we could obtain the maximum amount of useful long-period microseismic noise data for use in refining our long-period array recommendation. Because of the limited time available for the noise survey, and because of the limited instrumentation available, we recommended a compromise array on 23 November 1966. The Project Officer approved our recommendation with a request that we

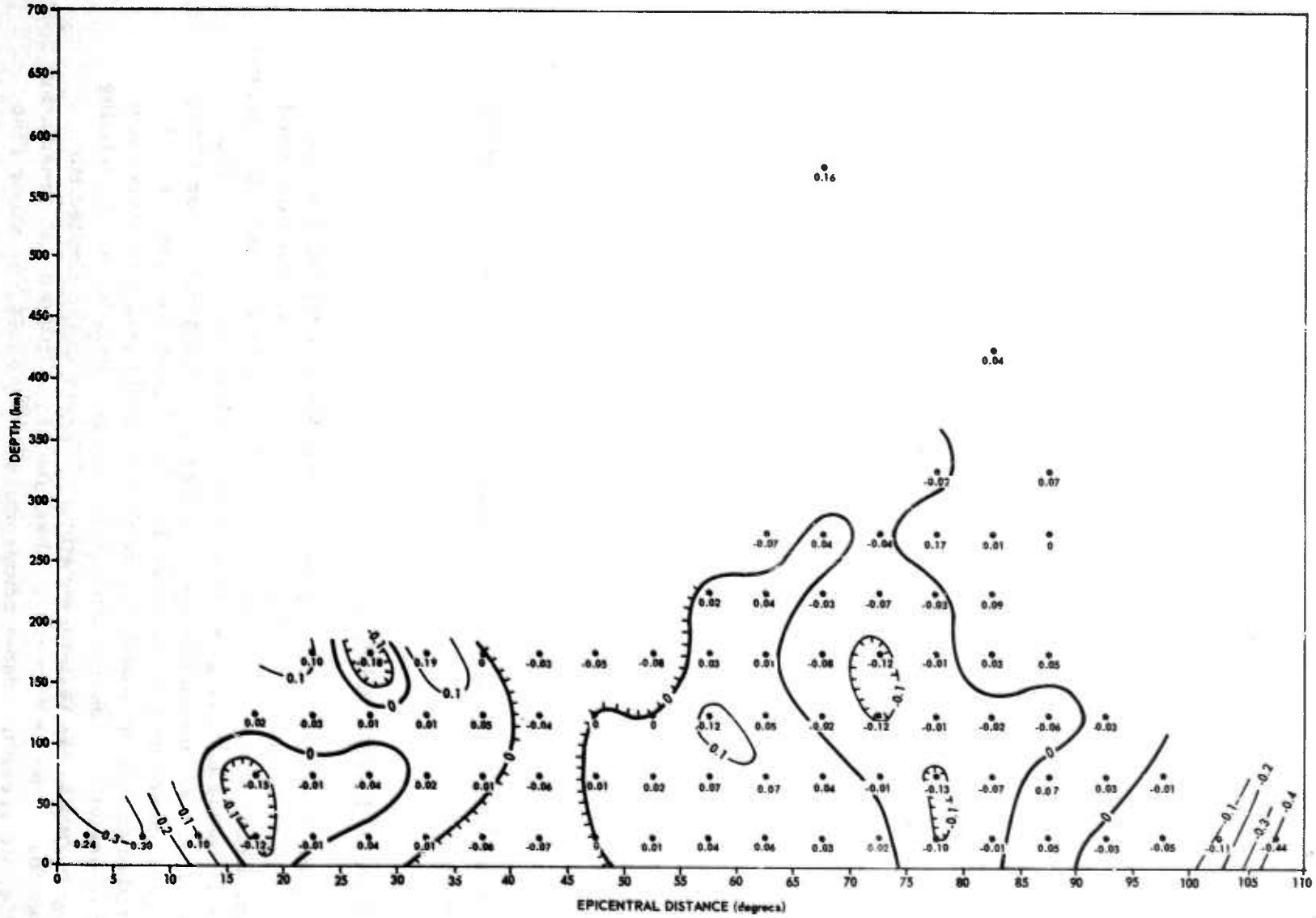

Figure 117. Estimated error ($\hat{\alpha}$) in Q_p (Δ, h) for those values of epicentral distance and hypocentral depth for which there were at least 10 observations

G 1432

reduce the spacing between three-component elements. All possible preliminary work necessary to install the array shown in figure 118, including the procurement of the necessary tank vaults, was accomplished before the end of Project VT/5055.

Because of their familiarity with the portable systems, we are of the opinion that the five LRSM systems can be installed and operated most economically by the LRSM personnel normally responsible for them. Accordingly, we plan to have the five employees normally assigned to the operation of the portable systems transport the systems to TFSO and install them, and we plan to assign two of these men to TFSO on temporary duty during the 2-month operating period.

Assuming that the useful operating magnification of the seismographs of the long-period test array is seismic-noise limited for extended intervals of time, we expect the test array to provide data for the determination of the coherency of the noise and the space stationarity of the noise power spectra over 10 distances ranging between 5 and about 30 kilometers. The array will also provide limited data regarding the azimuthal properties and velocities of the various components of the noise. We expect to successfully operate the seismographs simultaneously at magnifications of about 50K at 0.04 cps for some intervals during the term of the tests.

11. REPORTS AND DOCUMENTS PUBLISHED UNDER PROJECT VT/5055

Several reports and documents were published under Project VT/5055. Among the reports published were the following:

a. Fifty copies of TR 65-96, Operation of the Tonto Forest Seismological Observatory, Quarterly Report No. 1, Project VT/5055, 1 May through 31 July 1965, were mailed to the Project Officer on 17 August 1965.

b. Technical Report No. 65-129, Operation of TFSO, Quarterly Report No. 2, Project VT/5055, 1 August through 31 October 1965, was published on 12 November 1965.

c. Technical Report No. 66-14, Operation of TFSO, Quarterly Report No. 3, Project VT/5055, 1 November 1965 through 31 January 1966, was published on 14 February 1966

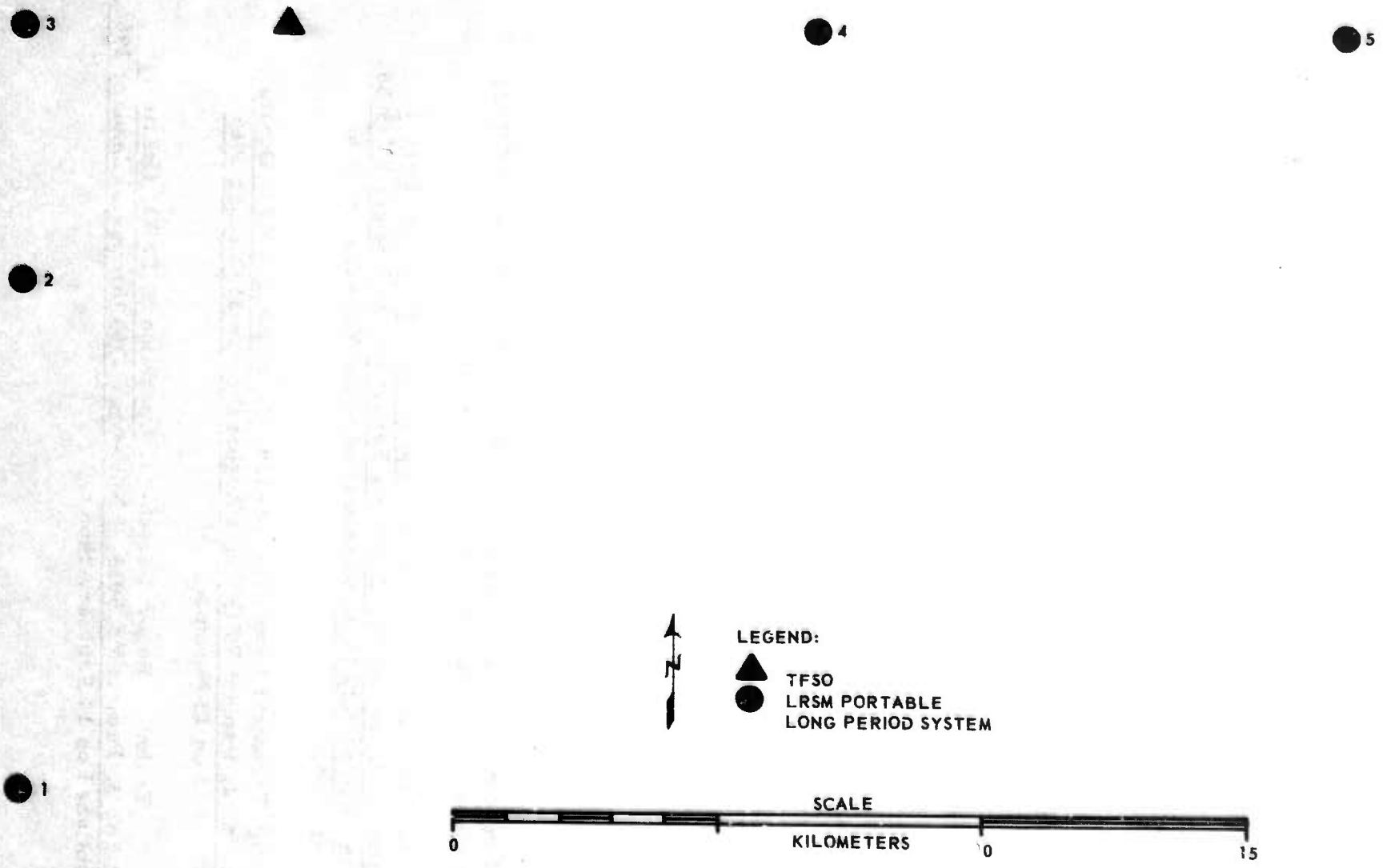

Figure 118. Long-period test array configuration

G 2088

d. Technical Report No. 66-53, Operation of TFSO, Quarterly Report No. 4, Project VT/5055, 1 February 1966 through 30 April 1966, was sent to the Project Officer on 9 May 1966.

e. Technical Report No. 66-85, Operation of TFSO, Quarterly Report No. 5, Project VT/5055, 1 May 1966 through 31 July 1966, was published on 17 August 1966.

f. Technical Report No. 66-109, Operation of TFSO, Quarterly Report No. 6, Project VT/5055, 1 August 1966 through 31 October 1966, was published on 1 December 1966.

g. The following letters of recommendation were submitted during the contract:

"Planned tests of shallow-hole seismograph system at TFSO," dated 9 November 1965:

"Request for approval to replace the crystal oscillator in the Hyperion timing system at TFSO" was submitted on 8 December 1965;

"Recommendations to improve the power system for frequency-regulated power at TFSO" was submitted on 17 January 1966;

"Recommendation for on-line operation of the Time Compensated Display Unit, Geotech Model 18621," dated 21 January 1966;

"Recommendation for adoption of weekly resistance measurements," dated 25 January 1966;

A recommendation to install dual output PTA's for TFSO's long-period seismographs was submitted to the Project Officer on 3 February 1966;

An outline of a study designed to determine the feasibility of classifying P waves using Pearson's correlation technique and requesting approval to conduct the study was sent to VSC on 10 February;

A recommendation that we improve the frequency regulated power system at TFSO by replacing the Bogen audio power amplifiers with a Model 22183 1000-watt power amplifier was submitted to the Project Officer on 23 February 1966;

A report of tests of the GS-13V geophone and a recommendation for the design of an improved high-frequency seismograph was submitted on 28 October 1966.

A request for authority to produce an engineering model of an improved high-frequency seismograph was submitted on 31 October 1966.

h. "Evaluation of the French Seismograph," letter report, dated 3 October 1966.

i. A report of tests conducted to confirm the proper operation of the Astrodata system was sent to the Project Officer on 31 August 1965.

j. A report on the operation of the TFSO high-frequency system was submitted on 22 September 1965. Blue-line prints of the high-frequency seismograms were mailed on 28 September 1965.

k. A list of Milestones was published, and a copy was sent to the Project Officer on 29 October 1965.

l. A Project Recommendation, P-624, for the design and testing of an improved high-frequency seismograph was delivered to the Project Officer on 18 April 1966.

m. Technical Report No. 66-73, Magnitude Studies Conducted under Projects VT/5054 and VT/5055, by Jack G. Swanson, was mailed on 31 August 1966.

n. Project Recommendation P-688, Recommended Orientation for the TFSO Seismograph Array, was submitted on 7 September 1966.

12. REFERENCES

Byrne, C. J., January 1961, Instrument noise in seismometers, Bulletin of the Seismological Society of America, vol. 51, no. 1, p. 69-89

Haubrich, Richard A. and MacKenzie, Glenn S., March 1965, Earth noise, 5 to 500 millicycles per second, Journal of Geophysical Research, vol. 70, no. 6, p. 1429-1440

Kovach, Robert L., 1965, Seismic surface waves: some observations and recent developments, Physics and Chemistry of the Earth, vol. 6, p. 251-314

Oliver, Jack, and Page, Robert, January 1963, Concurrent storms of long and ultralong period microseisms, Bulletin Seismological Society of America, vol. 53, p. 15-26

Taylor, V. W., UED, Investigation of system response as a function of azimuth from Tonto Forest Seismological Observatory, Project VT/070, TFSO Special Report No. 15, 14 August 1964.

Texas Instruments, Inc., 1961; Seismometer array and data processing system, final report phase I, project VT/077, contract AF 33(600)-41840

Texas Instrument, Inc., 1965; 1965; Array research semi-annual, technical report no. 3, contract AF 33(657)-12747, ARPA Order No. 104-60, Project Code 8100

Texas Instruments, Inc., 1966a, Array research special report no. 16; initial analysis of long-period, large-aperture data recorded at the Tonto Forest Seismological Observatory in 1965, contract AF 33(657)-12747, ARPA Order No. 104-60, Project Code 8100

Texas Instruments, Inc., 1966b, Array research wave number analysis of TFO long-noise sample, special report no. 17, project VT/4053, contract AF 33(657)-12747, ARPA Order No. 104-60, Project Code No. 8100

Texas Instruments, Inc., 1966c, Semi-annual technical report no. 5, project VT/4053, contract AF 33(657)-12747, ARPA Order No. 104-60, Project Code No. 8100

Rugg, Allen M., Jr. and Russell, Orville R., UED, Investigation of signal amplitude variations in the Tonto Forest Seismological Observatory array, VT/070, TFSO Special Report No. 31, 24 June 1965

The Geotechnical Corp., 1965, Evaluation of low-noise, low-frequency amplifiers and short-period seismometers, TR 65-69, Garland, Texas

APPENDIX TO TECHNICAL REPORT NO. 67-13

STATEMENT OF WORK TO BE DONE

STATEMENT OF WORK TO BE DONE
AFTAC PROJECT AUTHORIZATION NO. VELA T/5055

NOV 1 0 1964

1. Operation.

a. Operate the Tonto Forest Seismological Observatory (TFSO), normally recording data continuously.

b. Evaluate the seismic data to determine optimum operational characteristics and make changes in the operating parameters as may be required to provide the most effective observatory possible. Addition of new and modification of present on-line instrumentation are within the scope of work. However, such instrument additions and modifications, data evaluation, and major parameter changes are subject to prior technical approval by the AFTAC project officer.

c. Conduct routine daily analysis of seismic data and transmit daily seismic reports to the US Coast and Geodetic Survey, Washington, DC 20230, using the established report format and detailed instructions.

d. Record the results of daily analysis in a format compatible with the automated bulletin program (ABP) used by the Seismic Data Laboratory (SDL), 300 North Washington Street, Alexandria, Virginia 22314, in their preparation of the seismological bulletin of the VELA-UNIFORM seismological observatories. This format may be established by coordination with SDL through the AFTAC project officer. The schedule of routine shipments of this data to SDL will be established by the AFTAC project officer.

e. Conduct quality control (QC), as necessary, to assure the recording of high quality data on both magnetic tape and film. Past experience indicates that QC review of one magnetic tape per magnetic tape recorder per week is satisfactory unless QC tolerances have been exceeded and the necessity of additional QC arises. QC of magnetic tape should include, but need not necessarily be limited to, the following items:

(1) Completeness and accuracy of operation logs.

(2) Accuracy of observatory measurements of system noise and equivalent ground motion.

(3) Quality and completeness of voice comments.

(4) Examination of all calibrations to assure that no clipping occurs.

(5) Determination of relative phase shift among all array seismograph systems.

(6) Measurement of DC unbalance.

AF 33(657)-14444

REPRODUCTION

(7) Presence and accuracy of tape calibration and alignment.

(8) Check of uncompensated noise on each channel.

(9) Check of uncompensated signal-to-noise of channel 7.

(10) Check of general strength and quality of WWV time.

(11) Check of synchronization of digital time code with WWV.

f. Continue telephone service and VHF telemetry between TFSO and the mobile seismic vans (Project VELA T/4051) located along extensions of the TFSO crossed array.

g. Provide observatory facilities, accompanying technical assistance by observatory personnel, and seismological data to requesting organizations and individuals after AFTAC approval through the project officer.

h. Maintain, repair, protect, and preserve the facilities of TFSO in good physical condition in accordance with sound industrial practice.

2. Instrument Evaluation.

a. On approval by the AFTAC project officer, evaluate the performance characteristics of experimental and off-the-shelf equipment offering potential improvement in the performance of observatory seismograph systems. Operation and test of the instrumentation under field conditions should normally be preceded by laboratory test and evaluation.

b. To permit more thorough laboratory evaluations to be conducted at TFSO, improvements to TFSO laboratory capability may be necessary. The contractor should make recommendations for such improvements and, after approval by the AFTAC project officer, implement them.

3. Developmental Function. Operation and evaluation of the observatory's "standard" instrumentation and of "experimental" equipment may disclose the need for supplemental equipment, neither commercially available nor in development under the VELA-UNIFORM program, that could improve the performance and capability of the seismograph systems of TFSO and other VELA-UNIFORM observatories. The contractor should make recommendations on the development of such equipment and, after approval by the AFTAC project officer, proceed with developmental work.

4. Research Programs. On approval by or at the request of the AFTAC project officer, conduct research programs designed to upgrade the TFSO detection capability. Environmental conditions (geological, seismological, and meteorological) affecting the results of these research programs should not be neglected. Research might pursue investigations in, but are not necessarily limited to, the following areas of interest:

AF 33(657)-14444

REPRODUCTION

a. Microseismic Noise.

(1) Review all available TFSO noise data to guide the direction of additional work. Define and conduct additional surface noise studies as necessary.

(2) Examine noise at shallow depths using existing and additional shallow boreholes. The number, depth, and locations of the additional boreholes must be approved by the AFTAC project officer.

b. Array Detection Capability.

(1) Evaluate combinations of existing vertical and of existing horizontal surface array seismographs to determine the most effective array summations in detecting teleseismic signals. Determine TFSO overall detection capability when using these array summations along with the remaining seismograph systems.

(2) Under Project VELA T/5052, AFTAC has programmed the addition of a multiple array processor to the TFSO instrumentation for the summer of 1965; training in operation, maintenance, and calibration of the processor and in analysis techniques will be provided to appropriate TFSO personnel at the time of installation by the manufacturer, Texas Instruments Incorporated. Evaluate the detection capability of the processor and examine its enhancement, if any, of the overall TFSO capability.

(3) Mobile seismic vans (Project VELA T/4051) are temporarily located along extensions of the TFSO crossed array and the data (3-component short-period) from the vans are recorded at TFSO. Investigate the use of this extended array to improve the TFSO detection capability.

(4) Determine TFSO deficiencies, if any, that degrade the observatory's detection capability. Prepare and submit to the AFTAC project officer recommended improvements designed to eliminate such deficiencies and enhance the detection capability.

c. Visual Data Presentation. Investigate forms of visual data presentation which would improve detection of seismic signals by visual on-line analysis.

Programs implemented should be planned for completion during the contracted period of TFSO operation. Furthermore, prior to commencing any research program, AFTAC approval must be obtained of a comprehensive outline for each research program instituted.

REPRODUCTION